U.S.DEPARTMENT OF COMMERCE • ENVIRONMENTAL SCIENCE SERVICES ADMINISTRATION
Weather Bureau

TECHNICAL NOTE 9-SAIL-1

Proceedings of the Sea-Air Interaction Conference Tallahassee, Florida February 23-25, 1965

SEA-AIR INTERACTION LABORATORY
REPORT NO.1

WASHINGTON, D.C.
August 20, 1965

WEATHER BUREAU TECHNICAL NOTES

SEA-AIR INTERACTION LABORATORY REPORTS

The Sea-Air Interaction Laboratory of the Environmental Science Services Administration is responsible for the main research effort in problems concerning the physical aspects of exchange processes between the ocean and the atmosphere. The laboratory is also charged with the responsibility of coordinating the federal effort in air-sea interaction research and the development of a federal research program.

The laboratory's program encompasses research in an in-house basis such as storm surge research and the data collection program at sea. Other projects are accomplished on a contract basis by universities and other private agencies.

Reports by the laboratory staff, contractors, and cooperators will be preprinted in this series to allow immediate distribution of the information among the workers and other interested organizations. Since these reports may not be in completely polished form and are for limited reproduction and distribution they do not constitute formal scientific publication. Reference to a paper in this series should identify it as a preprinted report. Formal publi[illegible] made later in appropriate scier[illegible]

Scier[illegible] Clearinghouse for Federal
Build[illegible] S. Department of Commerce, Sills
[illegible]irginia 22151.

U.S. DEPARTMENT OF COMMERCE • John T. Connor, Secretary

ENVIRONMENTAL SCIENCE SERVICES ADMINISTRATION
Robert M. White, Administrator

Weather Bureau

TECHNICAL NOTE 9-SAIL-1

Proceedings of the Sea-Air Interaction Conference

Tallahassee, Florida, February 23-25, 1965

SPONSORED JOINTLY BY

FLORIDA STATE UNIVERSITY
DEPARTMENT OF METEOROLOGY AND OCEANOGRAPHY INSTITUTE,

AND

ENVIRONMENTAL SCIENCE SERVICES ADMINISTRATION,
SEA-AIR INTERACTION LABORATORY

WASHINGTON, D.C.
August 20, 1965

FOREWORD

The interactions between the atmosphere and the oceans have increasingly attracted the attention of meteorologists and oceanographers in recent years. It is generally agreed that progress in our understanding of, and ability to predict the behavior of the atmosphere and the oceans depends on a knowledge of the exchanges of matter, momentum, and energy between the two fluid systems. At the present time, adequate quantitative information on these exchange processes at the air-sea interface is lacking.

It has come to be recognized that a strong interdiciplinary research program in meteorology and oceanography is required for a more satisfactory comprehension of the interactions between the two parts of the coupled air-sea system. In several universities and other research institutions, joint programs of meteorological and oceanographic research are being conducted with emphasis on exchange phenomena at the sea surface, and in the atmospheric and oceanic boundary layers. The National Academy of Sciences has identified air-sea interaction research as one of the scientific areas requiring increased support, and the Federal Government has responded by establishing special programs for this purpose.

The Sea-Air Interaction Conference held in Tallahassee in February 23-25, 1965, was suggested and arranged by Prof. Charles L. Jordan, Chairman of the Department of Meteorology at Florida State University, in cooperation with the Oceanography Institute of the University. The conference was co-sponsored by the Sea-Air Interaction Laboratory (SAIL) of the Department of Commerce (a joint laboratory of the U.S. Weather Bureau and the U.S. Coast and Geodetic Survey). Mr. Feodor Ostapoff, acting director of SAIL, served as editor of the Proceedings and arranged for its publication.

In the congenial and informal atmosphere provided by the conference hosts at Florida State University, meteorologists and oceanographers from many universities, research institutions and government agencies exchanged views, reviewed programs and problems, and laid the groundwork for future cooperation in air-sea interaction studies.

The participation of all the conferees in the work of the conference, and the promptness with which they provided their papers to the editor for publication in these Proceedings, are gratefully acknowledged.

Jerome Spar
Director of Meteorological Research,
U. S. Weather Bureau

TABLE OF CONTENTS

Foreword.....iii

"Air Sea Exchange as a Factor in Synoptic-Scale Meteorology in Middle Latitudes, " by Jerome Spar..... 1

"The Three-Dimensional Ocean Circulation Driven by Density Gradients in an Enclosed Basin, " by Dr. Kirk Bryan..... 17

"On the Present State of Knowledge in Air-Sea Boundary Layer Problems, " by Dr. H. U. Roll..... 31

"A Survey of the Role of Sea-Air Interaction in Tropical Meteorology, " by Dr. Joanne Malkus Simpson..... 65

"Sensible and Latent Heat Exchange in Low Latitude Synoptic-Scale Systems," by Dr. Michael Garstang.....105

"Intensity of Hurricanes in Relation to Sea Surface Energy Exchange," by Irving Perlroth.....147

"The Gulf of Mexico after HILDA (Preliminary Results)," by Dr. Dale F. Leipper.....163

"Evidence of Surface Cooling Due to Typhoons," by Dr. C. L. Jordan....185

"The Modification of Water Temperatures by Hurricane CARLA," by Drs. Robert E. Stevenson and Reed S. Armstrong.....191

"On the Low Level Thermal Stratification of the Monsoon Air over the Arabian Sea and its Connection to the Water Temperature Field, " by Dr. José A. Colón.....209

"A Low-Level Jet Produced by Air, Sea, and Land Interactions," by Dr. Andrew F. Bunker.....225

"U. S. Fleet Numerical Weather Facility Activities Relating to Sea-Air Interactions on a Synoptic Scale," by Comdr. W. E. Hubert.....239

"Synoptic Scale Heat Exchange and its Relations to Weather," by Dr. Taivo Laevastu.....257

"Laboratory Studies of Wind Action on Water Standing in a Channel," by Drs. George M. Hidy and E. J. Plate.....285

"On the Instability of Ekman Boundary Flow," by Dr. Douglas K. Lilly..... 327

"Federal Research Programs in Air-Sea Interaction," by Feodor Ostapoff..... 331

Appendix I: Conference Program..... 341

Appendix II: Conference Participants..... 344

AIR-SEA EXCHANGE AS A FACTOR IN SYNOPTIC-SCALE METEOROLOGY IN MIDDLE LATITUDES

Jerome Spar
U. S. Weather Bureau, Washington, D.C.

INTRODUCTION

The subject of this conference is not a new one. Oceanographers and meteorologists have been concerned with exchanges across the air-sea boundary for many years and they do not need to be convinced of the importance of these exchange processes.

What we have assembled to discuss here, I presume are the unsolved problems of air-sea exchange, and the possibilities for solving these problems through new measurement programs, theoretical investigations, and computations. In particular, we need to concern ourselves now with improvements in our quantitative information about the exchange processes, and with the establishment of useful relationships between the microphysics of the exchange processes and the larger scale atmospheric and oceanic parameters.

One of the important subjects for this conference should be "interaction" in its full sense. Exchanges between the air and sea are generally viewed either from above or below -- rarely from both viewpoints simultaneously. Most of us tend to interpret "interaction" parochially as the transfer of property to or from our fluid (whether air or water) without regard to the subsequent effect on the other side of the boundary. I suppose we all cherish the long-term objective of treating the air-sea system as an integrated problem. At the moment, however, few of us are prepared to do very much about the real interaction problem. But perhaps we may be able soon to make a crude assessment of the relative importance of the reaction on one fluid of changes induced by that fluid in the other. How tightly are the air and sea linked? Are the interactions strong or weak? Do differences in the response times of the two fluids cause them to behave as if, for practical purposes, they do not interact, but only influence each other?

All oceanographers recognize that the atmosphere exerts an important influence on the oceans. Clouds affect the distribution of insolation. Rain falls into the sea. Evaporation varies with wind and humidity of the air. The wind stress drives currents, generates waves, produces upwelling, stirs the water, and creates spray. Atmospheric gases enter the sea, and heat is exchanged between the air and the sea.

Every meteorologist knows that the oceans have a profound influence on the atmosphere. Salt particles enter the air from the sea. Sea water evaporates into the air. Through surface wind stress, the atmosphere loses kinetic energy to the sea. And heat is exchanged between the sea and the air.

We have come to recognize that through these exchanges of matter and energy, a complex interaction takes place between the two fluid systems of the earth. Thus the wind stress on the sea surface may change the sea surface temperature distribution, which alters the heat transfer from the

sea to the air; and this in turn may change the atmospheric circulation, thus altering the wind stress.

Nevertheless, meteorologists have found it convenient -- when they have considered the oceans at all -- to think of the oceans and other large water bodies as inert systems with inifinite heat capacity. In this way we have been able to ignore "interactions" between sea and air entirely, and have treated the sea surface as fixed in time, and unaffected by the atmosphere.

To allow for the obviously non-negligible annual variation in sea surface temperatures, we may use climatological mean monthly sea surface temperatures, rather than mean annuals, and in some cases shorter time averages. But, for the most part, the meteorologist has taken the ocean state as "given" and has not attempted to predict it.

In extended and long-range weather forecasting and to a lesser extent in short-range forecasting, some attempts have been made to employ the water temperature anomalies as meteorological predictors. The underlying principle in these efforts, however, is again the relative persistence of oceanographic features -- in this case sea temperature anomalies -- compared with the variability of the atmosphere. A one-way transfer, from sea to air, without interaction, is implicit in these applications.

Of course, meteorologists are fully aware of the fact that the sea responds to the atmosphere. But we have generally been unable to incorporate oceanographic predictions in our work, either qualitatively or quantitatively. In fact we have made hardly any progress even with the relatively simpler one-way transfer problem.

We have come closest to dealing with a true air-sea interaction in practical meteorology in connection with the hurricane problem. Several investigators using synoptic ocean data, have presented interesting, albeit inconclusive evidence pointing to the possibility that hurricanes may tend to form over anomalously warm water, move along warm water anomaly "channels," avoid cold water, or dissipate over cold water. At the same time, these and other studies have shown that the hurricane -- whether through upwelling, stirring, evaporation or radiative-convective heat transfer -- cools the sea in its immediate vicinity, and appears to leave a cold water wake behind the storm. So large is this effect of the storm on the sea, that it is obviously unrealistic to assume a fixed sea temperature anomaly field in hurricane prediction.

To the oceanographer, looking at the underside of the air-sea boundary, oceanographic prediction depends almost entirely on accurate prediction of the atmosphere. Current anomalies, waves, and temperature anomalies -- as well as salinity, oxygen and other oceanic anomalies -- are ultimately meteorological in origin. The oceanographic prediction begins with a weather map. Because of the time lag between storm development and wave generation, plus the travel time of waves, a useful oceanographic prediction can (like a

useful river forecast) often be made from the current weather map. But in general the ocean forecaster requires prognostic weather maps. Abrupt and unpredicted deepending or filling of a cyclone near a continental coast -- a phenomenon that could conceivably be caused by a wind-generated oceanic anomaly -- can produce a disastrous failure in the prediction of sea state and coastal wave action.

The interdependence of meteorological and oceanographic predictions on all time scales is too obvious to belabor further except to note that while the atmospheric influence on the sea is reasonably well known, even quantitatively, the converse, i.e., the influence of the sea on the atmosphere, is not.

Given the wind stress at the sea surface, we can at least compute the steady state Ekman current as a function of depth. We can even generate from the wind a reasonably realistic wave spectrum. True we do not know too much about the depth to which the sea is mixed by surface wind action, and we cannot predict temperature anomalies caused by upwelling with satisfactory success -- but these problems appear to be amenable to solution.

The meteorological problem, on the other hand, seems to be much more difficult. The effect of the air on the sea is direct and measurable. The converse is neither direct nor measurable. The transfers across the sea surface that are likely to have an important influence on the atmosphere are of salt, water vapor, kinetic energy, momentum, and heat. None of these transfers is easily measured, especially in high winds. But even if we could measure them, we still have the problem of determining quantitatively the effects of these transfers on the atmosphere.

Does anomalously high storm activity at sea measurably increase the salt particle population of the atmosphere? How is the salt distributed? What is its residence time in the atmosphere? How does it affect the subsequent precipitation distribution? What is the nature of the dynamic feedback to the atmosphere of the latent heat thus released?

Similar questions may be asked regarding evaporative transfer, and again the questions are not easily answered. We note that in an east coastal cyclone (see, e.g., Petterssen,et al. 1962) most of the evaporative flux occurs in the cold air to the rear of the surface cyclone. What fraction of the transferred latent heat is realized locally in the cold air by cumulus development and showers, and what fraction is realized far from the source, perhaps in another system altogether? And what role does this energy play in the cyclone development?

The sensible heat transfer from the warm sea to a cold air mass (the major energy transfer according to Manabe, 1957) presents similar problems. What do we really know about the dynamical effects on the atmosphere of this sea-air heat transfer?

In the following I will try to review briefly some efforts that have been made to evaluate the quantitative effects of sea-air heat and vapor transfers on atmospheric circulation systems, largely in the context of the weather prediction problem. (I will not attempt to deal with the important salt transfer problem at all.)

QUANTITATIVE ESTIMATES OF SEA-AIR TRANSFER AND ITS EFFECT ON CIRCULATION

Investigations of this problem have almost universally ignored interaction effects, (i.e., thermodynamic feedback to the oceans), and it appears very likely that such feedbacks may indeed be second order effects. The ocean is thus taken as time-invariant.

Three approaches to the problem have been tried.

(1) Direct computations of the sea-air heat transfer (a) from the transfer equations, following the Eulerian approach of Sverdrup (e.g.,Jacobs, Petterssen, et al., Pyke), (b) empirically from trajectory (Langrangian, air mass modification) studies (e.g., Burke, Craddock, Spar), and (c) from line integral computations of energy flux divergence (Manabe).

(2) Indirect evaluation of sea-air heat transfers from a study of the errors generated by adiabatic NWP[1] models (e.g., Winston, Martin, Petterssen, et al., Pyke).

(3) NWP computations with diabatic models, including sea-air heat transfer (Bushby and Hinds, Reed, Spar).

A. Direct Transfer Computations

Direct computations of sea-air energy transfer do not really tell us what role the transfer plays in the generation of circulation. Nevertheless, the results are illuminating, and potentially useful for prediction.

To apply the Sverdrup-type transfer equations to the computation of sensible or latent heat transfer, as Petterssen, et al. (1962) and Pyke (1965) have done for diagnostic purposes, and others -- Bushy and Hinds (1955), Reed (1958) and Spar (1962), for example -- have done in prognostic exercises, one must have some knowledge of the transfer coefficients, and indeed one really needs to know the correct functional form of the transfer relation. While it is convenient to assume a linear relation between the transfer rate and the air-sea temperature or vapor pressure difference, and a linear dependence on wind speed, as well, these assumptions are really not strongly supported by data.

1/Numerical weather prediction

Empirical studies of two kinds have been conducted which could shed some light on the problems of the functional form of the transfer relation and the values of the transfer coefficients. However, these studies have not been carried far enough to solve the general problem, and the data from these studies have generally been used only to provide limited and immediate practical answers for some special needs.

The one general result which does appear to emerge from these studies is that we can assume zero sensible heat transfer in the stable case, i.e. where warm air passes over cold water, and probably zero latent heat transfer as well, as far as large scale dynamical effects are concerned. Obviously, the well-known modifications of the shallow surface layer are important for weather prediction; poleward moving surface air cools, and fog and stratus do form. But while these results must be included in the complete weather prediction computation, the total energy transfer involved is small, the effect does not penetrate very high, and its dynamical consequences are probably negligible.

The data from Burke's (1945) early experiment -- carried out at Sverdrup's suggestion -- are unfortunately not presented in a form that permits one to relate the sea-air energy transfer parametrically to macro-scale variables. Craddock's (1951) data are somewhat more useful in this regard. Several years ago (Spar, 1962) I tried to use the Lagrangian trajectory technique, as Burke and Carddock had done earlier in their studies of air mass modification, to evaluate the transfer coefficients for sensible heat and water vapor. The results, based on 238 12-hour trajectories off the east coast of the United States were the following:

In the case of "effective heat flux," (i.e. the sensible heat flux plus radiative heating plus that latent heat released locally in the cold air by cumulus formation and showers) the formula

$$H = 10\, V_o\, (T_s - T_o) \qquad (1)$$

(H in ly day^{-1}, V_o the average "surface" wind along the 12-hour trajectory in m sec^{-1}, T_s and T_o the average sea surface and "surface" air temperatures in degree C) gave "satisfactory" results in the sense that the correlation between the left and right hand sides of the formula was about 0.6.

The transfer coefficient above may be compared (although the comparison is not strictly valid) with some others (see Table I).

Table 1. Sensible (and effective) heat transfer coefficients, K_s, from various sources.

Dimensions: ly day^{-1} (m sec^{-1})$^{-1}$ degree $^{-1}$C.

K_s	Source
10.	Spar (1962)
3.6	Malkus (1962)
6.8	Jacobs (1942)

For water vapor the effort to evaluate a transfer coefficient from the 238 trajectories was less successful. The linear relation,

$$L = K_e V_o (q_s - q_o), \qquad (2)$$

(L, the latent heat transfer rate in ly day^{-1}, Vo the surface wind in m sec^{-1}, q_s and q_o the dimensionless specific humidity at the sea surface and in the "surface" air) could not be verified by the data because of the large scatter (low correlation). A value of K_e was determined, nonetheless, from mean values of $V_o (q_s - q_o)$ and L. Table 2 shows this (dubious) value of K_e together with some others.

Table 2. Latent heat transfer coefficients, K_e, from various sources.

Dimensions: ly day^{-1} (m sec^{-1})$^{-1}$

K_e (x 10^3)	Source
8.8	Spar (1962)
9.9	Marciano and Harbeck (1952)
8.5	Manabe (1958) (average over all speeds) 1/
8.6	Malkus (1962)
14.	Jacobs (1951)

Manabe (1958) has applied the line integral method for computing the horizontal flux divergence of latent and sensible heat to the Japan Sea with very satisfactory results. Unfortunately, Manabe did not use his data to test the parametric transfer formula for sensible heat as he did for evaporation. This task remains to be done.

B. Indirect Computations of Energy Transfer

The errors in adiabatic numerical prediction models are in part due to sea-air energy transfers, although other factors, notably condensation, may

1/ (Manabe's results show a change in K_e from 6.0 at low speeds - 6 m sec^{-1} - and a smooth surface, to 11. at higher speeds -8 m sec^{-1} - and presumably a rougher surface.)

be even more significant. Studies of these diabatic errors leave little doubt about the fact that they may be, on occasion, large and important, and justify the inclusion of diabatic processes in NWP.

Winston's (1955) study of the February 1950 cyclogenesis in the Gulf of Alaska, recently re-examined and extended by Pyke (1965), is an early example of the efforts to evaluate the sea-air transfer from prediction errors. A more comprehensive study of NWP errors by Martin (1962) demonstrated even more clearly the probably importance of the sea as an energy source for the atmosphere. Martin's computations were in remarkably good agreement with the independent computations of Manabe (1958) for the winter 1954-55 cold outbreak over the Japan Sea (with transfers of more than 1400 ly day^{-1}), and also with computations by Petterssen for the North Atlantic.

Petterssen, Bradbury, and Pedersen (1962) in a diagnostic study of cyclone development over the North Atlantic Ocean have attempted to develop the classical Norwegian cyclone models into a more complete dynamical model by computing the energy transfers from the sea to the air. The results have been somewhat disappointing. In the first place, the computed heat transfers show, as expected, the major heat transfer in the cold air mass to the rear of the cyclone -- but with no physical account of how (or if) this energy contributes to the cyclone development. Secondly, the paper essentially bypasses the question of how the heat source affects the circulation, because only the thickness (i.e., temperature) tendency is computed. Inclusion of the heat source term in the tendency calculation improves the predicted thickness tendency, as expected, but unfortunately, tells us nothing about the effect on the 500-mb circulation.

C. Diabatic Prediction Models

The effects of sea-air heat transfer on atmospheric circulation systems are so complex that it appears likely that nothing less than time integration of the complete diabatic system of equations can really tell us much about these phenomena. Such experiments have been attempted with models of varying degrees of complexity. Bushby and Hinds (1955) were probably the first to incorporate sea-air heat transfer in a numerical weather prediction model, followed a few years later by Reed (1958), who employed Fjørtoft's graphical (Lagrangian) method.

My own experiments (Spar, 1962), including heat of condensation as well as sea-air heat transfer, employed a somewhat less constrained model, but still only a two-level (vertically integrated) baroclinic model -- geographically limited and geostrophic. Despite these constraints, the experimental results may be of some interest.

In the computations with my prediction model, I have used the empirical transfer formulas (equations (1) and (2)) to compute (effective) sensible

heat transfer and evaporation. Input data included 1000 and 500 mb geopotential heights, integrated specific humidity (precipitable water), and ocean surface temperatures (time invariant). Output consisted of 1000 and 500 mb geopotential, precipitable water, cumulative precipitation, and vertically - averaged vertical motion. The forecasts shown are for 12 hours (computed in one-hour time steps).

The figures (Spar, et al., 1961) show the initial state, 12-hour forecasts, and verification maps for a case of rapid North American east-coastal cyclogenesis beginning at 0300 GMT 10 February 1957, and permit us to compare forecasts made with and without surface heat and vapor transfer.

The initial conditions for the forecast experiment are displayed in the three maps of Figure 1 which show the 500 mb geopotential and temperature, 1000 mb geopotential and 1000-500 mb geopotential thickness, and the vertically-averaged specific humidity.

Figure 2 illustrates the twelve-hour 500 mb forecasts computed (A) with a barotropic model, (B) with a baroclinic model including heat of condensation but no heat or vapor flux from the sea ("No Flux"), and (C) with a baroclinic model including sea-air fluxes as well as latent heat ("complete"). The verification contours are shown as dashed curves in Figure 2(A). It is noteworthy that the baroclinic model predicted the marked deepending that was missed by the barotropic forecast, but that the inclusion of the sea-air fluxes had no significant influence on the twelve hour forecasts.

The forecast 1000 mb maps, together with the predicted 1000-500 mb thickness patterns are shown in Figure 3 for the "No Flux" (A) and "complete" (B) models. Also shown is the verification map (C) for the 1000 mb level (solid curves) and the thickness (dashed curves). Again the forecasts made with and without sea-air fluxes do not differ significantly in this short time interval.

The conclusions drawn from these crude experiments were:

1. During cyclogenesis the diabatic effects (and this includes also the latent heat release) were second order effects compared with baroclinic effects. This conclusion, i.e., that potential to kinetic energy conversion is the dominant energy transformation in cyclogenesis, is in agreement with the results of many other investigators.

2. In 12 hours the dynamical effects of sea-air heat and vapor transfer were of little significance. It might be expected that over a longer period the air-sea effects might be more important. But it is noteworthy that the 12-hour period selected was the one when the cold outbreak over the water was strongest, and the heat transfer at its peak.

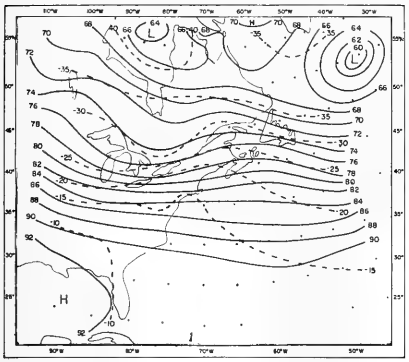

(A)

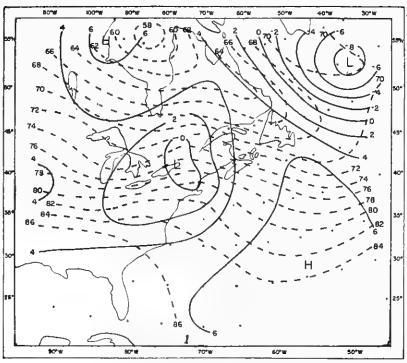

(B)

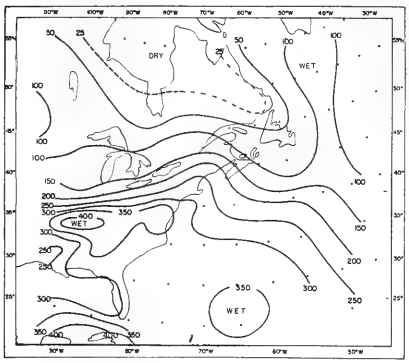

(C)

Figure 1. Initial conditions, 0300 GMT 10 February 1957. (A) 500 mb geopotential height (solid curves, labeled in hundreds of feet) and temperature (dashed curves, labeled in °C); (B) 1000 mb geopotential height (solid curves labeled in hundreds of feet) and 1000-500 mb geopotential thickness (dashed curves labeled in hundreds of feet), (C) mean specific humidity (parts per hundred thousand). See text page 10.

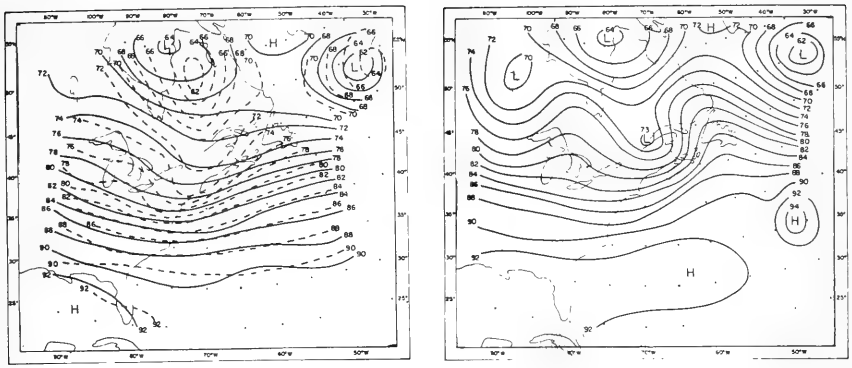

(A) (B)

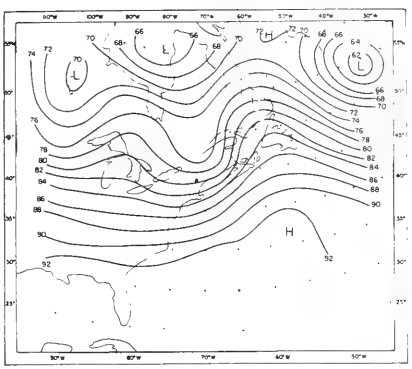

(C)

Figure 2. Twelve-hour 500 mb forecasts for 1500 GMT 10 February 1957. (A) Barotropic. Solid lines are the predicted contours; dashed lines are the observed contours. (B) "No Flux." (C) "Complete." Contours are drawn for an interval of 200 geopotential feet. See text page 10.

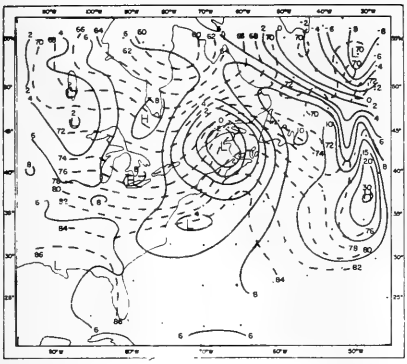

(A)

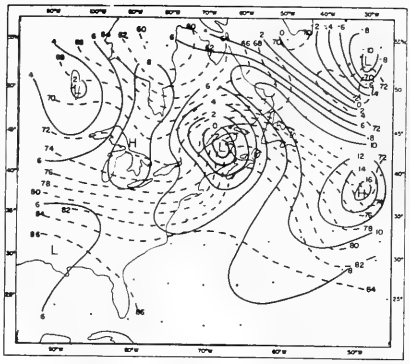

(B)

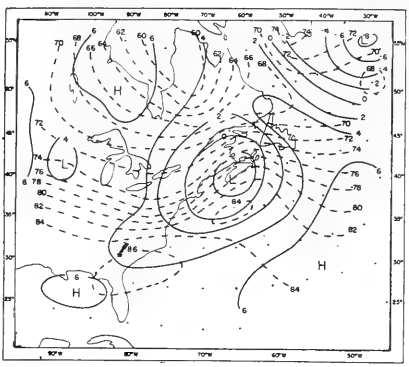

(C)

Figure 3. 1000 mb contours (solid lines) and 1000-500 mb thickness contours (dashed lines) drawn for interval of 200 geopotential feet. 1500 GMT, 10 February 1957. (A) "No Flux," and (B) "Complete" 12-hour forecasts. (C) Verification (observed) map. See text page 10.

3. Sea-air transfer did not affect the large scale vertical motion in the system significantly in 12 hours.

4. The sea-air transfer effects were shallow, failing to penetrate up through the 500 mb level.

These rather negative conclusions regarding the role of sea-air transfer in the dynamics of coastal cyclogenesis must be viewed warily. The model is constrained (notably in regard to the static stability); the experiments were few in number; the period of integration was short.

Nevertheless the conclusions are not greatly at variance with those of other investigators. Prof. Yale Mintz recently wrote the following to me, in reply to a request for his views on the subject:

> "I am sure this heating plays an important role in determining the temperature, wind and pressure fields, but in some complicated way affecting more than just the cyclone scale of motion."... "If I have to guess at an answer, I would say that the heat transfer from the sea affects the baroclinicity of the air and hence the subsequent cyclogenesis; but that a cyclone already in the developing state is, itself, relatively little affected by the heat transferred to it. But that is only a guess."

I am inclined to believe that this is a rather shrewd guess.

REFERENCES

Jacobs, W.C., 1942: On the energy exchange between sea and atmosphere. J. Mar. Res., 5, 37-66.

_____ 1951: The energy exchange between sea and atmosphere and some of its consequences. Bull. Scripps Inst. of Ocean., Univ. of Calif. 6, 27-122.

Petterssen, S.; D. L. Bradbury, and K. Pedersen, 1962: The Norwegian cyclone models in relation to heat and cold sources. Geophys. Publ. Geophys. Norwegica, 42, 243-280.

Pyke, Charles B. 1965: On the role of air-sea interaction in the development of cyclones. Bull. Amer. Met. Soc., 46, 4-15.

Burke, Cletus J. 1945: Transformation of polar continental air to polar maritime air., J. Meteor., 2, 94-113.

Craddock, J. M. 1951: The warming of Arctic air masses over the eastern North Atlantic. Quart. Jour. Roy. Meteor. Soc., 77, 355-365.

Spar, J. 1962: A vertically integrated wet diabatic model for the study of cyclogenesis. Proc. Int'l Symp. on Num. Wea. Pred., Tokyo, Nov. 7-13, 1960. 185-204, Met. Soc. of Japan.

Spar, J.; J. P. Gerrity, Jr.; L. A. Cohen 1961: Some results of experiments with an integrated, wet, diabatic weather prediction model. Sci. Rep. No. 2, Contract Nonr-285 (09). New York University. 28 pages.

Manabe, S. 1957: On the modification of air-mass over the Japan Sea when the outburst of cold air predominates. J. Met. Soc. Japan, 35, 311-326.

———————————— 1958: On the estimation of energy exchange between the Japan Sea and the atmosphere during winter based upon the energy budget of both the atmosphere and the sea. J. Met. Soc. Japan, 36, 123-133.

Winston, J.S. 1955: Physical aspects of rapid cyclogenesis in the Gulf of Alaska. Tellus, 7, 481-500.

Martin, D.C. 1962: The relation between non-adiabatic heating and the errors of numerical forecasts. Proc. Int'l. Symp. on Num. Wea. Pred., Tokyo, No. 7-13, 1960, 283-296. Met. Soc. of Japan.

Bushby, F. H. and M. K. Hinds 1955: Further computations of 24-hour pressure changes based on a two-parameter model. QJRMS, 81, 396-402.

Reed, R.J. 1958: A graphical prediction model incorporating a form of non-adiabatic heating. J. Meteor., 15, 1-8.

Malkus, J. S. 1962: Large scale interactions, Ch. 4 in The Sea, New York, John Wiley and Sons, pp. 88-94.

Marciano, J. J. and G. E. Harbeck 1952: Mass transfer studies. U. S. Dept. of the Interior, Geol. Survey, No. 229 Water Loss Investigations, Vol. I. Lake Hefner Studies. Tech. Report.

THE THREE-DIMENSIONAL OCEAN CIRCULATION DRIVEN BY DENSITY GRADIENTS IN AN ENCLOSED BASIN

Kirk Bryan
U. S. Weather Bureau, Washington, D.C.

ABSTRACT

Estimates of poleward transport of heat based on the heat balance of the ocean surface indicate that ocean currents in the North Atlantic transport from 10-20 percent as much heat poleward as the entire atmosphere in middle latitudes. Similar measurements for the Pacific based on heat balance are less reliable. An analysis of hydrographic data obtained during the IGY and NORPAC expeditions permits the examination of different components of the heat transport. Of particular interest are the two components associated with the thermohaline circulation, and the wind-driven subtropical gyre. The poleward heat transport by these two agencies is of the same order of magnitude. In the North Atlantic the thermohaline circulation and the wind-driven gyre both transport heat poleward. On the other hand, present evidence on the circulation of the North Pacific suggests that there these two important components tend to cancel each other. The relative contribution of smaller scale, transient motions is unknown.

A numerical model is proposed to gain further insight into the mechanism of poleward heat transport. Solutions are obtained for an enclosed basin of planetary scale bounded by two parallel meridians. The equations of the model closely correspond to the complete Navier- Stokes equations with viscosity and conductivity terms replaced by equivalent terms representing the effects of small-scale diffusion of momentum and heat, respectively. For the case of no wind, scale analysis suggests that the total poleward heat transport in the basin should be proportional to

$$\kappa L^2 \Delta\theta^*/d$$

where κ is the diffusion coefficient in the vertical, $\Delta\theta^*/L$ is the north-south temperature gradient imposed at the air-sea interface, and d is the scale depth of the thermocline. The constant of proportionality obtained by the numerical calculations is consistent with estimates of poleward heat transport based on the heat balance method, and empirical determinations of κ.

INTRODUCTION

An essential factor in determining the climate of the temperate zone of the Northern Hemisphere is a strong transfer of heat from the ocean to the atmosphere during the autumn and winter. Part of this heat (roughly half in the North Atlantic) has been received by the ocean during the previous spring and summer. The remainder is supplied by the lateral transfer of heat by ocean currents from other areas which receive a net surplus of heat on an annual basis. Detailed studies of the heat balance of the ocean offer one means of making a quantitative estimate of heat transfer. In Figure 1 estimates of the poleward transport of heat based on heat balance maps of Sverdrup (1957), Budyko (1956), and Albrecht (1960) are compared with direct measurements of energy transport in the atmosphere made by Starr and White (1954). Many features of the estimates in Figure 1 differ, but there is general agreement that a significant poleward transport of heat does occur in the Northern Hemisphere, the greater part of which takes place in the North Atlantic. A discussion of these estimates is given in an earlier paper (Bryan, 1962).

Most of the present-day knowledge of ocean circulation is based on detailed measurements of temperature and chemical properties. While this data is very important in tracing the origin and movement of water masses, it is difficult to use it directly in studying heat transfer by ocean currents. Mathematical models are needed to relate ideas gained from water mass analysis to the heat balance of the ocean and large-scale interaction with the atmosphere.

Recently, considerable attention has been devoted to the problem of the maintenance of the oceanic thermocline (Robinson and Stommel, 1959, Welander, 1959, Stommel and Webster, 1962, Blandford, 1965). These studies are directly relevant, since they deal principally with the manner in which heat is transferred from the surface to lower levels in the ocean. The steady-state solutions of the thermocline theories are intended to apply to the subtropical region of ocean basins, away from strong boundary currents. A disadvantage of these solutions is that they cannot easily be extended to include subarctic gyres and boundary regions. In particular, difficulties exist in treating regions in which the stratification is unstable, or nearly so.

These thermocline investigations form the point of departure for the present study. Solutions for an entire closed basin are obtained by numerical methods. To include regions in which convection may ocur, the vertical heat diffusion coefficient is a constant as in the model of Robinson and Stommel (1959). For unstable stratification this coefficient is effectively infinite. Since small, but significant departures from geostrophy exist in strong currents near lateral boundaries, the model includes the momentum equations in nearly complete form, without the geostrophic approximation.

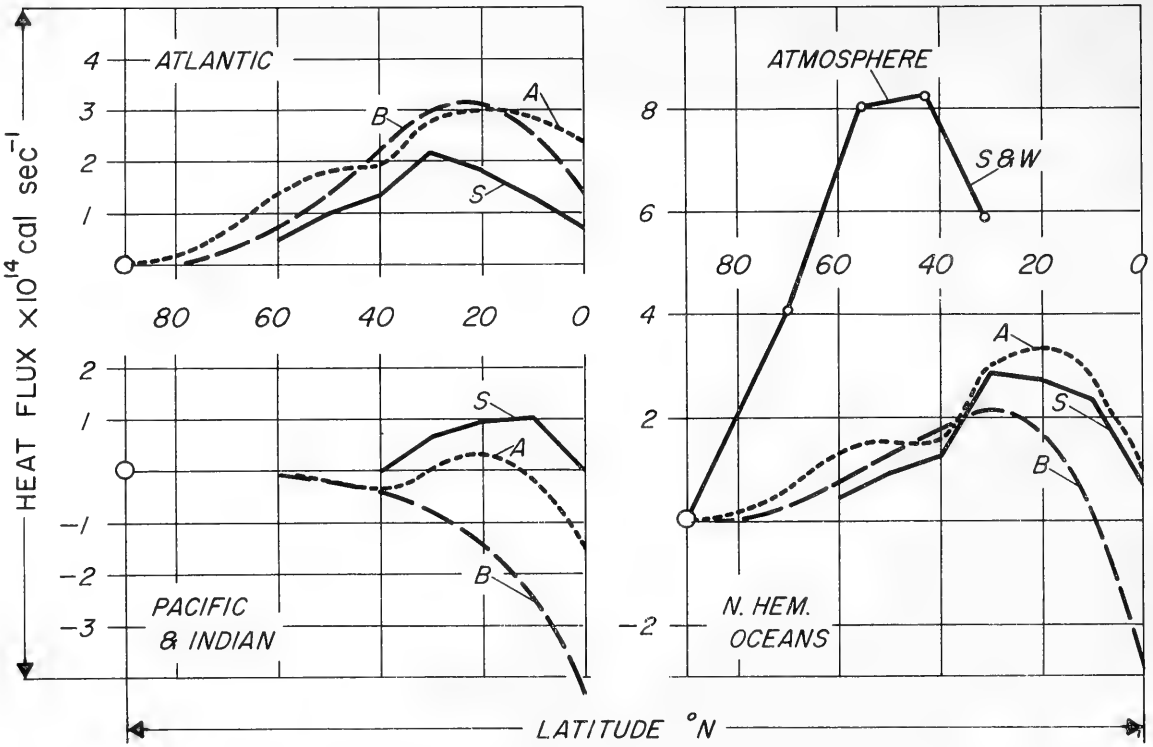

Figure 1. Northward heat transfer calculated by the heat balance method. A, B and S indicate Albrecht (1960), Budyko (1956) and Sverdrup (1957), respectively. S and W indicate Starr and White (1954).

The density anomaly of sea water is due to the distribution of both salinity and temperature. Source or sink regions at the ocean surface for salinity coincide with areas in which evaporation exceeds precipitation or vice versa. With exceptions like the equatorial rain belt, the surface of tropical oceans is a source region of both heat and salinity. On the other hand, cooling and an excess of precipitation make the ocean surface in subarctic areas a sink of both heat and salinity. To simplify the formulation of the present study of large-scale heat transfer by ocean currents it will be assumed that the boundary conditions of temperature and salinity have the same dependence on latitude and are independent of longitude. Neglecting second order terms the equation of state of the model is given as,

$$\rho = \rho_o[\, 1 - \alpha(T - T_o) + \sigma(S - S_o)]$$

where α and σ are the respective expansion coefficients for temperature, T, and salinity, S. Since T and S obey the same type of conservation law, and the boundary conditions are proportional, the two variables are no longer independent. A virtual temperature (Fofonoff, 1962) may be defined as

$$\theta = T - T_o - \frac{\sigma}{\alpha}(S - S_o)$$

The single variable, θ, then combines the effect of both T and S on the density field.

EQUATIONS OF THE MODEL

The basic equations are taken to be the Navier-Stokes equations, written for a Mercator projection in a rotating frame with the following assumptions: a) hydrostatic balance, b) variations in density neglected except where they appear as a coefficient of g (the gravitational acceleration), c) viscosity and conductivity are replaced by simplified terms representing the diffusion of momentum and heat by smaller scale transient disturbances.

Let $m = \sec \phi$

$n = \sin \phi$

where ϕ is the latitude. If λ is the longitude, and a the radius of the globe, x and y coordinates are defined as follows:

$$dx = a\,d\lambda$$

$$dy = a\,m\,d\phi$$

A and χ are respectively the eddy diffusion coefficients in the horizontal and vertical.

With this notation the equations of motion and continuity are:

$$u_T + muu_x + mvu_y + wu_z - 2n(\Omega + \frac{um}{a})v = -m(P/\rho_o)_x + \kappa u_{zz} + Am^2\nabla^2 u \qquad (1)$$

$$v_T + muv_x + mvv_y + wv_z + 2n(\Omega + \frac{um}{a})u = -m(P/\rho_o)_y + \kappa v_{zz} + Am^2\nabla^2 v \qquad (2)$$

$$g\rho/\rho_o = -(P/\rho_o)_z \qquad (3)$$

$$w_z = -m^2[(u/m)_x + (v/m)_y] \qquad (4)$$

The simplified equation of state used in these computations is then

$$\rho = \rho_o(1 - \alpha\theta)$$

The conservation equation for temperature is

$$\theta_t + mu\theta_x + mv\theta_y + w\theta_z = \frac{\kappa}{\delta}\theta_{zz} + Am^2\nabla^2\theta \qquad (5)$$

In (5), δ is

$$\delta = \begin{cases} 0 & \theta_z < 0 \\ 1 & \theta_z > 0 \end{cases}$$

indicating that for stable stratification the vertical mixing is a constant but for unstable cases effectively infinite.

The boundary conditions are the appropriate ones for a basin bounded on the east and west by two meridions one radian of longitude apart. To the north and south the basin is bounded by two parallels of latitude one radian of latitude apart. The south wall is placed 10^o of latitude away from the equator. Let x, y, z be the three coordinates of an interior point of the basin. Then

$$0 < x < X$$
$$0 < y < Y$$
$$-D < z < 0$$

The boundary conditions on temperature are such that no heat is diffused through the lateral walls or the ocean bottom.

$$\theta_x = 0 \qquad x = 0, X$$
$$\theta_y = 0 \qquad y = 0, Y$$
$$\theta_z = 0 \qquad z = -D$$

Temperature is prescribed at the upper surface as a linear function of latitude. Let $\Delta\theta^*$ be a scale temperature.

$$\theta(\phi) = \Delta\theta^*[\, 1 - (\phi - \phi_o)/\,(\phi_Y - \phi_o)], \qquad z = 0.$$

The boundary conditions on velocity in this preliminary investigation filter out external gravity waves, and eliminate any stresses acting at the bottom or at the upper surface.

$$w = u_z = v_z = 0 \qquad z = 0, -D.$$

Both the normal and the parallel components of velocity vanish at the lateral boundaries.

$$u = v = 0 \qquad \begin{matrix} x = 0, X \\ y = 0, Y \end{matrix}$$

Equations (1) - (5) are solved by finite differencing using a grid of 19 x 19 points with 6 levels in the vertical. In some cases a more refined net was used close to the western boundary to obtain a better resolution of the boundary current. The numerical scheme is based on ideas proposed by Arakawa[1/] and Lilly (1965). Details of the numerical method will be published in a separate paper.

RESULTS

In laboratory studies of hydrodynamic models scale analysis is an essential tool. It is also useful in a numerical study to isolate the important variables and eliminate redundant calculations. Following ideas proposed by Robinson (1960), a scale velocity, V*, and a scale depth of the thermocline may be defined in the following way. In terms of a geostrophic balance between the vertical variation of velocity and the horizontal temperature gradient,

$$2\,\Omega\, V^*/d = g\,\alpha\,\Delta\theta^*/L$$

The requirement that the vertical diffusion of heat be of the same order as the horizontal advection of heat may be expressed as,

$$V^*\,\Delta\theta^*/L = \kappa\Delta\theta^*/d^2$$

1/ Arakawa, "Computational Design for Long Numerical Integrations of the Equations for Atmospheric Motion," paper presented at the 44th Annual Meeting, A. G. U., Washington, April 1963.

A definition of V* and d may be obtained by combining these two relationships.

Scale analysis indicates that there are only three completely independent variables in the problem. A convenient formulation of these three dimensionless variables is given below. An estimate of their approximate magnitude in the case of the real ocean is also indicated.

$$R_1 = V^*D^2/(\kappa L) \qquad \sim 100$$

$$R_e = V^*L/A \qquad \sim 10 - 1000$$

$$R_o = V^*/2\Omega L \qquad \sim 10^{-5}$$

R_1 and R_e may be considered effective Reynolds numbers for the vertical and horizontal, respectively. R_o is a Rossby number. The estimate of the magnitude of the Rossby number is for the ocean interior. Much larger values would be appropriate for the type of flow in the western boundary current.

A useful nondimensional form of the total poleward heat transport in the basin is obtained by normalizing the calculated northward flux with the amount of heat transferred down to greater depths from over an area, L^2, through a vertical temperature gradient of $\Delta\theta^*/d$.

$$H/H^* = \frac{\text{Poleward Heat Flux}}{\kappa L^2 \, \Delta\theta^*/d}$$

From general considerations

$$H/H^* = F\,(R_1, R_e, R_o, t)$$

Numerical integrations of the model were performed to determine F as a function of the independent parameters for which the model ocean settled down to an equilibrium state.

In most cases the initial conditions are a state of uniform stratification and no motion. When a north-south density gradient is imposed through the surface boundary condition, convection takes place in the northern part of the basin. This in turn leads to the buildup of horizontal density gradients in the main body of the fluid. As the parameter, R_e, is increased, the effective horizontal mixing decreases. This allows an increasingly complex flow pattern to form. To resolve these complex patterns a detailed numerical grid and a large amount of calculation are necessary. The calculations of this study are therefore restricted to cases in which $R_e < 36$. Within this range an equilibrium is usually obtained after a numerical integration over the equivalent of a decade.

The behavior of the heat transport as a function of time is shown in Figure 2 for four different cases. These calculations show the effect of a four-fold change in the Rossby number with the other parameters kept

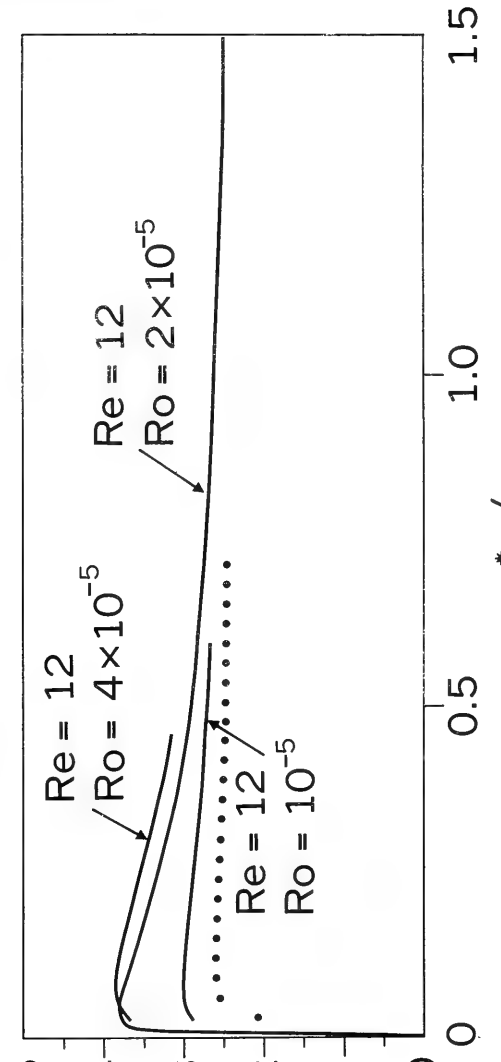

Figure 2. Nondimensional heat transport as a function of time. The solid curves are for $R_1 = 1000$. The dotted curve is for $R_o = 2 \times 10^{-5}$ and $R_1 = 100$.

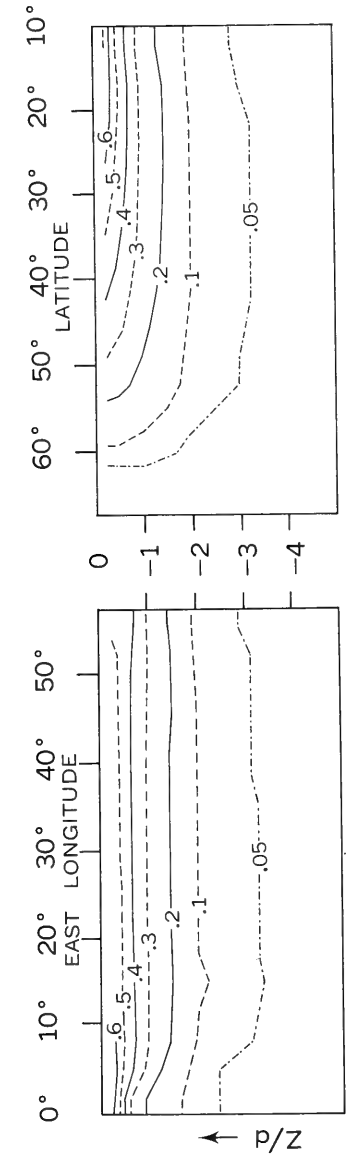

Figure 3. Temperature sections in the zonal plane at $\phi = 35°$ (left), and the meridional plane at $\lambda = 27°$ (right). For $\Delta\theta^* = 18°$, $\alpha = 2.5 \times 10^{-4}$ Deg.$^{-1}$, and $\kappa = 5$ cm^2/s. The scale depth, d, is 400 meters.

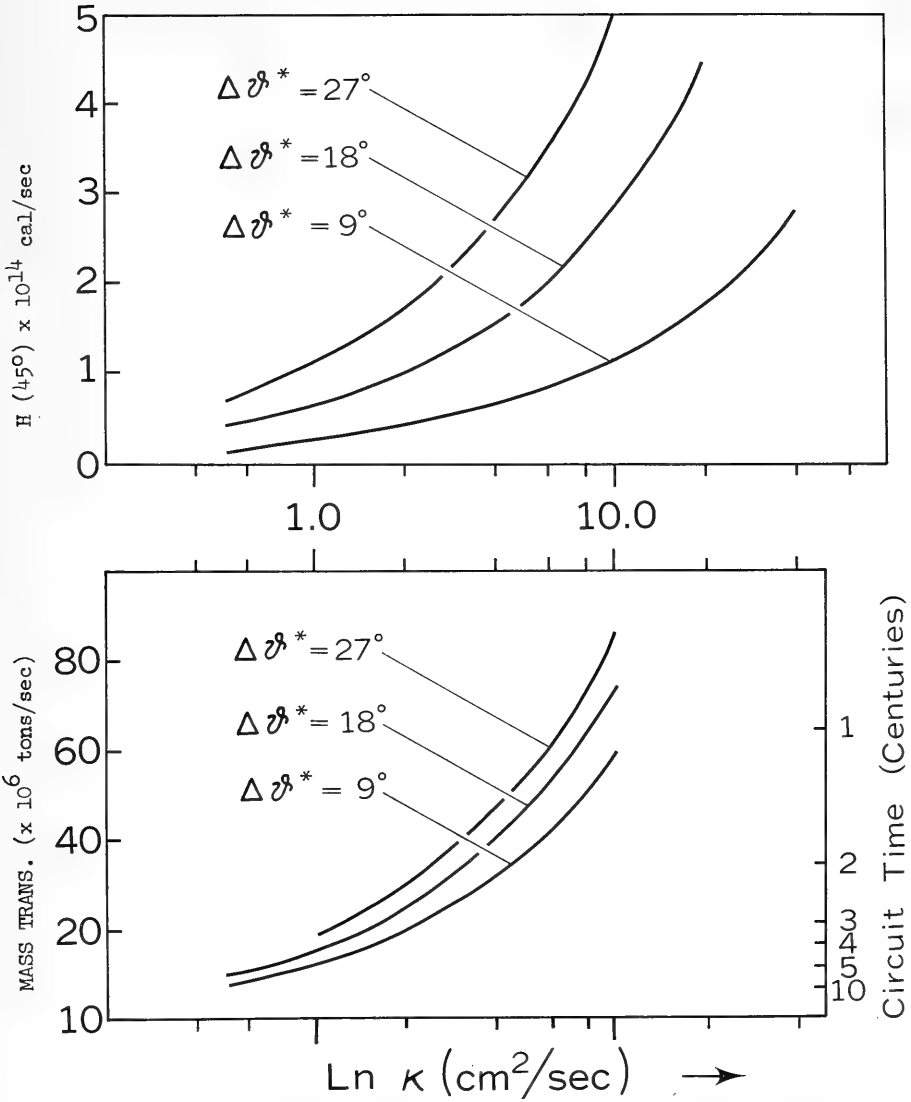

Figure 4. Above: Poleward heat transport estimated from the formula $H = .2H^*$, as a function of $\Delta\theta^*$ and κ. Below: The associated strength of the thermohaline circulation.

constant. For a value of κ equal to 5 cm^2/s the change in Rossby number would correspond to a change in the north-south temperature contrast from 9^o to 36^o. Note that this large change does not appear to have a correspondingly large effect on the nondimensional heat transport. The three solid curves in Figure 2 are for the cases in which R_1 is equal to 1000. The dotted curve represents a single test calculation made for R_o equal to 2×10^{-5} and R_1 equal to 100. The total depth, D, appears only in R_1. The test calculation shows that beyond a certain point, the purely thermal solution is insensitive to the total depth. A similar result has been obtained previously in the thermocline calculations of Stommel and Webster (1962).

Figure 3 shows vertical sections made for a zonal and meridional plane cutting the basin. The temperature has been normalized by dividing it by $\Delta\theta^*$. Note that the isotherms are fairly flat over most of the basin. Exceptions occur near the western boundary in a narrow zone, and in the northern part of the basin. The upturned isotherms near the western wall are associated with an intense, northward moving boundary current. A much slower, but deeper compensating current moving southward exists below. This western boundary current differs from that of the wind-driven ocean theories (Stommel, 1948) in that the net, vertically integrated mass transport is zero. This type of boundary current associated with the thermohaline circulation has been anticipated by Stommel (1958, page 157) in his prediction of an undercurrent in the vicinity of the Gulf Stream. Analytic solutions have been obtained only from a simplified linear model by Takano (1962).

Another set of calculations similar to those shown in Figure 2 indicate that H/H* depends markedly on the Reynolds number only in the range $0 < R_e < 10$. For larger Reynolds numbers horizontal mixing plays a rather small role in the poleward heat flux. Through an extrapolation of the results, it is estimated that the equilibrium value of H/H* for very large values of Reynolds numbers would be approximately .2, assuming that $R_1 = 100$ and the Rossby number is in the geophysical range. The oceanographic interpretation of this result is shown in Figure 4. Assuming that H/H* is 0.2, the total poleward heat flux is given as a function of the vertical diffusion coefficient, κ , and the total meridional temperature difference imposed at the surface. The Atlantic Ocean is known to have a direct thermal-haline circulation. For a rough comparison of heat transport in the model with observations we note from Figure 1 that the poleward flux at 45^o latitude in the North Atlantic is about 2×10^{14} cal/s. Allowing for the effect of salinity, a north-south virtual temperature difference of 18^oC is in best agreement with surface temperature data. From Figure 4 we see that a vertical diffusion of 5 cm^2/s would be required for the model to have a poleward heat flux of 2×10^{14} cal/s. This is a reasonable value of κ , since independent empirical estimates based on water mass analysis are all of the order of unity (Robinson and Stommel, 1959).

In the lower part of Figure 4 the strength of the thermohaline circulation is plotted, also based on an extrapolation of the numerical results to the case of very high Reynolds numbers. The total rate of overturning in

a vertical meridional plane for a temperature difference of $18^{\circ}C.$ and κ equal to 5 cm^2/s is 40 million tons/s. This is about 1/2 the observed transport of the Gulf Stream (Stommel, 1958). The average circuit time for water to sink to great depth and rise to the surface again is obtained by dividing the strength of the circulation into the volume of a basin 5 km deep. The right hand ordinate of Figure 4 indicates that the circuit time is of the order of centuries for the particular case under discussion.

Further calculations are in progress to test the effect of much larger variations in the Rossby number, and the modifications introduced by the effect of wind acting at the surface. It is hoped that such calculations will bridge the gap between theories of the thermocline and theories of purely wind-driven circulations. In principle there are no difficulties in including salinity in the model which will allow a much more realistic formulation of the boundary conditions. Robinson and Stommel (1959) have emphasized the importance of the vertical diffusion, κ, and have pointed out how little is known about the forced convection represented by this parameter. Based on the simplified density-driven model of this study, κ is shown to be the principal factor in determining the partitioning of poleward heat flux between the hydrosphere and the atmosphere.

REFERENCES

Albrecht, F. 1960 Ber. Deut. Wetterdienstes, 66, Bd. 9.

Blandford, R. 1965 J. Mar. Res. (In Press).

Bryan, K. 1962 J. Geophys. Res., 67, p. 3403.

Budyko, M. I. 1956 Atlas Teplovoga Balansa, Moscow

Fofonoff, N. 1962 The Sea, Vol I, M. N. Hill, Ed., Wiley, N. Y., London, p. 368

Lilly, D. K. 1965 Mon. Weather Rev., 93, p. 11

Robinson, A. R. and Stommel H. 1959 Tellus, 11, p. 295

Robinson, A. R. 1960 Deep-Sea Res., 6, p. 311

Starr, V. P. and White, R. M. 1954 Geophys. Res. Dir. Paper, 35, Bedford, Mass., U. S. A.

Stommel, H. 1948 Trans. Amer. Geophys. Un., 29, p. 202

1958 The Gulf Stream, Cambridge Univ. Press

Stommel, H. and Webster, J. 1962 J. Mar. Res., 20, p. 42

Sverdrup, H. U. 1947 Proc. Nat. Acad. Sci., 33, p. 318

1957 Handbuch der Physik, 48, Springer-Verlag, Berlin

Takano, K. 1962 Records Ocean. Works Japan, 6, p. 60

Welander, P. 1959 Tellus, 11, p. 309

ON THE PRESENT STATE OF KNOWLEDGE IN AIR-SEA BOUNDARY LAYER PROBLEMS

H. U. Roll
Florida State University
Department of Meteorology

INTRODUCTION

I hope that the title chosen for this talk has already indicated with sufficient clearness that I am going to deal with processes of small scale. We all are very well aware of the fact that air-sea interaction is not restricted to such small-scale processes but extends through the whole scale of motions comprising mesoscale and synoptic processes and reaching even the planetary scale by affecting the atmospheric circulation and the energy balance of the earth. Nevertheless, the limitation imposed on this lecture helps to focus our attention on the crucial region of air-sea interchange. This comparatively shallow layer with a thickness of only a few meters in air and water and characterized by vertical fluxes and energy transformations of different kinds apparently holds a key position in the interaction between the atmosphere and the ocean. All the motions and processes of other scales and related to air-sea interaction are in some way predetermined by the small-scale exchange occurring in the boundary layer air-sea. Therefore, any progress in our understanding of the interaction between ocean and atmosphere on the whole and in all its different parts cannot be accomplished without a simultaneous or preceding progress of our knowledge about the physics of this interchange in this shallow boundary layer.

This can be stated much more easily than it can be translated into action. The sea surface is distinguished from the atmospheric boundary conditions prevailing over land by very peculiar properties. On the continents, shape and size of the elements of surface roughness are clearly defined and comparatively easy to determine. Generally, their nature and locality are fixed and they neither vary with time nor do they depend strongly on atmospheric conditions. Their aerodynamics are relatively well defined and known.

Contrary to the boundary conditions found over land the surface roughness encountered at sea is composed of a great variety of moving elevations which are different in size, shape, and velocity as well as subject to continuous and irregular changes. The dimensions, the spatial distribution, and the temporal variations of the ocean waves are governed by statistical laws wherein the character and speed of the air flow play a decisive role. Moreover, the wind generates orbital motion and drift current in the sea and it is quite obvious that these water movements will react on the air flow. With increasing wind speed, the formation of foam and spray, which implies a disintegration of the sea surface, affects large areas and extends to a certain height, thus creating a transition zone between air and sea. Therefore we must realize that the boundary region between air and sea is an extremely variable, ill-defined, and hardly accessible zone where the coupling between atmosphere and ocean occurs in a very complicated manner.

These dynamic properties of the sea surface considerably increase the difficulties inherent in any investigation concerned with the mechanism of the air-sea boundary layer.

With a view to this severe handicap it is only of little comfort that, on the other hand, the sea surface also has a few pleasant properties. The local differences, which are most prominent over land, are substantially reduced on the oceans, these being much more uniform in this respect than the continents are. Their capability of acting as sources or sinks for heat and moisture shows but little variation from one place to another. For example, it has been recently reported by Brocks (1963) that, in the southern part of the North Sea, the correlation between simultaneous measurements of air temperature as well as between that of humidity or wind speed executed within a sea area of at least 25 nautical miles was found to range mostly between 0.9 and 1.0, which proves the high degree of spatial homogeneity at least for this area. Further, since the diurnal and annual variations are much smaller than those on land, there is also a pronounced uniformity in time at sea. Thus, in some respect, the oceans offer an ideal field for meteorological investigation provided that it is possible to overcome the experimental and theoretical difficulties mentioned before.

Every review must have a certain reference level from where it starts, i.e. a certain amount of knowledge which can be taken for granted, since it is impossible to give a complete treatment within a rather short time. Such a reference level can best be provided by a suitable publication. I am in the happy position of being able to make reference to two excellent reviews on our present subject. The first, given by E. L. Deacon and E. K. Webb (1962) provides a very concise and still detailed treatment of small-scale interactions air-sea. The viewpoint of the second review, which has been elaborated by 8 distinguished scientists (Benton et al., 1962) is more general, its main object obviously being to put the finger in the wound of insufficient knowledge and to show what should be done about it.

I shall take these two publications as a base for my discussion assuming that the state of affairs as it is reported therein is more or less known to the audience.

The interchange occurring in the boundary layer air-sea is manifold. When attempting to treat it systematically we may perhaps make a subdivision by separating

the exchange of energy from

the exchange of matter and from

the exchange of electrical charge.

Although the transfer of matter and of electrical charge through the boundary layer certainly has interesting or even fascinating aspects, I would rather like to confine my discussion to the exchange of energy thereby including the exchange of water which, owing to the latent heat of vaporization, must be considered as a - quite important - part of the energy transfer.

Primarily, there are four ways in which energy can be exchanged between the oceans and the atmosphere:

(1) by the transfer of momentum,

(2) by the radiative interaction,

(3) by conduction and convection of sensible heat, and

(4) by molecular and turbulent transport of latent heat in the form of water vapor.

I would like to deal with these different kinds of energy exchange in the order indicated above. When doing so I should emphasize that a complete review cannot be expected, because here in Tallahassee I do not have at hand my extensive and detailed file of references which, of course, I could not bring with me. Therefore, my presentation is certainly biased by a fair amount of randomness as far as the literature reported is concerned.

THE TRANSFER OF MOMENTUM

With a view to the well-known irregularity of motion near and at the sea surface our final aim must be to get a complete time record of the field of motion both in air and in water as well as of the distribution of pressure and stress in the marine boundary layer. These time records must show as high an amount of temporal resolution and must also be as long as would be necessary in order to allow (1) a spectral analysis of all fluctuations which may contribute to the transfer of momentum and (2) a reliable estimate of the vertical momentum flux. Further, a time record taken at only one point would certainly not be sufficient but must be supplemented by others taken nearby or by some suitable device which provides information about the spatial properties of the flow. On the base of such empirical information and using sound physical principles, theory must try to develop suitable models which can be applied for predicting purposes.

Looking first at some empirical evidence on the instantaneous wind field around moving ocean waves we can hardly see anything at all. The only measurements, which came to my knowledge and which at least supply a certain part of the information wanted, are those published by Pond, Stewart, and Burling (1963) and the - still unpublished - results obtained by Brocks and Hasse (1963).

Pond, Stewart, and Burling measured turbulence spectra of the "downstream" component of the wind over waves of approximately 30 cm height using a hot-wire anemometer. The probe was mounted at 1 to 2 m above the water level, at which height the mean wind speed was about 3 m/sec. No indication is given as to whether the measuring site was close to the shore or well on the open sea. But the smallness of the wave heights mentioned

therein leads us to believe that the anemometer was mounted on a fixed construction near the shore. The result obtained was presented in the form of a one-dimensional energy spectrum (Figure 1) giving the energy of the

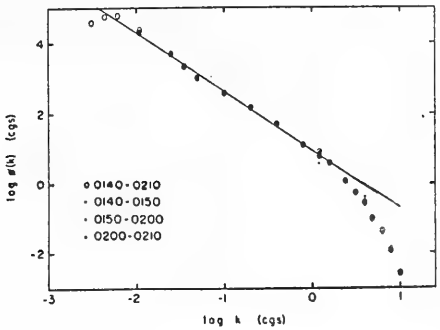

Figure 1. Energy spectra of the downstream component of the wind velocity fluctuation at a height of 1 to 2 m above the sea surface as a function of the wave number $k = 2\pi f/u$. Log-log plot. The run of 30 min. duration is broken down into subsections of 10 min. each to show the steadiness of the spectra. The straight line has a slope of -5/3 (from Pond, Stewart, and Burling, 1963).

---

fluctuations in the downstream wind component as a function of wave number k where

$$k = 2\pi f/u . \qquad (f = \text{frequency of fluctuations, } u = \text{mean wind speed})$$

The straight line corresponds to Kolmogoroff's theory of local isotropy and - in the double-logarithmic graph - has a slope of -5/3 which says that spectral energy density function goes with the -5/3 power of the wave number. As it can be taken from the graph, the results provide further support for Kolmogoroff's contention that there exists a universal form to the high number part of the spectrum of high Reynolds number turbulence.

A similar - as yet unpublished - result has kindly been communicated to me by Brock and Hasse (1963) who recorded the horizontal and vertical components of the wind speed and the air temperature as well. These measurements were made by means of a buoy (Figure 2) carrying a stabilized mast on which hot-wire anemometers and platinum resistance thermometers as well as vertical accelerometer were mounted. The measuring site was well away from land and - owing to the distance between buoy and research

Figure 2. Buoy with gyro-stabilized mast carrying sensors for recording the fluctuations in horizontal and vertical wind components and in air temperature. In the foreground: small buoy for recording the wind speed close to the sea surface. In the background: research vessel "Hermann Wattenberg" of the Oceanographic Institute at Kiel University connected by floating cable with the buoy. (By courtesy of Dr. K. Brocks.)

---

ship being about 250 m - also any disturbing influence from the ship was avoided. Brocks and Hasse computed variance spectra for the horizontal and vertical wind components and for the air temperature which again seem to support Kolmogoroff's -5/3 power relationship, apart from some deviations in the wind fluctuations at frequencies of 0.3 to 0.4 c/sec, which certainly originate from sea waves. Their results are reproduced in Figure 3 where the products of spectral intensity and frequency are plotted as functions of the spectral frequency f for the horizontal and vertical wind components u, w, for the air temperature θ as well as for the covariances $u'w'$ and $\theta'w'$.

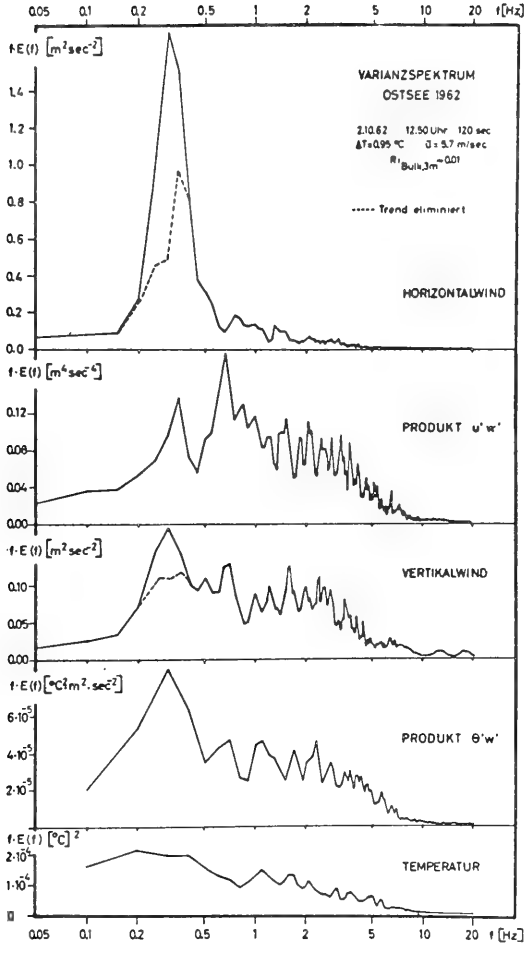

Figure 3. Variance spectra of horizontal wind component u,

covariance u'w'
vertical wind component w,
covariance θ'w'
air temperature θ .

The products of spectral intensities and frequency f are plotted versus spectral frequency f (Hz = c/sec). (By courtesy of Dr. K. Brocks.)

So far this is all that has come to my notice about measurements of the instantaneous wind field around ocean waves. The spectral analysis seems to be a suitable method of representing and studying such very irregular motions. However, I would wish that it may not only be applied to the wind field over the sea but also to the wave motion at and - if possible - below the sea surface. Simultaneously taken records of this sort would yield highly useful information on the mechanical interaction between air and sea, in particular if the measurements of the motion in both media were supplemented by records of the pressure distribution and its fluctuations. Apparently, plans and preparations for such an approach as well as preliminary field tests are being made at the University of British Columbia, Vancouver (Stewart and Burling, 1964).

Certainly the whole problem is easier to tackle by laboratory measurements, although the result obtained there may not always be meaningful with respect to open-sea conditions. One interesting paper of this kind has recently been published by Schooley (1963) who tried to measure the wind field above wind-generated water waves in a short tunnel by photographing the tracks of neutrally buoyant soap bubbles. The data could be summarized in form of vertical wind profiles (Figure 4) above certain points

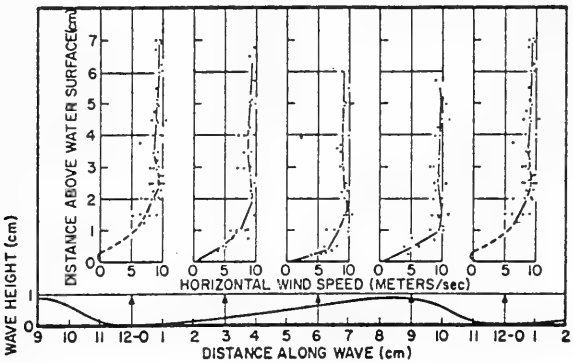

Figure 4. Vertical wind profiles above four different points along a water wave in a wind-water tunnel (from Schooley, 1963).

along the wave profile and show the expected strong increase of wind speed with height above the crest region as well as the less steep gradient above the trough. I said "expected" because a similar result had been obtained three decades ago by Motzfeld (1937) who investigated the air flow over a wavy

but solid wall in the institute of Prandtl. According to Schooley's findings (Figure 5) the flow has a maximum speed which occurs at about 1.5 to 2.5 cm above the water surface. This "jet" effect, as it is called by Schooley, points to a systematic deviation from the log-profile at a level of about 1.5 to 2.5 wave heights above the surface. This could be of importance as will be explained later.

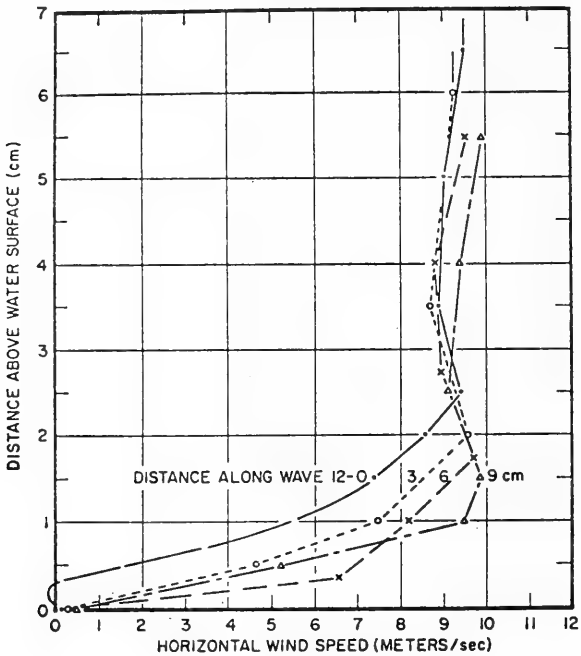

Figure 5. Vertical wind profiles above four different points along a water wave showing a maximum velocity just above the boundary layer. (from Schooley, 1963)

On the whole, laboratory measurements seem to be very promising, in particular for developing and checking theoretical models. I have been told that a study on the instantaneous wind field around moving water waves is being made at the National Center for Atmospheric Research by means of a rather sophisticated equipment. The results aspired to will be of great interest.

As long as measurements of the instantaneous wind field over the ocean waves are not available, the average vertical wind profile should at least furnish us some useful information which can be interpreted in the light of the turbulence theory developed and checked by means of measurements in laboratories or over land. Now a real trouble begins! I would not like to spend much time describing the observational problems, but let me only mention this: There are two possibilities of fixing the height of a certain mean wind speed:

(1) One can take the average distance from the wavy sea surface. This can be done by placing the anemometer on a fixed construction or on a floating base that does not participate substantially in the wave motion. No measurements in the wave troughs are taken in this case.

(2) The measurements are made at a point that has the same distance from the wave sea surface at any instant, i.e. the anemometer oscillates with the sea surface. This can be realized by using a float or a buoy as carrier of the instrument. In this case, measurements may include the trough region.

Up to now, it is not clear which procedure gives the better estimate of the mean wind profile. Naturally, the influences coming from the fixing of the zero level will only be significant in the immediate vicinity of the waves. Unfortunately, this is the very height range where the vertical wind profile is of particular interest and importance.

Apart from such observational difficulties, there are the problems of interpretation of the results. During the last years we were very happy that the majority of the vertical wind profiles measured showed a log-distribution which can be easily interpreted in terms of the turbulent boundary layer theory. Out of 26 studies I reviewed, 14 reported a log-profile, 3 could explain their deviations from the log-profile by the influence of thermal stratification, 3 did not say anything about it, because the wind speed was only measured at 2 levels (which certainly is the easiest way) and only 6 papers, mostly published before 1950, reported a pronounced deviation from the log-profile in the lowest levels (below 2 m). The occurrence of such a "kink" in the wind profile could, however, be explained by observational errors (determination of heights) or by disturbances originating from the carrier of the instruments, e.g. from the ship, float, etc. Thus, the validity of the log-profile appeared to be well established also for the marine boundary layer under adiabatic conditions, and many conclusions about the aerodynamic roughness and the friction coefficient of the sea surface as well as the wind stress at the sea surface were based on this fact.

Quite recently, however, some doubt has been shed on the validity of the log-profile for representing the mean vertical wind distribution over the sea. For instance, Takeda (1963) and others found a kink in the lower part of every log-profile they measured over the sea and, after having

checked every possible influence carefully, stated that this deviation was not caused by any instrumental or observational error. They were led to believe that the structure of the air flow over the undulating sea surface is different from that over land or along a solid wall. Theoretical arguments (Miles, 1957; Stewart, 1961) also suggest the existence of a critical layer in the wind profile over waves where the wind speed is equal to the phase velocity of the waves. Stewart predicts a nonturbulent, organized and wave-like motion below that level which is connected with a reduction of the turbulent stress and wind shear. At present it is yet too early to interpret the kink recently found in vertical wind profiles over the sea by referring to Miles' and Stewart's critical level. A systematic investigation of the fluctuations of flow, both immediately above the sea surface and at it, is necessary in order to bring this problem nearer to solution.

Before leaving this subject of vertical wind profiles over water let us cast a short glance at a diagram (Figure 6) which summarizes the results obtained from log-profiles by applying the turbulent boundary layer concept. Under adiabatic conditions those profiles yield corresponding values for the aerodynamic roughness z_0 and for the friction velocity u_* which is defined as the square root of the ratio surface wind stress τ_0 by air density ρ.

In the diagram z_0 is plotted as a function of u_*. We are confronted with a very confusing result, because some evidence for a decrease of z_0 with growing u_* can be found as well as some proof for its increase with growing u_* or its constancy. Thus we must state that this relationship is by no means well understood at present. Even the physical meaning of the so-called roughness parameter z_0 is obscure. In the boundary layer theory z_0 describes the scale of turbulence at the level where the mean wind speed $\bar{u}$ is equal to zero. Remember the well-known log-profile of wind speed

$$\bar{u} = \frac{u_*}{k} \ln \frac{z + z_0}{z_0} \qquad (1)$$

where $\bar{u} = 0$ for $z = 0$ and the turbulence present at this level is described by the mixing length $l = k\, z_0$ (k = von Karman constant). At sea there is, in general, no level at which the mean wind velocity $\bar{u} = 0$, since the water surface itself may move with appreciable speed (by about 4 percent of the wind speed taken at 10 m). Thus, the boundary layer model needs considerable amendment and refinement in order to be applicable to the complicated mechanism of air-sea interaction.

The results presented so far referred to the adiabatic wind profile. Regarding the wind profile under nonadiabatic stratification very little evidence is available from the sea which can be compared with the theoretical approaches given by Monin and Obukhov (1954), Ellison (1957), Yamamoto (1959), and Panofsky, Blackadar and McVehil (1960). The reason for this is that, in order to be able to apply these theories, data on the vertical heat flux are needed apart from the simultaneous measurement of the vertical momentum flux and wind profile. It is very difficult to get reliable information

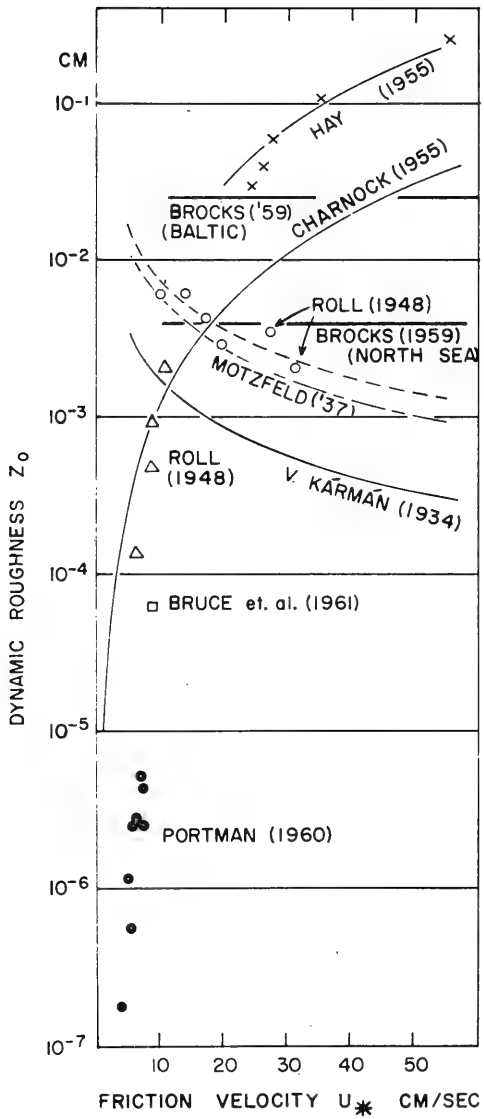

Figure 6. Dynamic roughness z_0 of the sea surface as a function of friction velocity u_*. Summarizing graph.

about these quantities over the sea. The small amount of information available seems to indicate that at sea the influence of thermal stratification on the wind profile can be taken into account in the same manner as this is done over land (Deacon, 1962).

In this connection the following seems to be important: The stability of the air above the sea does not only depend on the vertical temperature distribution. It is determined by the vertical variation of density, i.e. there may be an effect of the humidity gradient also. Kraus (1964) has drawn our attention to the fact that a strong humidity decrease with height in the lowest layer above the sea may even be sufficient to reverse the stabilizing effect of a small temperature increase with height. A decrease of water vapor pressure of 5 mb would compensate a temperature increase of $0.5^{\circ}C$. Therefore, according to Kraus, this effect must be taken into account under relevant circumstances, for example, by an additional term in the Richardson number which is normally used as a measure of stability.

So far I have been talking about the wind field in the marine boundary layer. The quantity that is of most importance in the field of mechanical interaction air-sea certainly is the wind stress acting on the sea surface. Very little is known as yet about the normal wind stress, its size and spectral distribution associated with the turbulent wind blowing over the water. This lack of knowledge is regrettable, as it seems we may be sure that the atmospheric pressure fluctuations play an important part in the generation of wind waves at the sea surface. Thus, we have not been able to check the theory advanced by Phillips (1957, 1958, 1962) who considered the initial waves generated by a resonance mechanism between the surface wave modes and the random pressure fluctuation associated with the turbulent wind blowing over the water and convected by the mean flow. There is, however, some very recent empirical evidence (Snyder, 1965) by which the importance of the resonance mechanism is questioned.

The tangential wind stress, however, has been the subject of considerable number of investigations, although one cannot say that all the problems connected with it have been solved. The tangential wind stress is equivalent to the vertical transport of horizontal momentum in a viscid fluid. In the turbulent boundary layer of the atmosphere the shear stress is usually considered as constant with height. Over the sea this may not be true as we know from the theories of Miles and Stewart, but up to now the vertical constancy of the wind stress is the generally accepted practice also for the marine boundary layer. Consequently, the tangential wind stress τ observed in the boundary layer is equal to the tangential wind stress $\tau = \tau_o$ exerted by the wind on the sea surface. The latter quantity is of importance for quite a number of air-sea interaction problems, e.g. generation and growth of ocean waves, of drift currents, and storm surges.

It is customary to express the surface drag τ_o of the wind at the sea surface in terms of the mean speed $\bar{u}_{10}$ at the height 10 m

$$\tau_o = \rho C_{10} \bar{u}_{10}^2 \qquad (2)$$

the factor of proportionality C_{10} being a dimensionless height-dependent quantity, termed resistance, drag, shear-stress, or friction coefficient. The problem of determining the surface stress τ_o is then reduced to ascertaining reliable values of C_{10}.

Estimates of the drag coefficient have been based largely on indirect evidence. The following five methods have been used so far:

In air: (1) Wind profile method: Under adiabatic conditions the drag coefficient can be easily calculated from the log profile. In fact, the drag coefficient is a function of the roughness length z_o and also of the height z. With a diabatic wind profile, the additional knowledge of the vertical heat flux is necessary. So far the wind profile method was used in about 22 studies in the field and in the laboratory and supplied quite useful results.

(2) Geostrophic departure method: The covariance $-\rho\overline{u'w'}$ of the turbulent fluctuations in the horizontal and vertical wind components is recorded and supplies an estimate for the turbulent Reynolds stress. This is a rather direct approach. Unfortunately, it needs a fixed or stabilized platform as well as sensing elements of sufficiently rapid response. Therefore, we have as yet only four or five studies of this kind. The data show a considerable scatter.

In water: (3) Sea surface tilt method: If an enclosed body of water is available and the wind has blown for a sufficiently long period as to assure steady state conditions, then the surface wind stress is assumed just to balance the hydrostatic forces due to the tilt of the surface. The surface slope provides an estimate for the wind stress or the drag coefficient. Quite a number of studies (18) were made up to now, partly in the field, partly in the laboratory. The necessary accuracy (10^{-7}) could mostly not be achieved with small wind speeds. Disturbing effects as stratification in the water, horizontal density gradients, near-shore effects due to waves, nonsteady state etc., may make the result uncertain.

At the water surface: (4) Surface film method: An insoluble monolayer is applied to the water surface. Its contraction under the action of the wind provides a measure of the wind stress. This seems to be essentially a laboratory method. Only one paper (Vines, 1959) has become known so far.

I would like to present the results obtained in a somewhat condensed form by showing a diagram (Figure 7) containing all the empirical relationships suggested between C_{10} and $\bar{u}_{10}$. There is, of course, a substantial scatter in the single measurements which are not reproduced here. Looking at these different results we are in a similar position as we were before with regard to the roughness length. There is no satisfactory agreement

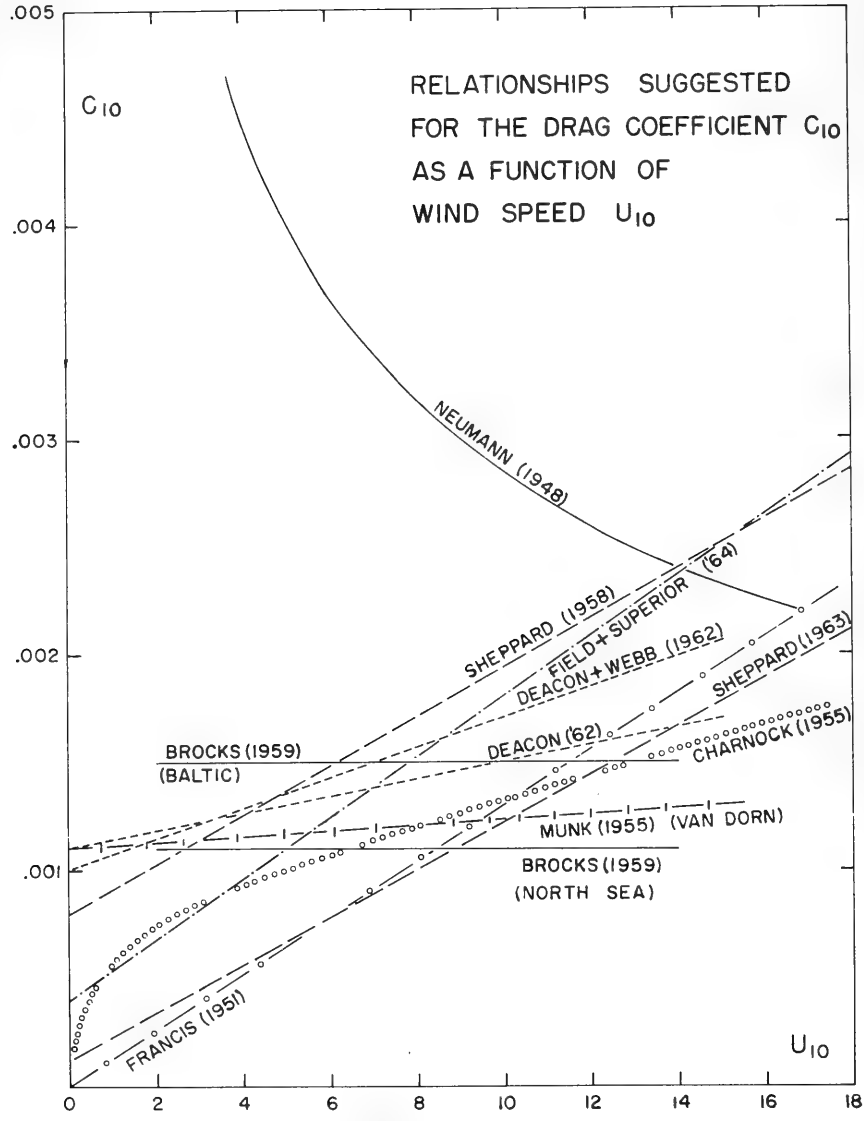

Figure 7. Relationship suggested for the drag coefficient C_{10} of the sea surface, as a function of the wind speed (at 10 m) u_{10}, in m/sec.

between the different authors and methods. The strong increase of the friction coefficient with decreasing wind speed, which characterizes Neumann's result, is now generally assumed to be biased by data of insufficent accuracy, however. Then the problem remains whether increase with growing speed or constancy is correct. During the last years, a certain tendency could be observed to diminish the slope and so to approach the contancy proposed by Brocks.

These values refer (or should refer) to adiabatic conditions. The question arises whether there is an influence of thermal stratification on the wind stress. Visual observations are in favor of such an effect. The ocean waves appear to be higher and steeper, the production of foam and spray is more intense with cold air over warm water than vice versa. Some relevant evidence was reported by Darbyshire (1955) who obtained stress coefficients that, for a given wind speed, were twice as great in unstable cases than in stable ones. More convincing measurements were reported by Garstang (1965). This stability effect can also be calculated with the help of the theories of Monin and Obukhov and of Ellison. We then may express the drag coefficient C_a at the level $z = a$ by the relation

$$C_a = \frac{k^2}{\left\{\ln\frac{a + z_o}{z_o} + \alpha\, Ri\right\}^2} \qquad (3)$$

where k is von Karman constant, α = constant (= 3.7), Ri = Richardson number.
This relationship remains to be checked by suitable measurements.

Regarding the possible influence of the fetch on the wind stress, there is no uniform result up to now. A few scientists found favorable evidence, whereas the majority could not verify such an effect. There is some reason to believe that the wind set-up measurements which indicated such an influence of fetch were biased by coastal wave effects.

The results reported so far on the variation of the drag coefficient with wind speed are empirical. There is only one theoretical approach, namely Munk's (1955) interpretation of Van Dorn's (1953) wind set-up data which is based on Jeffreys' "sheltering hypothesis." Herewith the existence of sheltered regions with eddies to the leeward of the wave crests is assumed, which implies a phase lag between the wave profile and the pressure distribution. Under the assumption that the Neumann spectrum is valid for the wave energy density Munk (1955) computed the form drag caused by a fully developed sea and found that the young high-frequency waves contribute much more to wave slope and form drag than the low-frequency waves do, which mainly determine the elevation statistics. Consequently, these low-frequency waves seem to be of little significance for the aerodynamics of the sea surface, a conclusion which confirms the findings of other scientists who were led to believe that the form drag is principally caused by the small, slowly moving ripples and wavelets. This would also explain that the drag is much less affected by limitations in fetch and duration than the wave

height, since the high-frequency waves which determine the form drag reach their final state much more rapidly than the low-frequency waves dominating the wave amplitude.

For the composite wind stress, which is composed of the tangential stress and the form drag, Munk obtained a cubic relationship with the wind speed. This would imply that the total drag coefficient increases linearly with wind speed. (The corresponding straight line is entered in Figure 7.) Thus, at least some theoretical support is provided for this kind of variation of the drag coefficient with wind speed.

On the whole, however, the state reached is far from being satisfactory. There is a distinct gap between empirical and theoretical work. On one side, theory is not yet able to interpret empirical findings sufficiently. On the other hand, theoreticians penetrate with their reasoning into regions which are not yet accessible to measuring. In the latter respect, I am thinking of quite a number of important papers concerned with the problem of wave generation (e.g. those published by Phillips (1957, 1958, 1962), Miles (1957, 1959, 1962) Hasselmann (1960), and others) which cannot be discussed here. The same is true with regard to the theoretical work recently done by Schmitz (1962) who studied the transfer of mechanical energy at the sea surface. He found for instance, that the equality of the vectors of mean flow on both sides of the sea surface is not a necessary condition (but, of course, a sufficient one) for the continuous transfer of mechanical energy, as it is usually thought. This can also be fulfilled if the mean values of flow in air and water immediately at the surface differ from each other, i.e. if the air glides over the water.

Thus, a concentrated effort, made both by experimenters and theoreticians, is needed in order to clarify the complicated process of mechanical interaction at the sea surface.

THE RADIATIVE INTERACTION

Passing now to a short treatment of the radiative processes in the marine boundary layer we enter a region which can perhaps be characterized best by the statement that here the importance of the subject is only surpassed by the imperfection and incompleteness of our knowledge about it. Although radiation forms the primary energy source of all processes in atmosphere and ocean, there is an almost complete lack of data measured in the boundary layer air-sea which however are indispensable when the radiative interaction between both media shall be studied. First we need a sufficient coverage of the oceans with climatological radiation data, but in addition to that some current information on radiation for the study of synoptic-scale processes will be necessary, because the empirical formula describing e.g. the effect of cloudiness on the different components of the radiative budget deviate substantially from each other. Laevastu (1960), has certainly taken great care in checking the diverse empirical relationships but finally it results that he gets a higher net radiation for the cloudiness of 4/10 than for a cloudless sky. This is caused by the fact that he assumes a

linear decrease of the effective back radiation with cloudiness while this decrease goes with the cube in the case of the incoming short-wave radiation. This example throws some light on the most difficult problem we are faced with: to develop formulae for the different components of the radiation balance in which the influence of cloudiness is adequately assessed. There may be some doubt about whether this will ever be possible with the present system of estimating only the amount and kind of clouds and the altitude of their base. In any case, much more routine measurements of the different components of radiation are urgently needed at sea.

Since more than 15 years ago a remarkable network of ocean weather ships has been working continuously and at fixed positions in the North Atlantic and the North Pacific Oceans. These stations have assembled an amount of meteorological data which are unique in marine meteorology. Unfortunately, radiation measurements have been included in the observational program of some of those stations but during the last years, practically since the International Geophysical Year (IGY). Now some relevant publications have come up. I would like to mention that of Ashburn (1963) which presents daily and mean monthly data on total incoming radiation from sun and sky for 2 years at the North Pacific ocean station "Papa" as well as some values of net radiation. With regard to the influence of cloudiness a new formula (the 11th as far as I can see) is offered which seems to represent the measured data better than the other ones. This is but a beginning. Many additional measurements will be necessary to determine the precision of the measurements and to develop an equation expressing the total incoming radiation received at the ocean surface as a function of the known physical variables such as cloud types, cloud thickness, solar zenith distance and albedo of the sea surface.

A more sophisticated approach regarding the influence of cloudiness was made by Lumb (1964). Using radiation measurements made on British ocean weather ships he suggested a relationship for the total incoming radiation during short periods (1 hour) depending on different cloud categories and the average solar altitude during that period.

These first results should be warmly welcomed but much more radiation measuring must be done on the oceans - both close to the sea surface and also at upper levels - before we will have sufficient evidence about the contribution of radiative fluxes to the energy balance of the atmosphere and the ocean surface and before we will arrive at a marine climatology of radiation which is based on really measured values. Certainly, the instrumental and operational difficulties are great but not insurmountable if scientists and engineers would recognize the challenge of this task. Substantial progress could then be achieved. In addition to radiometers installed on ships and buoys, such instruments could be carried by planes and satellites and thus fill the gaps between the necessarily wide network of radiation measuring stations in the marine boundary layer. Relevant investigations have already been made. I would like to refer to Clarke (1963) who presented observations of the long-wave radiative flux in the

downstream trade wind region by means of an airborne radiometer as well as to Rasool's (1964) evaluation of radiation data taken by the TIROS satellites.

SENSIBLE AND LATENT HEAT EXCHANGE

Considering the exchange of sensible and latent heat at the sea surface I think the present situation here is somewhat better than it is in the field of radiation, although it is not entirely satisfactory. The chief aim being to furnish reliable values of the turbulent fluxes of sensible and latent heat between ocean and atmosphere, we must try to derive formulae by means of which these transfer quantities can be calculated with sufficient reliability. It would be particularly welcome if such computations could be done by only using the meteorological elements which are usually measured on a routine basis at sea.

Remarkable success has already been achieved with relatively simple procedures. I am thinking of the so-called "bulk aerodynamice formulae" for the vertical fluxes of sensible and latent heat through the marine boundary layer which have been widely used, among others by Jacobs (1951) for his road-showing study on the climatology of air-sea interaction. However, these formulae are not without any problems. In addition, there are fundamental questions as e.g. the role of the molecular transport at the sea surface, the effect of sea spray, the influence of surface films, which require detailed consideration.

Let me first give a discussion of the bulk aerodynamic formulae. They are mostly derived in such a way that the ratios of the fluxes H (heat), E(evaporation), and τ (momentum) are formed

$$H/\tau = -c_p(\partial\overline{\theta}/\partial z)/(\partial\overline{u}/\partial z) \quad \text{and} \quad E/\tau = -(\partial\overline{q}/\partial z)\cdot(\partial\overline{u}/\partial z) \tag{4}$$

(c_p = spec. heat at constant pressure) which can be obtained by dividing the equations of definition of these fluxes and assuming that the turbulent exchange coefficients for momentum, heat, and moisture are equal. This is already a questionable assumption. Immediately at the sea surface, where molecular transfer comes into play, these exchange coefficients are certainly not equal. Further, the vertical gradients of mean wind speed $\overline{u}$, mean potential temperature $\overline{\theta}$ and mean specific humidity $\overline{q}$ are approximated by the vertical differences $\overline{u}$, $\Delta\overline{\theta}$, $\Delta\overline{q}$ between these meteorological quantities at a certain height and their values at the sea surface. When doing so we assume that at the sea surface the wind speed is equal to zero and the temperature and moisture of the air are determined by the temperature of the sea surface (saturation assumed). If finally the wind stress τ is replaced by the expression $\tau = \rho C_a \overline{u}_a^2$ we arrive at the bulk aerodynamic formulae

$$H = c_p\rho C_a(\overline{\theta}_o - \overline{\theta}_a)\overline{u}_a \quad \text{and} \quad E = \rho C_a(\overline{q}_o - \overline{q}_a)\overline{u}_a \tag{5}$$

where the subscripts 0 and a refer to the sea surface and the level z = a, respectively.

We see that the validity of this approach depends partly on the applicability of the drag coefficient C_a and partly on how well the vertical gradients can be approximated by the vertical differences air-sea. The first condition has already been dealt with and we are very well aware of the difficulties and limitations inherent in the C_a concept. But what is less well known, is the validity of the second assumption.

Therefore, I am going to examine this case more in detail. Some suitable diagrams have been published by Brocks (1963). Profile measurements of wind speed, air temperature, and water vapor pressure were made by means of a buoy well away from land and also without any disturbance from the accompanying vessel. The data used are averages each over a period of 15 minutes.

Figure 8 shows the vertical wind shear between the 10 m and the 1 m levels as a function of the wind speed measured at 10 m. On the whole

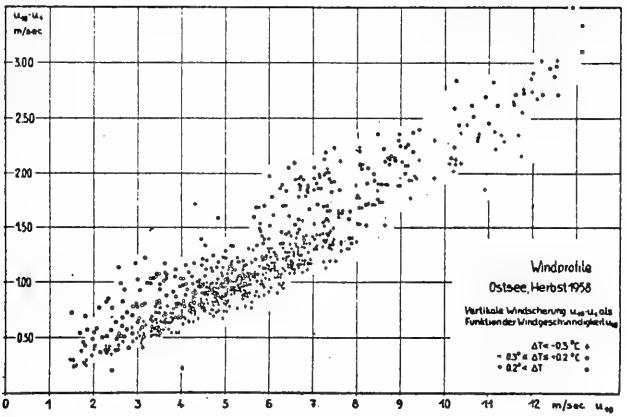

Figure 8. Vertical wind shear $u_{10}-u_1$ between the 10 m and 1 m levels as a function of wind speed u_{10} and grouped according to the temperature difference air-sea, ΔT. (from Brocks, 1963)

there is a clear relation between wind shear and wind speed but I am not sure that it is a linear one. In addition, there is also a substantial scatter caused by the thermal stratification as is indicated by the different notations. Under stable conditions, the wind shear recorded with a certain wind speed is distinctly greater than with adiabatic or unstable stratification. Thus, for the height level z = a, we may write

$$\partial\bar{u}/\partial z\Big|_a = f_1(\bar{u}_a, \Delta\bar{\theta}_a) \qquad (6)$$

if we try to be exact. Replacing the wind shear simply by the wind speed as it is usually done, would introduce an error which depends on stability. To avoid it, we must determine the function $f_1(\bar{u}_a\,\bar{\theta}_a)$.

Similar relationships can be found for the potential temperature and the humidity of the air. Figure 9 provides some evidence on the relation between temperature gradient and temperature difference air-sea. Again a definite - certainly non-linear - functional relationship is indicated,

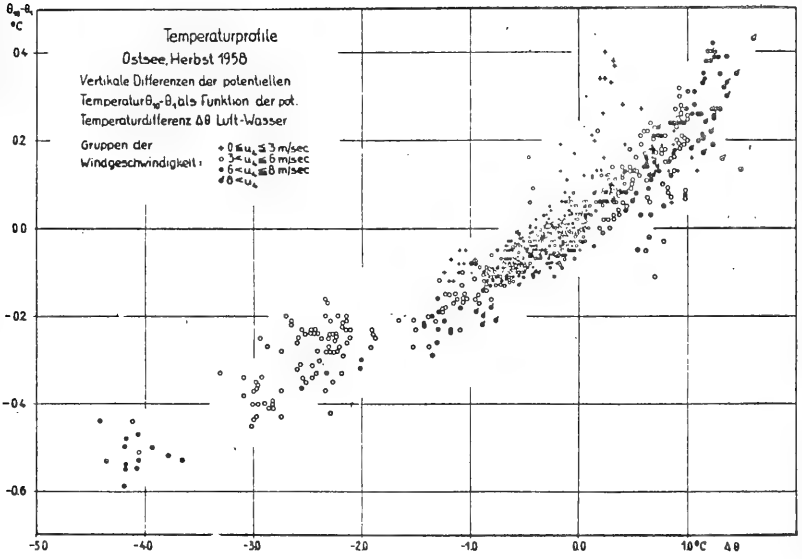

Figure 9. Vertical differences in potential air temperature $\theta_{10} - \theta_1$ between the 10 m and 1 m levels as a function of potential temperature difference air-sea $\Delta\theta$ and grouped according to the wind speed u_4 measured at 4 m height (from Brocks, 1963).

the scatter being caused by the wind speed as can be very distinctly seen in the stable region. Consequently, we would have

$$\partial\bar{\theta}/\partial z\Big|_a = f_2(\Delta\bar{\theta}_a, \bar{u}_a) \qquad (7)$$

Finally, when looking at the results obtained from vertical profiles of water vapor pressure (Figure 10) we recognize that a relation between

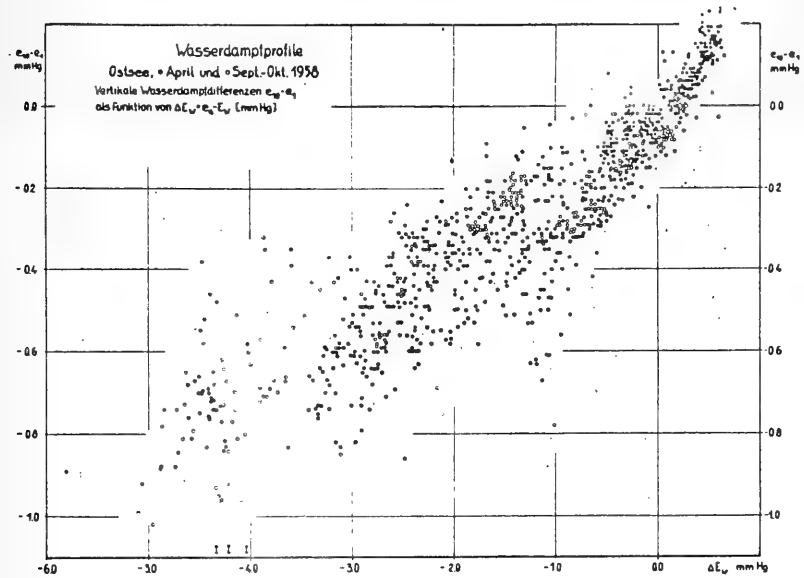

Figure 10. Vertical differences in water vapor pressure $e_{10}-e_1$ between the 10 m and 1 m levels as a function of water vapor pressure difference air-sea Δe. The results of two research trips are distinguished by different symbols (open and full circles). (from Brock, 1963)

---

gradient and difference air-sea apparently exists also here, but the scatter is rather large, because - in addition to the humidity difference air-sea - two other parameters - wind speed and stability - or dynamic and convective turbulence - determine the moisture exchange occurring in the boundary layer air-sea. In this case, we must write

$$\partial\bar{e}/\partial z\Big|_a = f_3(\Delta\bar{e}_a, \bar{u}_a, \Delta\bar{\theta}_a) \qquad (8)$$

After inserting the empirical functions f_1, f_2, f_3 into our initial equations (5) for the fluxes of sensible and latent heat we obtain

$$H = \frac{c_p \rho C_a f_2 (\Delta\bar{\theta}_a, \bar{u}_a) \bar{u}_a^2}{f_1 (\bar{u}_a, \Delta\bar{\theta}_a)}$$

$$E = \frac{\rho C_a f_3 (\Delta\bar{q}_a, \bar{u}_a, \Delta\bar{\theta}_a) \bar{u}_a^2}{f_1 (\bar{u}_a, \Delta\bar{\theta}_a)} \qquad (9)$$

These relations are considerably more complicated than the bulk aerodynamic formulae normally used and render themselves not so easily to practical application as the original relations do. They clearly show however the deficiencies inherent in the usual bulk aerodynamic approach. Even if we presume as a first approximation that the f-functions are linear in their main variable, we would not get rather much farther. Then we would have the following equations

$$H = c_p \rho C_a (\bar{\theta}_o - \bar{\theta}_a) \bar{u}_a f_4 (\bar{u}_a, \Delta\bar{\theta}_a)$$

$$E = \rho C_a (\bar{q}_o - \bar{q}_a) \bar{u}_a f_5 (\bar{u}_a, \Delta\bar{\theta}_a) \qquad (10)$$

which contain two other empirical functions and decisively differ from the original ones and from each other regarding their dependence on $\bar{u}_a$ and $\Delta\theta_a$.

Thus the bulk aerodynamic approach does no longer look as simple and as adequate for practical use as before. In order to get a quick check, let us assume that Brocks' graphs may be generally used and that further it is sufficient to approach each of them by one linear relationship in each case thus disregarding the other influences. Even with such a simplification we would obtain rather different coefficients for H and E, namely

$$H = 0.584 \quad c_p \rho C_a (\bar{\theta}_o - \bar{\theta}_a) \bar{u}_a$$

$$E = 0.841 \quad \rho C_a (\bar{q}_o - \bar{q}_a) \bar{u}_a \qquad (11)$$

This example shall only show what difficulties are implied when using the simple bulk aerodynamic formulae. Certainly, the differences mentioned

might be compensated by a proper determination of C_a. Therefore, great care should be taken in assessing a particular value of C_a separately for each of the two flux equations and for every special situation. Then a rather high accuracy can be expected from this approach as was shown by Webb (1960). Moreover, the concept of the so-called "profile coefficients" (which are simplified forms of the functions f_1, f_2, f_3) may be used here with some success.

After this critical treatment of the bulk aerodynamic approach let me pass to some problems occurring immediately at the sea surface. While the molecular viscosity does not play a decisive part, if any, in the exchange of momentum at the sea surface, things seem to be different with the transfer of heat and moisture. The momentum exchange is brought about by pressure forces acting on the roughness elements. However, this model cannot be applied to the exchange of sensible and latent heat, because, in this case, there is no equivalent to the pressure exerted on the waves.

Thus we are led to believe that the final exchange of heat and moisture between air and sea can only be effected by molecular processes. Consequently, an adequate representation of evaporation and heat transfer must include the molecular coefficients of conductivity and diffusivity. A suitable approach has been described by Sheppard (1958) who, in the basic exchange formulae, simply added the molecular constant ν_c and D to the turbulent coefficients, K_H and K_E.

$$H = - c_p \rho (K_H + \nu_c) \frac{\partial \bar{\theta}}{\partial z}$$

$$E = - \rho (K_E + D) \frac{\partial \bar{q}}{\partial z} \qquad (12)$$

Thus, there is no longer assumed a distinct layer of exclusively molecular transfer; molecular and turbulent exchanges are rather supposed to exist simultaneously. Since the turbulent coefficients decrease when the boundary is approached, the molecular constants will become important very close to the sea surface. I used this model with fair success for the computation of marine evaporation on the basis of profile data measured close to the sea surface.

Another phenomenon which is connected with the sea surface is the existence of the so-called "cool skin," i.e., a very shallow surface layer where the water temperature is about 0.5° C lower than measured with conventional methods which refer to a deeper layer. This cool skin, which originates from evaporation, may be of importance for the thermal intercourse between air and sea, since it is the actual sea surface temperature that determines the character of the convective and turbulent motions in the marine atmosphere. The observational evidence - given in part by small sensing elements, in part by radiometers which, depending on their optical properties, measure the water temperature of the uppermost layer of, say

1/10 mm - is somewhat varying. This may be explained by variable surface film effects. It is well-known that surface films, i.e. monomolecular layers consisting of organic matter or originating from artificial contamination can be found on the sea surface rather often. The transport of water through a compressed and, therefore, oriented monolayer is not an ordinary diffusion process which involves a small energy barrier but is to be considered as a process in which the water molecule must pass along a molecular pathway between long molecule chains, thus requiring a substantially higher amount of energy (La Mer, 1962). Consequently, a compressed monolayer results in a retardation of evaporation. Laboratory studies have shown (Haussler, 1955-56) that a cool skin does not occur in the presence of an oil film, which prevents evaporation but does not impede the transfer of heat. Thus it seems clear that the cool skin is actually due to evaporation and that it will only exist on those parts of the sea surface which are not covered by a monolayer. Hasse's (1963) paper provides further evidence for this.

Quite recently it has been reported (Jarvis, 1963) that monomolecular films not only retard evaporation but will also change the temperature of the sea surface, because of the effect of the film on the convective movement of surface water. The surface is constrained by such a film, convection is found to be inhibited with a consequent thickening of the surface layer and a rise of the surface temperature which is said to be quite independent of any reduction of evaporation.

Field measurements indicating the reduction of evaporation by natural surface films have been reported by Deardorff (1961). He compared the evaporation rates of two pans floating at the sea surface. One of these pans was filled with subsurface sea water while special care was taken in filling the second so that any surface film, which might have been present, would have been retained. The result showed a distinct reduction of evaporation, of the order of 20 percent, which was obviously caused by natural surface films. This surface film effect adds another item to the substantial list of difficulties encountered when trying to measure marine evaporation.

Only very little is known about the effect that sea spray might exert on evaporation, apart from that this influence must be present at higher wind velocities. It is indeed very difficult to get any quantitative information on this subject because field measurements of evaporation taken at the sea surface can only be made with light winds where there is no appreciable sea spray and, on the other hand, the problem seems hardly approachable by means of theoretical studies. Perhaps, quantitative information can best be expected from laboratory work. Relevant studies have been carried out by Okuda and Hayami (1959) in a wind-water channel of about 20 m in length. They observed the vertical distribution of the horizontal transport by sprayed water drops and found that the water transport by spray at 10 cm height was negligible below 10 m/sec wind speed but increased rapidly in the wind speed range of 12-13 m/sec. A strong decrease is found with height, the water transport by spray at 30 cm being only about 10 percent of its value observed at 10 cm height. The influence of sea spray on the

vertical moisture transport was studied in terms of the so-called "profile coefficient," a number which is proportional to this exchange. As is shown in Figure 11, a distinct increase of this profile coefficient is observed for wind speed about 15 m/sec which is accompanied by a corresponding increase of evaporation.

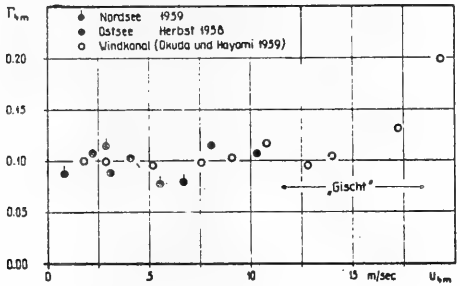

Figure 11. Profile coefficients Γ_e of water vapor pressure at 4 m height as a function of the wind speed u_4 measured at 4 m.
Full circles: Open sea (Brocks, 1959)
Open circles: Wind-water tunnel (Okuda and Hayami, 1959). (from Brocks, 1963)

Of course, it would be very welcome to get some evidence on the sea spray effect provided also by measurements in the field. Such measurements are of interest not only because of the expected effect of sea spray on the evaporation and vertical moisture transport, but also because it has been suggested that the larger droplets ejected from the sea surface will be accelerated by the wind and thereafter, when falling back into the sea, may contribute to the downward transport of horizontal momentum, i.e. to the wind stress acting on the sea surface. Relevant measurements have been undertaken quite recently during the Aruba Expedition of the Woods Hole Oceanographic Institution under the supervision of E. B. Kraus (1964). A second expedition is now under way. There is some hope that some useful results will be brought out with regard to the almost unknown effect of sea spray.

After the critical remarks I made with regard to the bulk aerodynamic method some suggestions would perhaps have been appropriate on how the vertical fluxes of sensible and latent heat could be estimated better. Certainly, there are methods that can be applied with considerably higher reliability, but they require a much greater instrumental expenditure. Measuring the fluctuations would be the most direct approach but also

profile measurements (at three levels) would furnish acceptable values. Finally, if these two possibilities cannot be used, some help can be expected from those "profile coefficients" which enter the refined bulk aerodynamic equations and which can be obtained from some general tabulations if wind speed and stability are known. It is, however, not possible here to give more details on these procedures.

CONCLUDING REMARKS

If some final conclusion shall be drawn after reviewing the present state of our knowledge on the physical exchange processes occurring at the sea surface, then it should perhaps be concerned with the question whether the relationships available at present for computing the vertical fluxes of momentum, heat, and moisture passing through the boundary layer air-sea might be serviceable and reliable enough for calculating these fluxes for large sea areas on a routine basis so that synoptic charts of air-sea exchange can be drawn in order to supply the necessary data for diverse meteorological and oceanographic forecasting purposes.

The bulk aerodynamic equations certainly are easy to apply, and their application can be based on such data as are normally available from the sea at present. But it seems questionable whether they equally give what we would like to have with sufficient precision. They appear to supply reliable results if the coefficients inherent can be determined separately for each quantity and also for each situation. However, I have some doubt whether this may be possible if a general and permanent application has to be made for a large sea area. Thus, the bulk aerodynamic formulae can only be considered as a very preliminary and incomplete procedure for application on a synoptic scale.

Therefore, we must look for other sources of information on the turbulent vertical transfer quantities. The direct measurement by applying the eddy correlation method certainly is not manageable generally because of the complicated instrumental expenditure needed. However, the profile method should be applicable in a general way. It would necessitate measurements of wind speed, air temperature and humidity each carried out at three levels, but it would be much better if their average vertical gradients at one level (say 5 m) could be directly recorded with sufficient accuracy. This object, of course, implies a considerable amount of development in instrumentation and engineering but, in principle, it should be possible. Using such devices we would get rid of all the problems connected with the drag coefficient and with the replacing of vertical gradients by differences air-sea.

Sometimes I dream of air-sea interaction buoys distributed over the oceans in a fairly dense network and broadcasting regularly their measured data on the mean vertical gradients which would enable us to draw reliable charts on air-sea interchange. Let us hope that this dream will not always remain a dream but will become true in not too distant future.

REFERENCES

Ashburn, E.V. 1963 The Radiative Budget of the Ocean-Atmosphere Interface. Deep-Sea Res., Vol. 10. 597-606.

Benton, G.S., Fleagle, R.G., Leipper, D.F., Montgomery, R.B., Rakestraw, N., Richardson, W.S., Riehl, H., and Snodgress, J 1962 Interaction Between the Atmosphere and the Ocean. Report of the Joint Panel on Air-Sea Interaction to the Comm. on Atmosph. Sci. and the Comm. on Oceanogr. Publ. 983, Nat. Ac. of Sci., Washington, D.C.

Brocks, K. 1959 Measurements of Wind Profiles Over the Sea and the Drag at the Sea Surface. Am. Assoc. Advanc. Sci., Intern. Oceanogr. Congr., New York, 1959, Preprints, pp. 742-743.

Brocks, K. 1963 Probleme der maritimen Grenzschicht der Atmosphäre. Ber. Deut. Wetterdienstes, Vol. 91, 34-46.

Brocks, K. and Hasse, L 1963 Fluctuation Measurements Made at Sea with a Gyroscopic Stabilised Floating Mast. Intern. Assoc. Meteorol. Atmos. Physics, Proc. IUGG Gen. Assembly, Berkeley, 1963. Publ. IAMAP No. 13, 117.

Bruce, J.P., Anderson, D.V., and Rodgers, G.K. 1961 Temperature, Humidity, and Wind Profiles Over the Great Lakes. Great Lakes Res. Div., Univ. of Michigan, Publ. No. 7, 65-70.

Charnock, H 1955 Wind Stress on a Water Surface. Quart. J. Roy. Meteorol. Soc., Vol. 81, 639-640

Clarke, D.B. 1963 Radiation Measurements With an Airborne Radiometer Over the Ocean East of Trinidad. J. Geophys. Res., Vol. 68, 235-244.

Darbyshire, J. and Darbyshire, M. 1955 Determination of Wind Stress on the Surface of Lough Neagh by Measurement of Tilt. Quart. J. Roy. Meteorol. Soc., Vol. 81. 333-339.

Deacon. E. L. 1962 Aerodynamic Roughness of the Sea. J. Geophys. Res., Vol. 67, 3167-3172.

Deacon, E. L. and Webb, E.K. 1962 Small-Scale Interactions. In "The Sea: Ideas and Observations." (M. N Hill, ed.), Vol. I, pp. 43-87, Wiley (Interscience), New York

Deardorff, J.W. 1961 Evaporation Reduction by Natural Surface Films. J Geophys. Res. Vol. 66, 3613-3614.

Ellison, T. H. 1957 Turbulent Transport of Heat and Momentum from an Infinite Rough Plane. J. Fluid Mech., Vol. 2, 456-466.

Field, R. T. and Superior, W.J. 1964 Study of Climatic Fluxes Over an Ocean Surface. C. W. Thornthwaite Assoc., Lab. of Climatol., Final Rpt. Contr. N62306-1236 (Mod. No. 1) U.S. Nav. Oceanogr. Office.

Francis, J.R.D. 1951 The Aerodynamic Drag of a Free Water Surface. Proc. Roy. Soc. (London) A, Vol. 206, 387-406.

Garstang, M. 1965 The Distribution and Mechanism of Energy Exchange Between the Tropical Oceans and Atmosphere. Ph.D. Thesis, Florida State University.

Hasse, L. 1963 On the Cooling of the Sea Surface by Evaporation and Heat Exchange. Tellus. Vol. 15, 363-366.

Hasselmann, K. 1960 Grundgleichungen der Seegangsvoraussage, Schiffstechnik, Vol. 7, No. 39.191-195.

Häussler, W. 1955/1956 Über Temperaturprofile beiderseits einer verdunstenden Wasserfläche. Wiss. Z. Tech. Hochschule Dresden. Vol. 5, 435-450.

Hay, J. S. 1955 Some Observations of Air Flow Over the Sea. Quart. J. Roy. Met. Soc., Vol. 81, 307-319.

Jacobs, W.C.	1951	Large-Scale Aspects of Energy Transformation Over the Oceans. Compendium Meteorol., pp. 1057-1070.
Jarvis, N.L.	1963	The Effect of Monomolecular Films on Surface Temperature and Convective Motion. Intern. Assoc. Meteorol. Atmos. Physics, Proc. IUGG Gen. Assembly, Berkeley, 1963. Publ. IAMAP, No. 13,125.
Kraus, E.B.	1964	Heat Flux and Surface Stress On and Near an Island in the Trade Wind Region. Report No. 4, Woods Hole Oceanogr. Inst., Ref. No. 64-36.
Laevastu, T.	1960	Factors Affecting the Temperature of the Surface Layer of the Sea. Soc. Sci. Fennica, Commentationes Phys. Math., Vol. 25, 1.
La Mer, V. K. (ed.)	1962	"Retardation of Evaporation by Monolayers," Academic Press, New York.
Lumb, F. E.	1964	The Influence of Cloud on Hourly Amounts of Total Solar Radiation at the Sea Surface. Quart. J. Roy, Meteorol. Soc., Vol. 90, 43-56.
Miles, J. W.	1957, 1959, 1960, 1962	On the Generation of Surface Waves by Shear Flows. J. Fluid Mech., Vol. 3, 185-204; Vol. 6, 568; Vol. 7. 469-478; Vol. 13, 433
Monin, A.S. and Obukhov, A.M.	1954	Basic Regularity in Turbulent Mixing in the Surface Layer of the Atmosphere. U.S.S.R. Acad. Sci. Geophys. Inst., No. 24, 151.
Motzfeld, H.	1937	Die Turbulente Strömung an Welligen Wänden. Z. Angew. Math. u. Mech., 17.
Munk, W. H.	1955	Wind Stress on Water: an Hypothesis. Quart. J. Roy. Meteorol. Soc., Vol.81, 320-322.
Neumann, G.	1948	Über den Tangentialdruck des Windes und die Rauhigkeit der Meeresoberfläche. Z. f. Meteorol., Vol. 2. 193-203.

Okuda S. and Hayami, S. 1959 Experiments on Evaporation from Wavy Water. Records. Oceanogr. Works, Japan (NS), Vol. 5, 6-13.

Panofsky, H.A., Blackadar, A.K. and McVehil, G.E. 1960 The Diabatic Wind Profile. Quart. J. Roy. Meteorol. Soc., Vol. 86, 390-398.

Phillips, O.M. 1957 On the Generation of Waves by a Turbulent Wind. J. Fluid Mech., Vol. 2, 417-445.

Phillips, O.M. 1958 The Equilibrium Range in the Spectrum of Wind-Generated Waves. J. Fluid Mech. Vol. 4, 426-434.

Phillips, O.M. 1962 Recent Developments in the Theory of Wave Generation by Wind. J. Geophys. Res., Vol. 67, 3135-3141.

Pond, S., Stewart, R.W., and Burling, R.W. 1963 Turbulent Spectra in the Wind Over Waves. J. Atmos. Sci., Vol. 20, No. 4, 319-324.

Portman, D.J. 1960 An Improved Technique for Measuring Wind and Temperature Profiles Over Water and Some Results Obtained for Light Winds. Great Lakes Res. Div., Univ. of Michigan, No. 4, 77-84.

Rasool, S.I. 1964 Global Distribution of the Net Energy Balance of the Atmosphere from Tiros Radiation Data. Science, Vol. 143, No. 3606, 567-569.

Rasool, S.I. 1964 Cloud Heights and Night Time Cloud Cover from Tiros Radiation Data. J. Atmos. Sci., Vol. 21, No. 2, 152-156.

Roll, H.U. 1948 Wassernahes Windprofil und Wellen auf dem Wattenmeer. Ann. Meteorol., Vol. 1, 139-151.

Schmitz, H. P. 1962 A Relation Between the Vectors of Stress, Wind, and Current at Water Surfaces and Between the Shearing Stress and Velocities at Solid Boundaries. Deut. Hydrograph, Z., Vol. 15, 23-36.

Schooley, A.H. 1963 Simple Tools for Measuring Wind Fields Above Wind-Generated Water Waves. J. Geophys. Res., Vol. 68, 5497-5504.

Sheppard, P.A. 1958 Transfer Across the Earth's Surface and Through the Air Above. Quart. J. Roy. Meteorol. Soc., Vol. 84, 205-224.

Sheppard, P.A. 1963 Momentum and Other Exchange Above a Water Surface. Intern. Assoc. Meteorol. Atmos. Physics, Proc. IUGG Gen. Assembly Berkeley, 1963. Publ. IAMAP, No. 13,117.

Snyder, R.L. 1965 The Wind Generation of Ocean Waves. Ph.D. Thesis, Univ. of Calif., San Diego.

Stewart, R.W. 1961 The Wave Drag of Wind Over Water. J. Fluid. Mech. Vol. 10, 189-194.

Stewart, R.W. and Burling, R.W. 1961 Some Preliminary Results from a Program of Air/Sea Interaction Studies. Trans. Amer. Geophys. Un., Vol. 45, No. 4,618.

Takeda, A. 1963 Wind Profiles Over Sea Waves. J. Oceanogr. Soc. Japan, Vol. 19, No. 3, 136-142.

Van Dorn, W.G. 1963 Wind Stress on an Artificial Pond. J. Marine Res., Vol. 12, 249-276.

Vines, R.G. 1959 Wind Stress on a Water Surface: Measurements at Low Wind Speeds With the Aid of Surface Films. Quart. J. Roy. Meteorol. Soc., Vol. 85, 159-162.

Webb, E.K. 1960 An Investigation of the Evaporation from Lake Eucumbene. Australia, C.S.I.R.O. Div. Meteorol. Phys., Tech. Paper No.10.

Yamamoto, G. 1959 Theory of Turbulent Transfer in Non-Neutral Conditions. J. Meteorol. Soc. Japan II, Vol. 37, 60.

A SURVEY OF THE ROLE OF SEA-AIR INTERACTION IN TROPICAL METEOROLOGY

Joanne Simpson
U. S. Weather Bureau, Washington, D. C.

Sea-air interaction affects every scale of motion and nearly every process in the tropical atmosphere. It enters every problem in which we attempt to make an explanation or a prediction - from interpreting the cloud forms we see on satellite pictures to the oceanic semi-diurnal convection cycle and the formation of hurricanes.

But what do we mean by sea-air interaction? How do the sea and air affect each other in the tropics? Since we are mainly discussing meteorology here and not physical oceanography or biology, let us examine more specifically how the physical interaction between the sea and the air affects the atmosphere. This takes place by means of exchanging of property: primarily moisture, heat, momentum and salt. Concerning each of these exchanges we must ask three main questions, namely:

1. What is its magnitude and distribution in space and time?

2. What is it controlled by, that is, what is its functional dependence?

3. What is its role in atmospheric processes and how important in this role?

Momentum flux is intimately coupled with the others, as is pointed out in the article by Roll in these Proceedings. Salt flux is probably important in atmospheric thermodynamics as well as in the condensation process; important research is going forward with its highly necessary documentation (cf. Woodcock, 1958). This article, however, will restrict its subject to moisture and heat fluxes, because of their large role in the energetics of air circulations.

First, we will examine their global distribution and role in planetary flows. This will lead naturally to a discussion of convection and cloud patterning and the role of exchange in these processes. Finally, we shall conclude with a more detailed consideration of the interaction between oceanic fluxes and air circulations in the trade-wind and equatorial trough zones of the tropics.

Knowledge of the role of sea-air exchange in atmospheric circulations has burgeoned since World War II - in some cases it has even been incorporated into models, both theoretical and numerical. There is, however, one major reservation which relates to the most serious bottleneck facing sea-air interaction studies and facing tropical meteorology - that is, for all practical purposes, we have no direct way to evaluate these fluxes. We cannot chart them from direct measurements, as we can sea temperature, for example.

Nearly all our knowledge of heat and moisture fluxes from sea to air is based on indirect calculations from the so-called transfer formulas or Jacobs formulas. These are partly empirical and partly based on a simplified

model of turbulent boundary layer processes occurring at the sea-air interface. This modeling should be best applicable when the windspeed is high and the static stability is near neutral - that is, for near-zero values of the Richardson number. The formulation gives increasingly bad results as the Richardson number increases, to either positive (stable) or negative (unstable) values.

This is not the place to develop the transfer formulas nor to discuss further their range of validity, although a lot of work and consideration has been recently devoted to this topic (Roll, 1965; Garstang, 1964). The fact remains that flux computations based upon them, good or bad, form one of the primary cornerstones upon which tropical meteorology has been built. Spot checks of these flux computations have been made, by methods which are themselves indirect and subject to errors and assumptions. Two main ways of checking are the energy budget method, which involves assessment of radiative fluxes, and the so-called "direct" method by aircraft measurements made at some height above the surface (Malkus, 1962). These results nearly always agree with those of the transfer formulas within a factor of two, and often to better than 25 percent. It is all very well to reiterate the truism that these fluxes just must be more accurately specified, to go forward with tropical meteorology, but no one has yet produced a way to do this, particularly on the necessary routine and frequent basis over wide expanse of ocean.

The second important point to make here about the Jacobs transfer formulas is that, to the extent that they are valid, they tell us that the atmosphere itself mainly controls the extent of its own heat and moisture input from the sea. We see this in the form of the equations, which is

$$\text{Flux} = \text{Coefficient} \times (\text{Air-Sea Property Difference}) \times \text{Windspeed} \qquad (1)$$

Since time fluctuations in the air-sea property difference are mainly governed by those in the lower air, we can see that the atmosphere opens and closes its own fuel line, making a very intriguing feed-back linkage; the fine beginning made by Kraus (1959) in modeling this has not been pursued as it deserves.

The coefficient in the transfer equations needs consideration prior to interpretation of any of its results. In most climatological maps of heat and moisture exchange, this coefficient is used as a constant. In his classical work, Jacobs (1951) obtained his constant coefficient by "calibration" with the energy budget method. There are more sophisticated but probably no physically sounder ways of evaluating the coefficient nowadays.

Boundary layer modeling indicates that the coefficient is a function of C_D, the so-called "drag coefficient," which relates momentum exchange at the interface to the windspeed. C_D must be empirically determined. Recently a number of workers have examined its dependence upon the atmospheric variables (cf. Garstang 1964; Roll, 1965; Deacon and Webb, 1962; Deacon,

Sheppard and Webb, 1956; Sheppard, 1958). It is found to increase with windspeed and with decreasing Richardson number - that is, the drag of the sea on the air appears to be greater at lower stability with the same windspeed. The drag coefficient roughly doubles as the wind increases from 2 to 14 meters per sec. Normal tropical variations in Richardson number contribute only about one-fourth this much variation.

Keeping these problems in mind, we turn to our first topic, namely the role of tropical sea-air fluxes in the planetary circulations. To examine this, we need the climatological picture of these fluxes - the magnitude of evaporation and sensible heat exchange - on annual global maps, and analysis of regional and seasonal variations.

The classical maps of Jacobs (1951) are shown again in Figures 1 and 2. Malkus (1962) and Garstang (1964) have compared these distributions with the later results of Budyko (1956) who also used the transfer formulas but does not divulge his data sources or method of analysis. In looking at these charts, we must keep in mind one further important limitation and that is the data problem. Even supposing that the transfer equations were exactly correct with an exactly known coefficient, for good results we would need a measurement network of air temperature and humidity, sea temperature and windspeed reporting every few hours. Then we should make the multiplications required by equation (1) from each set of data and average these products over month, season or year.

Of course, this is a visionary goal. Climatological mean values have to be plugged directly into the formulas and clearly this can lead to errors if there are correlations between air-sea property difference and windspeed - if, for example, the air temperature commonly drops in storm situations. This points the finger directly at synoptic disturbances.

Malkus (1962) and Garstang (1964) have made several case studies where the transfer calculation from fairly long-period means could be compared with averages of frequent measurements of the input into equation (1) from research vessels or Weather Ships. Suffice it to say here that in the strong and steady trades the correlation is unimportant, but wherever disturbances are predominant, such as in the equatorial trough, the error can become quite large. Garstang's (1964) results indicate that there it may be considerably larger than the earlier estimates by Malkus (1962).

Figures 1 and 2 show by and large the expected flux distributions, with some curious features, such as higher transfers in the Pacific than in the Atlantic, which exhibits negative sensible heat flux off North Africa. Budyko's (1956) values are greater in the Atlantic, suggesting that another scale of fluctuations has perhaps distorted the picture. Jacob's calculations were made using values at 1200 GCT, which is near midday in the Atlantic area and at night in the Pacific. We do not know what observations Budyko used, but the diurnal transfer cycle that we shall describe later suggests that he may have used these at 0000 GCT. In all transfer

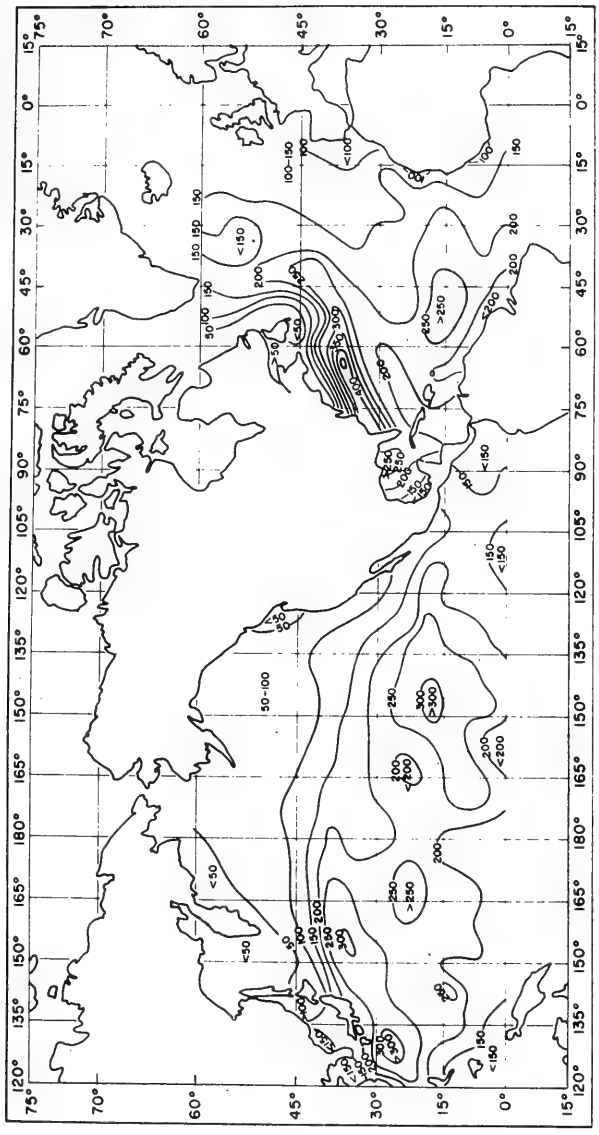

Figure 1 (after Jacobs, 1951). The mean annual distribution of evaportive heat transfer, Q_e, from sea to air over the North Atlantic and North Pacific, expressed in gram calories per square centimeter per day.

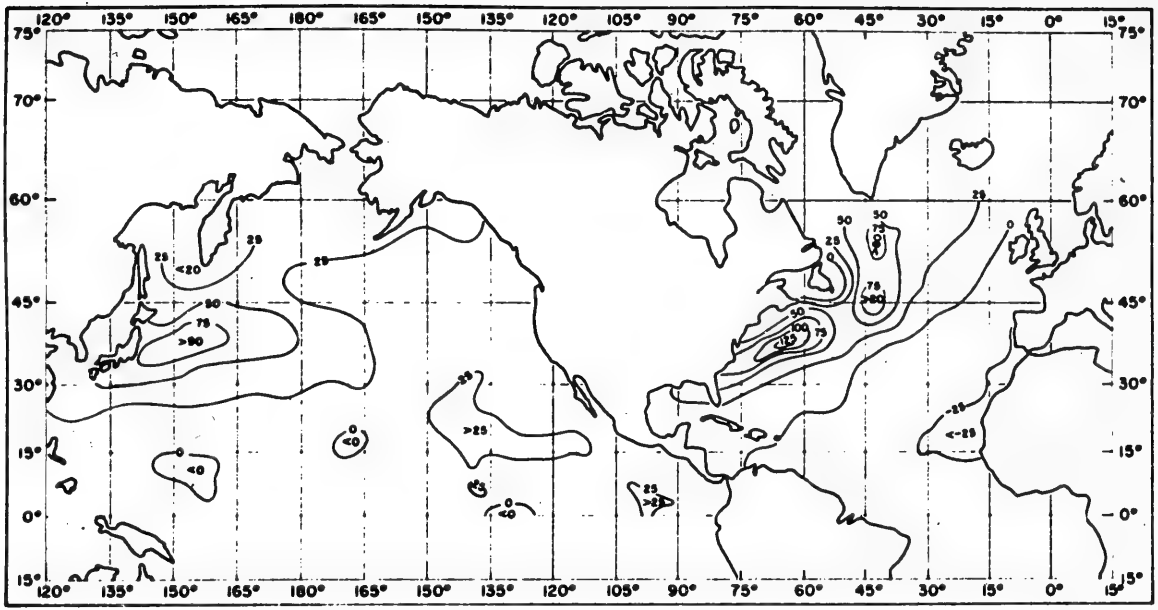

Figure 2 (after Jacobs, 1951). The mean annual rate of exchange of sensible heat, Q_s, between sea and air over the North Atlantic and North Pacific, expressed in gram calories per square centimeter per day.

calculations, we must know the data and their fluctuation scales to make a meaningful interpretation of results.

Figure 3 shows the evaporation integrated by latitude and broken down by seasons. Water vapor constitutes more than three-fourths of the atmosphere's energy source; this is provided by evaporating an average of just over 1 meter of sea water per year; about 75 percent enters the air equatorward of 30° latitude. Figure 4 shors the oceanic heat budget calculated by Budyko (1956), with roughly the same distribution of evaporative heat loss (Q_e = LE, where L is the latent heat of vaporization) as shown in Figure 3 from Jacobs. Note the very much smaller magnitude of Q_s, the sensible heat supply from sea to air; the ratio of Q_s to Q_e, however, rises outside the tropics, for reasons that are discussed later.

Budyko's Q_e shows a similar equatorward dip as Jacob's does, a deduction very crucial to the oceanographer as well as to the meteorologist. Q_{vo} is the oceanic heat flux divergence. In most studies, including Budyko's, this is deduced as a residual in the oceanic heat budget; it is essentially the difference between the radiation balance R and the heat loss by evaporation, Q_e. This heat energy difference is what the equatorial ocean has left to export to high-latitudes, to moderate their winter climates through warm currents such as Gulf Stream and Kuroshio. By integrating Q_{va} latitudinally, authors like Bryan (1962) use the only way extant to arrive at oceanic heat transports; these suggest that the oceans may carry as much as 15 - 20 percent of the heat energy transported by the general circulation of the atmosphere. Either this important result, or global radiation figures, must suffer an agonizing reappraisal if Q_e in equatorial regions undergoes significant alteration, as Garstang's contribution to these Proceedings suggests it must.

How does the air utilize these energy inputs from the oceans? To begin to answer this question, let us examine Figure 5, the heat budget of the atmosphere. First note the latitudinal uniformity of the radiation sink R_a, which corresponds to a cooling of about 0.75°C per day. From 60°N to 60°S, neither the sensible heating from the surface Q_s, nor heat flux convergence in the air ($-Q_{va}$) does much to make up this large radiational deficit - in fact the large negative peak in $-Q_{va}$ (air heat flux convergence) near the equator only compounds the air's heat losses in the tropics. As we see from the top curve in the diagram, LP (precipitation heating), is the vital atmospheric heat source which makes up both the radiational loss and provides for the heat export from the equatorial zone.[1]

Clearly the air must have converted the latent heat gained from evaporation into the usable or sensible form by making rain. Comparison of Figures 4 and 5 show clearly that the main input and the main utilization of the water vapor occur in quite different regions - our attention is directed to the wind circulations and cloud formation process to explain this difference.

1/ In latitudes poleward of 60°, heat flux convergence becomes as large or larger than precipitation warming.

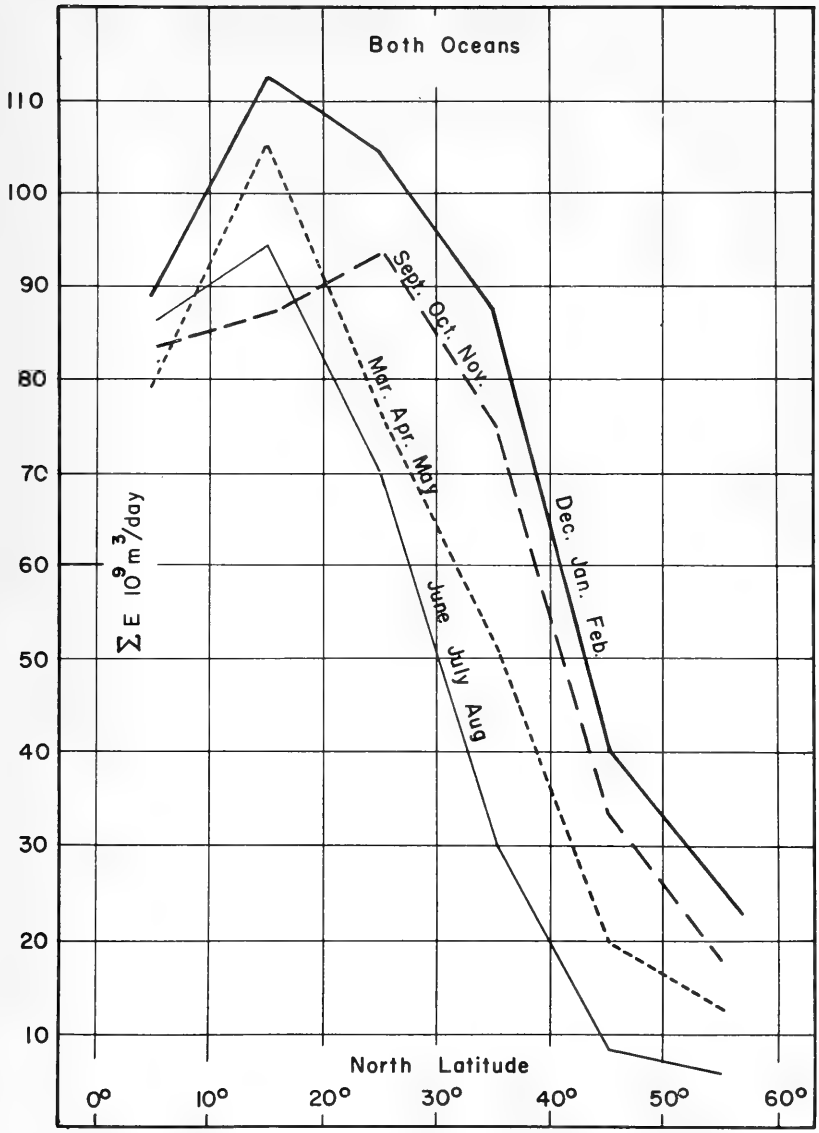

Figure 3 (after Jacobs, 1951a). Integrated latitudinal dependence of evaporation from N. Atlantic and N. Pacific Oceans together, by seasons. Units 10^9 m^3/day. Mean annual evaporative loss to both oceans: 112.5 cm $year^{-1}$.

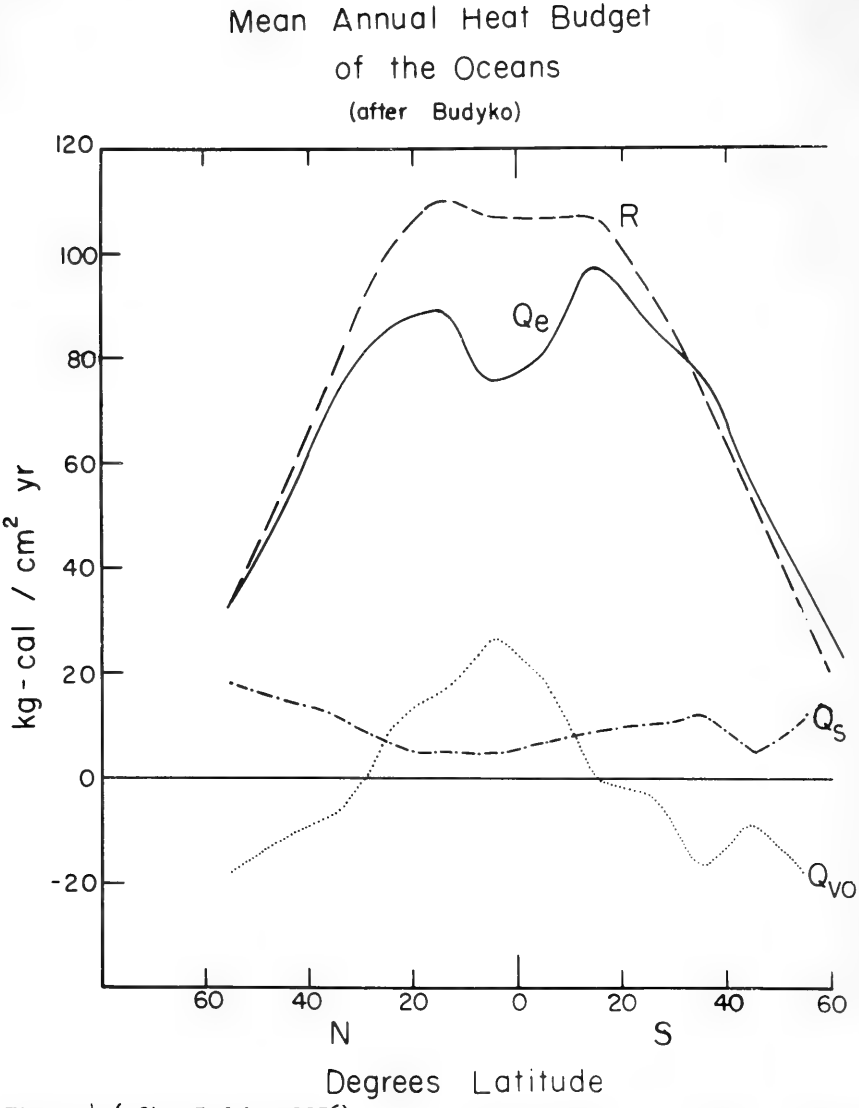

Figure 4 (after Budyko, 1956). Annual heat budget of the ocean. Units, kg calories per cm^2 per year. Q_e is evaporation; Q_s is sensible heat transfer; R is the radiation balance, and Q_{VO} is the oceanic flux divergence, computed as residual to balance the budget.

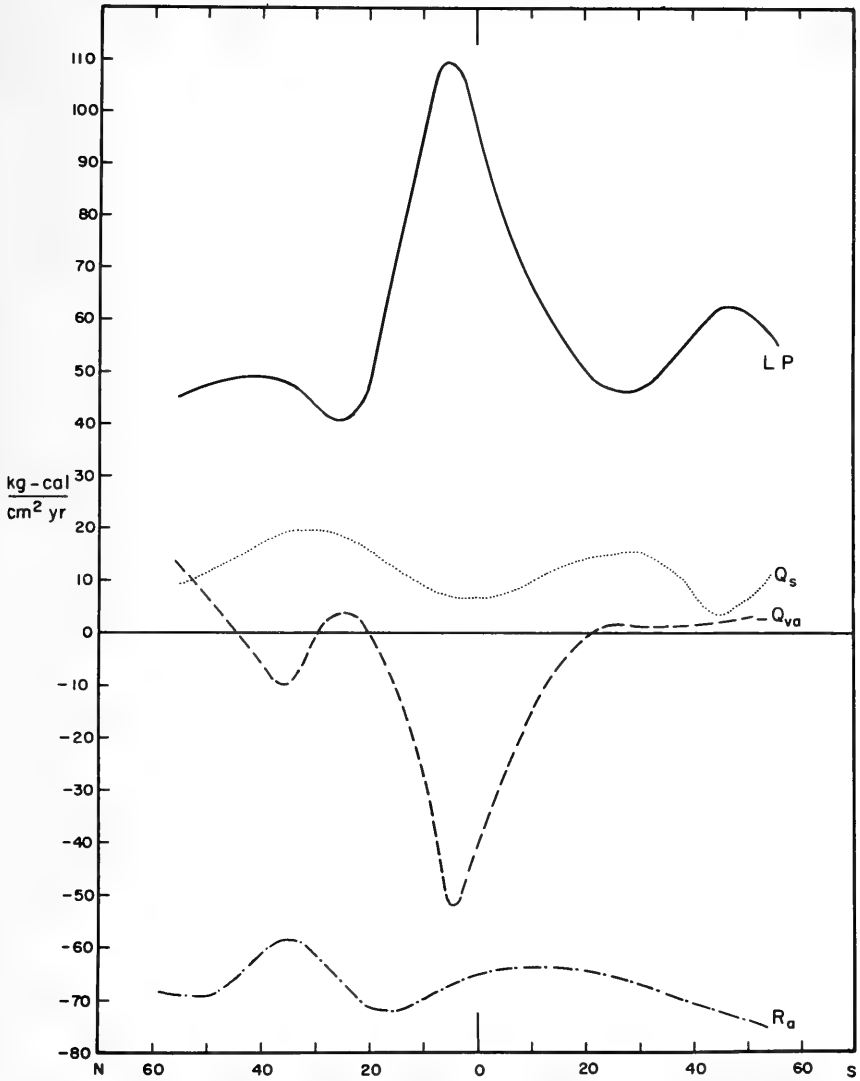

Figure 5 (after Budyko, 1956). Annual heat budget of the atmosphere. Units, kg calories per cm^2 per year. LP is precipitation warming where P is precipitation in cm and L is the latent heat of vaporization. Q_s is the sensible heat transfer from the ocean; $-Q_{va}$ is atmospheric flux convergence of sensible heat plus potential energy, and R_a is the radiation balance of the atmosphere.

In Figure 6, low-level wind patterns begin to delineate the intriguing paradox: equatorward - blowing trades carry the water vapor fuel unconverted into the convergent trough zone (solid line) - it is largely not processed locally in the input zone and from there exported poleward, but goes on this roundabout circuit because of the air's movements and differing cloud-building abilities.

Trade-wind clouds are normally stunted cumuli, as depicted in Figure 7, while in the equatorial regions, high cumulonimbus towers (Figure 8) often flourish. The latter are excellent latent heat converters and not the former which usually evaporate without dropping precipitation back into the ocean, which is the prerequisite that the heat stay in the air.

We see that the cloud and precipitation processes control the role of sea-air exchange products in the atmosphere - so again we return to air structure and motions and this time ask how these interact with clouds. In 1957 we made an airborne photogrammetic study in the Pacific to begin an attack on this question; the complete results have just been published (Malkus and Riehl, 1964). From the carefully time-lapsed movies, cloud maps were constructed and compared with sounding and synoptic data. Figures 9 and 10 show two typical trade-wind cases, the first with weak winds and the second with normally vigorous flow. In both, the ocean is presumed but not known to be warmer than the low-level air. To assess the role of sea-air interaction, comparison with Avsec's (1939) extension of Benard's classical convection cell studies was made. Figure 11 shows one of Avsec's laboratory experiments, with uniform heating from below and weak translation (weak shear between convecting fluid and lower boundary). Figure 9 suggests a similar admixture of polygonal cells with cells becoming elongated into rolls. In Figure 10, the stronger flow has presumably caused the rolls to predominate; our Pacific study confirmed the conditions, related to shear, for their orientation.

From satellite pictures, Krueger and Fritz (1961) have identified polygonal cells in some way apparently similar to those studied in the laboratory. Figure 12 is from one of the few cases where they had enough supplementary data to relate these patterns partially to sea-air interaction. The sea-air temperature excess was large ($\sim$ 3°c) and a strong trade-wind inversion confined the convection - its horizontal scale increased toward the southeast as the moist layer deepended. Three puzzling features were found, however, prohibiting the naive extrapolation of laboratory results.

Firstly, the winds were strong (15-20 knots) in the region (Figure 13) where the polygonal pattern was photographed - why were not the polygons elongated into rolls? Secondly, the horizontal cell size runs about 30 times the depth of the convective layer, exceeding the laboratory ratio by an order of magnitude. Thirdly, Figure 12 (upper) suggests each cell wall contains several cloud elements, or more than one scale of motion.

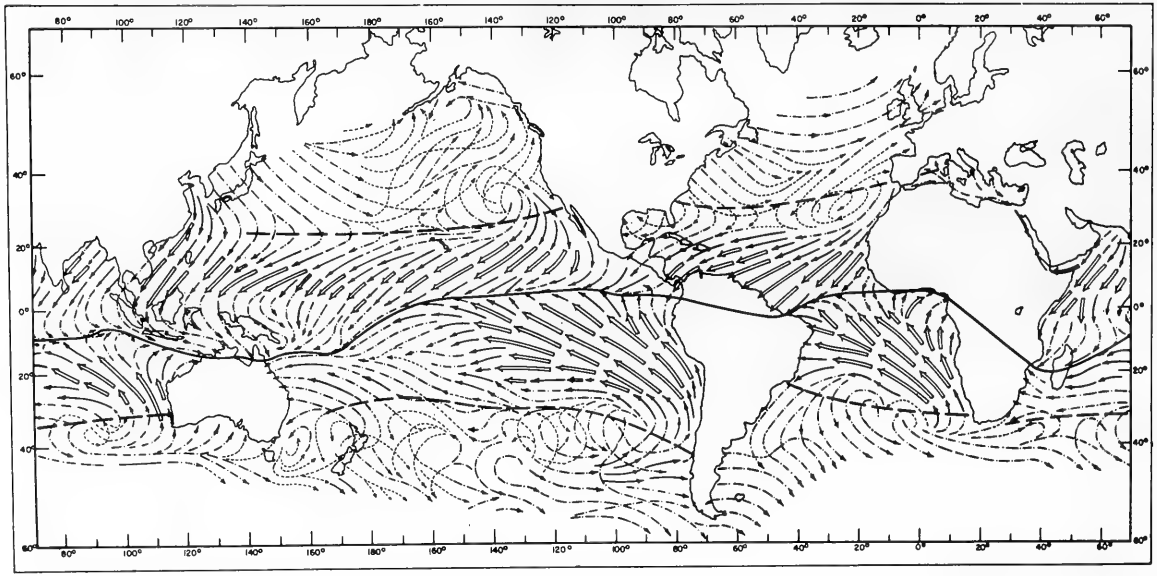

Figure 6 (after U.S. Weather Bureau, Atlas of Climatic Charts of the Oceans, 1938, Chart 3). Prevailing surface winds over the oceans in winter, direction and constancy in January. Direction lines based on dominant wind arrows computed for each 5-degree square, with directional constancy as follows: ⟹ 81 percent and over; ⟶ 61-80 percent; ⟶ 41-60 percent; - - -⟶ 25-40 percent of all winds from the quarter within which the line is a median.
Solid line: mean position of equatorial trough. Dashed lines: mean positions of subtropical ridges.

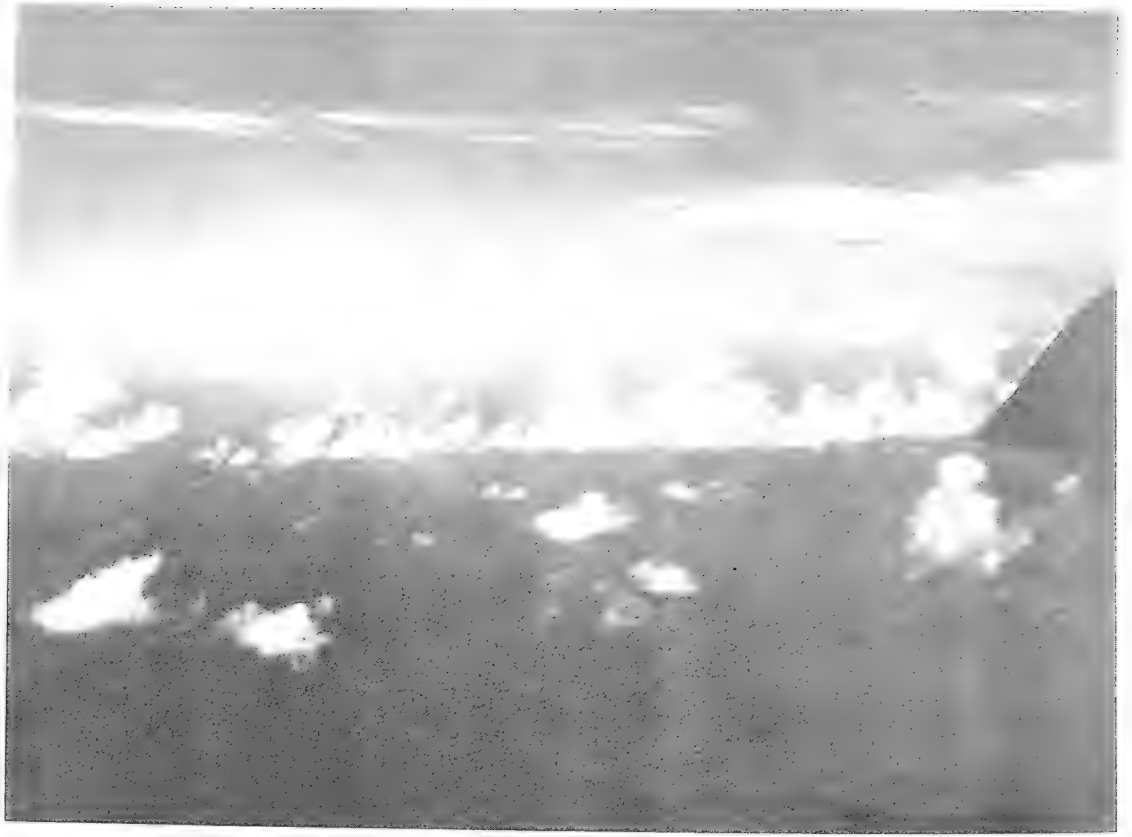

Figure 7. Typical photograph of trade-wind cumulus clouds in rows along the wind. Bases near 2000 ft; tops near 6000 ft.

Figure 8. (after Malkus and Riehl, 1964). Typical photograph of high cumulonimbus towers in an equatorial disturbance. Tops above 35,000 ft.

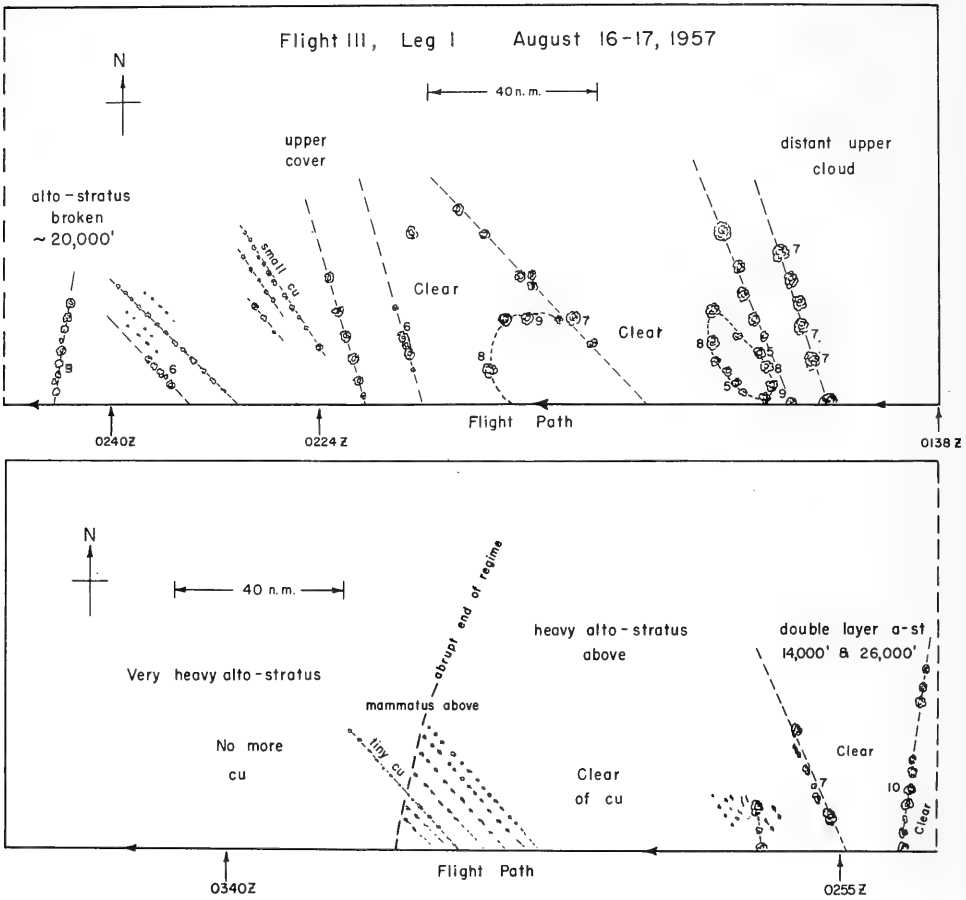

Figure 9 (after Malkus and Riehl, 1964). Trade-wind cloud map for weak wind conditions. Constructed from time-lapse movies: The numbers indicate heights of cumulus tops to the nearest thousand feet.

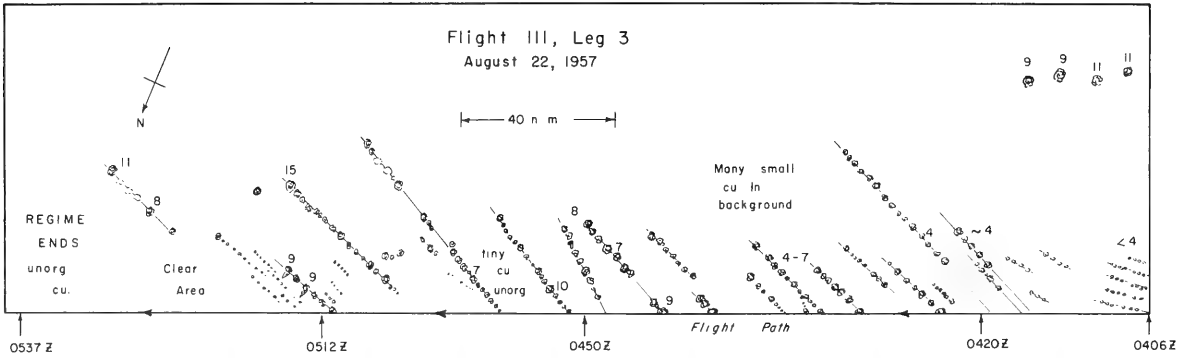

Figure 10 (after Malkus and Riehl, 1964). Trade-wind cloud map for normally vigorous wind conditions. The numbers indicate heights of cumulus tops to the nearest thousand feet. The wind is along the cloud rows from left to right.

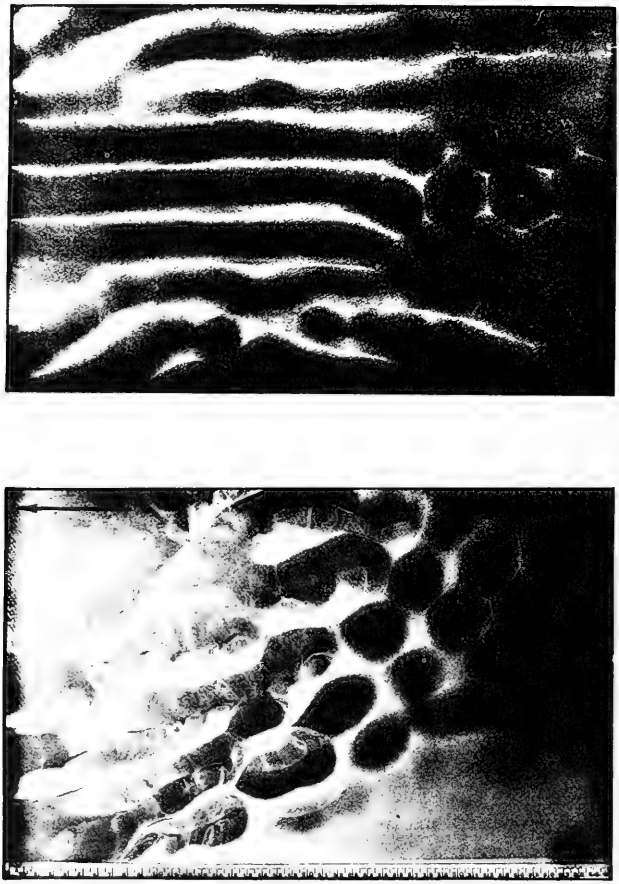

Figure 11 (after Avsec, 1939). Experimental transformation of polygonal cells into longitudinal bands, by the setting in motion of a layer of air heated from below. Depth of layer 20 mm. Compare with cloud map of Figure 9.

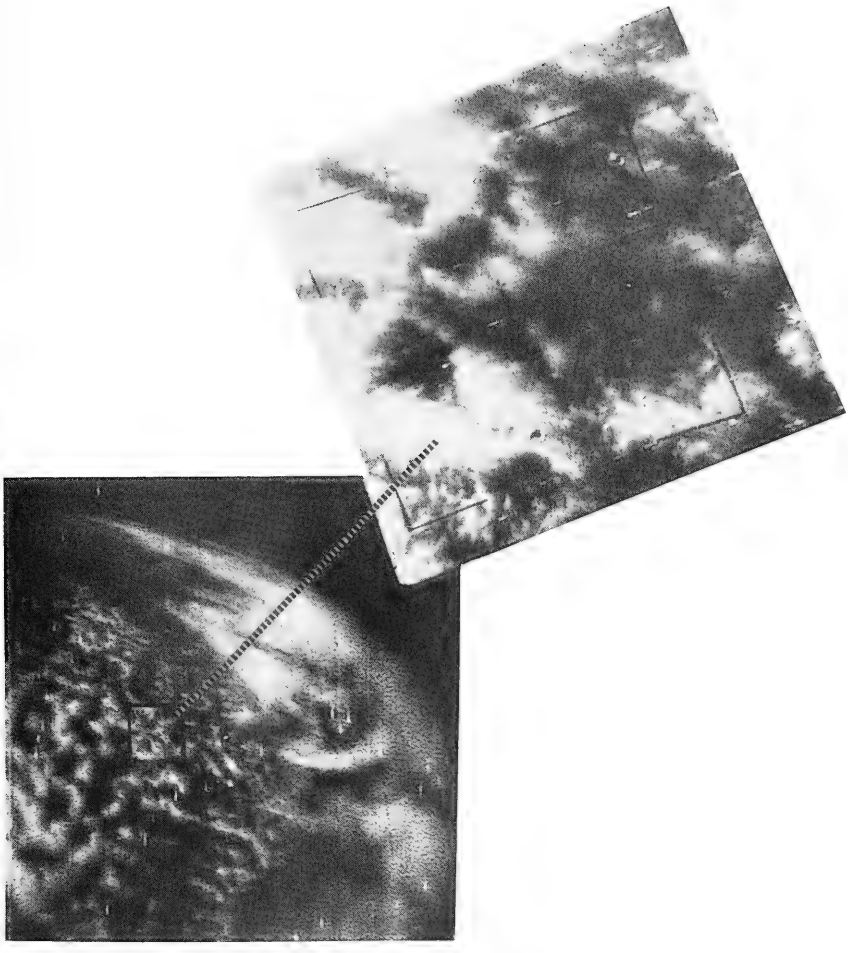

Figure 12 (after Krueger and Fritz, 1961). Case of polygonal cloud cells formed over subtropical Atlantic Ocean on April 4, 1960. Narrow angle picture (upper) corresponding to wide angle picture (lower). This outlined area is approximately 100 nautical miles square.

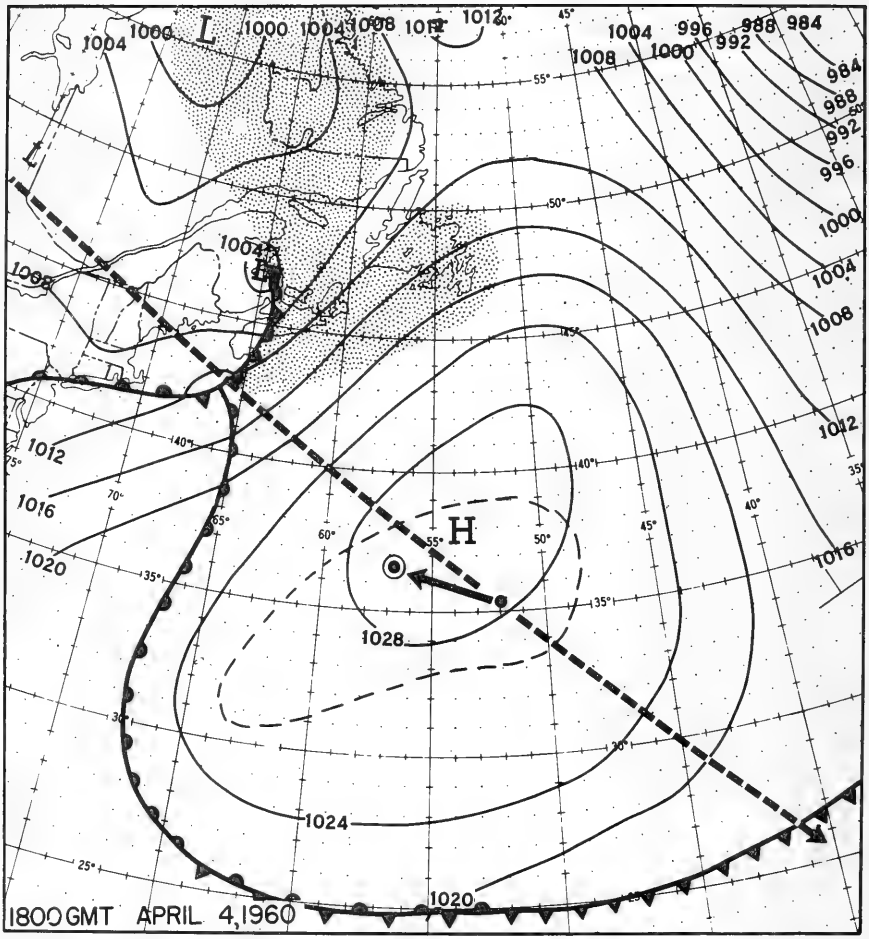

Figure 13 (after Krueger and Fritz, 1961). Surface weather map for 1800 GCT, April 4, 1960. Track of Tiros I, subsatellite point (dot), and picture center (circled dot) are indicated. The area occupied by cellular cloud pattern in Figure 12 is outlined by dashed line.

Clearly the fact the atmosphere is fully turbulent complicates the development of quantitative criteria for cloud patterning and makes difficult the assessment of the role of sea-air interaction in modifying or regulating these patterns. However, we can learn much more about these relations if we would only focus our existing observational resources simultaneously upon the sea-air boundary conditions, the air structure, and the cloud patterns. We do not yet know the relative roles of the first two in producing the fascinating cloud configurations that the satellites are showing us. For example, in Figure 14 as we move (from left to right) following the southeast trades toward the equator, the cloud patterns change from cellular to actinoform (Picture of the Month, 1963) to blob-like. Hubert 1/ has postulated that in going from cellular to actinoform, heating from below may be giving way to dominant cooling from above. The change to blob form in the equatorial zone may be due to deepening of the convective layer. No data exist to test these interesting and important suggestions. The potential of satellite pictures as a tool to understand and predict tropical weather, to interpret the role of sea-air interaction therein, cannot progress much farther until ship and aircraft observations are jointly focussed on these situations. The large necessary expenditure dwindles when compared to that of the space program.

A problem to isolate for the next step of the investigation might be the abrupt transitions in oceanic cloud forms. A typical example is shown in Figure 15. Are these common transitions, often almost infinitely sharp, related to sudden changes in sea temperature or are they governed by swift transitions in air motions? We know they are more abrupt than any likely structural changes in the atmospheric sounding, in terms of lapse rate or humidity stratification.

The beginnings of the required study were made with the Woods Hole Aircraft (Malkus, 1957) using an airborne radiometer, soundings, and cloud photography. "Warm spots" in the ocean upper layers were found, which were also documented by a research vessel with thermistors at several depths. These warm spots were related to trade cumulus groups observationally (Figure 16). The "heated island" and "equivalent thermal mountain" framework (Stern and Malkus, 1953) was used to explain the observations. Even these small-amplitude warm spots should produce an "equivalent thermal mountain" about 100 meters in elevation, which can be quite effective in triggering trade-wind clouds. In continuing these studies, a difficulty is that the airborne radiometer must be flown below 1000 ft., while cloud photomapping is much better performed at 10,000 ft. or more. Furthermore, a surface vessel is needed to calibrate the radiometer and to determine the depth of any oceanic temperature anomalies found. Despite these complications, such a program is mandatory to advance the interdependent fields of sea-air interaction, satellite interpretation, and tropical meteorology.

1/ Personal communication to the writer

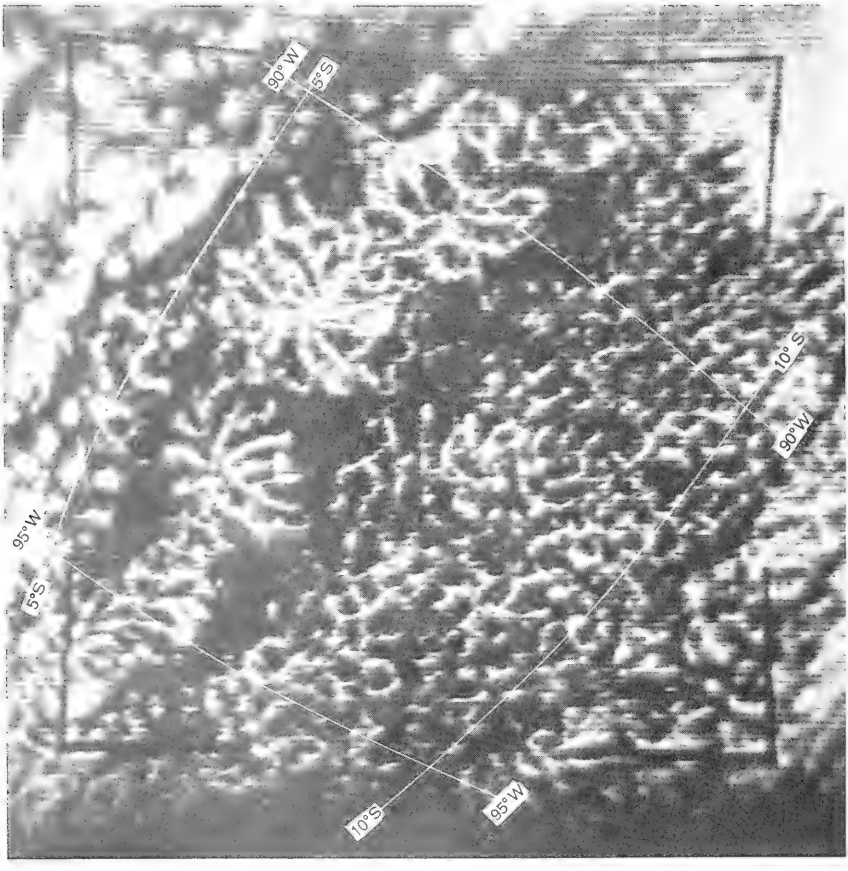

Figure 14 (after Picture of the Month, 1963). Tiros V, 1500 GMT, October 7, 1962. Tropical (southern hemisphere) cloud pattern.

Figure 15 (after Riehl and Malkus, 1964). Example of abrupt cessation of cumulus formations, followed by a completely clear area. Tropical North Pacific (Lat. 20°N; Long. 170°E), August 21, 1957.

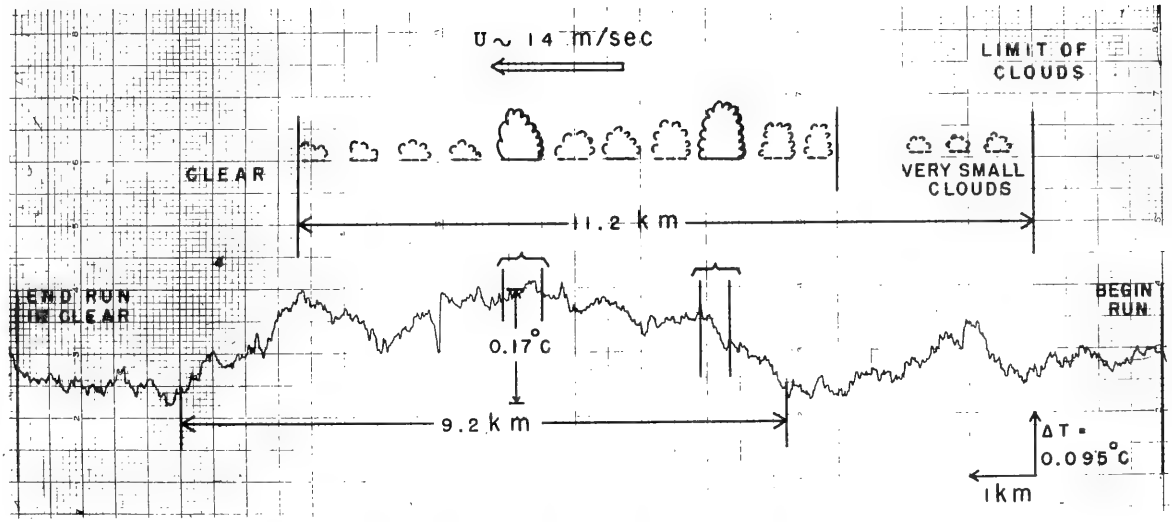

Figure 16 (after Malkus, 1957). A sea surface temperature record from airborne radiation thermometer on a day of strong wind off Jamaica, West Indies (Lat. 18°N; Long. 77°W). This persistent warm spot was also located by a surface vessel; the association with cumulus was determined by marking on the radiometer records and by time-lapse photography.

Figure 16 suggests the close relationship between active sea-air fluxes and cumulus convection. Although a temperature difference of 0.17°C may appear very small, it amounts to 30-50 percent of the common sea-air temperature difference in the trade-wind region. Therefore, we may presume that, over these warm spots, the flux of latent and sensible heat from sea to air is somewhat greater than in the surrounding regions, as are the vertical fluxes of heat and moisture in the well-mixed layer that characterizes the air below cloud base.

The important relation between variations in sea-air temperature difference, exchange and cumulus development is illustrated in the semi-diurnal cycle in convection over the tropical oceans.

A midday minimum in oceanic cumulus convection was long suspected and finally has been substantiated, primarily by the two cruises of Garstang (1964) with the Research Vessel CRAWFORD. Oceanic cumuli flourish best near dawn and sunset and undergo a suppressed period during the noonday hours. At least part of the cause appears to lie in a similar cycle of sensible heat flux (Figure 17). There is only a weak variation in latent heat flux (Figure 18). Figure 19 shows that the daily variation in sea-air temperature difference provides the main key to the transfer cycles, although there is also a weak wind minimum in the early afternoon, related by Lavoie (1963) to the S_2 component of atmospheric tide.

Interestingly enough, the convergence - divergence cycle of this tidal wind is quite nicely in phase with the cloudiness (Figure 20). Shibata (1964) showed that the amplitude of the convergence ($\sim 2 - 3 \times 10^{-7}$ sec^{-1}) and its attendant vertical motions can be related quantitatively to the cumulus variation. Which is cause and which effect? Does the semi-diurnal cycle in air-sea heat transfer help to drive the atmospheric tide via the cumulus process? Or does the tide, maintained solely in the high atmosphere, add to the air-sea interaction cycle in maintaining that of the cumulus? A very little more research could go a long way toward answering this intriguing question.

A recurring thread is clearly woven throughout all these examinations of the role played by exchange in tropical meteorology: This role is directed by clouds. How the atmosphere uses what it receives from the sea depends on what sort of clouds its circulation enables it to produce. And this, in turn, depends on large-scale atmospheric dynamics, or the air motions throughout the depth of the troposphere.

These points are illustrated by a comparison between the operation and energetics of the trade-wind zone and the equatorial trough. The amount of sensible and latent heat that the sea puts into the air does not differ highly between these two regions of the tropics. And yet, its usage is quite different, as is the cloud structure.

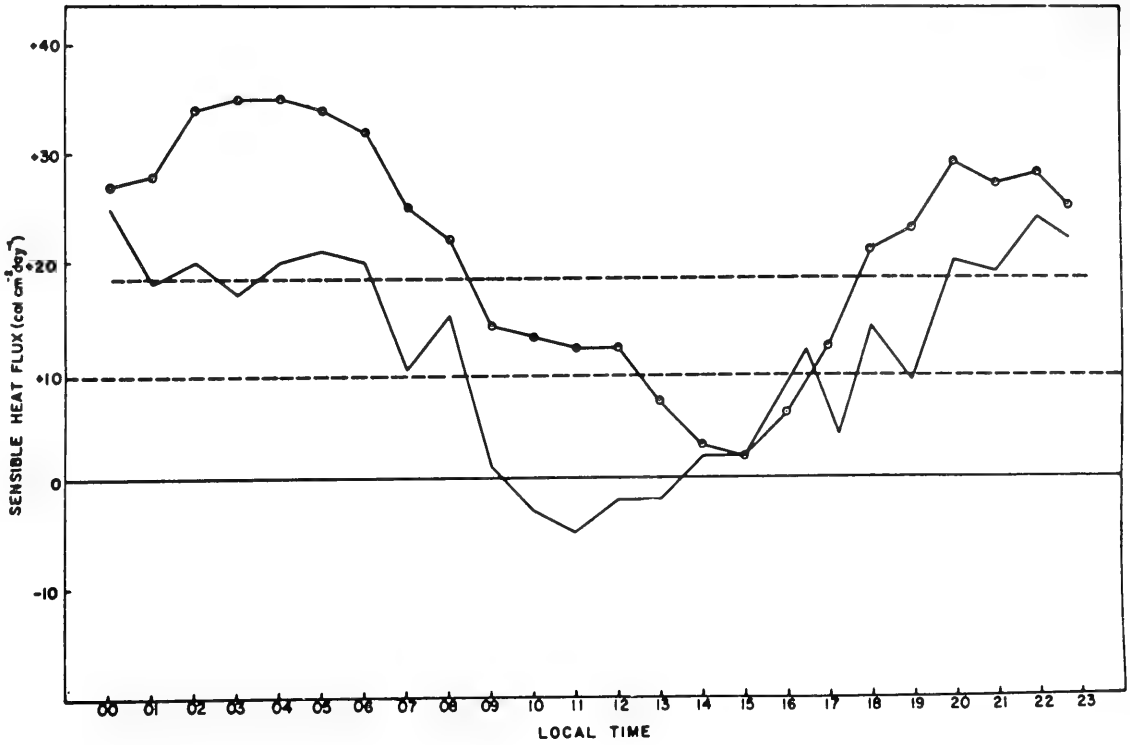

Figure 17 (after Garstang, 1964). Diurnal march of sensible heat transfer (cal cm^{-2} day^{-1}) between the ocean and atmosphere based upon the 1957 (plain line) and 1963 (line with dots) R. V. CRAWFORD data. This ship was stationed for 23 days in 1957 at 11°N, 52°W and for a similar period in 1963 at 13°N, 55°W.

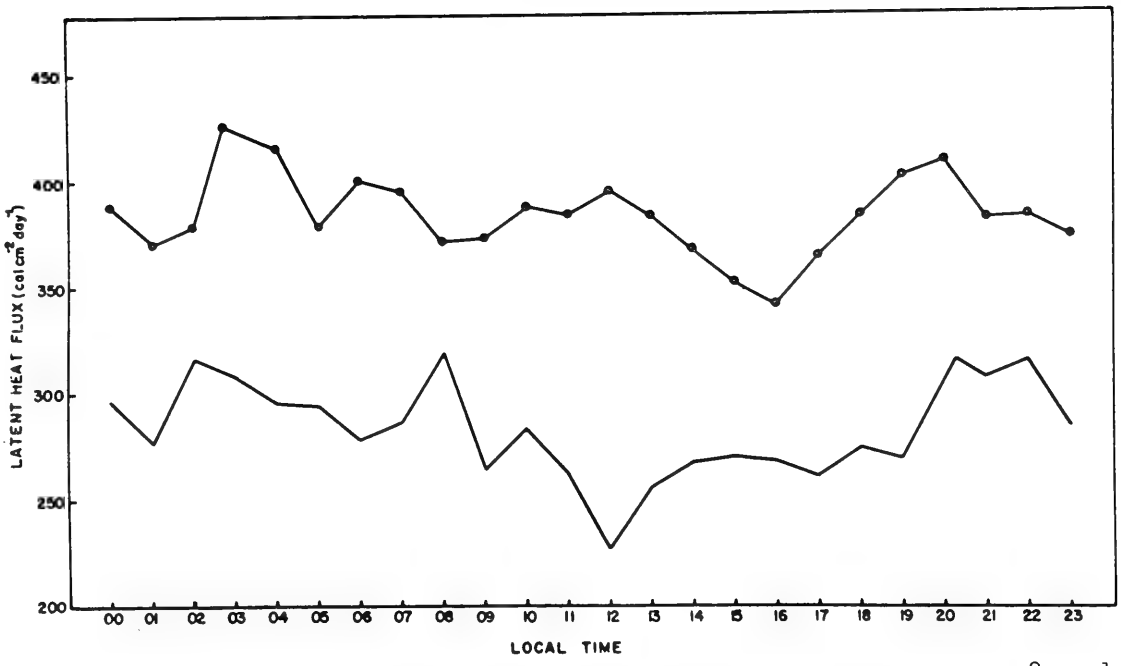

Figure 18 (after Garstang, 1964). Diurnal march of latent heat transport (cal cm^{-2} day^{-1}) between the ocean and atmosphere based upon the 1957 (plain line) and 1963 (line with dots) R. V. CRAWFORD data.

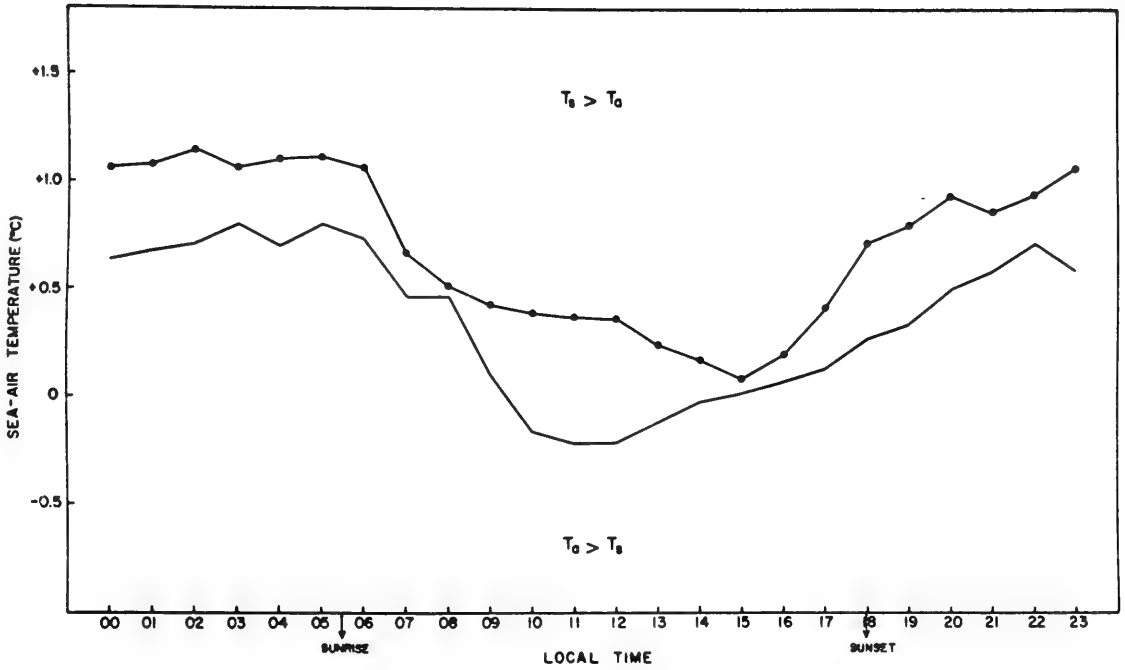

Figure 19. Diurnal march of sea-air temperature difference from R. V. CRAWFORD data. Plain line for 1957 period; line with circles for 1963 period.

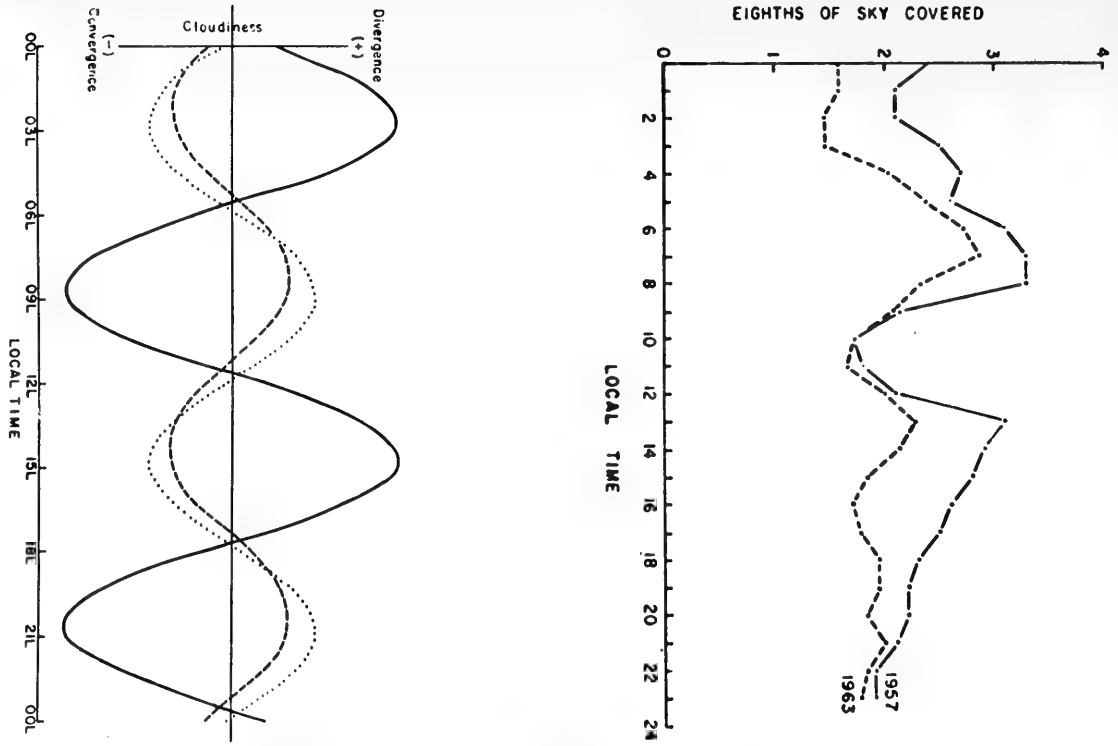

Figure 20 (after Shibata, 1964). Upper diagram: Diurnal march of low cloud cover (cumulus) in oktas of sky covered during the 1957 and 1963 R. V. CRAWFORD cruises. Lower diagram: comparison between divergence of atmosphere tidal wind (integrated over lowest 3 km) and second harmonic of cloudiness. The divergence amplitude is about 2×10^{-7} sec^{-1} while that of the cloudiness is arbitrary. Dashed line, all days of R. V. CRAWFORD cruises; dotted line, undisturbed days only.

In the trade-wind stream, the cloud development (Figure 21) is restricted by the trade-wind inversion, so that only about 25 percent of the latent heat gained is released by local precipitation. The remainder is accumulated in a deepening moist layer and is shipped toward the equator by the trades (Figure 22). The rain release occurs at fairly low-levels, and together with Q_s, provides a net heat source and "pressure head" which sustains the lower trades. A preliminary mathematical model of this system has been constructed (Malkus, 1956). The upper trades live on more sporadic imports from the equatorial trough zone.

Figure 23 summarizes the energetics of the region and the role of exchange therein. Sensible heat plus potential energy ($h = C_pT + Agz$) is budgeted on the left and latent heat L_q (q is specific humidity) on the right. Three layers are treated separately; in ascending order. These are roughly consistent with the mixed layer, cloud layer and above-inversion layer (although 500 mb is generally above cloud tops). The important point is that the sum of $Q_e + Q_s$ (1.87 units) is easily enough to balance the total radiation loss (1.32 units) but cannot do so, since 1.41 units of latent are exported. Half of Q_s balances the radiation loss below cloud, and the other half, together with all the precipitation, does not quite balance the radiation loss of the middle layer. The heat import at high levels makes up the difference. The upward - directed dashed arrows show the important "heat pump" function of the cumuli.

Convective clouds play an even more crucial role in the operation and energetics of the equatorial zone; they provide the release mechanism for most of the latent heat energy acquired from the sea over the entire tropics. Here giant cumulonimbus towers abound (Figure 24) but intermittently, bunched into the wavelike and vortical perturbations, with horizontal diversions ranging from about 200 to 2000 km.

The heat budget for the equatorial zone is dissected in Figure 25. Here we are examining total heat content ($Q = C_pT + Agz + L_q$) The input from the ocean is computed as 70 percent that of the trade-wind belt. Q_e was obtained from the transfer formula and Q_s was found as residual in an energy budget which may have exaggerated its magnitude, but not by a two factor. The main feature is the high heat export aloft. In their detailed study, Riehl and Malkus (1958) showed that the penetrative cloud towers were necessary to get this heat energy upward, balancing radiation losses and providing the crucial export.

In trade zone and trough together, the ocean provides a total $Q_s + Q_e$ of 3.18 units. Of this, 73 percent is eventually lost locally by radiation from the tropical atmosphere, leaving only 27 percent of the heat energy to ship poleward across the subtropical ridge. Only a few percent of this heat is ever converted into motions. As well as an inefficient heat engine, we see that the atmosphere also operates a very leaky fuel pump!

Figure 21 (after Wyman et al., 1946). Typical photograph of tropical cumulus seen from 20,000 ft. The easterly trade blows from left to right. Made north of Puerto Rico on April 25, 1946.

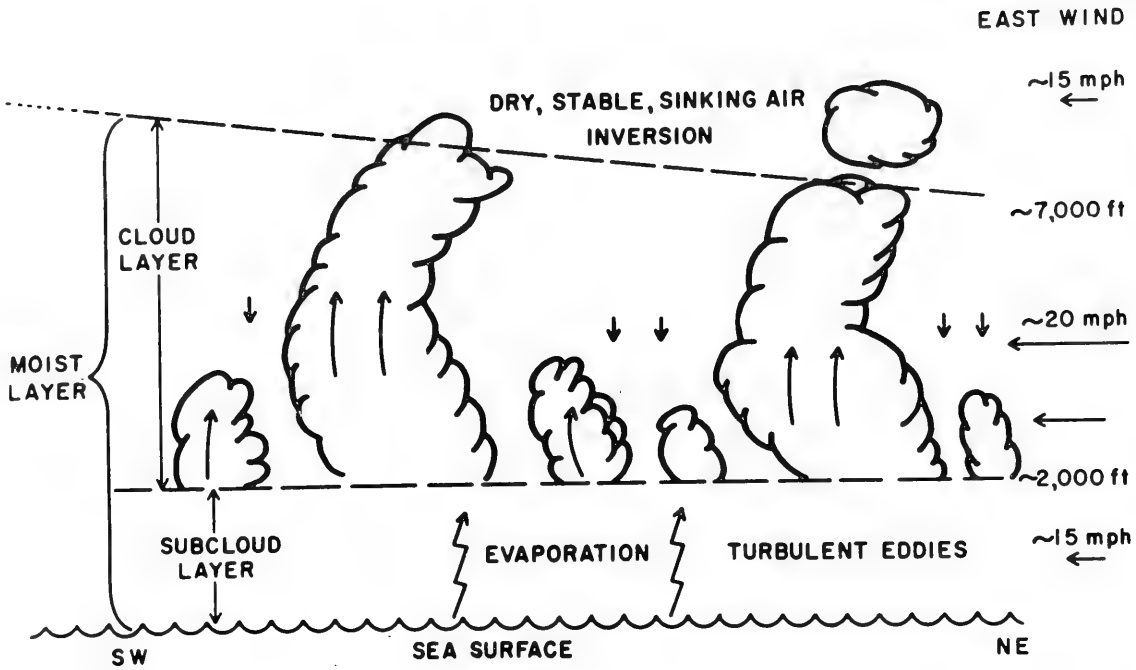

Figure 22 (after Malkus, 1962). Schematic vertical cross-section along the path of the trade winds.

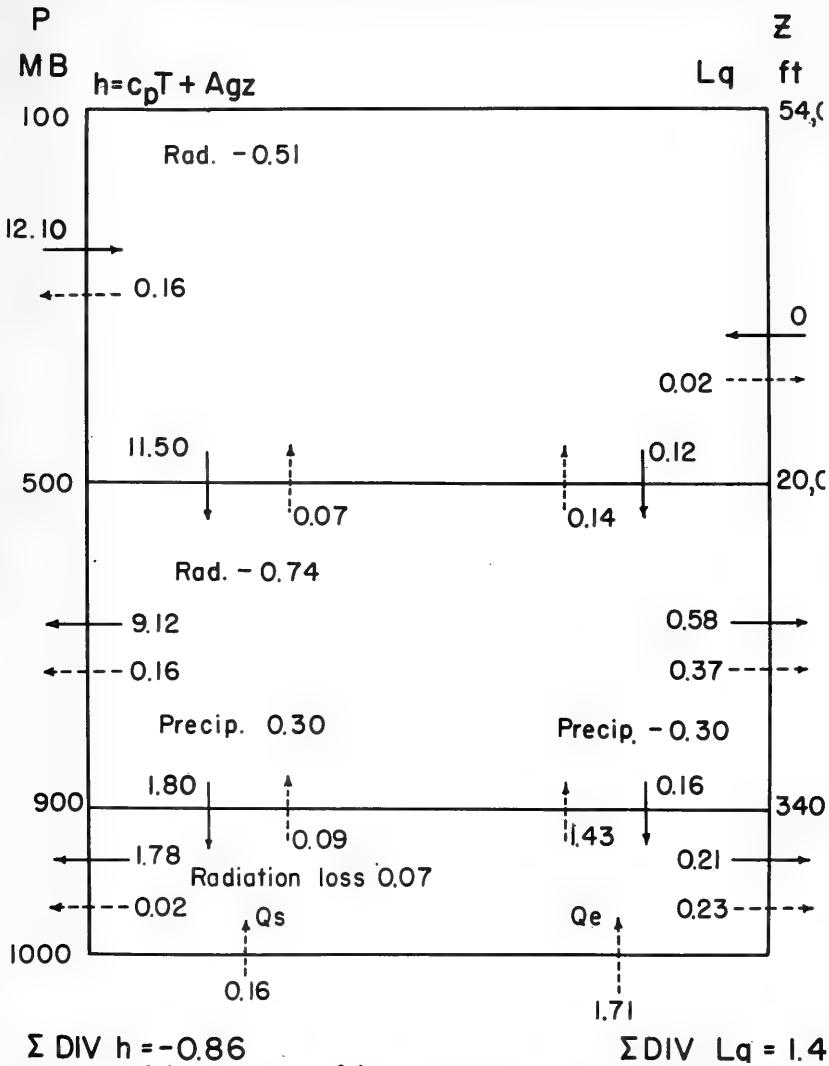

Figure 23 (after Colon, 1960). Heat energy budget of the trade-wind belt 10-20°N. Unit 10^{15} cal/sec, Left: Sensible heat plus potential energy. Right: Latent heat. Horizontal solid arrows: imports and exports due to average mean motions. Dotted horizontal arrows: Imports and exports due to departures from mean motions. Solid vertical arrows: Transports due to mean large-scale subsidence. Dashed vertical arrows: Transports due to cumulus clouds.

Figure 24 (after Malkus, 1962). Typical photograph of giant cumulonimbus in equatorial trough zone. Cloud tops 35,000-40,000 ft in incipient disturbance.

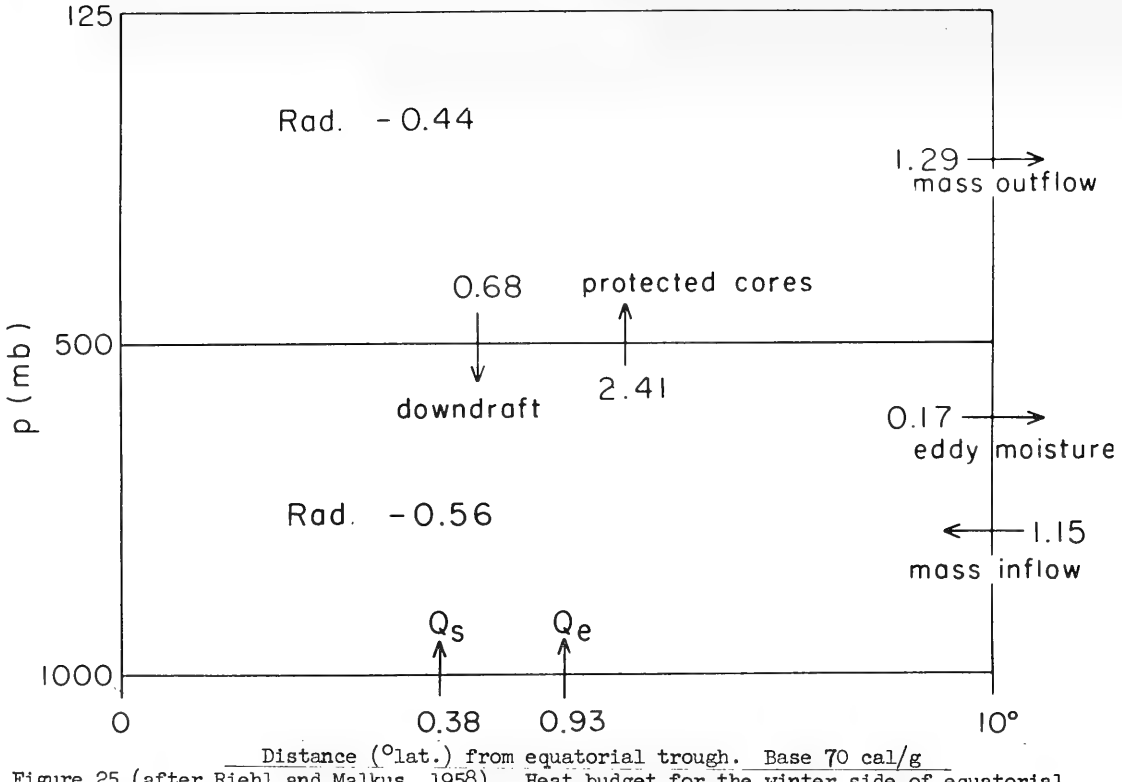

Figure 25 (after Riehl and Malkus, 1958). Heat budget for the winter side of equatorial trough zone. Fluxes in 10^{15} cal/sec are for total heat energy ($Q = C_pT + Agz + Lq$) for 10°-latitude belt. Troposphere divided into two layers, 1000-500 mb and 500-125 mb. Vertical arrows denote fluxes required for joint heat energy and mass balance in each layer, hypothesized due to protected cumulonimbus cores partially compensated by downdrafts.

The interaction between exchange and air circulation has been re-emphasized in this last discussion. The patterns of exchange are patently somewhat different in the equatorial trough zone from what they are in the trades - their relations to convective clouds and cloud distributions are also strikingly different.

The fluxes themselves are more variable in the trough zone than in the steadier trades. Frequent disturbances dominate the scene here, particularly in summer. By producing large clouds, these disturbances provide the mechanism which make the main product of sea-air exchange (moisture) usable in the atmosphere.

In the trough zone, another imprint of the disturbances is the much increased Q_s/Q_e ratio. The important documentation of why and how this ratio is higher in disturbed zones is taken up by Garstang in the following contribution to these Proceedings. We merely conclude here with two important questions which bridge the two topices; these are:

1. How do disturbances affect sea-air interaction in the tropics?

2. What role does sea-air interaction play in the life and growth of disturbances?

Concerning the first question, the foregoing has already given a clear indication that tropical disturbances are critical in regulating sea-air exchange. Garstang's work illustrates this in a rather disturbing way, in that the results suggest that we may have to make drastic changes in the accepted climatological exchange picture. This could upset the global budgets and part of oceanography as well.

In respect to the second question, we have firm evidence that in the hurricane stage, local sea-air fluxes play a large and crucial role in the machinery of the storm's heat engine (Malkus and Riehl, 1960). In sub-hurricane disturbances, we do not know what the role of local exchange is, nor do we yet have adequate models to form a framework for such a study. Quantitative observational studies of the sort described in the following paper by Garstang thus constitute the essential next step.

REFERENCES

Avsec. D. 1939: Thermoconvective eddies in air. Application to meteorology. Scientific and technical pub. of Air Ministry Work of Inst. of Fluid Mech. of Fac. of Sci., Paris, No. 155. Published (in French) at Ed. Blondel la Rougery., 7, Rue St. Lazare, Paris.

Bryan, K. 1962: Measurements of meridional heat transports by ocean currents. Jour. Geophys. Res., 67, 3403-3414.

Budyko, M. I. 1956: The heat balance of the earth's surface. Gidrometeorologicheskoe izdatel'stvo, Leningrad, 255 pp. (Translated by Nina A. Stepanova; translation distributed by U. S. Weather Bureau, Washington,D.C.1958).

Colón, J. 1960: On the heat balance of the troposphere and water body of the Caribbean Sea. National Hurricane Res. Proj., Rep't No. 41, U. S. Dept. of Commerce, Washington, D.C. 65 pp.

Deacon, E. L.; P.A. Sheppard; and E. K Webb 1956: Wind profiles over the sea and the drag at the sea surface. Austral. J. Phys., 9, 511-541.

Deacon, E. L. and E. K. Webb 1962: Interchange of properties between sea and air. Small-scale interactions. Chap 3, The Sea, Vol., 1, 43-87. Interscience Publishers, New York and London.

Garstang, M. 1964: The distribution and mechanism of energy exchange between the tropical oceans and atmosphere. Phd Dissertation, Dept. of Meteorology, The Florida State University, Tallahassee, Florida. 177 pp.

Jacobs, W. C. 1951: Large-scale aspects of energy transformations over the oceans. Compendium of Meteorology, Amer. Met. Soc., 1057-1070.

Jacobs, W. C. 1951a: The energy exchange between the sea and the atmosphere and some of its consequences. Bull. Scripps Inst. Oceanog., Univ. of Calif., 6, 27-122.

Kraus, E. B. 1959: The evaporation-precipitation cycle of the trades. Tellus, 11, 147-158.

Krueger, A.F. and S. Fritz 1961: Cellular cloud patterns revealed by Tiros I. Tellus, 13, 1-7.

Lavoie, R. L. 1963: Some aspects of the meteorology of the tropical Pacific viewed from an atoll. Sci. Rep't. No. 5, Meteorology Div., Hawaii Inst. of Geophysics, Univ. of Hawaii.

Malkus, J. S. 1956: On the maintenance of the trade winds. Tellus, 8, 335-350.

Malkus, J. S. 1957: Trade cumulus cloud groups: Some observations suggesting a mechanism of their origin. Tellus, 9, 33-44.

Malkus, J. S. 1962: Interchange of properties between sea and air. Large-scale interactions. Chap. 4, The Sea, Vol., 1, 88-294.

Malkus, J. S. and H. Riehl 1960: On the dynamics and energy transformation in steady state hurricanes. Tellus, 12, 1-20.

Malkus, J. S. and H. Riehl 1964: Cloud structure and distributions over the tropical Pacific Ocean. Univ. of Calif. Press, Berkeley, Calif., 229 pp.

Picture of the Month 1963: Monthly Weather Review, 91, 2.

Riehl, H. and J. S. Malkus 1958: On the heat balance in the equatorial trough zone. Geophysica (Helsinki), 6 (3-4), 503-538.

Roll, H. U. 1965: On the present state of knowledge on air-sea boundary layer problems. Proc. Sea-Air Interaction Conf., Tallahassee, Florida, Feb. 1965, pp 31-63.

Sheppard, P. A. 1958: Transfer across the earth's surface and through the air above. Q. J. Roy. Met. Soc., 84, 205-224.

Shibata, E. 1964: The atmospheric tide hypothesis on the diurnal variation of cloudiness in the tropics. M. A. dissertation, Dept. of Meteorology, Univ. of Calif. (Los Angeles), 82 pp.

Stern, M. E. and J. S. Malkus 1953: The flow of a stable atmosphere over a heated island, II. J. Meteor., 10, 105-120.

U. S. Weather Bureau 1938: Atlas of Climatic Charts of the Oceans. Gov't. Printing Office, Washington, D. C., Weather Bureau No. 1247, 130 pp.

Woodcock, A. H 1958: The release of latent heat in tropical storms due to the fall-out of sea-salt particles. Tellus, 10, 355-371.

Wyman, J. et al. 1946: Vertical motion and exchange of heat and water between the air and sea in the region of the trades. Unpublished report on file at The Woods Hole Oceanographic Institute, Woods Hole, Mass.

SENSIBLE AND LATENT HEAT EXCHANGE IN LOW LATITUDE SYNOPTIC SCALE SYSTEMS

Michael Garstang
Florida State University
Tallahassee, Florida

ABSTRACT

The transfer equations are applied to a set of 46 days of data collected from an oceanographic research vessel on a station in the low latitude western Atlantic. In this region the lapse rate and shear in the boundary layer of the atmosphere is such that the transfer equations may be applied with a reasonable degree of confidence. In particular, the most accurate results are likely when large transfers occur, the least accurate when small transfers occur. Under these conditions a linear dependence of the eddy exchange coefficient with wind speed and stability were used to compute latent and sensible heat transfer from time averages over 1 hour of specific humidity, temperature and wind speed at 6 m and at the sea surface. Sea surface temperatures were measured at 10 cm and compared with infrared radiometer measurements.

Individual synoptic scale systems that moved over or close to the point of observation are examined. Over limited regions of these disturbances latent and sensible heat transfers are found to increase by an order of magnitude. Integrated over the whole disturbance the energy flux is found to be double the undisturbed values. By using both streamline analysis and a rainfall amount and occurrence technique, the frequency and size of synoptic systems are determined. This makes possible the construction of summer, winter and annual maps of latent and sensible heat transfer for the tropical Atlantic. Significant differences are found when compared with results of earlier workers. The role of synoptic scale disturbances in the atmospheric energy balance is emphasized by these results.

I. INTRODUCTION

Considerations of the energy sources, conversions and transports in the earth-atmosphere system soon lead to the conclusion that the tropical oceans play an extremely important role in the heat and energy balance of the atmosphere. The greater part of the incoming short wave solar radiation in either direct or diffuse form is absorbed at the earth's surface. Before this energy can be utilized by the atmosphere it must be transferred across the earth-atmosphere interface. Therefore, the atmosphere is fuelled mainly from below. As shown by Malkus (1962, p. 93) and others, the most important transfer process at the earth-atmosphere interface is evaporation which provides about half of the atmosphere's fuel in the latent form of water vapor. More than half of this water vapor fuel is supplied to the lower troposphere by the tropical oceans between 30°N and 30°S latitude. If we add to these considerations the observation that the overall radiation balance of the earth-atmosphere system is positive between about 35°N and 35°S latitude and negative poleward, the validity of the opening statement is justified in general terms.

In the tropical regions of heat input the net transfer of water vapor and sensible heat is from the ocean to the atmosphere. Shear turbulence within the first tens of meters of the trades insures thorough mixing and upward transport of both water vapor and sensible heat. Turbulent eddies continue the upward transport through the subcloud layer to the cloud layer where convective cells, in the form of cumulus clouds, probably play the dominant role in the vertical transport of energy. Within the undisturbed trades high values of wind steadiness occur through a considerable depth of the lower troposphere. Under these undisturbed conditions, gradients are likely to stabilize and the energy input at the surface will reach an equilibrium value dependent upon the vertical removal from the surface and upward transportation of energy. Riehl, Malkus and others (1951) demonstrated that these processes create a moist convective layer gradually deepening along the airflow. In the trade wind regions of high evaporation most of the moisture is retained in vapor form rather than rained back into the oceans. This accumulated water vapor is transported equatorward "at a rate of energy export easily two orders of magnitude greater than the rate of kinetic energy consumption by all the global winds and sea currents combined." (Malkus, 1962.)

Within the equatorial trough region much of this water vapor is condensed, releasing its latent heat, which is carried to great heights in cumulonimbus clouds. Riehl and Malkus (1958) have shown that relatively few such large clouds concentrated in a limited number of synoptic scale systems (e.g., the vortical and wave-like pertubations common in this region) are able to transport this energy, now in the form of sensible heat and potential energy. But now a distinction should be made between suggestions based upon mean budget conditions and deductions based upon day-to-day synoptic changes. If average trade wind conditions prevail for some period of time, gradients

of water vapor and temperature will approach some constant value and the magnitude of the energy transports in the trades will be governed by this. Within the trade wind-equatorial trough system synoptic scale disturbances will produce internal convergences of water vapor and sensible heat and a vertical flux of energy. But synoptic scale systems, as was shown by the CRAWFORD cruise of 1957 (Garstang, 1958), significantly increase the transport of both latent and sensible heat from the ocean to the atmosphere. Gradients, particularly of temperature, in the air immediately above the sea surface steepen markedly and wind speeds increase during synoptic disturbances. The total flux of water vapor and sensible heat at the surface over the area of a synoptic disturbance is, therefore, likely to be significantly greater than during undisturbed conditions. Thus the mean picture is constrained by overall planetary budget requirements and departures from it are primarily due to the travelling synoptic systems which form a vital link between the ocean and the atmosphere. An attempt will be made here to evaluate the role that organized synoptic scale disturbances play in determining the distribution of latent and sensible heat transfer over the tropical oceans.

II. ANALYTICAL TOOLS AND AVAILABLE DATA

In restricting our attention to the tropical oceans we encounter the fortunate situation that the lower decameters of the tropical atmosphere are by and large barotropic and close to neutral stratification. Under these circumstances, the most practical equations for the computation of the flux of latent and sensible heat are the bulk aerodynamic equations expressed below:

$$LE = Q_e = \rho\, L\, C_D\, (\bar{q}_o - \bar{q}_a)\, \bar{u}_a \qquad (1)$$

$$Q_s = \rho\, C_p\, C_D\, (\bar{\theta}_o - \bar{\theta}_a)\, \bar{u}_a\,, \qquad (2)$$

where Q_e and Q_s are, respectively, the eddy vertical transport of latent and sensible heat and are directly proportional to the differences between the mean specific humidity and mean potential temperature measured at the surface and at some point above the surface multiplied by the mean wind speed measured at the same point above the surface. If the atmosphere above the sea surface is close to neutral stratification, then the most restrictive assumptions that must be made in order to arrive at the equations are most nearly satisfied.

Forty-six days of observations were made on two separate cruises, each of 23 days duration, on a fixed station. Both cruises took place during the months of August and September. The first in 1957 when the ship (R. V. CRAWFORD, Woods Hole Oceanographic Institution, Garstang (1958)) was stationed near 11°N 52°W; the second in 1963 when the same ship was stationed near 13°N 55°W (La Seur and Garstang (1964)).

The degree to which conditions in the air above the water departed from neutral stratification was assessed by computing hourly values for the bulk Richardson Number, R_B,

$$R_B = \frac{g}{T} z \frac{\Gamma_h}{\Gamma_m^2} \frac{\bar{\theta}_a - \bar{\theta}_s}{\bar{u}_a^2} \qquad (3)$$

where g is the acceleration of gravity; T is the air temperature in degrees Kelvin at height a; z is the height of the observation (6.0 m) above the sea surface; $\bar{\theta}_a$ the potential temperature at 6.0 m; $\bar{\theta}_s$ the potential temperature at the sea surface; $\bar{u}_a$ the wind speed at 6.0 m; each of the latter quantities averaged over 1 hour centered on the hour. The coefficients Γ_h and Γ_m represent the gradients of heat and momentum, and are defined as

$$\Gamma_m = \frac{1}{\bar{u}_a} \frac{\delta u}{\delta \ln z} \qquad (4)$$

and

$$\Gamma_h = \frac{1}{\bar{\theta}_a - \bar{\theta}_s} \frac{\delta \theta}{\delta \ln z} \qquad (5)$$

According to Deacon and Webb (1962) at heights of about 4.0 to 8.0 m and for conditions from neutral to moderate thermal stratification, Γ_h and Γ_m have values around 0.1. Thus the ratio in (3) was taken as equal to 10.

Ninety-six percent of the observations obtained on the CRAWFORD fall in the range

$$-0.325 < R_B < +0.025 \quad ;$$

sixty percent fall in the range

$$-0.040 < R_B < +0.020.$$

Conditions are, therefore, relatively close to neutral stratification. The departure from neutral stratification is a combined effect of lapse rate and wind shear. If we consider the bulk of the observations in the range $-0.325 < R_B < +0.025$ and assume a mean wind speed of 5.0 m sec^{-1}, an air-sea temperature difference ranging between -4.06C (sea warmer than air) and +0.21C (air warmer than sea) can be predicted from equation (3). The actual maximum range (except for three observations in showers) observed was -2.88C to +0.17C . It is, therefore, concluded that the most critical parameter in determining stability is the wind speed and, more important, the stronger the wind, the more closely governing conditions are met.

The saving grace for formulations such as (1) and (2) for the computation of sea-air energy transfers is that, by and large, the higher the transfer, the more accurately these formulae predict it. As will be shown in later sections, the largest exchange occurs at times of strong winds. Here the shearing is unlikely to permit maintenance of large lapse rates over the open ocean and, even if these did occur, the strong wind shear keeps the Richardson number in a reasonable range. When the wind approaches calm and the air-sea temperature difference remains large (unlikely), the formulae are in trouble and give particularly bad results for sensible heat exchange. But all the exchanges are then relatively small and perhaps even negligible for large scale budget and dynamic considerations.

The preceding establishes the fact that if the bulk aerodynamic equations can be used at all, they can probably be best applied to conditions prevailing over the tropical oceans. However, it is also quite clear that the drag coefficient, C_D, is not a constant but is a function of, at least, height (z); wind speed ($\bar{u}$) and stability (R_B). By applying considerations outlined by Monin and Obukhov (1954) it can be shown that

$$C_6^* - C_{11}^* \left(\frac{\bar{u}_{11}}{\bar{u}_6}\right)^2 = a\, R_B \left[C_6^{*3/2} - C_{11}^{*3/2} \left(\frac{\bar{u}_{11}}{\bar{u}_6}\right)^2 \right] \qquad (6)$$

where C^* is the drag coefficient for neutral or adiabatic conditions and the subscripts 6 and 11 refer to heights (in meters) above the sea surface. A linear dependence of the drag coefficient upon height and wind speed under adiabatic conditions was assumed using values obtained by Deacon and Webb (1962). In practice (6) was approximated and the contribution of the term in brackets on the right hand side was neglected. Figure 1 shows the functional relationship between the remaining terms of the above expression. Based upon these considerations the drag coefficient was then computed from

$$C_6 = (1.46 + 0.07\, \bar{u}_6 - 4.2\, R_B) \times 10^{-3} \quad . \qquad (7)$$

Finally, before using equations (1), (2) and (7) to compute the transfer of latent and sensible heat, an evaluation of the accuracy of the measurements must be made. Wet- and dry-bulb temperatures and wind speeds were measured at 6.0 m above the sea surface at a point 4.7 m on a pulpit ahead of the bow of the vessel. Sea surface temperatures were measured 10 cm below the surface and 4.5 m ahead of the vessel. The temperature sensors were thermistors and the wind speed was obtained from a recording cup anemometer. Care was taken to avoid radiation effects. Supplementary temperature measurements were made around the ship (out to 140 ft) on three different occasions. These measurements were used to determine any extraneous effects on the pulpit observations. Wind speeds were checked for ship effect in a manner similar to that described by Deacon et al. (1956). It is felt that

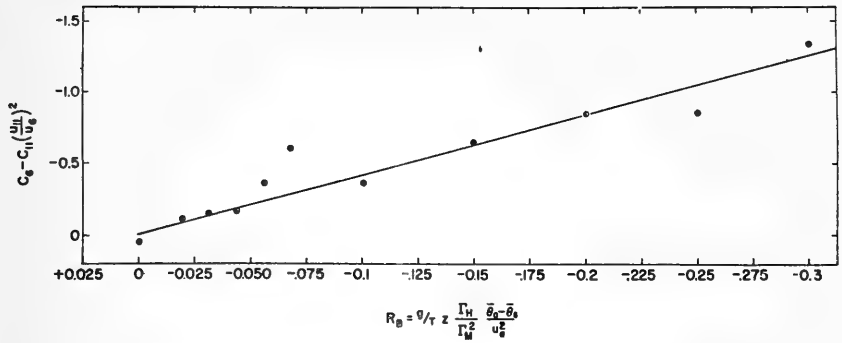

Figure 1. Departures from the neutral value of the drag coefficient at 6.0 m as a function of stability expressed in terms of the bulk Richardson number.

with these precautions and the corrections later applied, the observations are representative of ambient conditions over the open ocean. 1/

III. SYNOPTIC VARIATIONS OF LATENT AND SENSIBLE HEAT TRANSPORT

In order to examine the distributions of latent and sensible heat transfer under varying synoptic scale conditions, each observing period was subjected to careful analysis. The objective was twofold:

1. To delineate synoptic scale disturbances and categorize each system with respect to intensity;

2. To relate the observations made by the ship to each system and delineate the sector intensity that was sampled.

To achieve this, conventional methods of analysis were supplemented by a number of other techniques. Among these were: divergence, vorticity and vertical motion computations using the Bellamy (1949) triangle method for each of the five triangles shown in Figure 2, rainfall analysis of six islands in the Lesser Antilles using a classification based upon occurrence and amount, and a method using wind speed and steadiness as a measure of the occurrence and strength of a synoptic scale disturbance.

1/ A more complete treatment of ship effect is contained in a doctoral dissertation(Garstang (1964)). Similarly, details of analysis and computation referred to in subsequent sections of this paper may be found in the same source.

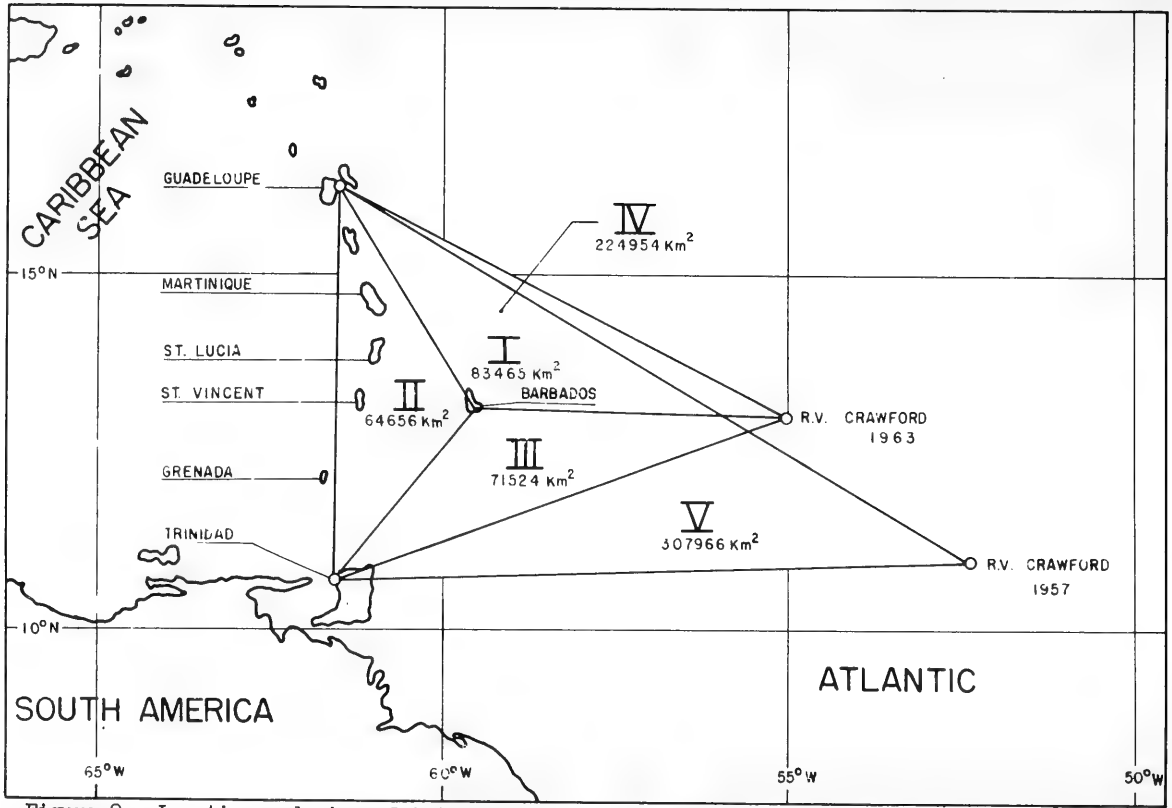

Figure 2. Location and size of triangles used for the computation of divergence, relative vorticity and vertical motion:
(I) CRAWFORD (1963) / Guadeloupe / Barbados;
(II) Guadeloupe / Trinidad / Barbados;
(III) Barbados / Trinidad / CRAWFORD (1963);
(IV) CRAWFORD (1963) / Guadeloupe / Trinidad;
(V) CRAWFORD (1957) / Guadeloups / Trinidad.

Once the systems had been identified, time distributions of latent and sensible heat could be obtained by calculating the hourly values for all 46 days and obtaining average values ($\overline{Q}_e$ and $\overline{Q}_s$) for each of the systems. Table 1 shows the initial broadscale breakdown. In the first two rows all undisturbed states can be compared with all disturbed states. The results from both sets of observations show the same trend: more heat is transferred from the ocean to the atmosphere under disturbed conditions than during undisturbed conditions. The increase in latent heat transfer is not as large as in the case of sensible heat transfer. The ratio of $\overline{Q}_e$ undisturbed versus $\overline{Q}_e$ disturbed is 1.17 in 1957 and 1.07 in 1963; but for $\overline{Q}_s$ it is 7.74 and 2.04, respectively. On each cruise weakly disturbed modes were fairly frequent and strong trade wind conditions relatively few, so that it is perhaps more meaningful to examine the transfers under weak and moderate trades and moderately disturbed modes. Under these conditions the ratio of undisturbed to disturbed for $\overline{Q}_e$ increases to 1.94 in 1957 and 1.25 in 1963; and for $\overline{Q}_s$ 11.70 and 2.16, respectively. The relative increase in the Bowen ratio remains essentially the same for both of the above comparisons. While the amount of sensible heat made available to the atmosphere never exceeds 8 percent of the latent heat transfer, it is significant to note that:

1. This is an average figure throughout the whole disturbed period;

2. For periods up to 6 hours within a disturbed region, the ratio of sensible heat to latent heat may be greater than 0.20 as opposed to undisturbed conditions when, for similar period, the sensible heat transfer may be in the opposite direction, i.e., from the atmosphere to the ocean.

3. This energy is directly available to contribute to the instability of the subcloud layer and the development of convective cloud.

Therefore, it is suggested that the role of sensible heat transfer in the formative and developing stages of tropical disturbances is a critical one.

The synoptic scale fluctuations of exchanges are examined in more detail in Table 2. The mean values for each regime or mode are based upon values computed for each hour through each state. Little change in Δq is noted between the various states. The mean temperature difference, $\Delta\overline{T}$ however, shows a systematic and fairly large change from undisturbed to disturbed conditions. Mean sea-air temperature differences in excess of 1C occur during the disturbed modes, while under the strong trade regime $\Delta\overline{T}$ is less than 0.3C. Sea surface temperatures were observed to vary little between periods, although slightly lower temperatures were noted during the strong trade wind regime as opposed to the weak regime. The dominant control upon $\Delta\overline{T}$ is produced by variations in air temperatures. Lower air temperatures during the disturbed modes are ascribed to reduced insolation due to cloud cover, direct cooling by rain showers, as well as the descent from aloft of cool air associated with the condensation-precipitation cycle. These processes

TABLE 1

HEAT TRANSPORT FROM THE OCEAN TO THE ATMOSPHERE UNDER VARYING SYNOPTIC CONDITIONS

	$\bar{Q}_e$		$\bar{Q}_s$		$\bar{Q}$		Bowen Ratio	
	1957	1963	1957	1963	1957	1963	1957	1963
Undisturbed trades	265.2	371.8	3.1	14.0	268.3	385.8	0.012	0.038
Disturbed modes	309.4	396.2	24.0	28.5	333.4	424.7	0.078	0.071
Weak and moderate trades	254.2	326.0	3.0	14.4	257.2	340.4	0.012	0.044
Moderately disturbed modes	492.8	408.2	35.1	31.2	527.9	439.4	0.071	0.076

TABLE 2

SYNOPTIC SCALE EXCHANGE FLUCTUATIONS IN THE VICINITY OF 11°N TO 13°N, 52°W TO 55°W DURING THE MONTH OF AUGUST AND PART OF SEPTEMBER FROM THE 1957 AND 1963 R. V. CRAWFORD CRUISES

	$\bar{\Delta T}$ C	$\bar{\Delta q}$ g kg^{-1}	$\bar{u}$ m sec^{-1}	$\bar{C}_{D_3}$ 10^{-3}	$\bar{R}_B$	$\bar{Q}_e$ cal cm^{-2} day^{-1}	$\bar{Q}_s$ cal cm^{-2} day^{-1}	$\bar{Q}$ cal cm^{-2} day^{-1}	Mean Bowen Ratio
Strong trade regime $\bar{u}$ >7.7 m sec^{-1} $\bar{S}$ > 98%	0.290	5.54	8.12	2.062	-0.008	544.6	12.6	557.2	0.026
	0.002	4.47	7.68	1.992	0.001	407.4	3.6	411.1	0.009
Moderate trade regime 5.01-7.6 m sec^{-1} $\bar{S}$ > 97%	0.50	5.24	5.71	2.020	-0.037	356.5	13.4	369.9	0.040
	-0.08	4.61	5.47	1.827	0.004	272.0	-0.6	271.4	-0.002
	0.54	4.78	5.23	2.004	-0.042	295.7	15.4	311.1	0.049
	0.09	5.36	5.15	1.913	-0.022	314.8	3.9	318.7	0.012
	0.20	4.39	5.04	1.933	-0.029	245.4	5.2	250.8	0.046
Weak trade regime < 5.0 m sec^{-1} $\bar{S}$ > 97%	0.53	5.65	4.75	2.043	-0.060	312.6	12.5	325.1	0.041
	0.68	6.06	4.73	2.047	-0.062	340.0	17.8	357.8	0.048
	0.52	5.16	3.96	1.963	-0.054	227.3	5.4	232.8	0.030
	0.10	5.31	4.47	1.903	-0.031	254.4	2.4	256.8	0.032

(Continued)

TABLE 2, (Continued)

Weakly	0.60	5.39	5.43	2.011	-0.044	350.7	18.5	369.2	0.480
disturbed	1.09	4.56	5.02	2.791	-0.361	325.0	32.9	357.9	0.102
mode	0.76	4.41	4.33	2.475	-0.223	255.8	22.6	278.7	0.079
$\bar{u}$ 5.5	1.06	5.21	2.86	3.351	-0.418	282.1	40.5	322.7	0.123
m sec^{-1}	0.50	5.34	4.00	2.053	-0.268	268.7	12.6	284.0	0.050
$\bar{S}$ 75%	0.32	4.69	5.48	1.913	-0.016	293.2	9.5	302.8	0.035
Moderately	1.01	4.83	5.79	2.187	-0.078	355.0	32.6	387.6	0.095
disturbed	0.72	4.75	6.99	2.108	-0.038	419.2	27.2	442.5	0.083
mode									
5.5 $\bar{u}$ 7.5									
90% $\bar{S}$ 75%									
Strongly	0.74	5.27	7.67	2.109	-0.027	505.1	29.0	534.1	0.057
disturbed	0.71	4.84	9.30	2.213	-0.024	570.1	43.4	612.1	0.081
mode									
$\bar{u}$ 7.5									
m sec^{-1}									
95% $\bar{S}$ 90%									

are clearly not advective in origin, but are associated with the dynamics of the disturbance involved. While these differences between the undisturbed regime and the disturbed mode are noted, Figures 3 and 4 show that, with the exception of $\overline{\Delta T}$ in the disturbed case, there is little variation within each mode or regime. The greater dependence of $T_s - T_a$ upon wind speed in the disturbed mode is related to the fact that much lower air temperatures are observed at lower wind speeds under these conditions, as opposed to the undisturbed regime. This leads to the reverse effect in $\overline{\Delta q}$ which is higher at low wind speeds for the undisturbed case. The scalar average wind speed is similar within similar intensity categories, i.e., the weak trade regime speed is similar to the weakly disturbed mode wind speed. While it follows from the above that, given similar $\overline{\Delta q}$ and $\overline{u}$, similar $\overline{Q_e}$ should be obtained, it is also illustrated in Table 2 that the stability changes. Under the strong trade regime the stability, as indicated by R_B, is on the average, close to neutral. Maximum instability is reached in the weakly disturbed mode, returning to weakly unstable in the strongly disturbed mode. When a drag coefficient with a dependence upon stability is used, then these changes in stability are reflected in changes in C_D. The changes in C_D produce an increase in latent heat transfer during disturbed conditions even though the wind speeds and specific humidity differences are similar to those of undisturbed conditions.

Since there is a fairly systematic increase in $\overline{\Delta T}$ there is a corresponding increase in sensible heat transfer during disturbed conditions. Changes in the Bowen ratio show that this increase is greatest with respect to latent heat transfer in cases categorized under the weakly disturbed mode. This suggests that sensible heat transfer may play an important role in both the formative stages of a disturbance and in the peripheral regions of an organized disturbance.

The maximum exchange of total energy, $\overline{Q}$, takes place in the disturbed mode. The largest exchanges take place when conditions are closest to neutral stratification and, in consequence, closest to conditions which are assumed in the development of the exchange equations. Almost all of the relatively large amount of total energy transferred from the ocean to the atmosphere during undisturbed conditions is in latent form. It has been clearly established by other workers such as Riehl (1954, p. 56) and confirmed in this region by La Seur and Garstang (1964a), that the greater proportion (> 50 per cent)of tropical precipitation falls in organized synoptic disturbances. The proporation over the oceans may, in fact, be far larger than this figure. Hence, before a significant proporation of the latent heat accumulated in the tropics can be made available to the atmosphere, it must be advected into organized synoptic disturbances. Condensation and precipitation processes will release part of this latent heat directly into the disturbance. This available energy may then be used both to fuel the disturbance itself, as well as increase the potential energy in the upper levels of the tropical and equatorial atmosphere. Therefore, the synoptic disturbances, not only represent a localized maximum of energy flux, but are also regions of horizontal convergence and vertical transport of the energy supplied to the atmosphere over large regions of the tropics. The extent to which individual synoptic disturbances contribute to the energy budget of the atmosphere is examined below.

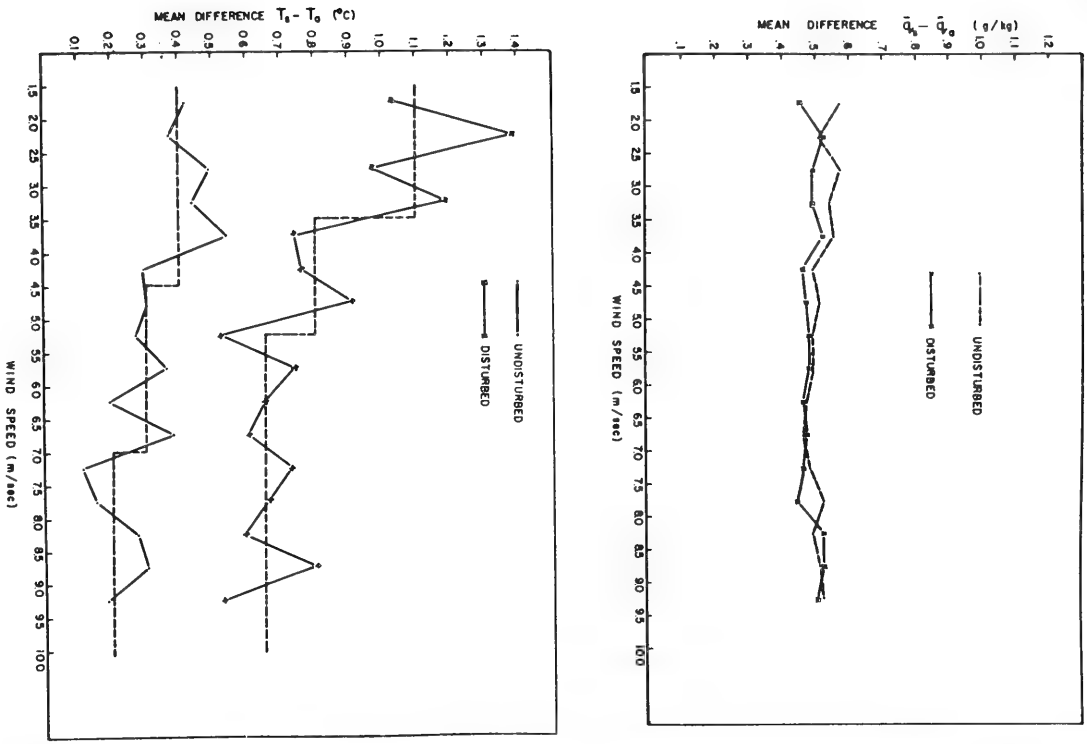

Figure 3 (Above): $\Delta\overline{q}$ as a function of wind speed for all the disturbed modes and for all the undisturbed regimes.

Figure 4 (Below): $\Delta\overline{T}$ as a function of wind speed for all the disturbed modes and for all the undisturbed regimes.

The temperature and specific humidity distributions shown in Figures 3 and 4 suggest that the time sequences presented up to this point may, given the wind field, be extended into space sequences. Table 3 shows constant values for six conditions. The spatial variation will, as pointed out above, depend upon adequate representation of the wind field. This was done by compiling composite maps for each of the disturbances considered. Surface streamline analysis, utilizing both reconnaissance and research aircraft reports and satellite pictures (in 1963), was carried out for each storm at intervals of 12 hours. Each 12-hourly chart consisted of a composite of at least 6-hourly reports. Three-hourly reports were added when available. In each of the disturbances the CRAWFORD was located well within the circulation of the system. The time section and detailed surface reports at the ship were incorporated into the analysis. A series of 12-hourly streamline analyses was then obtained for each vortex. A period, which varied between 12 hours and 102 hours, in which the storm approximated a steady state at the surface was selected. A composite of each storm was then constructed. This was done by locating all observations on the individual streamline analyses with respect to the center and neutral point. The observations were then transferred and relocated on a composite map. An isogon-isotach analysis was carried out for each composite map and the resulting streamline isotach analysis used to perform a component analysis, from which the low level field of divergence was computed. This was done for three cases. Too few observations prevented detailed kinematic analysis of the fourth case, but the streamline field could be delineated and the relative motion of the vortex shown with respect to the stationary ship. Since this happened to be the only vortex of which the center moved past the ship on the equatorial side, it is the only example where flux measurements could be made through the strong wind regions of the disturbance.

Two examples of the composite streamline fields and the associated divergence and weather are presented in Figures 5 and 9. The values of $\Delta\bar{q}$ and $\Delta\bar{T}$ given in Table 3 are shown in Figures 6 and 10, each region being defined by one or both of two criteria:

1. The speed field (limits given in Table 3);

2. The division between disturbed and undisturbed conditions given by the line of zero divergence and by the distribution of the weather.

The energy transports associated with the first example are shown in Figures 7 and 8. The dependence upon wind speed controls the major features of the distribution of Q_e, maximum values occurring within the speed maxima around the center and to the north of the center, while minimum values of Q_e are associated with the speed minima around the cols and center. Within the regions of maximum latent heat transport, values of Q_e are associated with the speed minima around the cols and center. Within the regions of maximum latent heat transport, values of Q_e exceed 600 cal $cm^{-2}day^{-1}$ over fairly large areas. These large transports are concentrated within the regions usually associated with maximum precipitation. Five centimeters of

TABLE 3

AIR-SEA PROPERTY DIFFERENCES BASED UPON TABLE 2 AND FIGS. 3 AND 4, USED TO COMPUTE ENERGY TRANSFERS FOR THE COMPOSITE DISTURBANCES

	$\bar{\Delta T}$ (C)	$\bar{\Delta q}$ (g kg^{-1})
Strong trade 7.7 m sec^{-1}	0.20	5.0
Moderate trade 5.0-7.7 m sec^{-1}	0.30	5.0
Weak trade < 5.0 m sec^{-1}	0.40	5.5
Weakly disturbed A < 3.5 m sec^{-1}	1.10	5.0
Weakly disturbed B 3.5-5.25 m sec^{-1}	0.80	5.0
Moderately and strongly disturbed > 5.25 m sec^{-1}	0.65	5.0

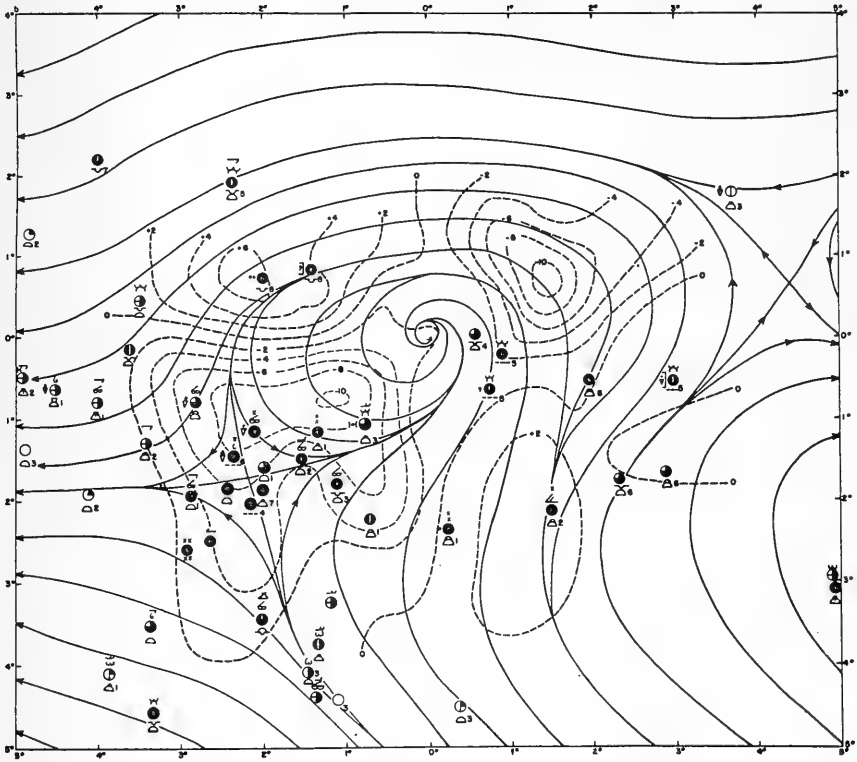

Figure 5. Streamlines (solid), divergence (dotted in units of 10^{-5}sec^{-1}) and weather based upon observations composited over the period from 0000 GMT on 15 August to 0600 GMT on 19 August 1957.

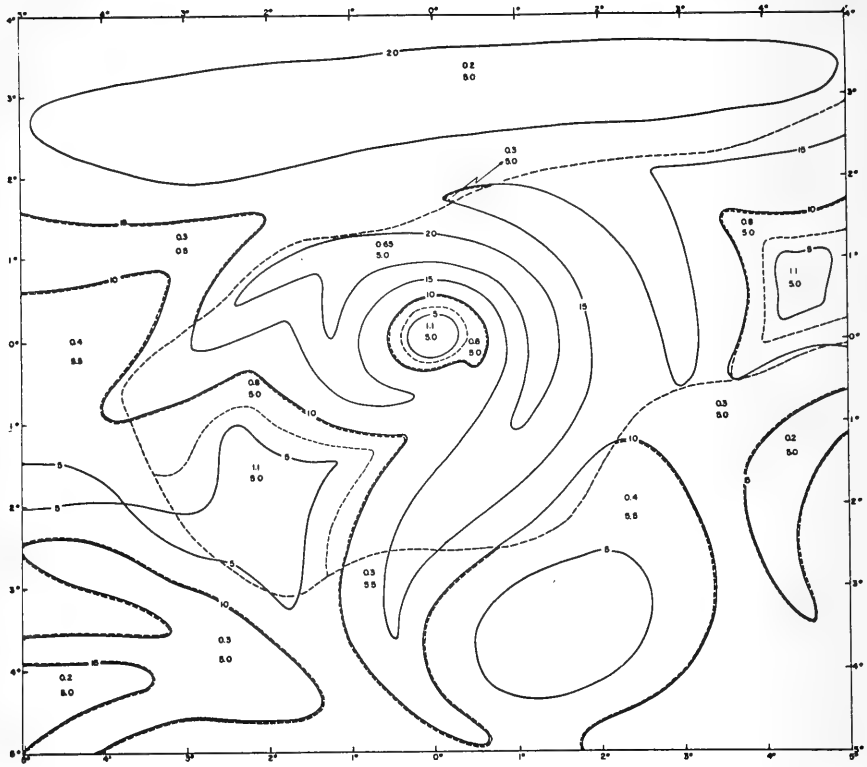

Figure 6. Isotachs (solid) and regions of constant $\Delta\overline{q}$ and $\Delta\overline{T}$ (dotted) based upon (a) the delineation of the distrubed region of the storm using the zero line of divergence and distribution of weather in Figure 5 as a guide; (b) the classification in Table 3. $\Delta\overline{T}$ is the upper and $\Delta\overline{q}$ is the lower figure in each region.

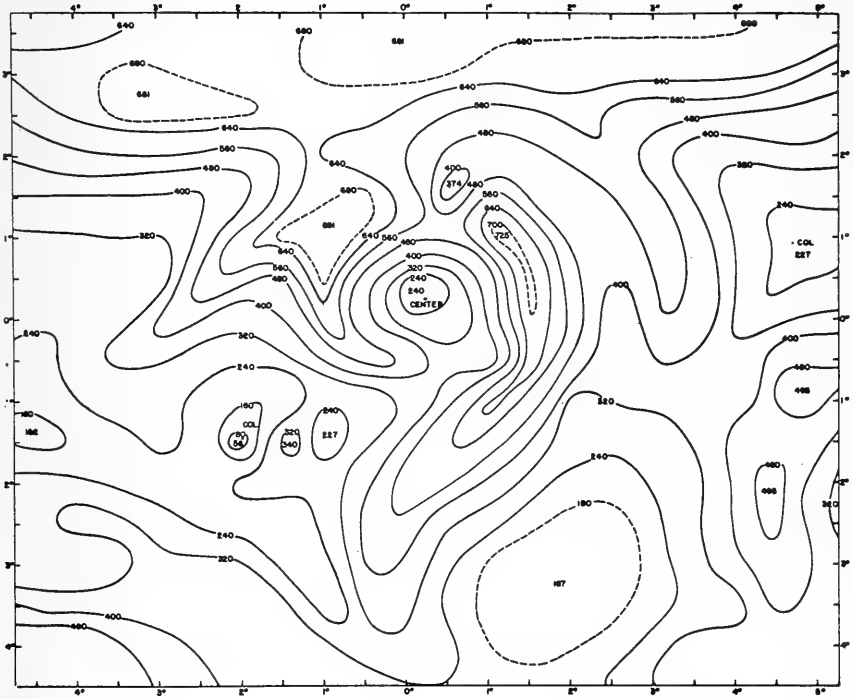

Figure 7. Latent heat transfer in units of cal cm^{-2} day^{-1} based upon Figures 5 and 6. The central values represent the highest and lowest value computed in each closed region.

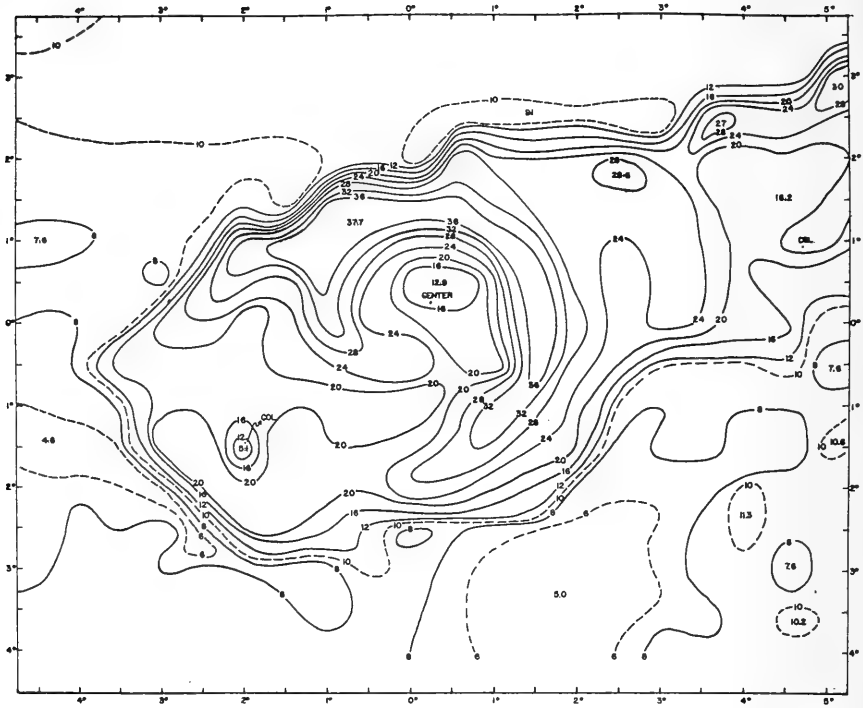

Figure 8. Sensible heat transfer in units of cal cm^{-2} day^{-1} based upon Figures 5 and 6. Notation as for Figure 7.

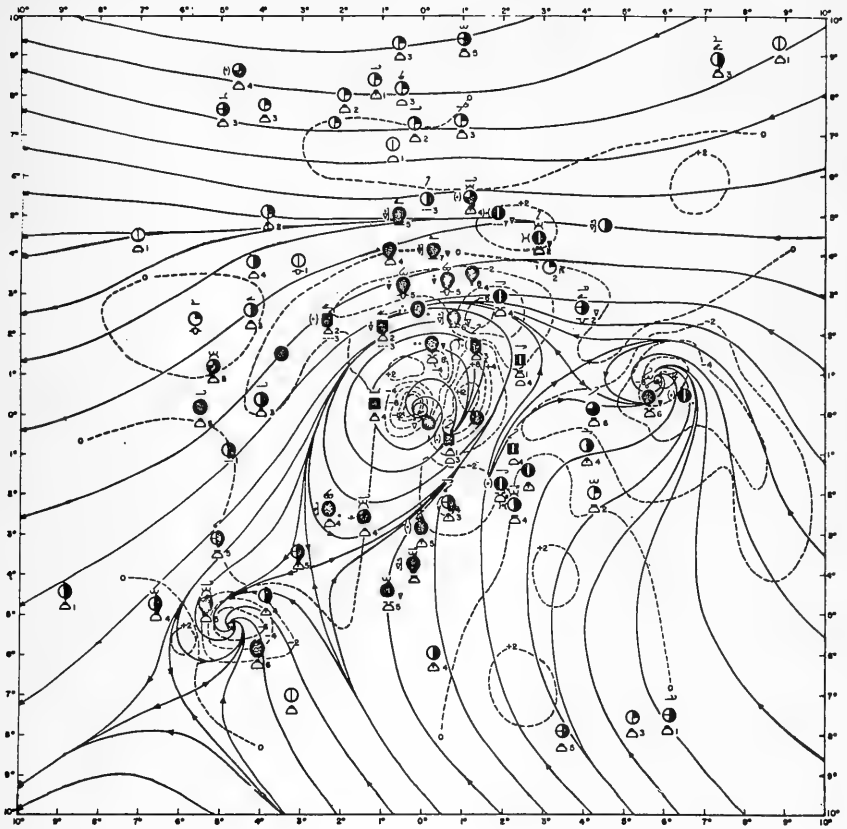

Figure 9. Streamlines (solid), divergence (dotted in units of 10^{-5} sec^{-1}) and weather based upon observations composited over the period 0600 GMT on 21 August to 1200 GMT on 21 August 1963.

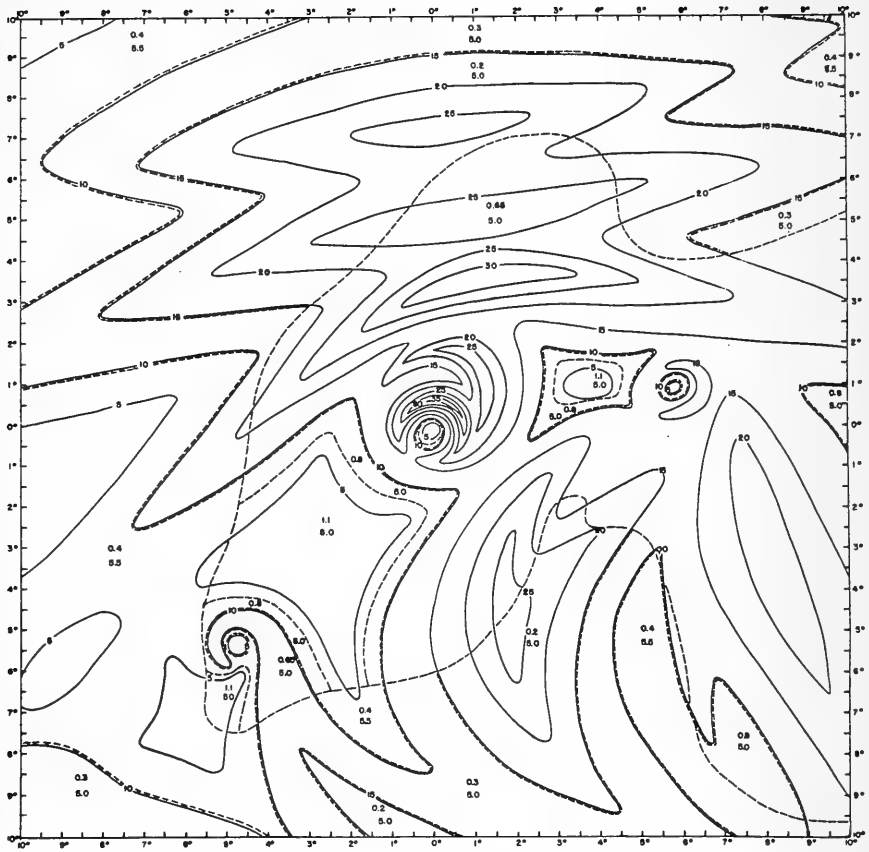

Figure 10. Isotachs (solid) and regions of constant $\Delta\overline{q}$ and $\Delta\overline{T}$ (dotted) based upon (a) the delineation of the distrubed region of the storm using the zero line of divergence and distribution of weather in Figure 9 as a guide; (b) the classification in Table 3. $\Delta\overline{T}$ is the upper and $\Delta\overline{q}$ is the lower figure in each region.

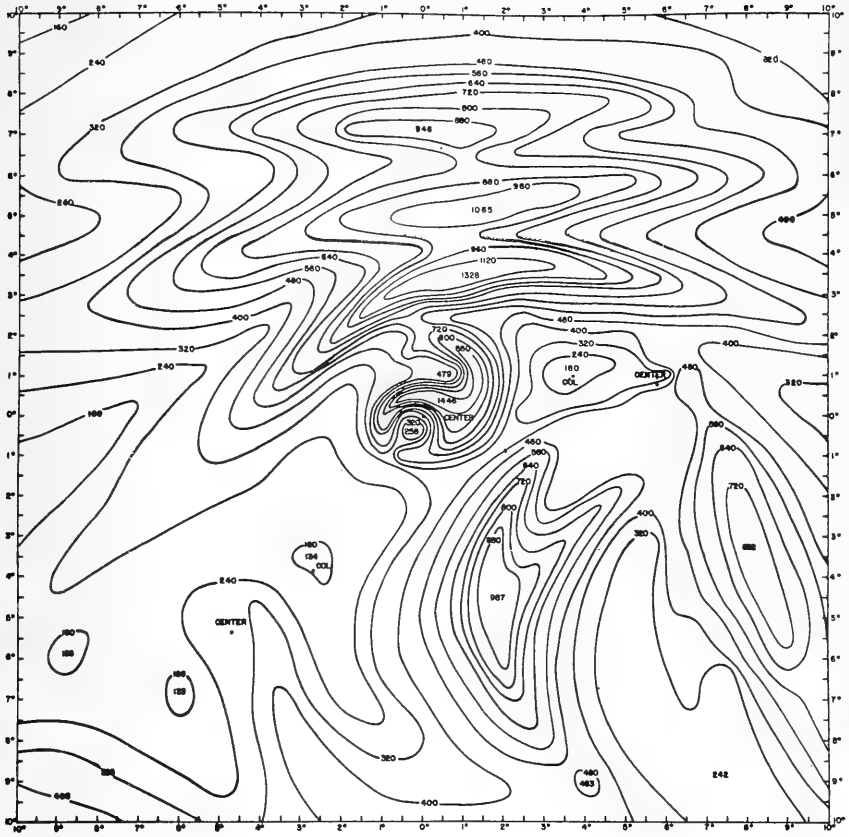

Figure 11. Latent heat transfer in units of cal cm^{-2} day^{-1} based upon Figures 9 and 10. The central values represent the highest and lowest value computed in each closed region.

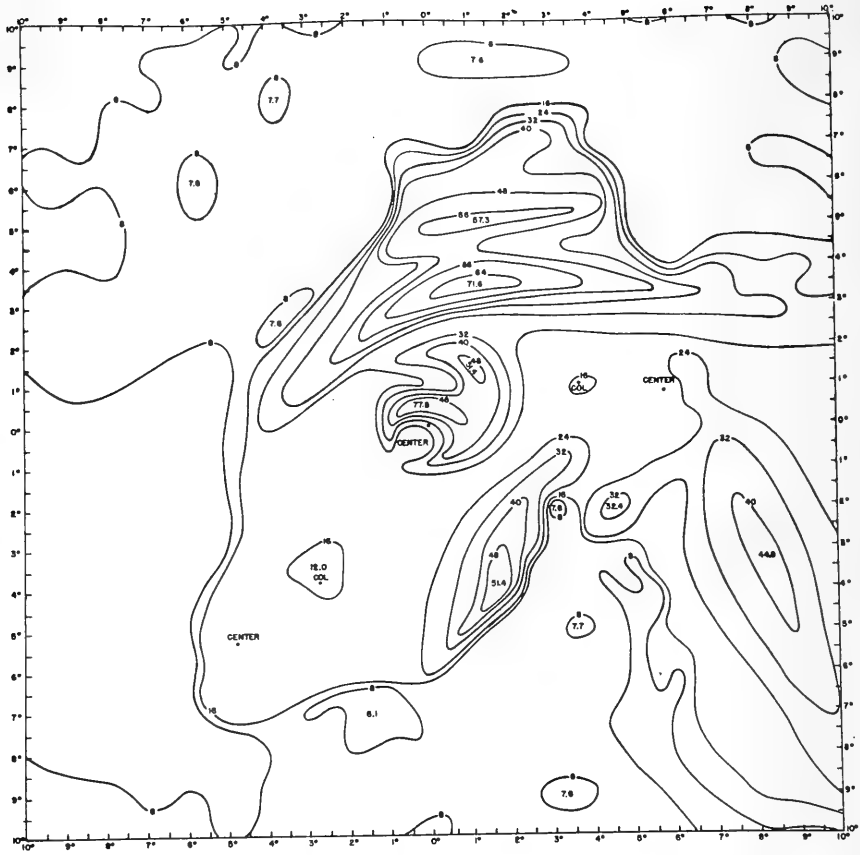

Figure 12. Sensible heat transfer in units of cal cm^{-2} day^{-1} based upon Figures 9 and 10. Notation as for Figure 11.

rain in such a region in 1 day would represent a release of about 3000 cal $cm^{-2}day^{-1}$. While the greater fraction of water vapor represented in such an energy conversion must be due to horizontal advection, a significant amount could be accounted for by the transfer processes taking place within such a region. The distribution of sensible heat transport is similar to that of the latent heat transport, with the exception that strong gradients coincide with the boundary between disturbed and undisturbed states. Since this is the boundary between the regions of maximum and minimum cloudiness and weather, maximum values of Q_s are found within the disturbed region. Values of Q_s in excess of 36 cal $cm^{-2}day^{-1}$ are observed over a wide crescent around the center of the disturbance. This means that maximum convective instability should be concentrated within this region. Total energy Q is, therefore, at a maximum within this region, exceeding 650 cal $cm^{-2}day^{-1}$ in the northern quadrant of the storm. The distributions of Q_e and Q_s for the second example are shown in Figures 11 and 12. The main features are unchanged, but there is considerable increase in the size of the transports. Latent heat transport reaches a maximum of 1446 cal $cm^{-2}day^{-1}$, and sensible heat transport, 78 cal $cm^{-2}day^{-1}$. These values can be compared with the maximum values computed by Petterssen, et al., (1962) from typical winter cases of cyclones in the western North Atlantic. Maximum values of 1440 cal $cm^{-2}day^{-1}$ for latent heat flux and 720 cal $cm^{-2}day^{-1}$ for sensible heat flux were obtained. Pyke (1964) computed values for a cyclone in the Gulf of Alaska and obtained values of 350 cal $cm^{-2}day^{-1}$ for Q_e and 216 cal $cm^{-2}day^{-1}$ for Q_s. Malkus and Riehl (1959), assuming equations essentially the same as (1) and (2), computed latent and sensible heat fluxes for a moderate hurricane within 90 km of the center of 2420 cal $cm^{-2}day^{-1}$ and 720 cal $cm^{-2}day^{-1}$. Consistent with the above, they assumed small changes in $q_s - q_a$, a decrease of 5.2 g kg^{-1} in the region 90 to 70 km to 3.5 g kg^{-1} 50 to 30 km from the center. Thus the increase in latent heat from the values observed in the above disturbances and in the trade wind regions is due to an increase in wind speed. They assumed a constant sea-air temperature difference of 2.0C. This they ascribe to adiabatic expansion during horizontal motion toward lower pressure rather than the cooling mechanisms called upon in the above disturbances. This large $\Delta\overline{T}$, together with high wind speeds, gives a large sensible heat transfer. In comparison with this value, the highest hourly mean value of Q_s observed on the CRAWFORD was 201 cal cm^{-2} day^{-1}. The values utilized by Malkus and Riehl for the moderate hurricane are, therefore, quite consistent with those values computed from the composite storm data. In turn, these are consistent with values of latent heat transfer computed for higher latitudes. The values of sensible heat transfer appear, at the most, to be 40 percent of the values observed at higher latitudes where pronounced sea-air temperature differences are observed.

Figure 13 shows the observed values of latent and sensible heat transfer every 2 hours through a composite streamline field of an equatorial vortex encountered during the 1963 cruise. Latent heat flux ranges from 252 to 938 cal $cm^{-2}day^{-1}$, while sensible heat flux ranges from -2 to 201 cal cm^{-2} day^{-1}. Regions of maximum and minimum transfer coincide with the distribution noted in the composite models presented in Figures 5 through 12.

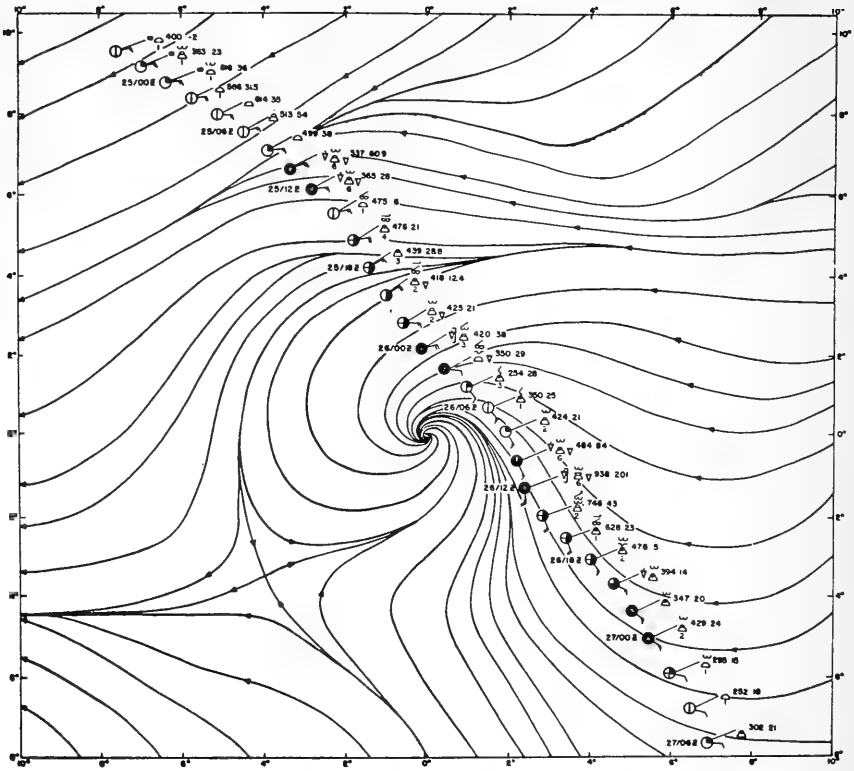

Figure 13. Streamlines based upon observations composited over the period 0000 GMT on 25 August to 0000 GMT on 27 August 1963. Observations made on the CRAWFORD are plotted every 2 hours with the corresponding values of latent and sensible heat in cal $cm^{-2}day^{-1}$ on the upper right hand side of the plotting model.

The integrated transport of latent and sensible heat was computed for all disturbances and mean values for the whole area are presented in Table 4. These mean values are compared with values which would have been obtained had the whole region been covered by a uniform trade wind, maintaining an average speed within the limits specified, for periods of 1 to 4 days. Climatic charts for the Atlantic from 15°S to 15°N from September to November (Mac Donald, 1938) show that average wind speeds are everywhere less than 6.7 m sec^{-1}, and over most of the region less than 5.0 m sec^{-1}. From Table 4 the average value of Q_e would be between 180 and 380 cal $cm^{-2}day^{-1}$ and of Q_s between 5.4 and 10.5 cal cm-2 day^{-1}. The occurrence of a moderate synoptic disturbance of dimensions similar to those considered above would greatly alter the distribution of energy input within these latitudes. Only during the months of November through May do average winds in excess of 7.2 m sec^{-1} cover a significant portion of the region 15°N to 15°S. At this time of the year within the moderate to strong trade wind regions, the latent heat flux would approach that associated with moderate to strong disturbances. For the remainder of the year, i.e., June through September, the net input of energy from the surface of the ocean in this region will depend significantly upon the frequency and distribution of such synoptic scale disturbances.

Detailed analysis of the tropical Atlantic for the International Geophysical Year of 1958 is being carried out by Dean (Dean and La Seur, work in progress in Dept. Meteor., Florida State Univ.). The frequency of equatorial vortices for each month in 1958 has been obtained. Preliminary results suggest a frequency of 10 to 15 vortices per month during August, September, and October. As shown in Figure 14, development generally takes place off the West African coast in the vicinity of 5°N to 10°N, with some vortices apparently emerging from the continent itself. As the equatorial trough region migrates equatorward, the number of vortices diminishes and they can be tracked into the Atlantic for limited distances only. During the months of January and February, only a few weak vortices appear in the eastern equatorial Atlantic, none of which migrates into the central Atlantic. Phenomena in the mid- and upper-troposphere (such as the tropical easterly jet) appear to play an important role in this seasonal fluctuation in the frequency of these equatorial systems. Figure 14 shows the tracks of 11 equatorial or tropical cyclones. At least nine of these systems followed a track confined to an extremely narrow belt. As shown by Figure 15, the mean map reflects this concentration as an asymptote in the streamline field.

For the region near the asymptote, a mean number of 10 vortices per month can be accepted for the wet season months (July through October), with 1 to 4 per month during the dry season (January through May). If, in the mean, the disturbance covered 15 x 15 degrees of latitude and moved at a mean rate of 300 nautical miles within 24 hours, or 5 degrees of latitude per day, then within a belt 15 degrees wide across the tropical Atlantic centered on the mean asymptote during any wet season month, the mean sensible and latent heat flux would correspond to the values computed for the composite storms. The choice of a belt 15 degrees wide is suggested not only by the mean size of the disturbances examined, but is also reflected

TABLE 4

COMPARISON BETWEEN LATENT AND SENSIBLE HEAT TRANSFER UNDER CONSTANT TRADE WIND CONDITIONS AND SYNOPTIC SCALE DISTURBANCES OVER AREAS OF 10 BY 10 AND 20 BY 20 DEGREES OF LATITUDE

	Average Energy Fluxes in the Trade Wind Region		Average Energy Fluxes in Disturbed Conditions	
			Disturbance I averaged over 100° lat^2	Disturbances II and III averaged over 400° lat^2
	Q_e	Q_s	Q_e	Q_s
Weak trade $u<2.5$ m sec^{-1}	$Q_e<180$	$Q_s<5.4$		
Weak to moderate trade $2.5<u<5.0$	$180<Q_e<314$	$5.4<Q_s<9.4$		
Weak disturbance			418	15
Moderate trade $5.0<u<7.7$	$314<Q_e<450$	$9.4<Q_s<11.3$		
Moderate disturbance < tropical storm			435	17
Strong trade $u>7.7$	$Q_e>450$	$Q_s>7.6$		
Strong disturbance < hurricane			480	22

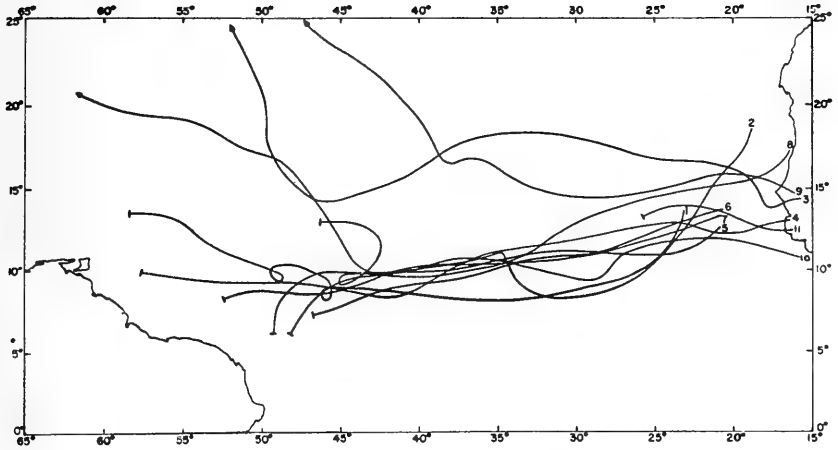

Figure 14. Tracks of equatorial cyclones for the month of August 1958. The cyclones have been identified in the surface streamline analysis and tracked until the circulation could no longer be identified. Tracks of systems originating in July and persisting into August have not been included. (After Dean, Dept. Meteor., Florida State Univ.)

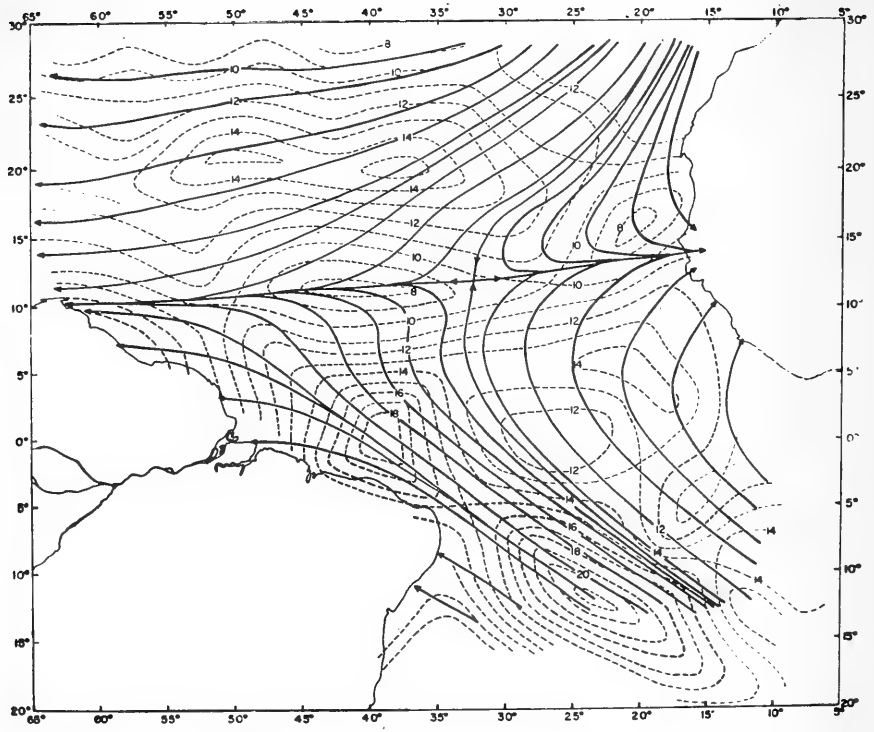

Figure 15. Mean streamlines (solid) and mean wind speeds, irrespective of direction (dashed) for the tropical Atlantic based upon all ship reports within 5 degree latitude-longitude squares for August 1958. (After Dean, Dept. Meteor., Florida State Univ.)

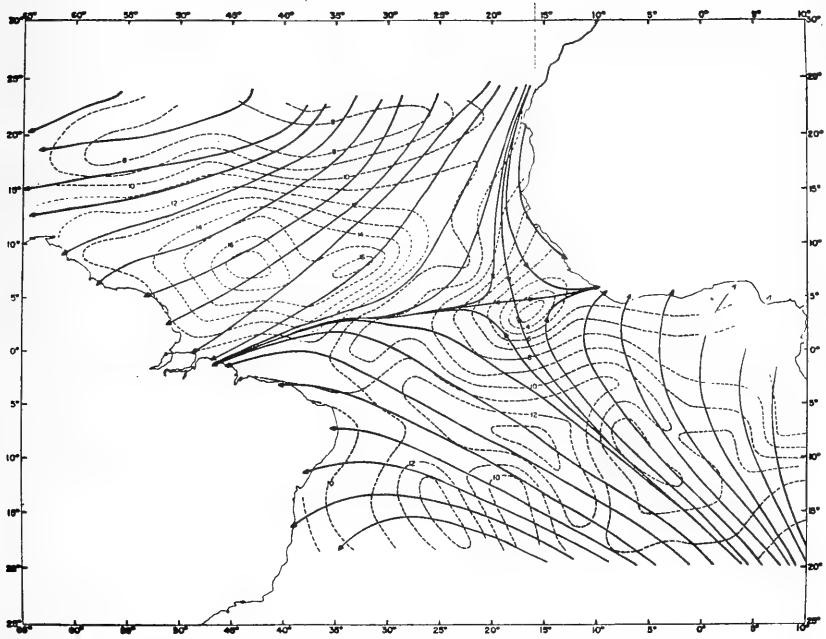

Figure 16. Mean streamlines (solid) and mean wind speeds, irrespective of direction (dashed) for the tropical Atlantic based upon all ship reports within 5 degree latitude-longitude squares for February 1958. (After Dean, Sept. Meteor., Florida State Univ.)

by the charts of wind constancy (e.g., MacDonald, 1938). For the months of July through October a belt 15 degrees wide with wind constancies of 80 percent or less exist about the equatorial trough zone. A constancy of 80 percent signifies that during 80 percent of the time steadiness is better than 90 percent. Therefore, the 80 percent constancy boundary roughly corresponds to the division between disturbed and undisturbed conditions used above. Outside this belt other synoptic systems would affect the distribution of energy flux, but within the stronger and more persistent trade wind belts such fluctuations would have less effect upon the net transport than is the case in the vicinity of the equatorial trough.

The month of August was chosen as representative of the wet season and the month of February as representative of the dry season. Computations for the tropical Atlantic have, in each case, been based upon the mean wind speed values depicted in Figures 15 and 16. On the August map the 15-degree wide region under the influence of disturbances has been centered on the position of the mean asymptote. Latitudinal means were obtained for Q_e and Q_s at 1-degree intervals from the values computed for the composite storms. These values were applied to 24 of the days of August, the remaining 7 days represent undisturbed conditions. The region between ±7.5 degrees of the asymptote and about 30°N and 20°S was then subdivided on the basis of mean sea surface temperatures (MacDonald, 1938). Based upon these values, the air-sea temperature difference was scaled according to observed values from the 1957 and 1963 data. The difference between the saturated specific humidity and the humidity at 6.0 m was assumed constant at 5.0 g kg^{-1}. Computations (as before) of Q_e and Q_s were then made for 5-degree squares. This procedure of computing Q_e and Q_s outside the equatorial trough region in August was applied to the whole area in February. Transport during the transition months between wet and dry seasons will depend upon the occurrence and frequency of synoptic disturbances. Thus, an annual mean map of Q_e and Q_s has been constructed from an average of the August and February maps. These six maps are presented in Figures 17 through 22. The mean value of Q_e for the month of August shown in Figure 17 shows similarities with the mean annual map of Budyko (1956) only near 30°N. On Figure 17 a well defined maximum now appears to the north of the asymptote as a result of synoptic scale systems. A secondary maximum appears in the southwestern tropical Atlantic in association with the maximum in the winter trade of that hemisphere. The overall results indicate a pronounced increase in latent heat transport within the equatorial and southern tropical Atlantic.

The mean sensible heat transport for August shown in Figure 18 indicates, in general, lower values than reported by Budyko (1956) but higher values than Jacobs (1951). Within the equatorial trough regions values are close to those shown by Budyko. This is due to the added transport associated with synoptic systems. Outside this region the values reported in Figure 18 are lower than those of Budyko. This is in large part due to the exclusion of diurnal effects, a factor not considered by Budyko.

During February the mean transport of latent heat shown in Figure 19 corresponds in the southern hemisphere to that obtained by Budyko (1956) on

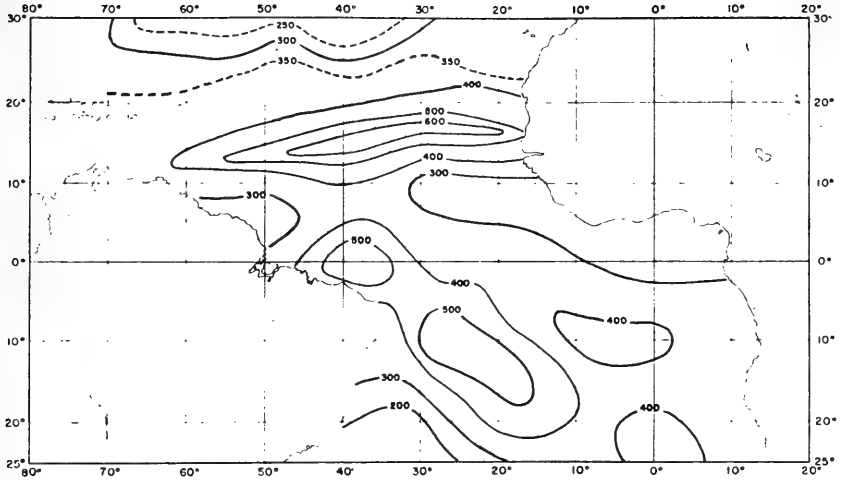

Figure 17. Mean values of latent heat transport in cal cm^{-2} day^{-1} for the tropical Atlantic for the month of August, computed on the basis of methods outlined in the text.

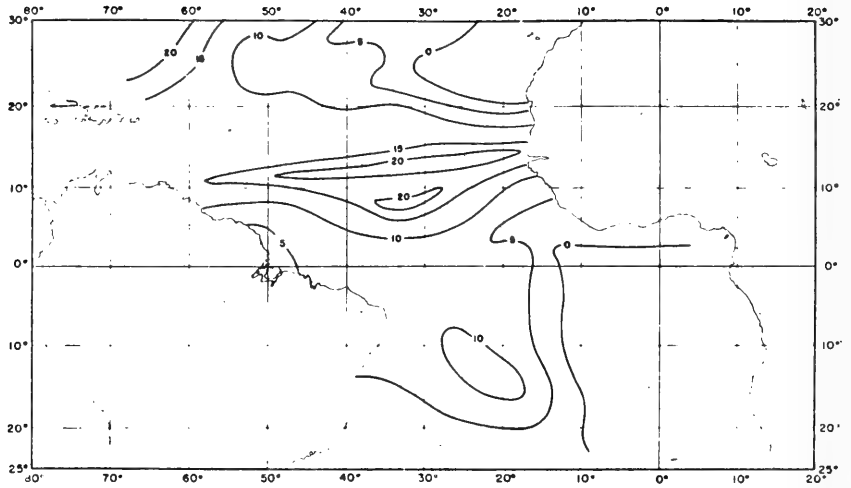

Figure 18. Mean values of sensible heat transport in cal cm^{-2} day^{-1} for the tropical Atlantic for the month of August, computed on the basis of methods outlined in the text.

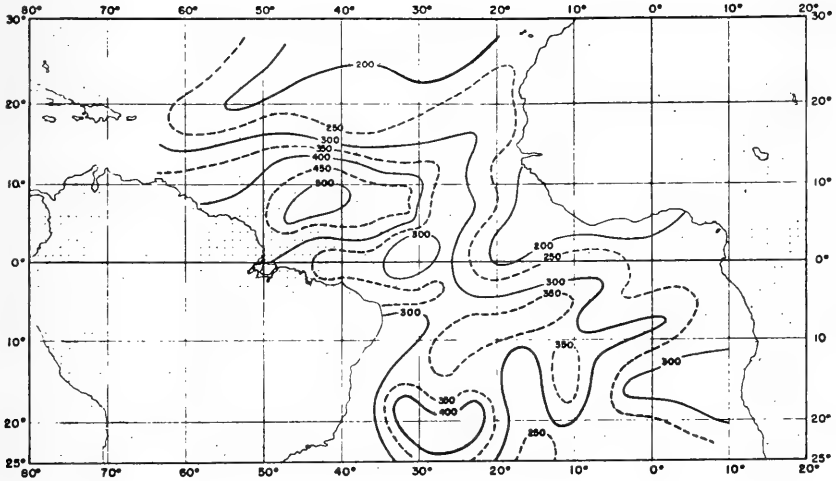

Figure 19. Mean values of latent heat transport in cal cm^{-2} day^{-1} for the tropical Atlantic for the month of February, computed on the basis of methods outlined in the text.

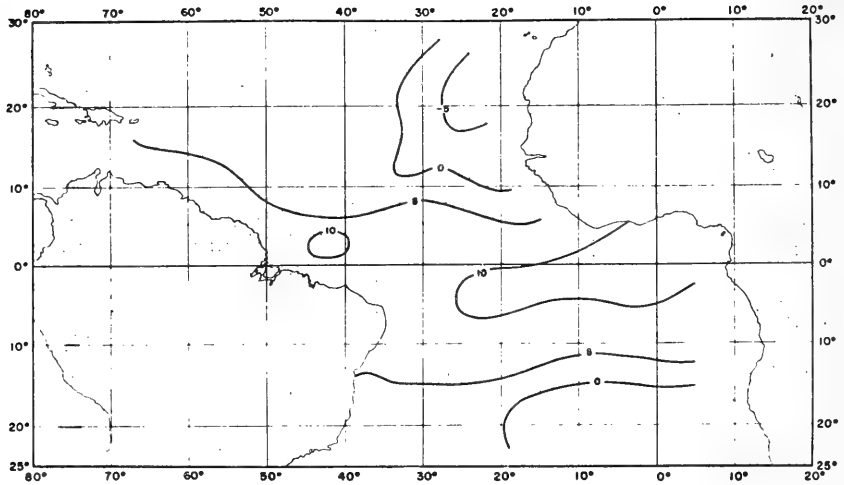

Figure 20. Mean values of sensible heat transport in cal cm^{-2} day^{-1} for the tropical Atlantic for the month of February, computed on the basis of methods outlined in the text.

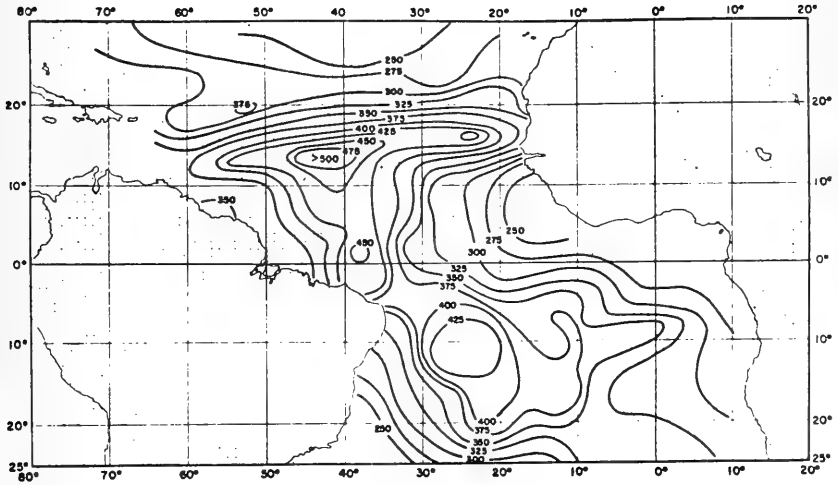

Figure 21. Mean annual values of latent heat transport in cal $cm^{-2}day^{-1}$ for the tropical Atlantic based upon Figures 17 and 19.

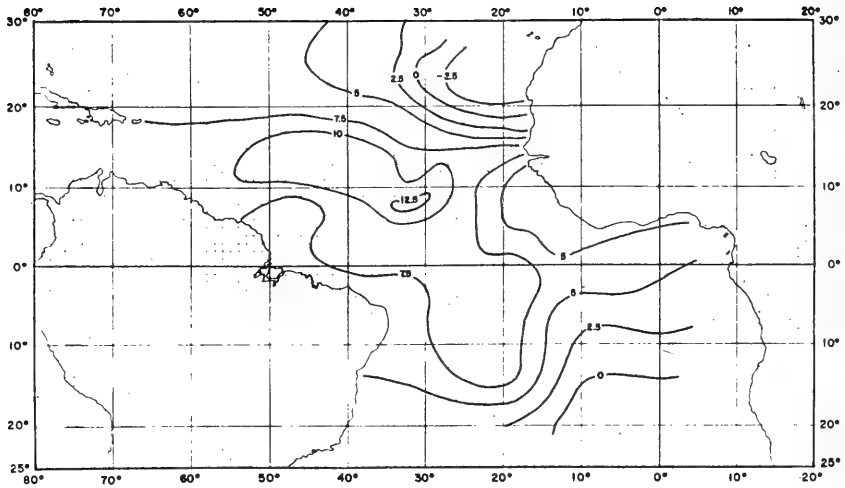

Figure 22. Mean annual values of sensible heat transport in cal $cm^{-2}day^{-1}$ for the tropical Atlantic based upon Figures 18 and 20.

an annual basis in the northern tropical Atlantic. A maximum associated with the trade-wind maximum of the winter hemisphere appears again.

A marked decrease in the transport of sensible heat during February is shown in Figure 20. This is not only due to the inclusion of diurnal effects but also to the fact that fair weather is a mean condition over most of the region during this month.

Figures 21 and 22 show the mean annual distribution of Q_e and Q_s for the tropical Atlantic as calculated in this paper. In the case of latent heat the most significant features remain the maximum in the equatorial trough region associated with synoptic scale disturbances, and the higher values shown over much of the southern tropical Atlantic. The integrated effect still produces a maximum within the eastern and central equatorial trough region.

The inclusion of both the synoptic and diurnal effects on the transport of sensible and latent heat produces pronounced variations in both the monthly means and the annual distributions. The inclusion of the drag coefficient as a function of both wind speed and stability results in an increase in the transport of heat, particularly in the regions of high mean wind speeds. Clearly, these effects will apply in all tropical ocean areas. In the central and western Pacific, where the mean annual frequency of synoptic disturbances is higher than in the Atlantic, the effect will be even more pronounced than shown to be the case in the Atlantic.

IV. CONCLUSIONS

The strong dependence of latent and sensible heat transport upon synoptic scale disturbances implies that the role of the equatorial trough region in the heat balance of the atmosphere may be even more important than has heretofore been suspected. Not only do the disturbances in this region perform the function of horizontal and vertical advection of vast quantities of energy generated within the trade wind regions, but a large increase in energy transfer occurs within the region of the disturbance. Through the condensation-precipitation cycle, the disturbance then provides a means of releasing this energy. In the mean, the concentration, vertical and horizontal transports of energy in this region prescribe one of the fundamental constraints on the heat balance of the atmosphere.

While it is considered that the magnitudes of the transports derived in the text may be more accurate than those previously published, it is important to note that changes in the coefficients used would not change the direction of the transport, the sense of the synoptic variations or the fact that synoptic systems produce large amounts of latent and sensible heat at the surface. Verification of the absolute magnitude is indeed desirable but there seems little doubt that a region of maximum transport will occur just poleward of the equatorial trough and that this region will have maximum values in excess of those appearing on current maps (e.g., Budyko (1956)). These conclusions cast some doubt upon the relative magnitude of the various terms in

the presently accepted heat budget of the ocean and the atmosphere. In particular, it may suggest a revision of the current estimate of the radiation balance and oceanic heat flux (Budyko, 1956). However, before such a revision could be made, the uncertainties that have entered into the computations made in this paper would have to be removed.

REFERENCES

Bellamy, J.C. 1949: Objective calculations of divergence, vertical velocity and vorticity. Bull. Amer. meteor. Soc., 30, 45-49.

Budyko, M. I. 1956: The heat balance of the earth's surface. Leningrad, Gidrometeorologicheskoe izdatel'stvo, 255 pp. (translated by Nina A. Stephanova; translation distributed by the U S. Weather Bureau, 1958).

Deacon, E. L.; P. A. Sheppard; and E. K. Webb 1956: Wind profiles over the sea and the drag at the sea surface. Austral. J. Phys., 9, 511-541.

_____; and E. K. Webb 1962: Interchange of properties between sea and air. The Sea, Vol. 1, M. N. Hill, Gen Ed., New York, John Wiley and Sons, 43-87.

Garstang, M. 1958: Some meteorological aspects of the low-latitude tropical western Atlantic: results of CRAWFORD cruise No. 15, Woods Hole Oceanog. Inst., Ref. No. 58-72, unpublished manuscript.

_____, 1964: The distribution of mechanism of energy exchange between the tropical oceans and atmosphere. Florida State Univ., doctoral dissertation.

Jacobs, W. C. 1951: The energy exchange between the sea and atmosphere and some of its consequences. Bull. Scripps Inst. Ocean. Univ. Calif., 6, 27-122.

La Seur, N.E. and M. Garstang 1964: Rainfall distributions in the tropics. Proc. Conf. Tropical Meteor., Fort Monmouth, to be published.

_____, 1964a: Tropical convective and synoptic scale weather systems and their statistical contributions to tropical meteorology. Final Rept. to U. S. Army E. R. D. L., Dept. Meteor., Florida State Univ., 55 pp.

MacDonald, W. F. 1938: Atlas of climatic charts of the oceans. Washington, U. S. Weather Bureau.

Malkus, J. S. 1962: Large scale interactions. The Sea, Vol. 1, M. N. Hill, Gen Ed., New York, Wiley and Sons, 88-294.

_____and H. Riehl 1959: On the dynamics and energy transformations in steady-state hurricanes. Nat. Hur. Res. Proj., Rept. No. 31, U. S. Weather Bureau, 31 pp.

Monin, A. S. and A. M. Obukhov 1954: Basic regularity in turbulent mixing in the surface layer of the atmosphere. U. S. S. R. Acad. Sci. Geophys. Inst., No. 24.

Petterssen, S.; D. L. Bradbury and K. Pedersen 1962: The Norwegian cyclone models in relation to heat and cold sources. Geofys. Publ. Geophysica Norvegica, 24, 243-250.

Pyke, C. B. 1964: On the role of air-sea interaction in the development of cyclones. Dept. Meteor., Univ. Calif., unpublished manuscript.

Riehl, H. 1954: Tropical meteorology. New York, McGraw-Hill Book Company, Inc., 392 pp.

_____and J. S. Malkus 1958: On the heat balance in the equatorial trough zone. Geophysica (Helsinki), 6, 503-538.

_____; T. C. Yeh; J. S. Malkus; and N. E. La Seur 1951: The northeast trade in the Pacific Ocean. Quart. J. R. meteor. Soc., 77, 598-626.

INTENSITY OF HURRICANES IN RELATION TO SEA SURFACE ENERGY EXCHANGE

Irving Perlroth
National Oceanographic Data Center, Washington, D.C.

ABSTRACT

The following study, based on the apparent relationship existing between variations of central pressure of a hurricane and the sea-surface temperature pattern, indicates that hurricane intensity is affected by the eddy flux of energy from sea to air. The effect is investigated by constructing synoptic composite sea-surface temperature and related energy exchange charts, employing Jacobs' equations for determining the energy removed from the sea.

INTRODUCTION

The relationship between sea-surface temperatures and the intensity of hurricanes is becoming more evident with the increasing comprehension of the oceanographic environment. Recent studies by Fisher (1957), Perlroth (1962), and Tisdale and Clapp (1963) indicate that energy exchange between sea and air is one of the major factors governing hurricane structure. Namias (1962) found similar evidence in studying the behavior of typhoon Freda in September 1962. For the following study on the effects of energy exchange upon the behavior of hurricanes, the author has selected hurricane Ginny (October 1963) as the main example to serve his purpose.

To fully understand the interaction between the sea and the atmosphere, we need a detailed analysis of the sea-surface temperature field. Due to the inherent difficulties in obtaining sea-surface temperatures in the immediate vicinity of hurricanes, a composite data anlysis was performed immediately before the storm's passage.

Previous studies by Gibson (1962) and Perlroth (1962) have shown that construction of 10-day composite sea-surface temperature charts with definable temperature patterns is possible. It is believed that the extent of order and stability of 10-day composite sea-surface temperature patterns permit such charts to be representative of the steady-state structure of the temperature field for any given day during the indicated period.

In this study attempts are made to relate the fluctuation of hurricane intensity with the sea-surface temperature pattern. No conclusive evidence is present that a hurricane follows a track which lies over the warmest water (Fisher, 1957); however, hurricane Ginny (October 1963) appeared to traverse the core of the Gulf Stream for a long time. It is believed that under unusual atmospheric conditions (devoid of any major steering currents), the paths of hurricanes may be influenced by areas of maximum energy exchange. The cycloidal character of many hurricane tracks might be attributed to the influence of pronounced sea-surface temperature patterns.

It is also believed that energy obtained from the sea is not the sole controlling factor governing hurricane intensity and fluctuation of central pressure; however, if a hurricane remains tropical in its character and is not extensively influenced by any cold fronts or extratropical troughs, there appears to be substantial evidence of the effect of energy exchange on hurricane structure.

HEAT-EXCHANGE COMPUTATIONS

Data for the analyses of Figures 1 and 2 were obtained from ships, located in the western Atlantic, which transmitted radio teletype reports of synoptic weather observations to the U. S. Weather Bureau. The basic data used were air and sea temperatures, dew point, and wind velocity.

Jacobs' (1942) final equations for the energy removed from the sea are as follows:

$$Q_e = 145.4\ (e_w - e_a)\ W_a \text{ g cal/cm}^2 \text{ day}$$

$$Q_c = \frac{0.01(-t_w - t_a)\ Q_e \text{ g cal/cm}^2 \text{ day}}{e_w - e_a)}$$

$$Q_a = 145.4\ (e_w - e_a) + 0.01\ (t_w - t_a\ )\ W_a$$

where

Q_e = energy used for evaporation

Q_c = sensible heat exchanged between sea and atmosphere through convection

Q_a = sum of Q_e and Q_c, representing total energy exchange between sea and atmosphere

e_a = vapor pressure at height a, in inches

e_w = vapor pressure at sea surface, in inches

W_a = wind speed at height a, in knots

t_w = sea surface temperature, in degrees F

t_a = air temperature at height a, in degrees F

Since in many previous studies computations for total eddy transfer of heat have been averaged over large ocean areas (5- and 10-degree squares), only generalized estimates can be made of the physical processes that may exist; the resulting relationships therefore are incomplete. As pointed out by Jacobs, the constants in the above equations are intended to apply only to the marine climatic data which were used by him in his computations of seasonal values over the oceans. Nevertheless, his constants have been used subsequently in the more-or-less synoptic sense by a number of investigators; the results have almost invariably provided the proper order of magnitude and have satisfied continuity, except when the constants were used under conditions of extreme atmospheric instability. It should be pointed out, however, that the validity of the constants has not been established

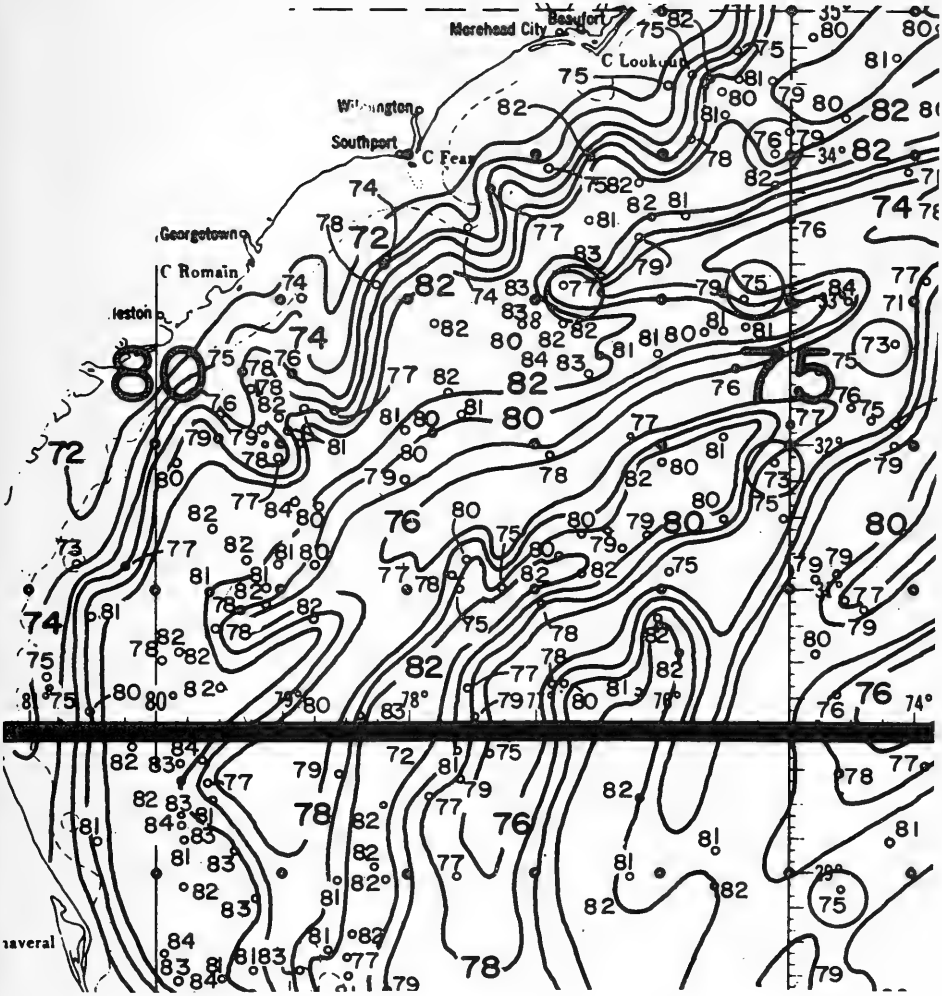

Figure 1. Sea Surface Temperature Pattern
11-19 October 1963

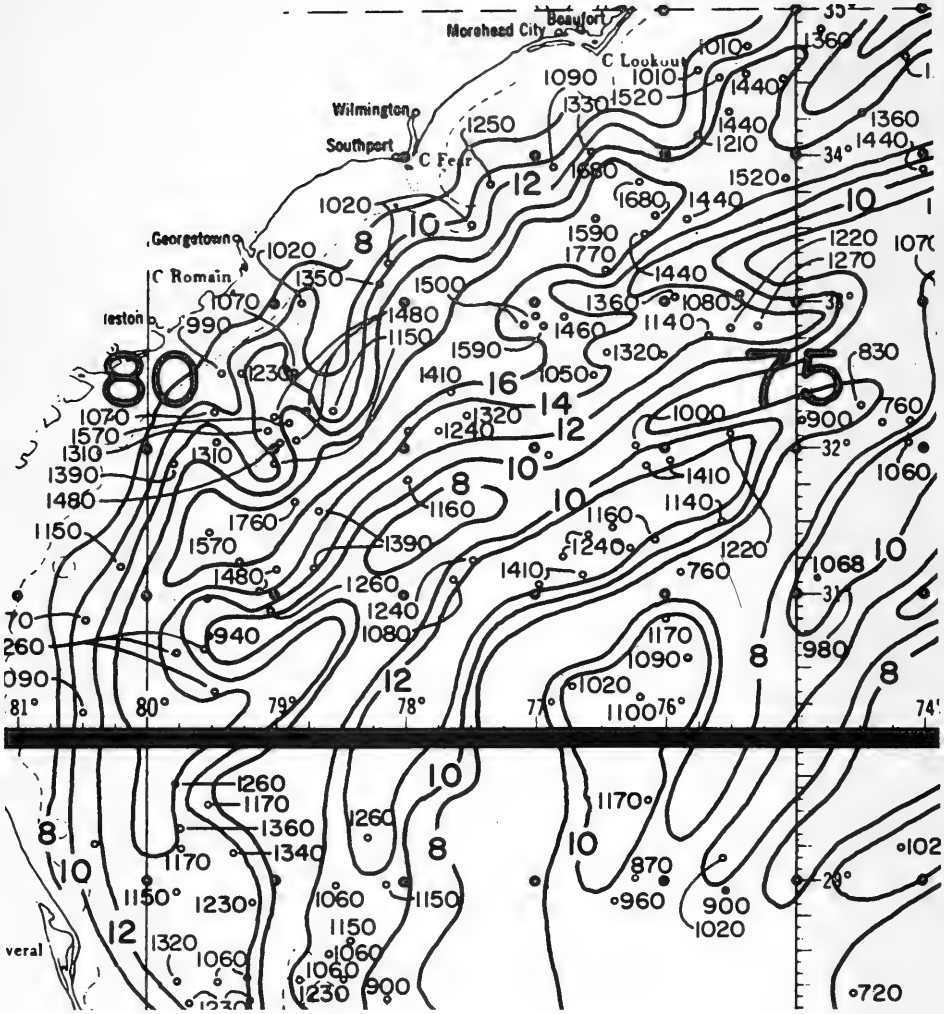

Figure 2. Heat Exchange Pattern 11-19 October 1963
(Values in hundredths g cal/cm^2 day)

when the computations involved the excessively high wind speeds found in the vicinity of hurricane centers. Figure 2 represents an attempt to construct a composite heat-exchange chart for the 10-day period just before the passage of hurricane Ginny. The pattern shows only the existing heat exchange, unaffected by the passage of the hurricane. Dew points, air-sea temperature differences, and wind velocity were averaged for this 10-day period by 1-degree squares. Sea-surface temperatures and air temperatures for each synoptic observation were used in the calculation of the total heat exchange in each 1-degree square. By employing this method, a composite energy exchange chart, based on a corresponding composite sea-surface temperature analysis, was constructed (Figure 1). Patterns of warm and cool water masses and of maximum and minimum energy exchange areas are shown in Figures 1 and 2.

Extensive calculation errors which may occur in the preparation of total heat-exchange charts can be minimized by using data from composite sea-surface temperature charts. The most obvious errors in determining sea-surface temperatures can be eliminated by mass data coverage (Figure 1). Consequently, Jacobs' equations can be used in computing individual synoptic data, and reliable results can be obtained.

OCEANOGRAPHY AND ANALYSIS

To construct the 10-day composite chart shown in Figure 1, sea-surface temperature data for October 11-19, 1963, were used. An analysis of these data was performed; doubtful data were circled and not used in the computations. The chart shows that the temperature patterns for certain ocean areas maintain a high degree of persistence. For shorter time periods (10 days or less), these patterns appear to be conservative; they are, however, extremely complex. Berson (1962) endorses the existence of quasi-meridionally oriented bands of thermally differentiated water, with significantly varying layer depth, having dimensions of 20 to 60 km in width and 500 km or more in length. The surprisingly stable correlations with current velocity suggest long-term persistence of these bands. This persistence is in agreement with strong indications of quasi-geostrophic balance prevailing in the long-term seasonal averages of the current component along the bands. It is thus quite possible that these standing oceanic eddies, on a mesoscale, form an integral part of the mechanism for secular-scale meridional heat transport in the oceans. According to Laevastu (1963), pronounced patterns of heat-exchange components are relatively persistent from day to day, with slight changes in position and intensity.

Figure 1 shows the axis of the Gulf Stream and the adjacent cold water of the continental shelf. Horizontal surface temperature gradients of 8 to 10°F exist within the few miles between these two water masses. The alternating warm and cool bands of water are quite notable; however, their surface temperature gradients are less than those along the Gulf Stream.

The total heat-exchange pattern shown in Figure 2 is very similar to

the sea-surface temperature pattern. Computations of total energy flux (sea to air) in the core of the Gulf Stream exceed 1600 g cal/cm^2 day; yet only a few miles seaward, approximately half of this value was obtained. The maximum heat-exchange areas coincide with bands of warmer water, and minimum heat-exchange areas coincide with bands of cooler water.

The absolute values of sea-surface temperature and heat exchange undergo a change upon the passage of a hurricane; however, the relationship between temperature and heat exchange remains the same during the passage of a hurricane. In the Gulf Stream, near the center of hurricane Ginny, calculations of total heat exchange exceed 3000 g cal/cm^2 day.

Bathythermogram studies of the vertical temperature structure of the ocean in the numerous water bands have indicated interesting relationships. The warmer water bands, particularly the core of the Gulf Stream, are generally isothermal to 150-250 feet during this time of year (October); the cooler water bands show a mixed layer of less than 50 feet. As the hurricane passes over the cooler water, a notable decrease of the surface temperature can be expected, while the deeper layers of isothermal water are less affected. It could be concluded, therefore, that the surface temperature gradients do not dissipate as is shown by Figure 6. The sea-surface temperature and hurricane pressure curves indicate a unique relationship.

HURRICANE GINNY

Hurricane Ginny formed in the western Atlantic, in the vicinity of the southeastern Bahamas, on October 16, 1963. In her formative stages, this storm appeared to be extratropical in nature. Figures 3 and 4 represent the surface weather chart and 500-mb chart for 12 UT on October 19. The available data at 500 mb indicate the presence of a deep polar trough along the southeast coast of the United States, with an apparent cold pool of air in its axis. However, transformation of the cold core to a warm-core low had apparently occurred by October 22 when the reconnaissance aircraft found that the storm had acquired tropical characteristics.

For study purposes, hurricane Ginny might be classified as an "ideal" storm, primarily because of its erratic motion, slow movement, and the coincidence of its track with the axis of the Gulf Stream. The "Yankee Storm" in November 1935 followed a similar track. It developed in the vicinity of Bermuda, moved westward to the vicinity of Cape Hatteras, and from there curved southwestward to the south coast of Florida.

In this evaluation, the track of hurricane Ginny during October 22-28 is being studied (Figure 5). Hurricane positions indicated in Figure 5 were obtained from the U. S. Weather Bureau radio teletype summaries of reconnaissance aircraft penetrating the eye of the storm. It is notable that a considerable increase in the intensity of the storm occurred between October 24, 1400 UT, and October 25, 0100 UT, when the eye of the hurricane entered the core of the Gulf Stream. The increase in intensity was apparently due to the increase

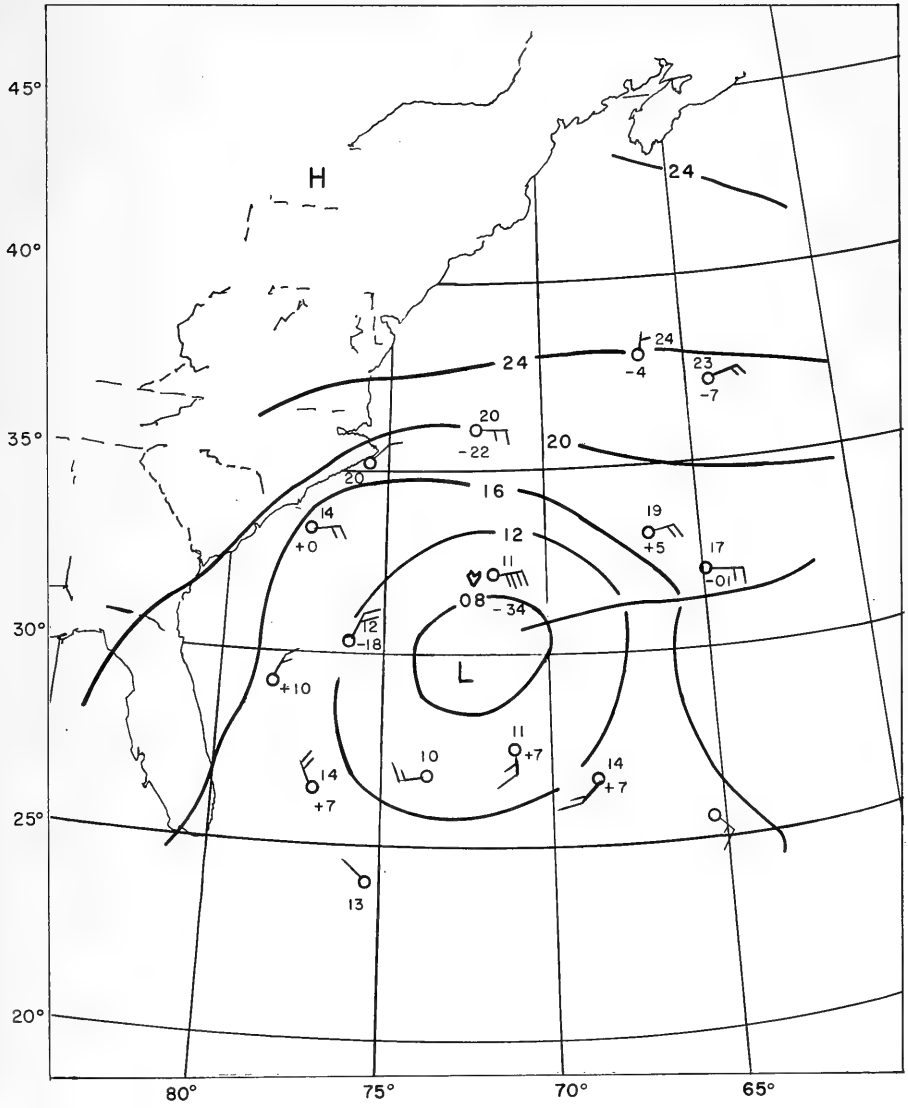

Figure 3. Surface Weather Chart 12Z 19 October 1963

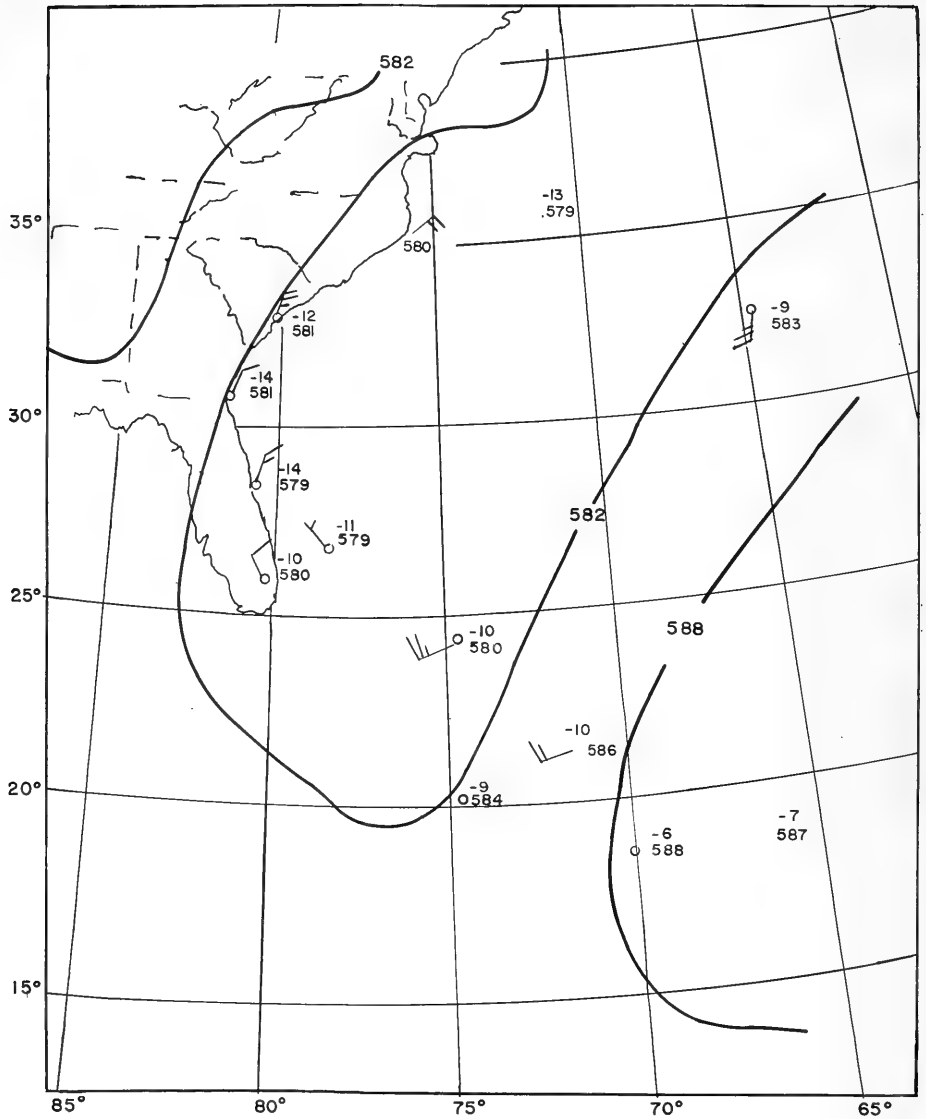

Figure 4. 500 mb Weather Chart 12Z 19 October 1963

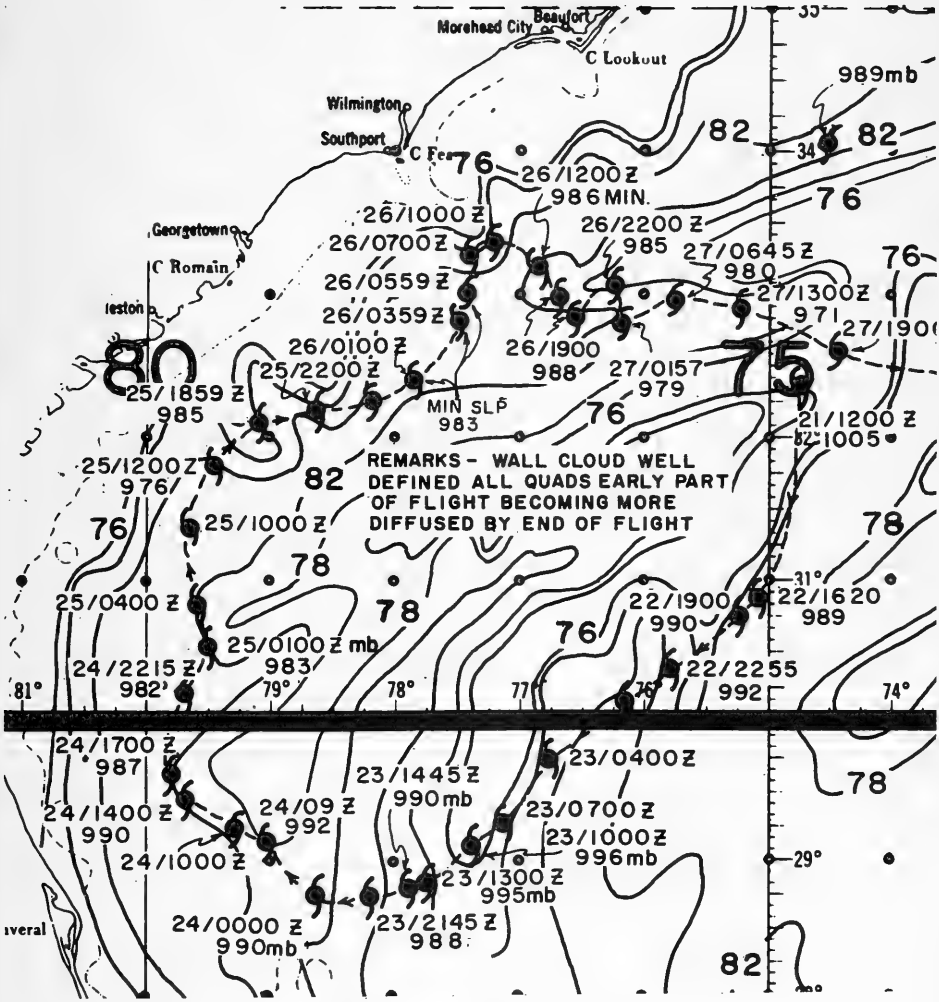

Figure 5. Track of Hurricane Ginny 21-28 October 1963

in sea-surface temperature and the resulting increase in total energy exchange; the eye and wall cloud of the hurricane became better defined, and the central pressure dropped 7 mb in 7 hours. The intensification continued as the storm's track lay over the axis of the warm water stream.

Dunn and Miller (1960) indicate that in the absence of mid-tropospheric ventilation, the vertical temperature structure of the hurricane core is determined by the heat and moisture content of the subcloud air which, in turn, is closely related to the temperatures of the underlying water surfaces. For instance, hurricane Janet (1955) deepened over warm water, and hurricane Carrie (1957) weakened over cool water; however, the rate of change in hurricane intensity depends upon the length of time it takes a hurricane to traverse a particular water mass.

Riehl (1963) points out that a relationship exists between the development of hurricanes and the small anomalies of local temperatures. Perlroth (1962) exemplifies this relationship between hurricane intensity and the air-sea interaction in a comprehensive study of hurricane Esther (1961).

The sea-surface temperature and hurricane-pressure relationship is illustrated in Figure 6. For this relationship to be coincident, the sea-surface temperature pattern during the 10-day period must have remained conservative. As shown in Figure 5, when the hurricane eye and wall cloud entered part of the cold shelf water on October 25, a marked decrease in intensity occurred. The central pressure of 976 mb was observed at October 25, 1200 UT, while by October 25, 1859 UT, a reading of 985 mb was obtained. The storm then turned sharply to the east-northeast and once more entered the axis of the Gulf Stream. The central pressure of hurricane Ginny again began to deepen and by October 26, 0359 UT, reached 983 mb. On October 26, the hurricane appeared to be headed for Wilmington, N. C.. Once again, as the eye passed over the cold shelf water, a notable decrease in intensity was observed. Aircraft reconnaissance indicated that the wall cloud was becoming diffuse, and a central pressure reading of 988 mb was observed. These observations indicate that the storm structure responds spontaneously to the total energy flux from sea to air in the vicinity of the hurricane eye.

On October 28, the steering of hurricane Ginny became influenced by a deepening polar trough forming along the east coast, consequently causing a rapid acceleration of the hurricane to the northeast. Because of the influence of this trough, correlations of hurricane intensity and sea-surface temperature were not determined. The hurricane reached the maximum intensity east of New England as it accelerated rapidly north-northeastward.

CONCLUSIONS

The results of this study imply that a relationship exists between hurricane intensity and the total energy flux from sea to air. The evidence produced in this and other studies brings out the significance of this relationship.

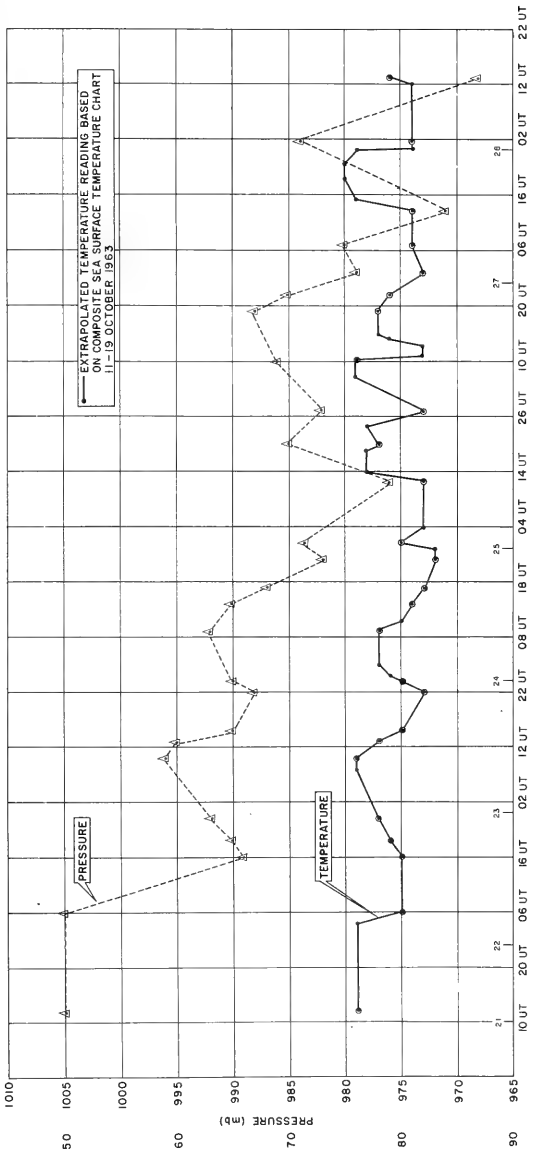

Figure 6. Central Pressure Versus Sea Surface Temperature

It is apparent that where sea-surface temperatures are relatively low (weaker energy exchange), hurricanes are cut off from their heat source and tend to weaken; where the sea-surface temperatures are relatively high (maximum energy exchange), hurricanes tend to intensify. (Figure 6 shows the spontaneous response of hurricane central pressure to the sea-surface temperature field.)

It is interesting that the facts brought out in this study would aid the hurricane forecaster in predicting variations in hurricane intensity. Construction of 10-day composite sea-surface temperature charts for the east coast, Gulf of Mexico, or any other areas influenced by the presence of tropical storms is desirable. The construction of total heat-exchange charts can be performed on a mesoscale, to provide the forecaster with a better understanding of potential areas of hurricane intensification or weakening along its projected track. It must be realized however, that outside the major shipping lanes (tropical Atlantic) lack in density of synoptic observations may prevent a detailed analysis.

Numerous hurricanes, for instance the one of September 1938, of September 1944, and hurricane Hazel in 1954, have reached maximum intensity in the northern latitudes. These hurricanes maintained or even increased their intensity after moving over colder coastal waters or over land. These effects may be attributed to polar trough intensification which affected the motions of these storms and also provided new sources of energy for extratropical development. (This study is intended to relate only the fluctuations of the central pressure of hurricanes in relationship with the sea-surface temperature pattern of storms that remained tropical in their nature.)

Hurricane Ginny appeared to follow a track over the Gulf Stream; however, it is believed that this track coincided with the prevailing weak steering current. There is no substantial evidence to prove that the paths of hurricanes follow the warmer water bands; for instance, hurricane Esther (1961) assumed a track at right angles to the alternating warm and cool water masses.

Although only a relatively small number of hurricanes has been studied for determining the relationship of heat exchange with hurricane pressure, there is sufficient evidence that hurricane intensity is related to sea-surface temperature patterns. This concept should be fully investigated.

Acknowledgement - I am indebted to Dr. W. C. Jacobs for constructive comments and criticism in preparing this study for publication and to the U. S. Weather Bureau, Washington, D. C., National Airport, for use of their files of synoptic weather maps.

REFERENCES

Berson, F.A. 1962: On the influence of variable large-scale wind systems on the heat balance in the active layer of the ocean, Tech. Mem. 25, National Meteorological Center, U. S. Weather Bureau.

Dunn, G.E., and Miller, B. I. 1960: Atlantic Hurricanes, Louisiana State University Press.

Fisher, E. L. 1957: Hurricanes and the sea surface temperature field, the exchange of energy between the sea and the atmosphere in relation to hurricane behavior. Report 8, Parts 1 and 2, National Hurricane Research Project.

Gibson, B. 1962: The nature of the sea surface as deduced from composite temperature analyses, Deut. Hydrograph. Z.

Jacobs, W. C. 1942: On the energy exchange between sea and atmosphere, J. Marine Res., 5(1), 37-66.

Laevastu, T. 1963: Energy exchange in the North Pacific; its relations to weather and its oceanographic consequences, Oceanography Division, Hawaii Institute of Geophysics, University of Hawaii.

Namias, J. 1962: Large-scale air-sea interactions over the North Pacific from summer 1962 through the subsequent winter, J. Geophys. Res., 68(22), 6171-6186.

Perlroth, I. 1962: (A) Persistence of composite sea surface temperature patterns, Undersea Technology, 3(4), 16-22. (B) Relationship of central pressure of hurricane Esther (1961) and the sea surface temperature field, Tellus, 14(4), 403-408,1962.

Riehl, H. 1963: On the origin and possible modification of hurricanes, Science, 141 (3585).

Tisdale, C. F., and Clapp, P. F. 1963: Origin and paths of hurricanes and tropical storms related to certain physical parameters at the air-sea interface, J. Appl. Meteorol., 2(3).

THE GULF OF MEXICO AFTER HILDA (PRELIMINARY RESULTS)

Dale F. Leipper
Department of Oceanography and Meteorology
Texas A&M University

ABSTRACT

Hurricane HILDA crossed the Gulf of Mexico in the period September 30, to October 4, 1964, developing to a very severe hurricane in the central Gulf. Sea temperature data available prior to the storm indicated what is probably a typical late summer situation with some surface temperatures running above 30°C. Beginning on October 5, a 7-day cruise was conducted over the area where hurricane winds had been observed. Using the Bureau of Commercial Fisheries vessel GUS III, four crossing of the hurricane path were made, one where the maximum 150 mph winds were observed, one south of that where the winds had first reached 120, one north where they had decreased to 120, and one in shallow water (40 fathoms), where prior data had been collected by the U. S. Fish and Wildlife Service from their Galveston Biological Laboratory. Bathythermograms were taken regularly to depths of 270 meters and hydrographic casts to 125 meters. All four sections of observations indicated similar patterns of upwelling. During the passage of the hurricane it appears that sea surface temperatures over an area of some 70 by 220 miles decreased by more than 5°C, and that a cyclonic ocean current system was established around this area. The data collected on the GUS cruise appear to be the first systematic oceanographic observations available in such a situation. Although they do not permit a full description of the changes which occurred, they are suitable to serve as a basis for a model from which, for example, total amounts of heat lost to the atmosphere might roughly be estimated.

INTRODUCTION

Most of the other papers presented at this Conference have dealt with the influences of the underlying sea upon the atmosphere. This one illustrates an exchange in the opposite direction, a situation where intense atmospheric phenomena brought about significant and observable changes in the underlying sea. Although changes of similar type probably are caused by certain less extreme weather conditions, it is seldom that features as distinct as those created by hurricane HILDA may be observed.

Figure 1 shows the path of HILDA across the Gulf of Mexico. It may be noted that the most intense stage of the hurricane occurred when it was centered 250 miles offshore in waters of over 1000 fms depth. Thus, the effects of the hurricane upon the sea would quite likely be similar to those resulting from similar storms in the larger ocean basins. Entering the Gulf of Mexico with winds less than 80 mph, the hurricane intensified to the 150-mile stage and the winds again decreased to less than 120 mph during the passage across the Gulf. The width of the zone having winds of hurricane velocity is indicated in Figure 1. The average propagation speed of the storm may be obtained from recorded dates and times.

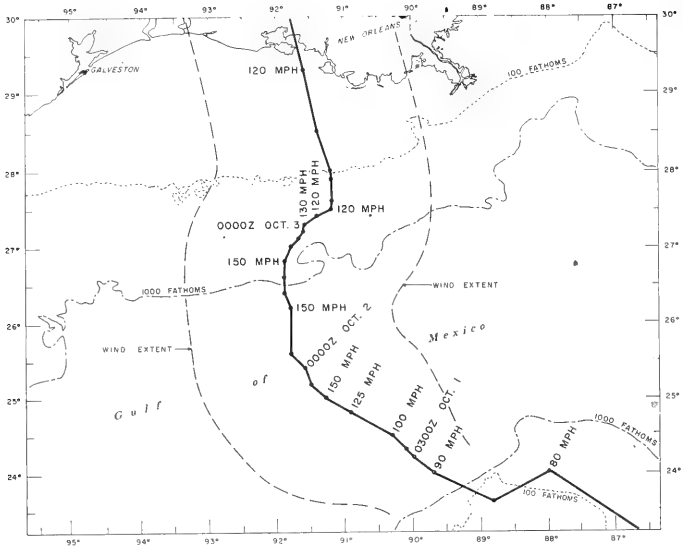

Path of Hurricane Hilda, 1964

Figure 1. Positions are those of the center of the eye at dates and times shown. Wind speeds indicated at center positions are as reported by the Weather Bureau in the advisory transmissions. The dashed lines show the distances from the center to which hurricane speed winds were thought to extend. Latitude (north) and longitude (west) are indicated on the margins.

On September 30, when HILDA entered the Gulf, the conditions encountered were apparently those typical of late summer, the Gulf not having been disturbed by any previous hurricanes nor by any widespread and severe northers. The surface waters over much of the Gulf were of relatively uniform temperature, approximately 29 - 30°C, as indicated in Figure 2. The temperature depth structure, based upon a few bathythermograms, collected prior to hurricane HILDA and upon the limited available climatic data, consisted of a well mixed layer from the surface to approximately 60 meters depth with a normal seasonal thermocline beneath. In Figure 2, the path of the hurricane during its development stage may be seen to have followed along approximately the center of the initially high temperature zone.

CRUISE PLANS

As hurricane HILDA became a severe hurricane on October 2, efforts were made to locate a research vessel which could be used to make a survey in the hurricane area immediately after the passage of the storm. The Galveston Biological Laboratory in Galveston, Texas, was able to provide the 90-foot shrimp boat GUS III, and a decision was made on October 2 to begin the cruise on October 6. The Laboratory provided the crew of the vessel together with scientific observers David Harrington and Stewart Law and Captain Jim McMurrey. From Florida State University came Reed Armstrong, a graduate student under Dr. Robert Stevenson Accompanying the author from Texas A&M University was chief marine technician Kenneth S. Bottom.

At the outset, there was no fixed cruise plan. The first objective was to retrace a line containing observations made immediately prior to hurricane HILDA from the R/V ALAMINOS of Texas A&M University. The plan, as completed, is shown in Figure 3. When the point H-9 was reached the boundary of the cold water area was reached and sea temperature conditions appeared to be at almost prehurricane HILDA values. It was decided to make a section from there perpendicular to the hurricane path. This section was made so as to pass the position of the anchored buoy NOMAD from which regular observations were being collected. The next section to the north was chosen across the path at the point of maximum hurricane intensity. In the final run from BT 57 to 63, Figure 3, a line was repeated along which observations had been made prior to the hurricane by the Bureau of Commercial Fisheries. Most of the observations collected on the cruise of the GUS III were made at times 5 to 10 days after passage of the storm at the same station locations.

Although there apparently had been no systematic observations previously under similar circumstances, there are indications in the literature that areas of low sea-surface temperature are often found in the wake of a hurricane, (Fisher, 1958, and Jordan and Frank, 1964). Hidaka, 1955, reported similar cold areas and developed a theory which indicated that there would be considerable upwelling in the center of a hurricane and that a cyclonic current

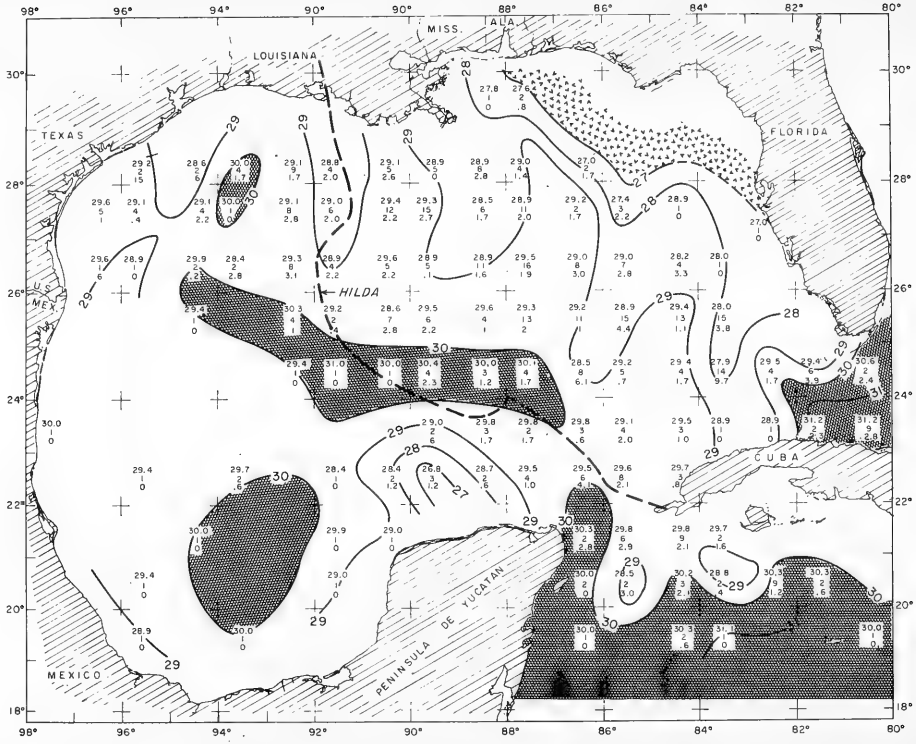

Figure 2. Sea Surface Temperature Before Hilda - September 24-30 Inclusive Based Upon Merchant Ship Data Collected By The U. S. Weather Bureau Averaged By 1° Quadrangles, Number Of Observations And Temperature Range Indicated Below Averages

Temperature > 30°

Temperature < 27°

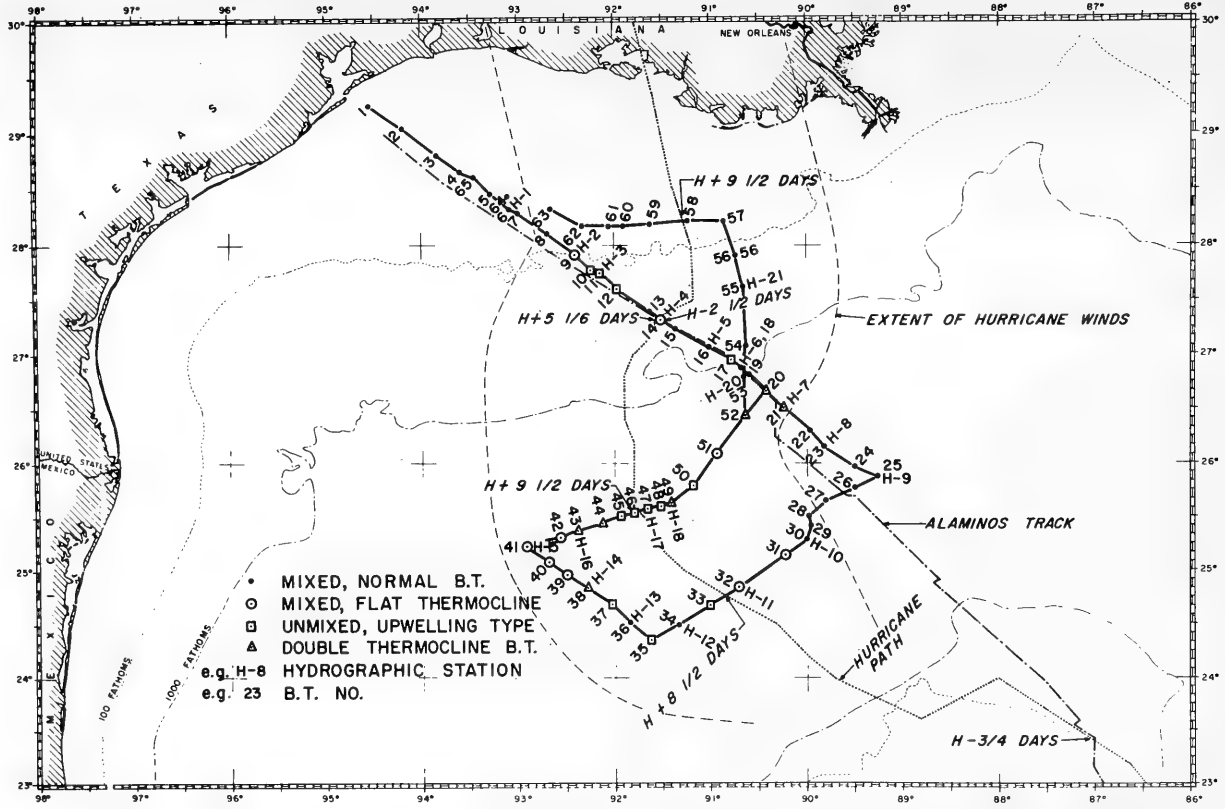

Figure 3. Position Chart for Hurricane Hilda and Observation Cruises

would be formed around the low pressure area. Stevenson (in press) reported on shallow water ocean conditions associated with hurricane CARLA in 1961.

A MODEL

The observations collected on the GUS III cruise may be fitted into a simple model based primarily upon the concept of wind-driven current. V. W. Ekman, 1905, concluded that the effect of the wind upon the sea surface is to set up a surface current 45° to the right of the wind. As depth increases, the direction of the flow turns to the right and the speed decreases. When the ends of vectors representing velocity at different depths are projected on a horizontal plane they form a spiral which has been called the Ekman Spiral. The net transport of water in this layer of wind-driven current can be shown to be 90° to the right of the wind direction in the Northern Hemisphere.

Figure 4 is a schematic diagram of a hurricane similar to HILDA. As may be observed, the winds at any given time create an Ekman net transport outward from the center.

Since the hurricane is moving and since the actual transport direction and speed vary with depth the full pattern is more complicated. In all events, the passage of a hurricane causes the surface layers of the ocean to diverge from the center. The surface waters which are moved aside must be replaced, and the only source of replenishment is from below. Thus, cold water from considerable depths appears at the surface in the hurricane eye.

Figure 5 shows schematically the change in isotherms in a section across the hurricane path. It allows a comparison of the isotherms as they would appear in the normal summer situation in the Gulf with those which would appear after a hurricane passage.

Since the upwelled water arrives at the surface only after the winds have blown for a considerable time, these waters would lose little heat to the atmosphere through evaporation and conduction. The major loss of this type would be from the warm mixed layer of surface water upon which the winds acted directly and which was pushed aside in the Ekman drift.

THE DATA

With this model in mind, the data may now be considered. The surface temperature pattern prior to the hurricane was shown in Figure 2. The comparable pattern after the passage of the hurricane is given in Figure 6. The darkest shaded areas indicate warm water, above 28°. These areas appear to represent the original warm surface layer which has undergone the normal seasonal cooling through the 12 to 14 days involved. The cold upwelled

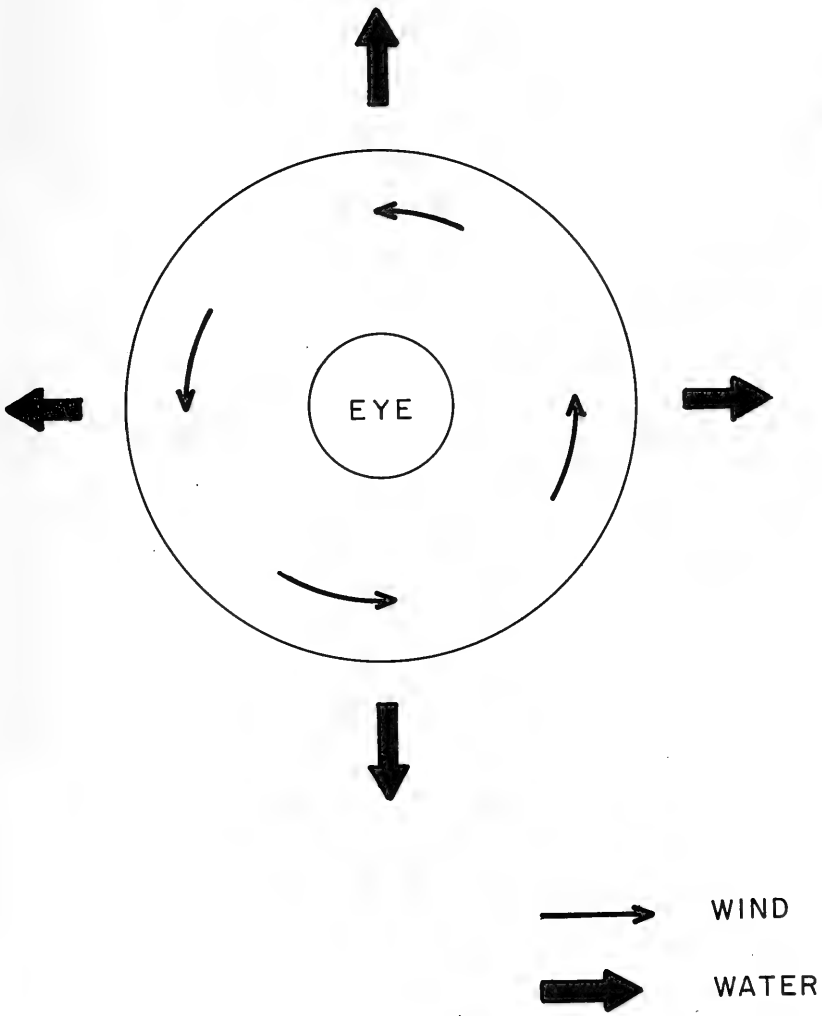

Figure 4

Schematic Diagram of Hurricane and Associated Net Water Transport

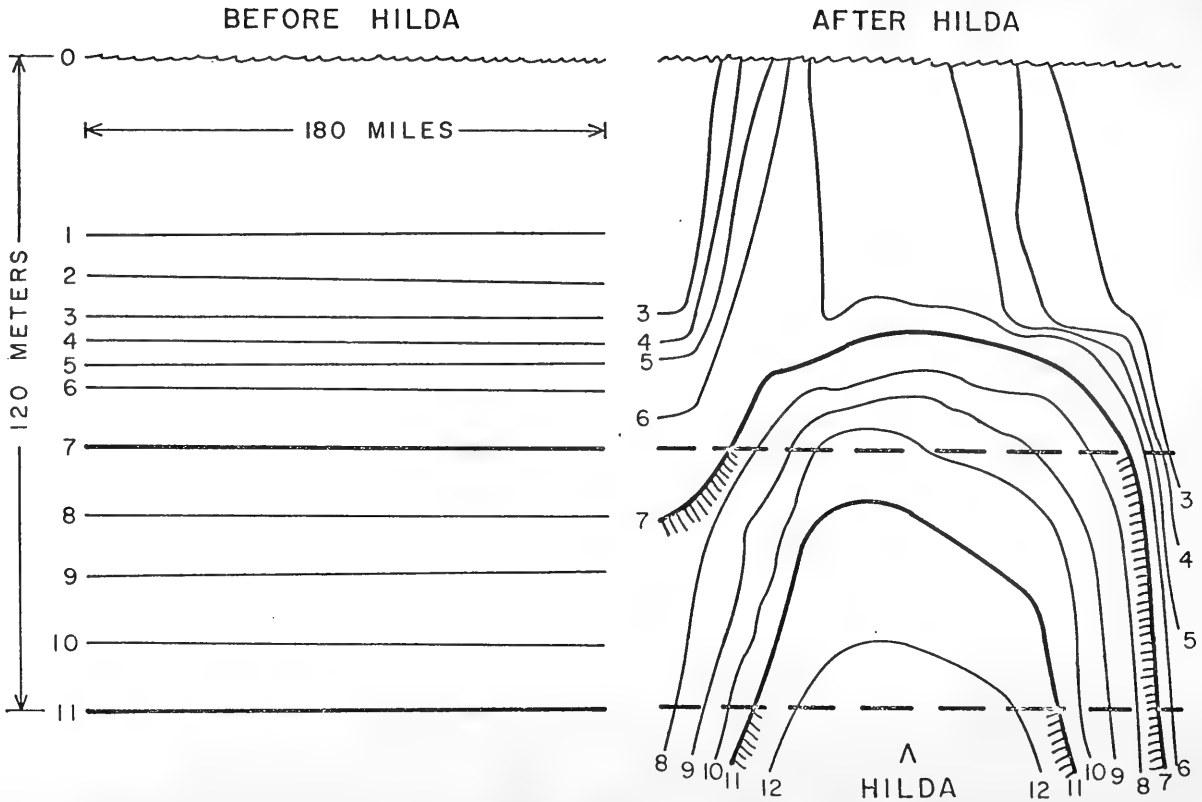

Figure 5. Section Across Path Showing Schematically the Change in Depth of Isotherms

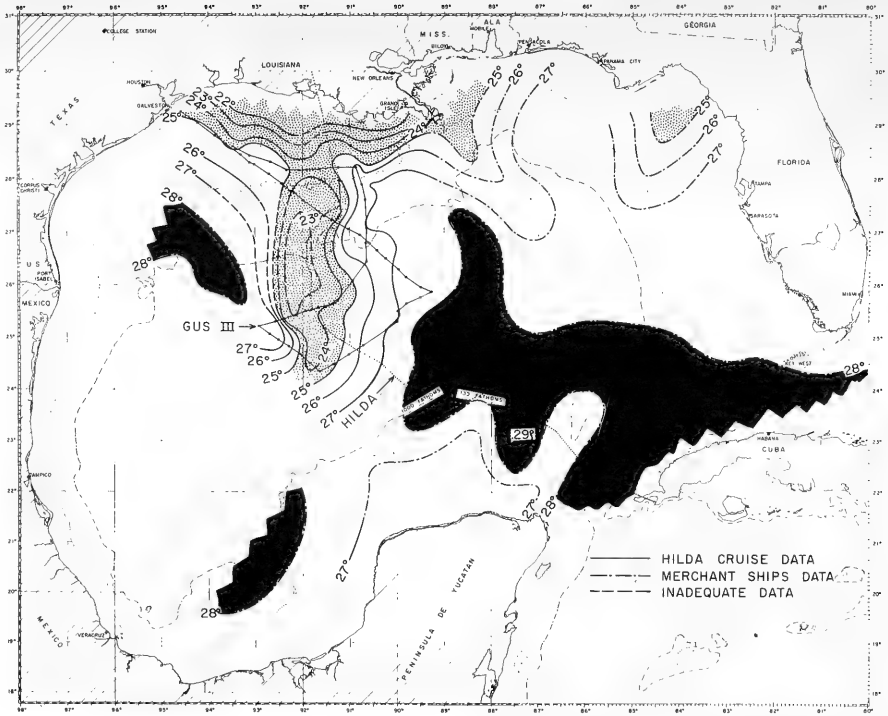

Figure 6. Sea Surface Temperature After Hilda - October 1-13 Inclusive Including Cruise Hilda And BCF Data

Shaded Area > 28°

Stippled Area < 25°

waters appear along the path of the hurricane, 23° water appearing where temperatures of 29° had been observed. The cold band along the Gulf Coast in shallow water is probably not a part of this upwelling pattern, but is in part due to the fact that the time interval between observations in this area before and after HILDA was 24 days compared to a time interval of less than one-half that for the other data. Also, northerly winds in October probably caused considerable cooling and mixing in these shallow waters.

Figure 7 shows the pattern of temperature change between Figures 2 and 5. The climatic atlases indicate a normal seasonal change of less than one and one-half degrees per month at this time. Thus, the change brought about by hurricane HILDA appears to be some 5° in excess of this.

To illustrate the depth of isotherms along the section where winds had been highest, 150 mph, Figure 8 was prepared. Since the path of the ship was deflected from a straight line by currents, the section was drawn along a straight line determined by the observations on the western end and by projecting on to this line in the eastern extent the positions of stations near it. The portion of the section based upon these projected stations is indicated by dashed lines for the isotherms. Several features of the section may be significant. The warm surface waters have been pushed to the left and to the right. A strengthening of the thermocline is indicated by the closer spacing of several of the isotherms separating these uniform warm water bodies from the upwelled water. The isotherms seem to rise rapidly on both sides of the hurricane and the coldest water at the surface appears slightly west of the hurricane path. The warm surface layer is deeper at the eastern end of the section.

Salinities were obtained to a depth of 125 meters and these, together with temperature values, permit the computation of the density anomaly sigma t. In Figure 9, lines of equal value of sigma t are plotted against depth and distance. The shallowest depth of the more dense water is noted at the hurricane path. Near the surface, as shown by the constant values of sigma t, is a layer of mixed water. Proceeding both to the east and the west from the path of HILDA, the depth of this mixed layer increases to a distance approximately 100 miles from the path.

The temperature structure across section C may be indicated in a different manner by copying the temperature depth traces from bathythermograms. In Figure 10, the BT's from section C, as well as those from the other sections surveyed on the cruise of the GUS III, are shown. Water warmer than 25° is indicated by the crosshatched areas. All of this water is seen to lie away from the path to the east and west. This water is well mixed, the mixing apparently having been caused by the hurricane winds and by the heat loss to the atmosphere which lowered the temperatures of the whole water layer from 29 - 30° to 27 - 28°.

The coldest water is that near the path of the hurricane. The BT's in this sector do not show the surface isothermal layers characteristic of surface cooling and mixing but rather have the rounded characteristic which

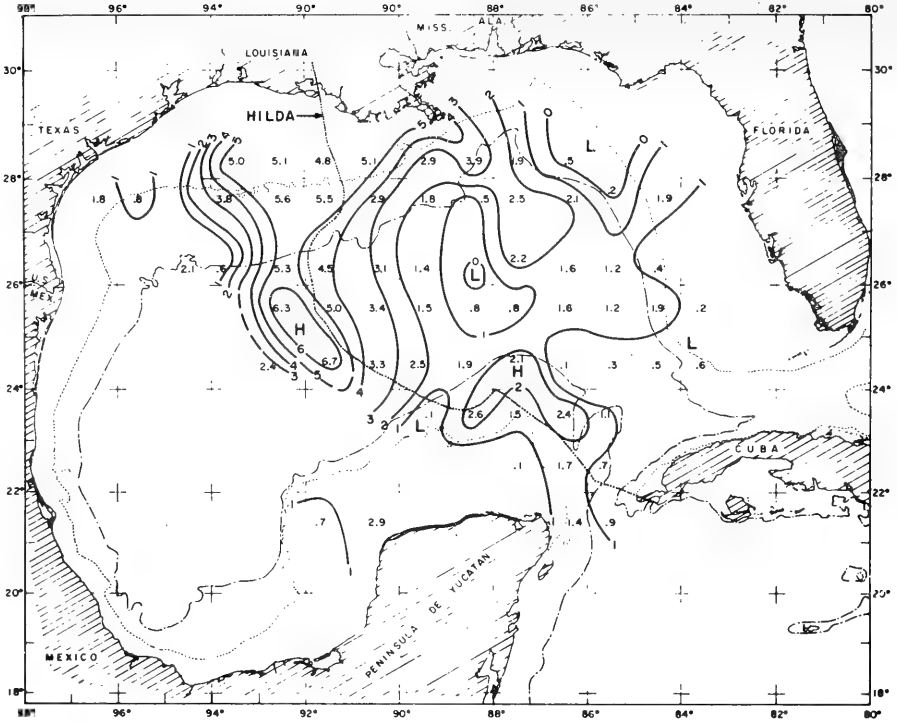

Figure 7. Sea Surface Temperature Decrease in ^{o}C Before Hilda To After Hilda

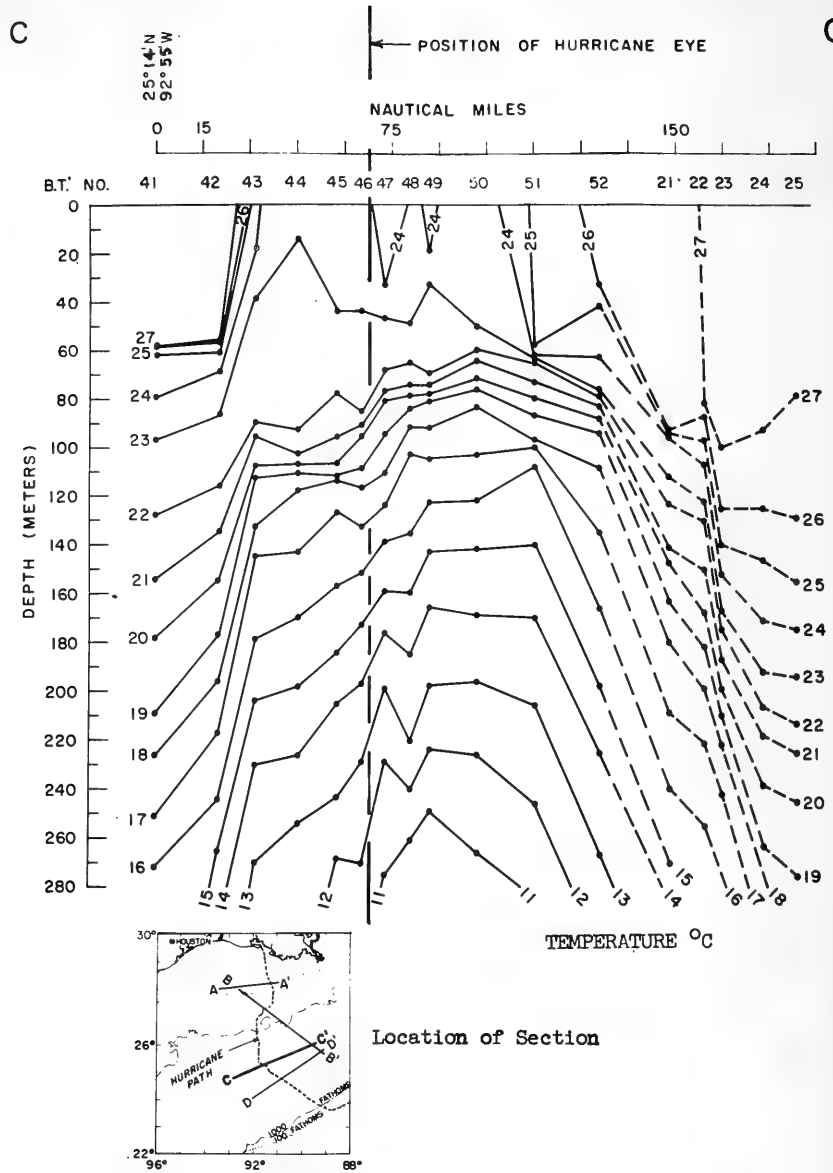

Figure 8. Depth of Isotherms in Section Across Path after Hilda

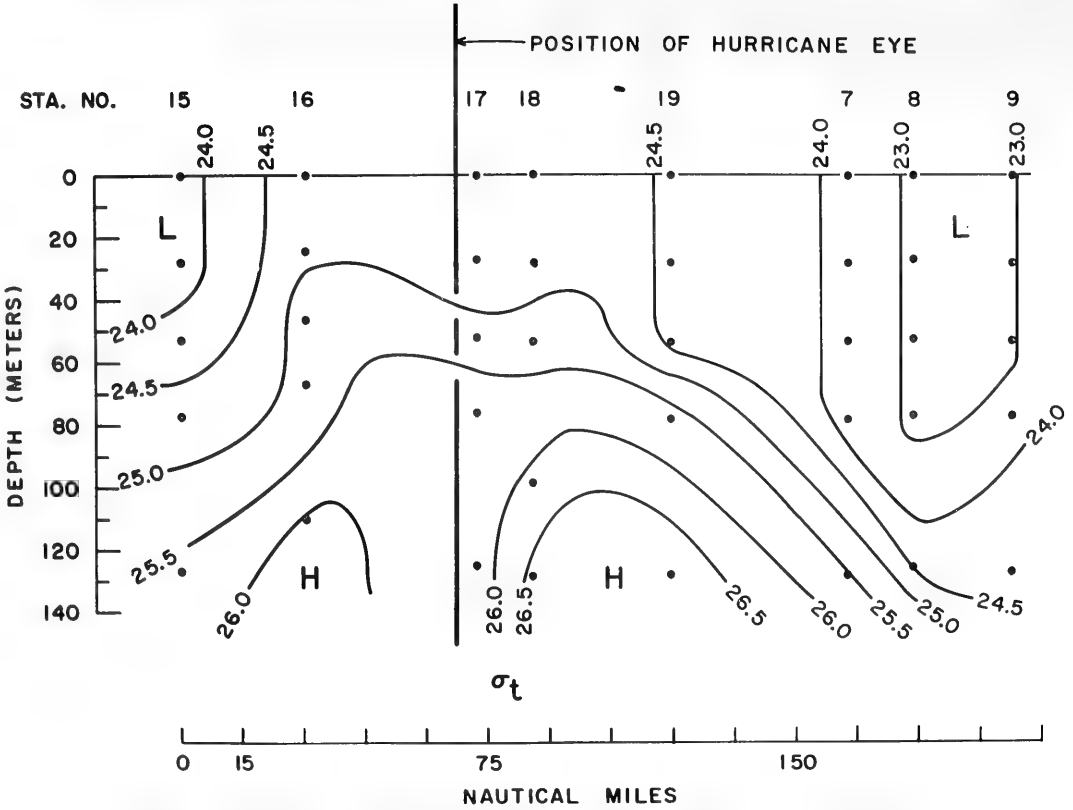

Figure 9. Depth of Contours of Density Anomaly Sigma t Across Path After HILDA, Section C-C[1], (see Fig. 8).

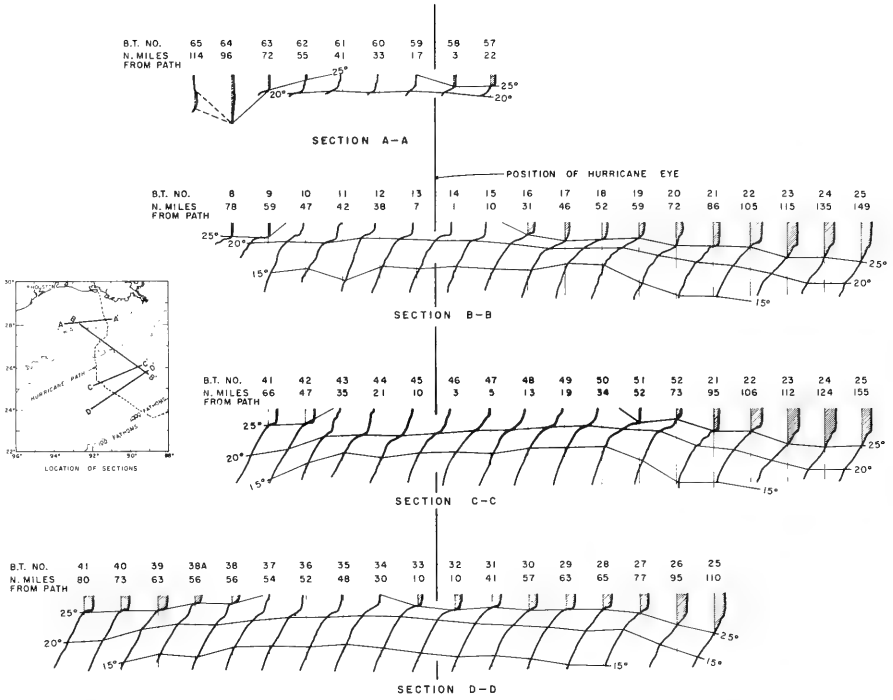

Figure 10. Copies of B. T. Traces Along Sections Crossing Path of Hilda (Shaded Portions > 25°)

is typical of recently upwelled water. The other three sections show characteristics similar to section C.

In proceeding from Station 41 to the eastward along C (see Figure 3), the heading of the GUS III was maintained without change. However, later determination of position indicated a strong drift to the north as indicated at Stations 51 and 52. Also, in the vicinity of Stations 56 and 57 there appeared to be a set to the west. These drifts indicated the existence of an unusual current. Since salinity observations had been made to depths of 125 meters it was possible to compute the density distribution to these depths. Further, since temperature observations reached 250 meters depth and since there was a close correlation between temperature and salinity values, the salinities could be inferred from the temperatures at depths between 125 and 250 meters and densities could be computed here. From the densities, the dynamic height of the sea surface above the 250 meter reference level could be determined. The topography is indicated in Figure 11. Associated with this topography would be a relative geostrophic current of approximately 1 knot. This, then, is the current related to the distribution of mass established during the hurricane passage by the wind drift current.

Since there were some bathythermograph observations made from the ALAMINOS and from the GUS III prior to the passage of HILDA, it is possible to represent the local change in temperature at some six positions. The superimposed temperature structures at each of these positions before and after the hurricane are shown in Figure 12. The three upper positions, which may be located in Figure 3, are in shallow water and the observed change is what one might expect from mixing along with some cooling.

At the three positions in deep water, all of which were along section A, (indicated in the insert on Figure 8) there are several general features. In general, the depth of the mixed layer before the hurricane was less than that after, and the temperature of the mixed layer was higher than it was after HILDA. It should be noted that all three of these observation stations were located east of the path in a region to which the warm layer of surface water would have been displaced from the center of the hurricane.

Considerable further study is needed before the data collected may be fully interpreted. Present plans call for the preparation of one brief article about the surface temperature change alone, another somewhat along the lines of the present paper but organized for final publication, one on the estimated energy redistribution (which requires considerable additional research on conditions existing before the hurricane) and, finally, one on the duration of the cold spot and the cyclonic circulation which was observed on the GUS III cruise.

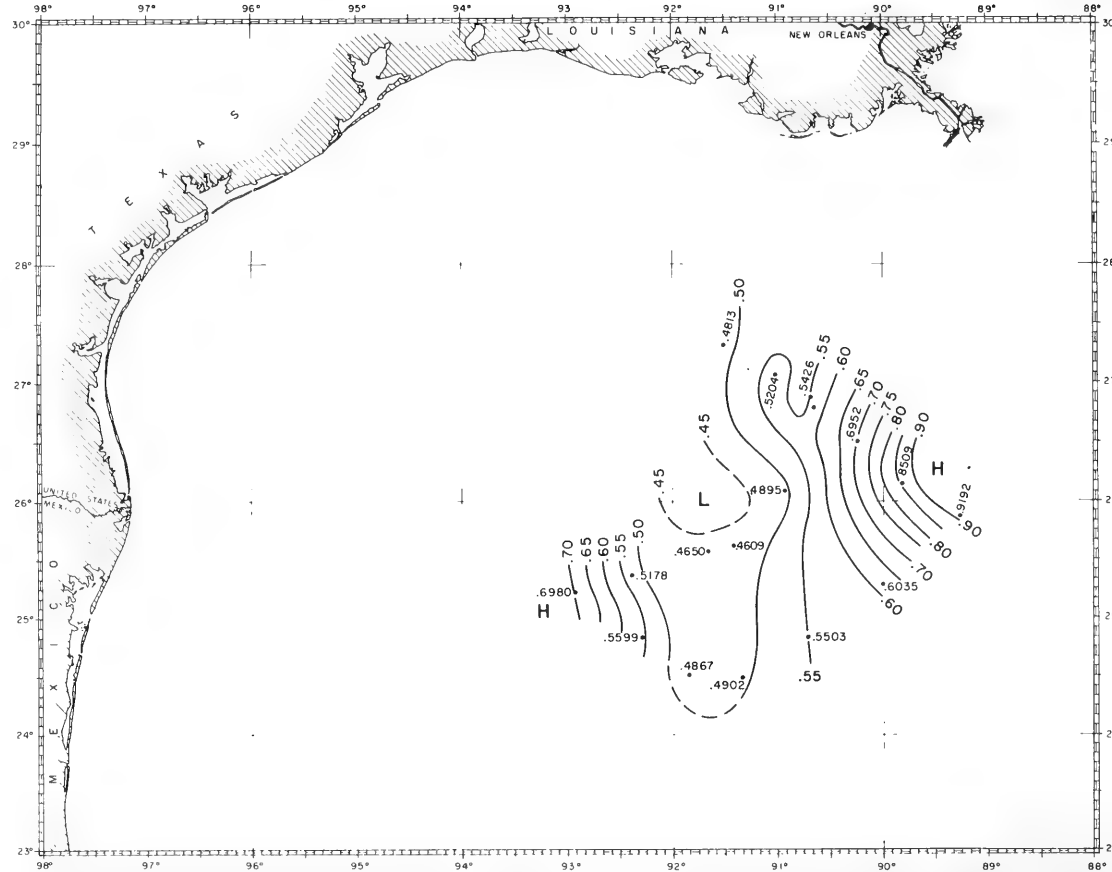

Figure 11. Dynamic Height of the Sea Surface Referred to 250 m. Cruise Hilda, 1964

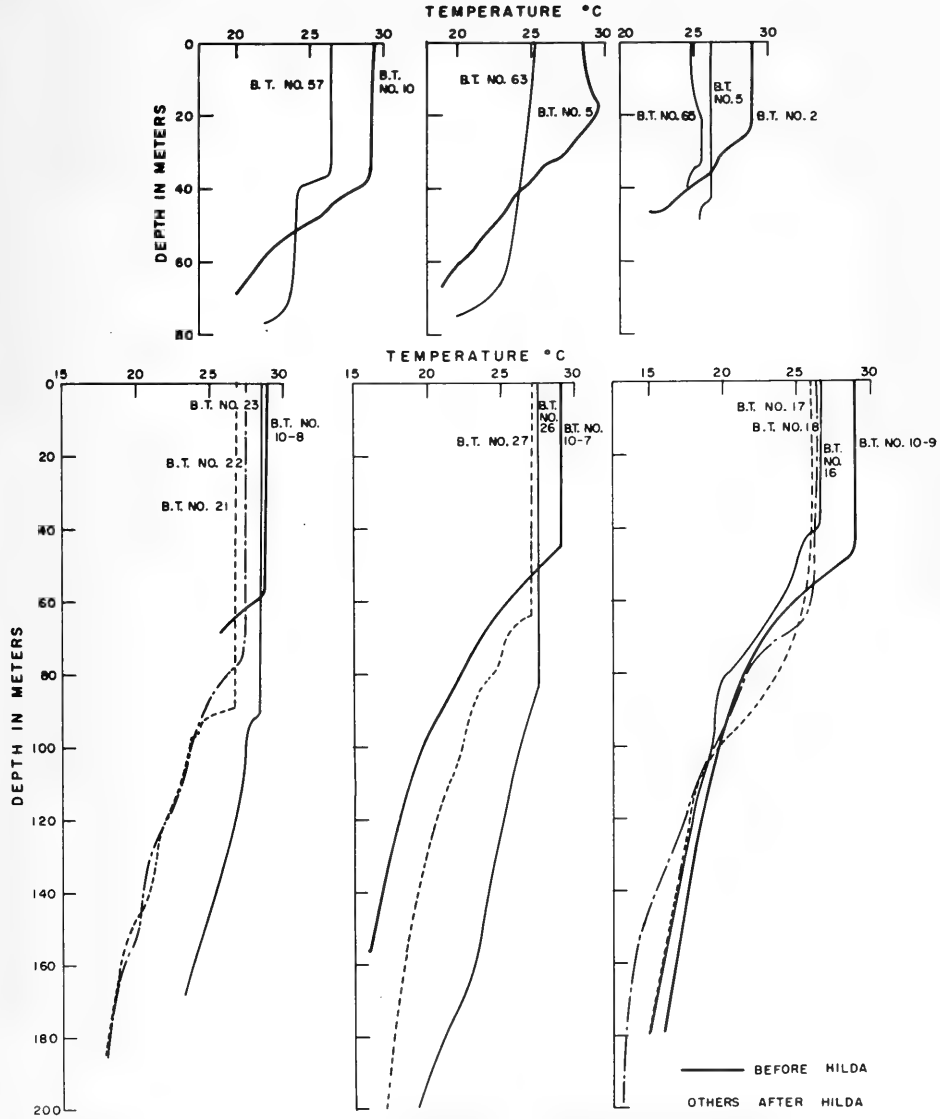

Figure 12. BT Traces at Six Positions, Showing Temperature Structure Before and After HILDA at Each Position. (See Fig. 3 for locations)

ACKNOWLEDGEMENTS

The work of the author was supported by the Geophysics Branch of the Office of Naval Research through the Texas A&M Research Foundation. The vessel GUS III together with her crew and two observers were provided by the Galveston Biological Laboratory of the Bureau of Commercial Fisheries, U. S. Department of the Interior. Technical assistance was provided by Larry Brennan and secretarial work was done by Lydia Fenner.

REFERENCES

Fisher, E. L. 1958 Hurricanes and the Sea-Surface Temperature Field. Journal of Meteorology, 15, pp. 328-333

Jordan, C. L. and Frank, Neil L. 1964 Project Report, On the Influence of Tropical Cyclones on the Sea Surface Temperature Field, Florida State University. NSF Grant GP-621.

Hidaka, Koji and Akiba, Yosßio 1955 Upwelling Induced by a Circular Wind System. Records of Oceanographic Works in Japan, Vol 2, No. 1, March 1955.

Stevenson, Robert E. and Armstrong, Reed S. The Modification of Water Temperatures by Hurricane CARLA. Florida State University. In press.

Ekman, V. W. 1905 On the Influence of the Earth's Rotation on Ocean Currents. Arkiv for Matematick, Astronomi och Fysik 2 (11), pp. 1-52.

EVIDENCE OF SURFACE COOLING DUE TO TYPHOONS

C. L. Jordan
Florida State University

Evidence of marked cooling in the surface layers of the ocean, as shown by the preceding paper by Leipper, has been noted in association with some intense typhoons in the western Pacific. As discussed in a recent report /1/, cooling of this type is often clearly indicated by 15-day mean charts but the cooling shown between successive 15-day periods seldom exceeds 5° F. Individual ship traverses through areas over which intense typhoons have passed have indicated cooling of the same magnitude shown by Leipper.

The sea surface temperature given in routine synoptic reports are subject to quite large errors /2/ but the errors tend to be systematic for an individual ship. Consequently the temperature changes indicated along a ship track are usually much more reliable than those deduced by combining observations from several ships. Observations of this type have been used to present two cases of unusually low sea surface temperature in the western Pacific (Figures 1 and 2). The data for the ship which passed through the area traversed by typhoon Wanda of 1956 (Figure 1) were taken less than

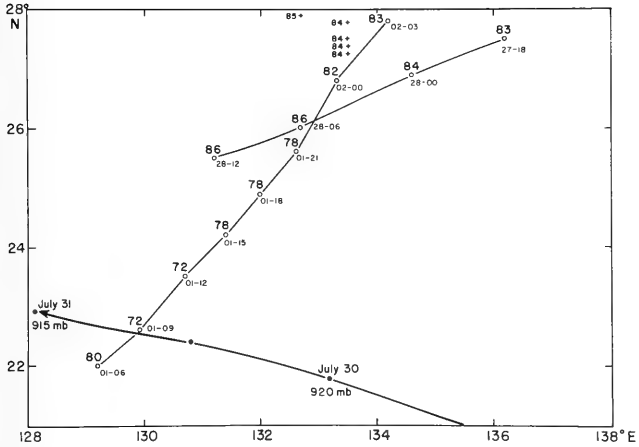

Figure 1. Ship traverses prior to and following typhoon Wanda of 1956. The positions of the storm center and its central pressure at 0000 GMT are shown along the storm track. Temperature values (in °F) are given along the two ship traverses with dates and times shown below the individual reports. The additional reports of sea surface temperature were made on July 30 and 31.

36 hours following the passage of the storm. The two reports of 72°F are 10° colder than those reported by the same ship some 250-300 miles to the northeast and up to 14°F lower than values reported by ships 150-300 miles to the north and northeast 1 to 2 days earlier. The ship traverse across the track of typhoon Nina of 1953 (Figure 2). which occurred about 48 hours after the storm, reported temperature as low as 74°F. These values are some

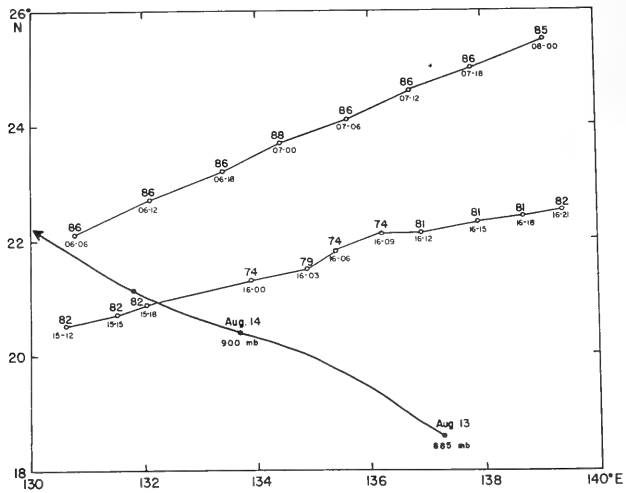

Figure 2. Same as Figure 1 except for typhoon Nina of 1953.

10° lower than the climatological average for the area and season and up to 14°F lower than reports from a ship traversing the area 150-200 miles to the north about a week before the typhoon passage.

The extent of cooling of the surface waters brought about by a tropical cyclone is undoubtedly related to storm intensity and to the vertical temperature distribution in the ocean. Typhoons Wanda and Nina were unusually large and intense and there is little doubt that most tropical cyclones do not result in cooling of the magnitude suggested by Figures 1 or 2 (or by the previous paper by Leipper). However, ship reports following tropical cyclones suggest that rather marked cooling occurs in many cases. Fisher /3/ noted cold pools in the sea surface temperature field following several hurricanes in the 1953-1955 period and ship reports in the western Gulf of

Mexico indicate a significant decrease in surface temperatures following hurricane Carla of 1961. The extent of cooling in this latter case can be judged by the following sea surface temperature statistics for the area 26-29°N, 90-96°W. In the 4-day period prior to the storm passage there were 11 reports of temperatures ranging from 85° to 88°F, with a mean value of 86.0°F. In the 5-day period following the storm the reports in the same area ranged from 78° to 82°F with a mean of 79.6°F.

In the report cited previously /1/, the conclusion was reached that vertical mixing was the primary factor in the cooling of the surface layers of the ocean during a tropical cyclone. However, in contrast to the results presented in the preceding paper by Leipper, the observations led to the tentative conclusion that mechanical stirring was probably more important than organized upwelling in the cooling process. This conclusion was reached mainly from the observation that cooling was much more pronounced on the right hand of the storm track (Figures 1 and 2) where wind and wave action are known to be most pronounced.

REFERENCES

1. Jordan, C. L. and Frank, N. L. 1964 On the Influence of Tropical Cyclones on the Sea Surface Temperature Field. Scientific Report. Department of Meteorology, Florida State University. 31 pp.

2. Saur, J. F. T. 1963 A Study of the Quality of Sea Water Temperatures Reported in Logs of Ships' Weather Observation. Journal of Applied Meteorology, 2, 417-425.

3. Fisher, E. L. 1958 Hurricanes and the Sea-Surface Temperature Field. Journal of Meteorology, 15, 328-333.

THE MODIFICATION OF WATER TEMPERATURES BY HURRICANE CARLA

Robert E. Stevenson and Reed S. Armstrong
Oceanographic Institute
Florida State University

INTRODUCTION

Hurricane Carla entered the Gulf of Mexico through the Yucatan Straits on September 7, 1961. From there it traveled in a northwesterly direction and grew to be one of the five severest hurricanes to invade the Gulf since 1837. By September 10, as it approached the Texas Coast (Figure 1,), pressures in the center were 931.2 mb, and winds of 130 knots whirled around the eye. Because of the early and continuous advisories issued by the U. S. Weather Bureau, nearly 500,000 people evacuated the coastal regions. Thus, despite the fury of the storm and the accompanying storm surges (a maximum of 7 meters where the storm crossed the coast), few persons were injured.

The energy exchange between the sea and the atmosphere is several orders of magnitude greater during a hurricane than in less severe tropical cyclones. Hurricanes provide, therefore, a unique 'laboratory' for investigations of air-sea interaction. However, the taking of in situ measurements of water temperature changes is virtually impossible. Aboard ship, nothing can be done but to practice survival techniques, and even these are unsuccessful on many occasions. Weather buoys have broken from their moorings, never again to be seen, and towers have foundered.

It was, therefore, a fortuitous set of circumstances by which changes in the water temperature distribution affected by hurricane Carla were 'preserved' for investigation at a more peaceful time.

NORTHWEST GULF WATERS IN THE FALL OF 1961

Throughout the year a low-salinity layer of water lies along the coast of the northwest Gulf. The variations in the salinity, width, and thickness of the layer are dependent primarily upon the volume of river runoff coming through the numerous estuaries and lagoons. Usually the surface salinity is approximately 30.00 per mil close to the shore. A salinity of 36.50 per mil is normal at distances of 30 to 50 km from the coast. The water of 30.00 per mil may extend to depths of 20 to 30 meters, below which salinities of 36.00 per mil are encountered at 40 to 50 meters.

In September 1961, the brackish surface water lay in a bulge which extended some 120 km from the coast between the Mexican border and Galveston, Texas. It was over this bulge that hurricane Carla swept on September 10 and 11 (Figure 1).

A month later, between October 4-9, scientists cruised aboard the R/V HIDALGO, of the A&M College of Texas, to investigate the distribution of temperatures and salinity. Many of the traces from bathythermograph casts revealed temperature inversions, with magnitudes as great as 2.5°C, extending to depths of 83 meters (Figure 2). The inversions were all within the area of the brackish bulge (Figure 3). Salinities of 29.76 per mil were encountered near shore, and salinities of 30.00 to 31.00 per mil were measured though depths of 40 meters. In most of this area, water of 36.00 per mil lay below 100 meters, although at 70 to 80 meters the salinities were usually

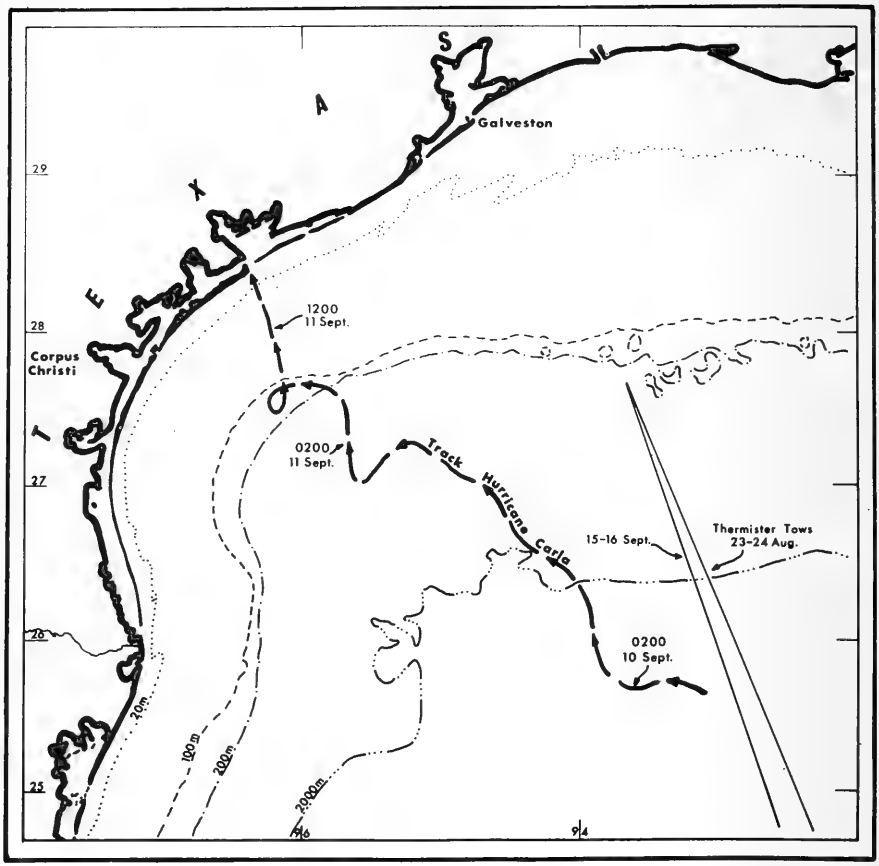

Figure 1. The Track of Hurricane Carla on September 10 and 11, 1961, as Plotted by U. S. Weather Bureau Radar at Corpus Christi and Galveston, Texas, and Locations of Thermistor-Chain Tows Made from the R/V HIDALGO

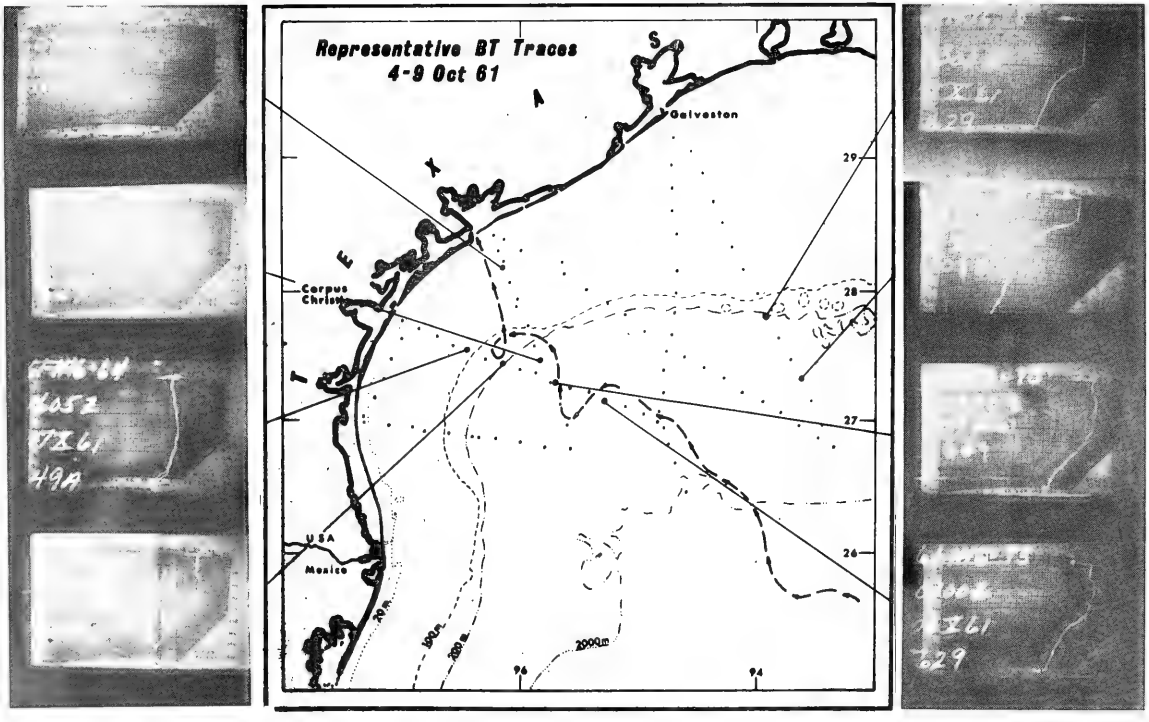

Figure 2. Location of Bathythermograph Casts Made from the R/V HIDALGO on October 4-9, 1961, and Representative Temperature Traces.

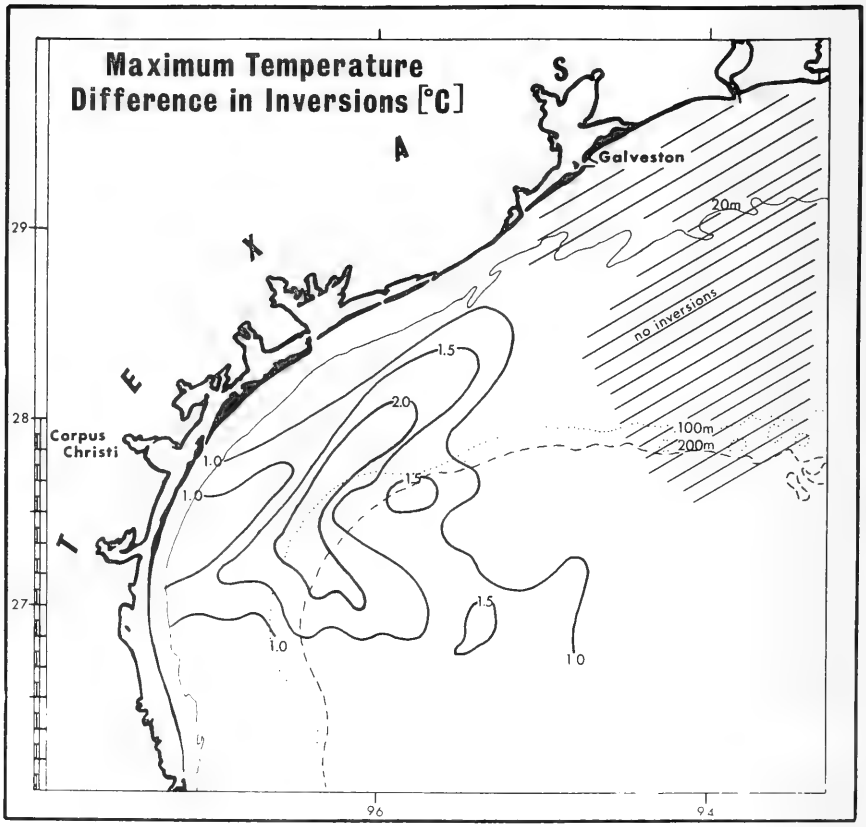

Figure 3. The Distribution of Maximum Temperature Differences in Inversions as Deduced from Data Gathered on October 4-9, 1961.

near 35.00 per mil (Figure 4A and B). Waters with the steepest salinity gradient were within 110 km of the shore, and surface waters having salinities of 33.00 per mil, or less, extended to 210 km from shore (Figure 4A). The typically steep salinity gradients are noted from the curve in Figure 4B.

The loss of heat in the surface waters to the hurricane atmosphere lowered the water temperatures, forming the inversions, and, because of the brackish layer, the lowered temperatures did not result in a density instability in the water. From climatologic records and previous data collected during research cruises in the northwest Gulf, it is known that changes in water temperatures in September and October are negligible. This has been substantiated by applying the techniques presented by Laevastu (1960) to the factors influencing heating and cooling of surface waters. Furthermore, a careful examination of the 91 bathythermograms taken on the October 4-9 cruise showed no indication of heating, or cooling, of the surface waters.

In the weeks following the occurrence of hurricane Carla, winds over the waters of the northwest Gulf blew at low velocities, and there were several successive days of light and variable airs. The wind directions were, as normal, from the southeast. However, the low velocities produced wind-drift currents of little consequence in re-establishing normal temperature distribution. Isosteric surfaces, computed from data gathered on October 4-9, were essentially flat. Therefore, no significant density currents were present.

With these considerations in mind, it was concluded that the water-temperature structure of the northwest Gulf retained, for at least the succeeding 4 weeks, the dominant characteristics formed during hurricane Carla. The inversions which were measured during October 4-9 were believed little modified from the configuration immediately following the hurricane.

To the southeast of Galveston, where the vertical distribution of salinity was nearly isohaline, the heat loss from the surface caused instability in the upper layers. The consequent convective stirring produced an isothermal layer which extended to depths of 60 meters (Figure 2).

THE TEMPERATURE DISTRIBUTION

The distribution of surface water temperatures in the early days of October reflected the influence of Carla (Figure 5). Warmer water was centered in the area where the hurricane deviated from its northwesterly course, whereas colder water was situated near the outer boundaries of the low-salinity layer and over that part of the shallow shelf which was beneath the track of the storm.

At depths of 50 meters (Figure 6), the main 'cells' of warm and cold water were even more sharply defined. The effects of the temperature inversions were noted where temperatures were slightly greater than 28.0°C, which was just more than 0.5°C warmer than those at the immediately overlying surface. Farther from shore and to the right of the hurricane track, the

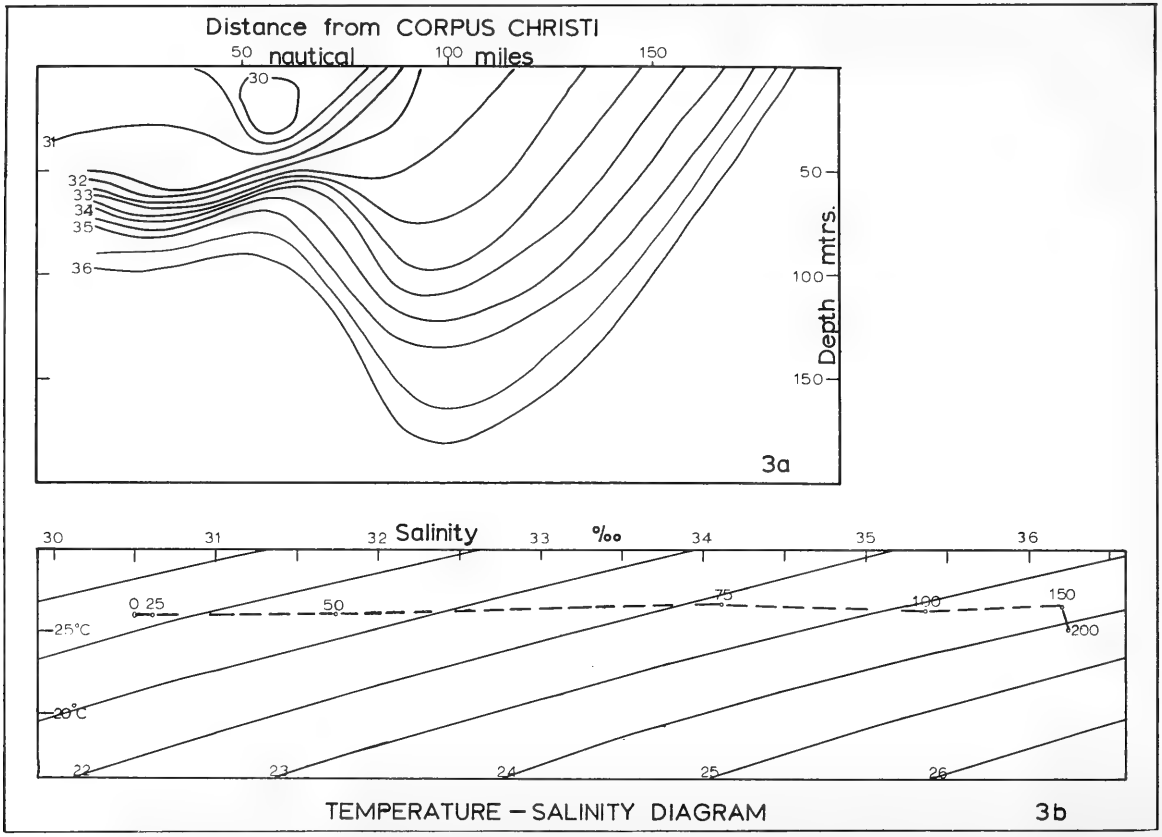

Figure 4(a): Salinity Profile Extending East of Corpus Christi, Texas. The Samples Were Collected on October 7 and 8, 1961.

4(b): Temperature-Salinity Diagram at HIDALGO Station 10 (see Figure 4a.) on October 7, 1961.

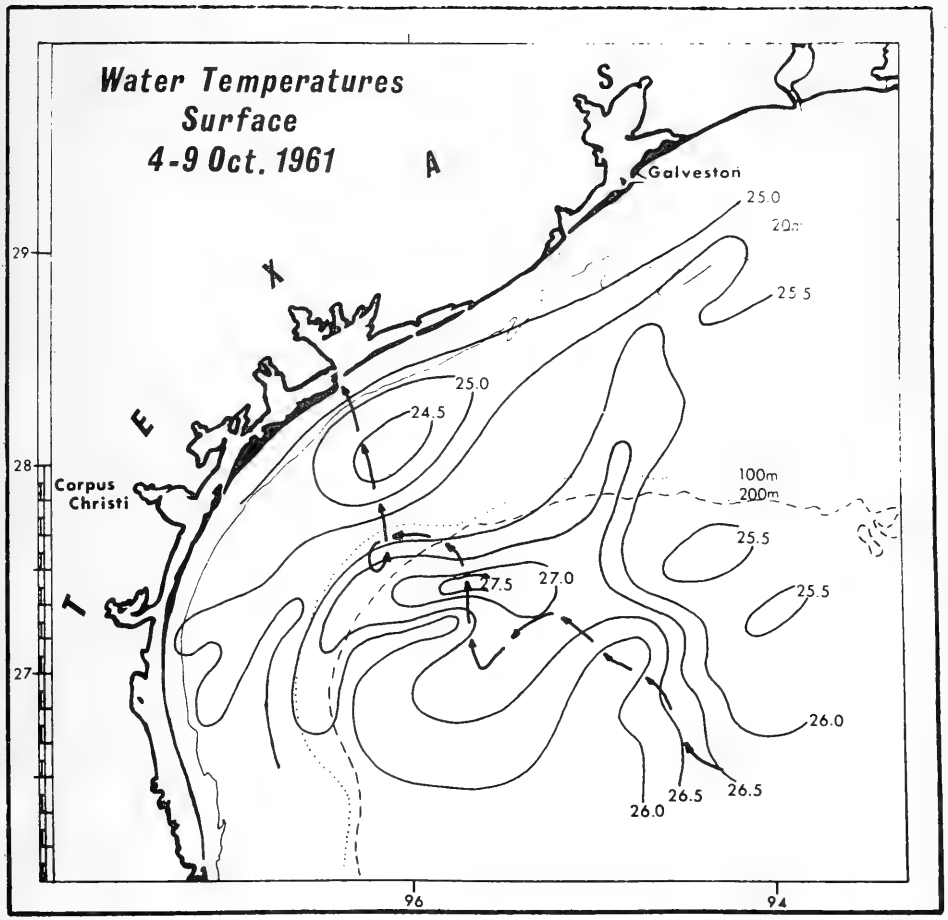

Figure 5. The Distribution of Surface Water Temperatures on October 4-9, 1961.

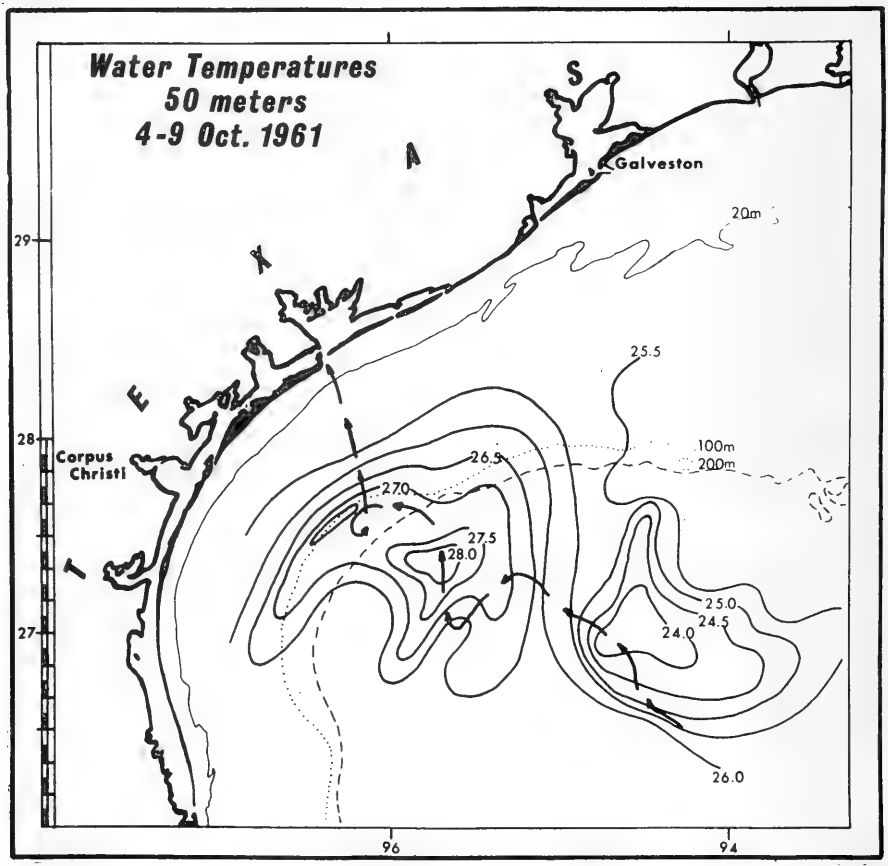

Figure 6. The Distribution of Water Temperatures at a Depth of 50 Meters on October 4-9, 1961.

cooler water indicated modified temperature structures where typical Gulf-water salinities occurred.

The influence of the hurricane was not restricted to the surface layers, for there was an upward transport of heat from depths greater than 100 meters. This was best exemplified by changes which took place in the vertical and horizontal configuration of the thermocline. For Figures 7 and 8, semi-diagrammatic sketches were drawn from data gathered by thermistor-chain tows along the tracks indicated in Figure 1. (It must be noted here that Figures 7 and 8 were drawn from average values of the data obtained by the thermistor-chain. The temperatures and the depths of the isotherms differ to some extent, therefore, from those plotted directly from the bathythermograms.) On August 23 there was a thermocline typical of these Gulf waters, exhibiting a flat surface at depths of 65 to 70 meters. The thickness of the thermocline decreased in an offshore direction, but the 26°C isotherm remained as the upper limit throughout the length of water measured.

During the hurricane, 26°C water was carried into the disturbed surface layer, and the 25°C isotherm marked the upper part of the thermocline on September 15 (Figure 8). The surface of the thermocline was no longer flat, having been depressed to the shoreward and seaward of the region where the tracks of the hurricane and thermistor tow crossed. A comparison of the two profiles (Figures 7 and 8) reveals that after the storm the 24° and 25°C isotherms were deeper in the near-shore area and that those below the thermocline were from 18 to 70 meters shallower than on August 25. The greater upward displacement was in the deeper water (note the 20°C isotherm, for example).

The topography of the 25°C isotherm (top of the thermocline) during the days of October 4-9 closely resembled the configuration of the temperature distribution. Whereas south of Galveston and seaward of the shelf break, the thermoclinal surface was generally between 50 and 75 meters, to the west it was depressed to depths of 102 meters (Figure 9). From the edge of the shelf shoreward, the depth to the thermocline decreased abruptly, and, along the track of the hurricane, it was absent in waters shoaler than 50 meters (see Figure 2).

Authors' Note: A more complete paper was prepared for presentation at the Third International Conference on Hurricanes and Tropical Meteorology held in Mexico City in June 1963. That paper is now in press in Geofisica Internacional as part of the Conference proceedings.

In presenting this condensed version at Wakulla Springs in February 1965, it was the authors' intent to show the similarities and differences in the water temperature distribution in the northwest Gulf in 1961 as compared with that existing after hurricane Hilda (see Leipper, this volume).

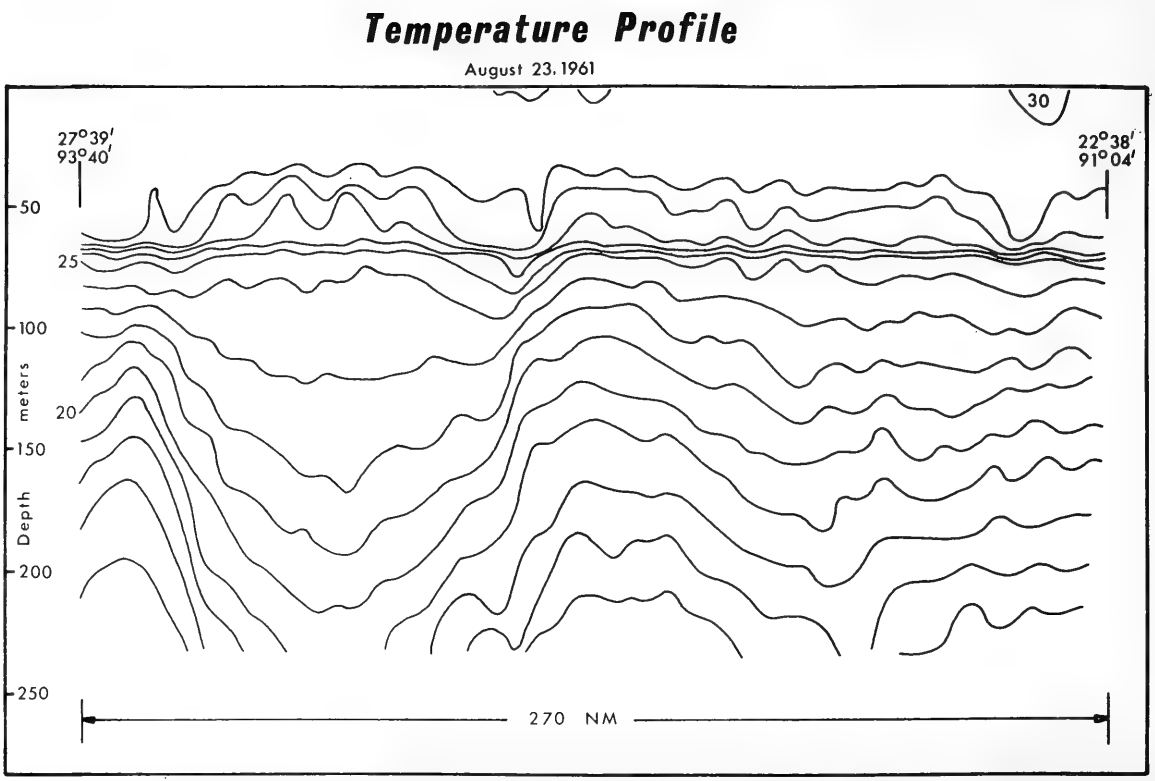

Figure 7. A Semidiagrammatic Representation of the Vertical Water Temperature Distribution South of Galveston on August 23, 1961. Data Were Obtained from a Thermistor-Chain Tow Made from the R/V HIDALGO.

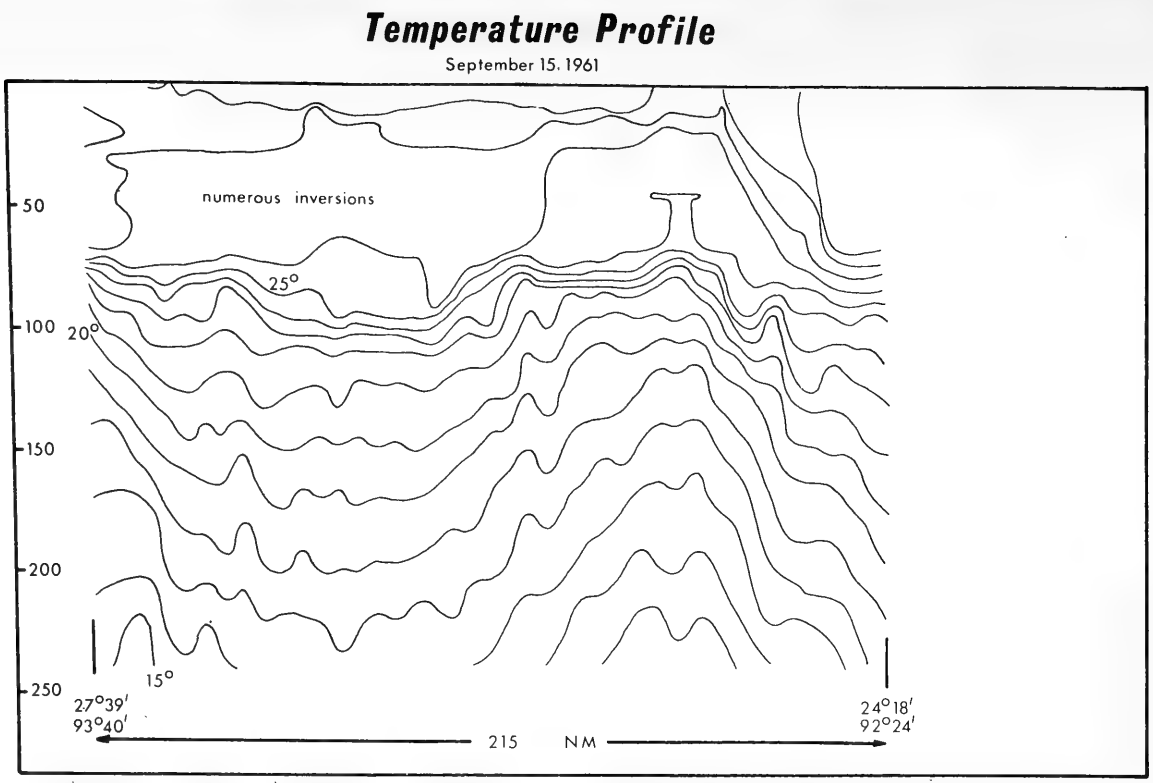

Figure 8. A Semidiagrammatic Representation of the Vertical Water Temperature Distribution South of Galveston on September 15, 1961. Data Were Obtained from a Thermistor-Chain Tow Made from the R/V HIDALGO.

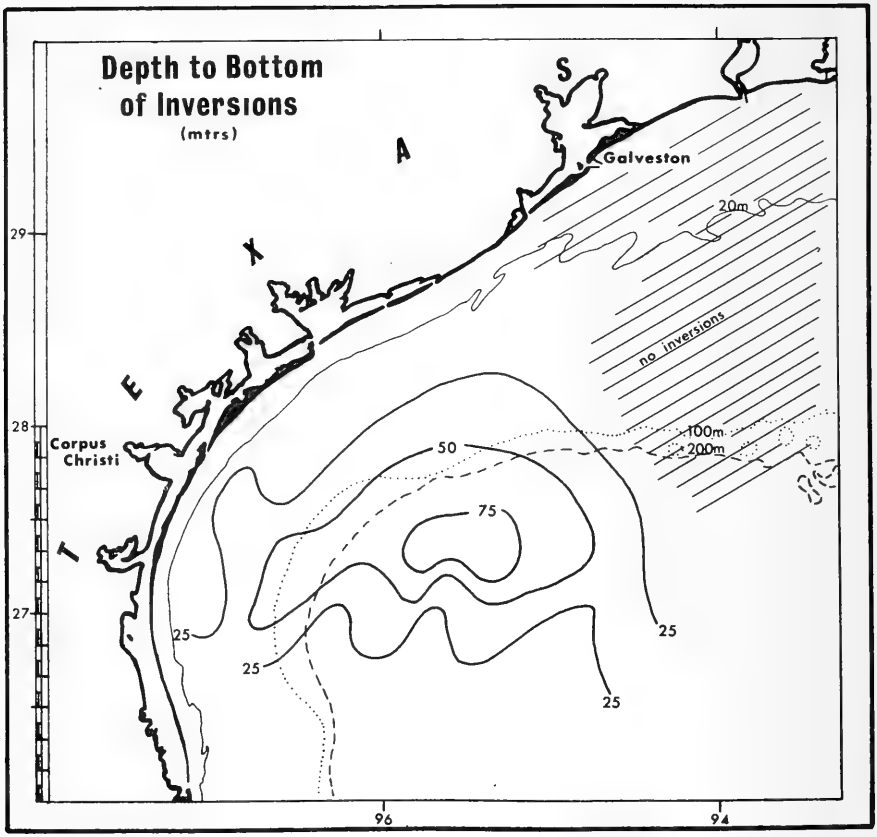

Figure 9. The Distribution of Depths to the Base of Temperature Inversions on October 4-9, 1961.

The cruises of the R/V HIDALGO in 1961 were certainly "cruises of opportunity," for the extent and magnitude of changes in the waters following a hurricane passage were unknown. Nevertheless, the temperature profile obtained on September 15, 1961 (Figure 8), is quite similar to those from data gathered in 1964. The "stovepipe" effect beneath the "eye position" is easily noted, as is the depression of the thermocline on either side. It would appear that Leipper's analysis is correct; that the warmer surface water was transported from the areas of the "eye" to lie in "trough" along the borders of the "eye track," and that the removal of the surface water beneath the "eye" developed a divergence which resulted in the upwelling of deeper and cooler water.

One recognizes also, as from the data presented by Leipper, that the isotherms below the thermocline were at lesser depths following hurricane Carla than before (compared Figures 7 and 8). This is the case at least to the depths measured; i.e., about 230 meters. However, the configuration of the isotherms below 100 meters (perhaps even 75 meters) on September 15, was nearly identical to that existing before the hurricane. It was strictly fortuitous that the path of hurricane Carla crossed the southern border of the western Gulf eddy. Thus, the configuration of the isotherms below the thermocline existed before the hurricane and clearly was not altered as the result of any reaction to the storm.

Water temperatures collected in the northwest Gulf in October 1961 differed from those in the north-central Gulf in October 1964. In only the shallow nearshore waters in the north-central Gulf were there temperature inversions, whereas deep inversions were widespread in the northwest Gulf after Carla (Figure 3). In each case, the inversions occurred only where low salinity water made up the surface layer.

Hurricane Hilda travelled over Gulf waters of normal salinity (@ 36.00 per mil) throughout most of its course. Hurricane Carla, on the other hand, travelled over waters which had surface salinities of near 30.00 per mil. Thus, the water temperatures resulting from the two hurricanes differed significantly, and any comparison must be subjective.

It is unlikely that the temperature inversions which were measured in 1961 can have resulted from any mechanism other than cooling; i.e., heat loss. Upwelling does not produce such vertical temperature distributions. An introduction of cool, low-salinity water could allow inversions similar to those observed to develop. However, the source of low-salinity water is the estuarine system of the Texas coast which, during the later summer, contains water with temperatures of 28°-32°C. Furthermore, and as discussed by Leipper (this volume), the wind field around the hurricanes develops a wind drift (in these cases, storm surges) which drives water into, rather than out of, the lagoons and estuaries.

Considering, then, that the inversions represent a certain amount of heat loss from the waters, the magnitude and depth of the inversions could be controlled by (1) the thickness and salinity difference of the surface

layer, (2) the intensity of the storm and the consequent reaction of the water, or (3) a combination of both.

Were the temperature decrease sufficient, in any water, to produce a density instability, convective stirring must take place (in addition to mechanical stirring by wave action). In such cases, inversions would be eliminated and a thoroughly mixed layer formed (as noted by Leipper in waters of normal salinity in the north-central Gulf, and by the authors in the waters southeast of Galveston). If cooling were insufficient to cause a convective stirring in the brackish surface water, but extended below the low-salinity layer, a mixed zone below the inversions would be expected. None was noted (see Figure 2). A more precise determination could be made if there were adequate salinity data. However, in October 1961, we obtained too few salinity samples to analyze the depth distribution of the brackish water in detail. Thus, we must rely on an interpretation of the temperature data.

The lesser salinity of the surface waters could, as mentioned, control the magnitude of the temperature inversions. Again, should the cooling be so great as to produce a density instability, convective mixing would result. Conceivably, then, cooling could produce greater temperature differences than observed in the inversions, but the depth and magnitude of the inversions would be limited by the consequent instability of the water column.

The temperature-salinity curve in Figure 4b shows that the water to 150 meters (at this station) was far less stable than that normally encountered, but still did not reach a neutral stability (a frequent condition in the Gulf during the winter). The temperature decrease was not, therefore, the maximum possible under the prevailing water conditions. It is clear, then, that the depth and magnitude of the inversions were the result of the reaction of the water to the storm.

UPWELLING AND COOLING

The discussion by Leipper of the water temperatures after hurricane Hilda impressively described the mass transport of surface water from the region underlying the "eye." Such a picture is not obvious from the data obtained after hurricane Carla. Rather, the temperature inversions ascribe to cooling of the water.

Conversely, the temperature distribution after hurricane Hilda presented great difficulties in defining a degree of heat loss from the water. One cannot but presume that both mass transport and cooling take place. However, to fit the two together from the available data is not a simple matter, nor have we tried, other than by mental ruminations.

Certainly, were one to place a magnitude of upwelling to the inversions measured in 1961, then it is clear that cooling extended to a greater depth

than indicated by the temperature curves. With the data we have, any estimation of how much greater would be pure folly. Nonetheless, it now seems apparent that the heat loss from the water must have been orders of magnitude more than the 2.2×10^{18} cal/24 hours originally calculated.

Acknowledgements - Financial support for this work was from the Office of Naval Research, under contract NONR 2119(04) NR 083-036.

REFERENCES

Laevastu, T. 1960: Factors affecting the temperature of the surface layer of the sea, Societas Scientiarm Fennica, Comm. Physico-Math XXV 1

ON THE LOW LEVEL THERMAL STRATIFICATION OF THE MONSOON AIR OVER THE ARABIAN SEA AND ITS CONNECTION TO THE WATER TEMPERATURE FIELD

José A. Colón
U. S. Weather Bureau
San Juan, Puerto Rico

ABSTRACT

During the period August 7 to September 28, 1963 the research vessel R/V ATLANTIS II, while participating in the program of the International Indian Ocean Expedition, made several E-W cross sections across the Arabian Sea carrying out a program of meteorological and oceanographic observations which included daily radiosondes. This collection of raob data was analyzed in the form of time and space atmospheric cross sections in order to study the general properties of the monsoon air.

The southwest monsoon regime is generally established over the Arabian Sea around the latter part of May and is maintained as a fairly steady and persistent current until the latter part of September. Therefore, the data collected by the ATLANTIS II showed characteristic properties of the monsoon current at the height of the season.

The thermal structure consisted essentially of two layers of air: a shallow layer of humid air near the surface and a dry, relatively unstable air mass on top, separated by a pronounced thermal inversion. The nature of the monsoon inversion and of its distribution over the Arabian Sea was investigated.

The properties of the surface moist layer and the modifications during its path downstream will be discussed also in relation to the water temperature field and the weather-producing processes responsible for monsoon rains.

INTRODUCTION

This report deals with the low level thermal stratification of the atmosphere over the Arabian Sea during the summer monsoon season, its relation to the water temperature field, and to the general atmospheric circulation in the area. In order to understand better the problems involved, we should review briefly the general characteristics of the Indian monsoon circulation, although these are fairly well known to most readers.

The mean circulation near the surface over the Arabian Sea, once the southwest monsoon current is well established, can be illustrated by the mean chart for August (Figure 1). The monsoon circulation is usually established over the northern Indian Ocean by early June. The flow pattern shown in Figure 1 persists with little variation from June until late September. The surface flow over the Indian Ocean northward from about latitude 20°S consists essentially of a current formed by the southeast trades of the southern Indian Ocean turning in a clockwise direction near the equator to continue as a broad southwest current over the Arabian Sea into the Indian subcontinent and southeast Asia.

During the 1963 season we had the opportunity to analyze and study the Indian monsoon weather while stationed in Bombay participating in the activities of the International Indian Ocean Expedition. One of the features noted with great interest was the persistent and steady character of the circulation over the Arabian Sea which showed very little interdiurnal variations in a picture that day after day differed little from what appears in Figure 1. The daily charts showed important variations in wind speed, but only small variations in the direction of flow.

The establishment of the southwest monsoon current over the Arabian Sea brings about significant change in the oceanic circulation and distribution of water temperatures. There is as a result a large variety of air-sea interactions going on over this oceanic area during the monsoon, with significant effects on both the properties of the oceanic surface layers and of the atmospheric layer above. Some of these effects were studied in an earlier report (Colón, 1964). The Arabian Sea during the summer season presents as varied and striking evidence of air-sea interactions as can be found anywhere else in the globe. Some of these developments assume even greater importance when considered in the light of the vast production of rain which normally takes place a little farther downstream over India.

Among the activities carried out during 1963 in Bombay were a series of aircraft flights over the Arabian Sea by the U. S. Weather Bureau-Research Flight Facility and by the Woods Hole aircraft operated by Dr. Andrew Bunker to investigate the monsoon flow over the ocean. One important reconnaissance mission consisted of a flight upstream following the surface streamlines, which in a period of 2 days covered the path all the way from Bombay to the

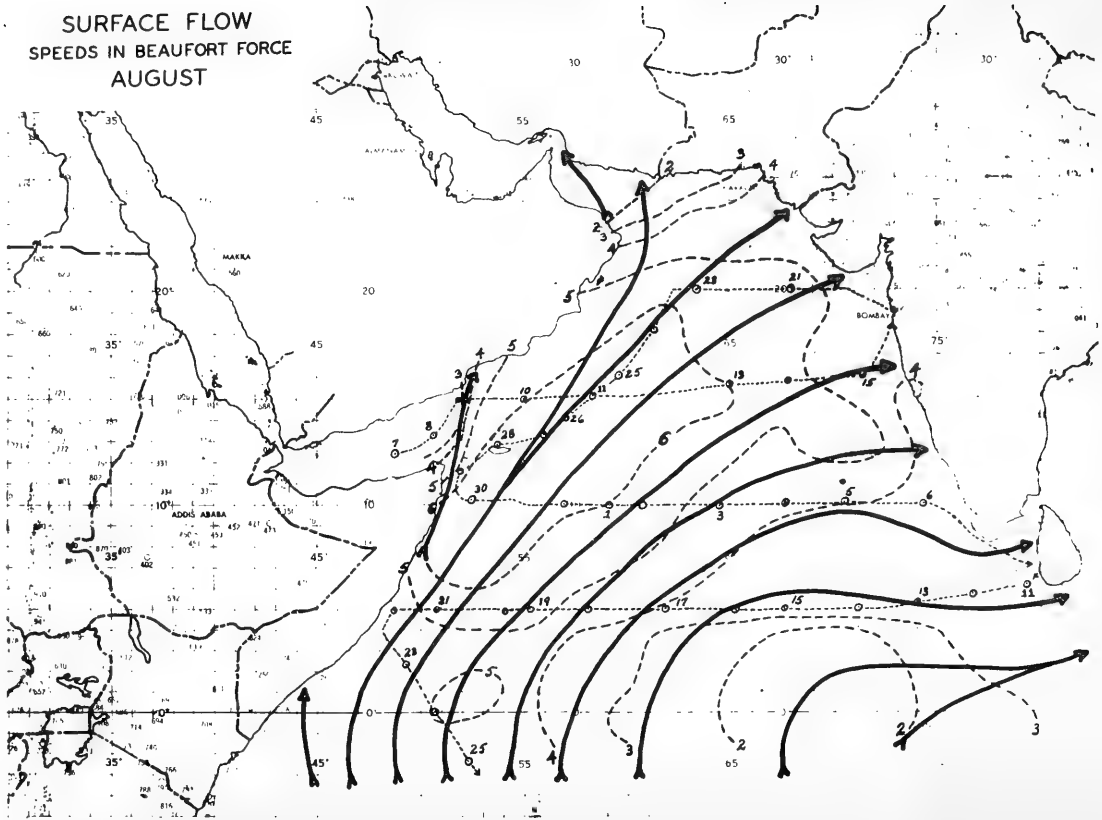

Figure 1. Mean Surface Circulation Over Arabian Sea for August. Dashed Curves Are Isotachs in Beaufort Force. Dotted Path Shows Track of R/V ATLANTIS II, August 7 - September 25, 1963, With Positions of Raob Observations Indicated.

equator near the coast of Africa. That mission contributed greatly to our knowledge and understanding of the atmospheric properties and weather features over that oceanic body. Another important source of data were the cruises by the research vessels RV ATLANTIS II and RV ANTON BRUUN. The ATLANTIS II carried out an extensive survey over most of the Arabian Sea during the period August 7 - September 28, 1963.

The present study is mainly concerned with some aspects of the raob data collected by the ATLANTIS II. A collection of about 45 soundings made aboard the ATLANTIS II were studied and analyzed in various forms which revealed well the general characteristics of the thermal stratification over the ocean. We also had access to 10-12 soundings made aboard the RV ANTON BRUUN from August 11-26, 1963, and to innumerable dropsondes made by the research aircraft.

TRACK OF THE ATLANTIS II IN RELATION TO THE FLOW AND WATER TEMPERATURE FIELDS

The track of the ATLANTIS II in relation to the monsoon circulation is illustrated in Figure 1. The monsoon current shows a significant velocity maximum in the western side of the sea near the coast of Somali, with speeds decreasing downstream. In the mean picture the velocity maximum is around 30-35 knots, but velocities of around 50 knots were measured by aircraft in that area. Very significant upwelling of the cold subsurface water is also observed in that area.

One interesting and significant feature of the flow is that nearly all the surface air that enters into India seems to have an oceanic source originating in the Southern Hemisphere. However, flow charts at some distance above the surface, for example 850 mb, reveal flow off the African Continent and the Arabian peninsula moving eastward toward India. Thus, the southwest oceanic current is extremely shallow.

The ATLANTIS II made four latitudinal cross sections between the east and west sides of the sea. She cruised from Aden to Bombay along latitude 15°N from August 6 to 15. From Bombay she cruised westward along latitude 20°N and southward to the region of upwelling near Somali; then eastward along latitude 10°N, arriving in Colombo, Ceylon on September 7. From Colombo she proceeded westward along latitude 5°N, to the coast of Africa, then went southward arriving in Zanzibar on September 28.

This track turned out to be quite good from the point of view of a study of the monsoon current. The latitudinal paths were to large extent across the flow in the western Arabian Sea, but nearly parallel to it in the east side. The track from August 23 to 30 followed for a distance of about 1000 miles a direction upstream closely parallel to the flow, terminating in the cold-water region near the coast of Somali.

The distribution of water temperatures is shown in Figure 2. The isotherms are oriented in a general southwest-northeast direction with very cold temperatures of 22-23°C in the western coastal areas in the regions of upwelling and warm centers of 27-28°C in the east side. The influence of the atmospheric circulation on the distribution of temperatures can be easily visualized. We can note with interest the extremely warm temperatures in the Gulf of Aden and the thermal gradient between the Gulf and the Arabian Sea. The track of the ATLANTIS II is also reproduced in Figure 2 to show the distribution of data with respect to the water temperature field.

THERMAL STRATIFICATION - THE MONSOON INVERSION

Two soundings obtained by the ATLANTIS II in the central Arabian Sea, reproduced in Figure 3, illustrate the essential characteristic of the thermal stratification of the monsoon air over the ocean. One was obtained on August 11, 1963, near 15°N, and 58°E, and the other on August 14, 1963, near 16°N, and 63°E. Only the dew-point curve for August 14 is illustrated.

Figure 3 indicates a well-mixed, humid layer of air near the surface, a pronounced inversion immediately above in the levels from about 900 to 800 mb, and a relatively warm, dry-air mass aloft. The lapse rate is close to dry adiabatic in the surface layer, stable in the inversion, relatively unstable from the top of the inversion to the 500-mb level and close to the moist adiabatic in the high troposphere. The humidity is large in the surface layer and drops off significantly at the base of the inversion. These data illustrate a moist air mass below, evidently dominated by oceanic influences and a dry hot-air mass aloft, presumably of continental origin. Figure 3 shows a larger depth of the moist layer, or higher base of the inversion, in the position farther east.

The presence of such a pronounced inversion so close upstream from the coast of India was detected quite early in our studies of the monsoon air over the ocean and presented some interesting questions concerning the mechanisms for development of monsoon rains.

The soundings were analyzed in the form of five cross sections; four of them along latitudinal directions and one along a direction parallel to the flow. They all presented a consistent picture of a low inversion in the western edge of the sea, which rose eastward toward India and showed a pronounced tendency for dissolution near the Indian coast. The cross section along latitude 15N showed a rather deep stable layer in the western end with a warm center of over 20°C temperatures at the 825 mb level, which was about 8°C warmer than at the same level in the east side of the ocean. The top of the moist layer or base of the inversion rose from the 960 mb level at longitude 50°E to the 850 mb level at longitude 68°E. A sounding obtained near the Indian coast on August 15 showed no presence of the inversion. The other E-W cross sections along latitudes 10°N and 5°N showed more or less similar characteristics.

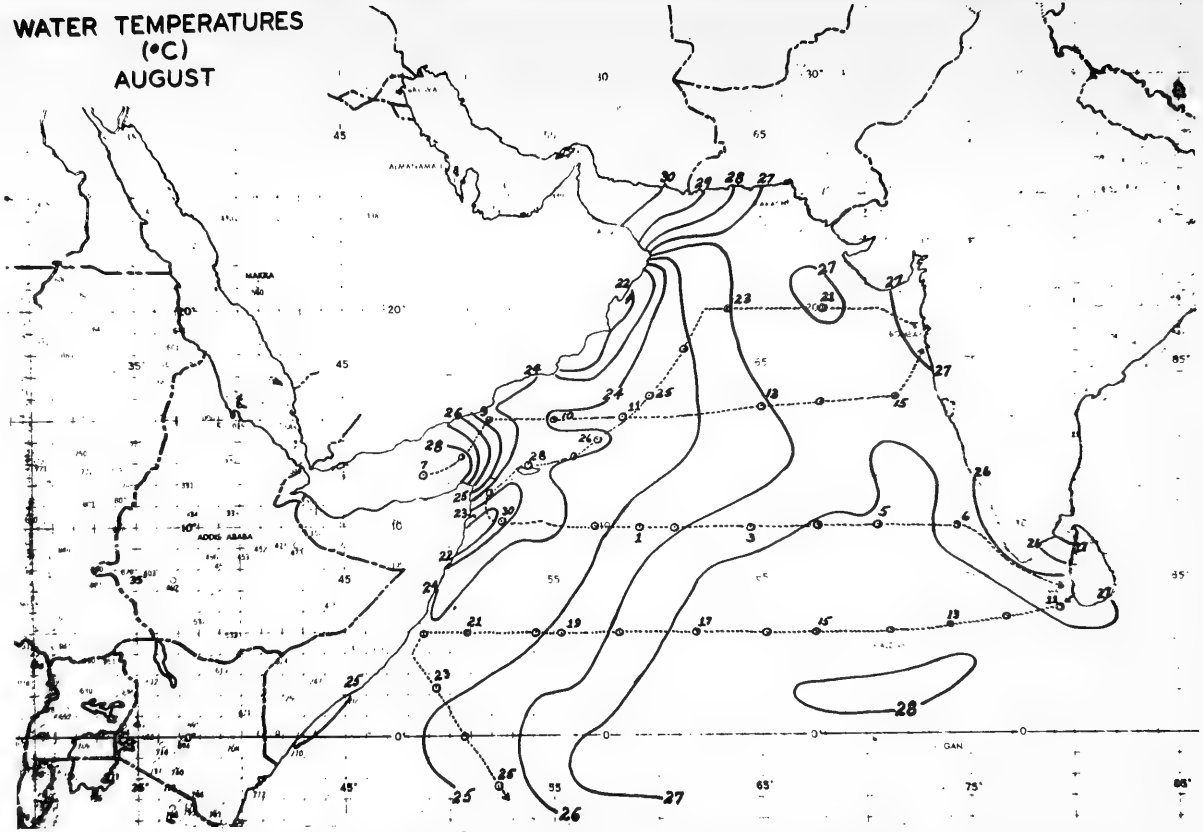

Figure 2. Mean Water Temperature (°C) Distribution, Arabian Sea, August. Dotted Path Shows Track of RV ATLANTIS II, August 7 - September 25, 1963, With Positions of Raob Observations indicated.

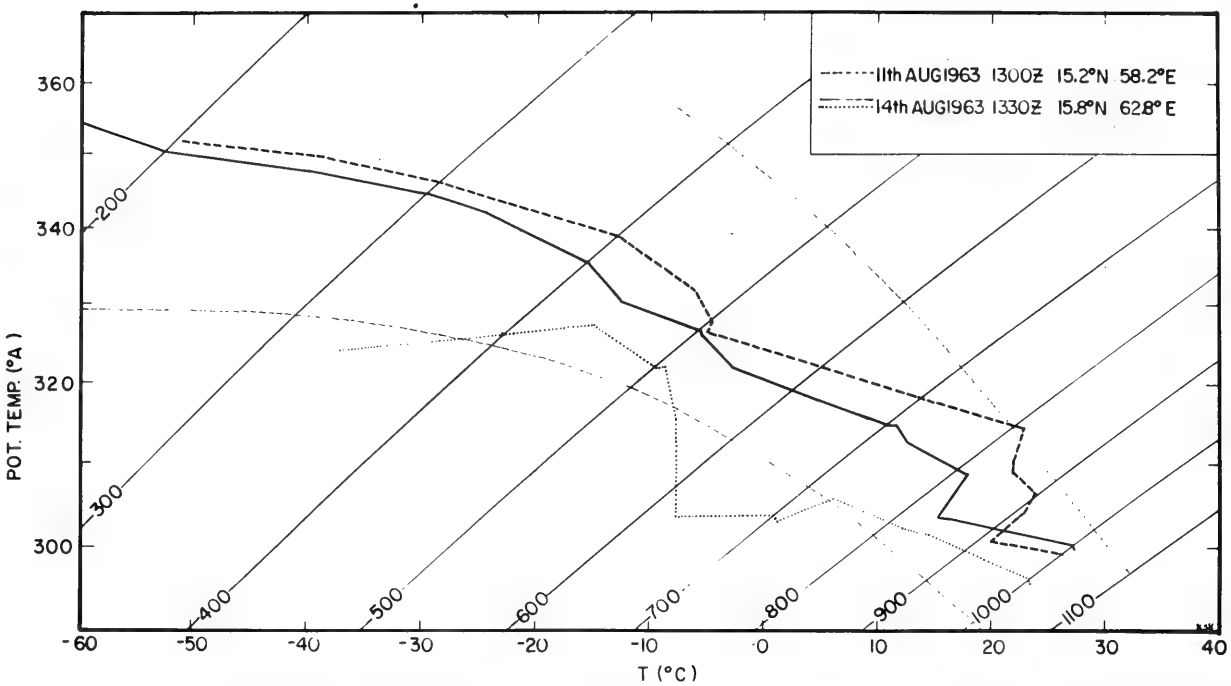

Figure 3. Tephigram With Temperature Soundings Over Arabian Sea Recorded Aboard RV ATLANTIS II on August 11 and 14, 1963.

The cross section made from August 23-30, which extended in a line closely parallel to the direction of flow and indicates well the modifications introduced as the air moved downstream over the sea surface is illustrated in Figures 4 to 6. It starts in a position near 10°N, and 57°E, very close to the center of colder temperatures, and extends to a position near 20°N, and 63°E. Figure 4 shows the temperature field. The base of the inversion or top of the moist layer appears at the 960 mb level in the upstream end; it rises slightly in the first 600 miles, and more rapidly afterward. In the downstream end it was observed at the 850 mb level. The depth of the stable layer did not vary much downstream. At the surface there was an increase in temperature from 24° to 26°C between the upstream and downstream end, which no doubt resulted from heating from the water surface. At the 850 mb level the temperature decreased from 20-21°C in the upstream end to around 16°C in the northeastern or downstream end.

The field of potential temperature, Figure 5, indicates as one of its most interesting features that the 300°K line followed closely the level of the base of the inversion. The 304°K isoline also followed closely variations in height of the inversion layer. This is evidence of rising adiabatic motion as the monsoon air moved downstream over the ocean, since in the lower layer we can presume with a great degree of validity that the flow followed closely along the cross section line. At upper levels it cannot be similarly assumed that the flow followed parallel to the cross section. The potential temperature lines above the inversion were displaced generally downward downstream. An attempt to construct an isentropic chart for a level in the dry air mass aloft was not too successful, but there appeared to be a tendency for downslope motion between the west and east sides of the sea, a tendency that is also supported by the data in Figure 5.

The most important feature of the moisture distribution (Figure 6) is the increase in moisture content downstream near the surface, evidence also of the exchange processes between the sea surface and the air above. The tendency for higher moisture content in the upper levels near 500 mb in the eastern end of the section is also evident. In computations carried out over the central Arabian Sea average evaporation rates of 600-700 cal cm^{-2} day^{-1} were obtained.

An analysis of the distribution of the height of the base of the inversion or mean depth of the surface moist layer is shown in Figure 7. It indicates a shallow moist layer or low inversion in the western section of the Arabian Sea, specially near the coasts of Arabia and Somali, and a rise eastward toward the coast of India.

In the western half of the Arabian Sea all available soundings revealed the presence of the inversion near the surface. A few aircraft soundings available in the northern corner near Arabia and Pakistan revealed a very pronounced inversion close to the surface. In the eastern third, near the coast of India, most of the available observations showed absence of the inversion. The stratification was generally indicative of disturbed weather conditions with lapse rates close to the moist adiabatic and high moisture content extending to 500 mb and above. To the south, near the equator, the

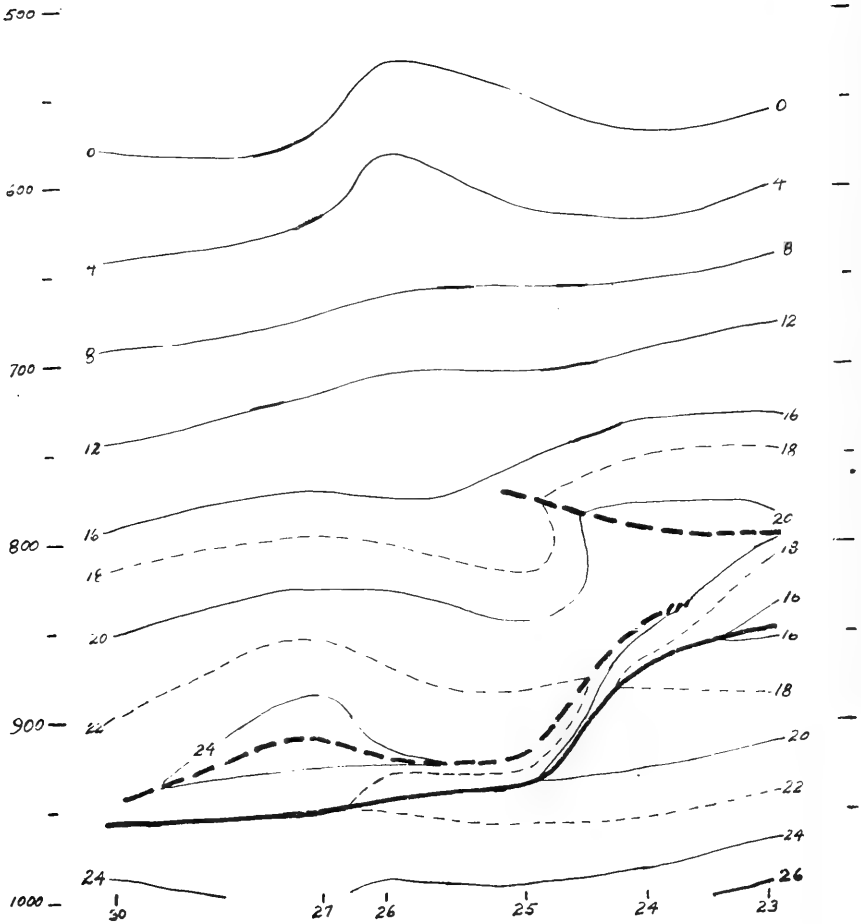

Figure 4. Temperature (°C) cross section based on data collected by RV ATLANTIS II between positions 20°N, 63.5°E, and 10°N, 52.5°E, August 23-30, 1963. Heavy solid line shows base and heavy dashed line top thermal inversion.

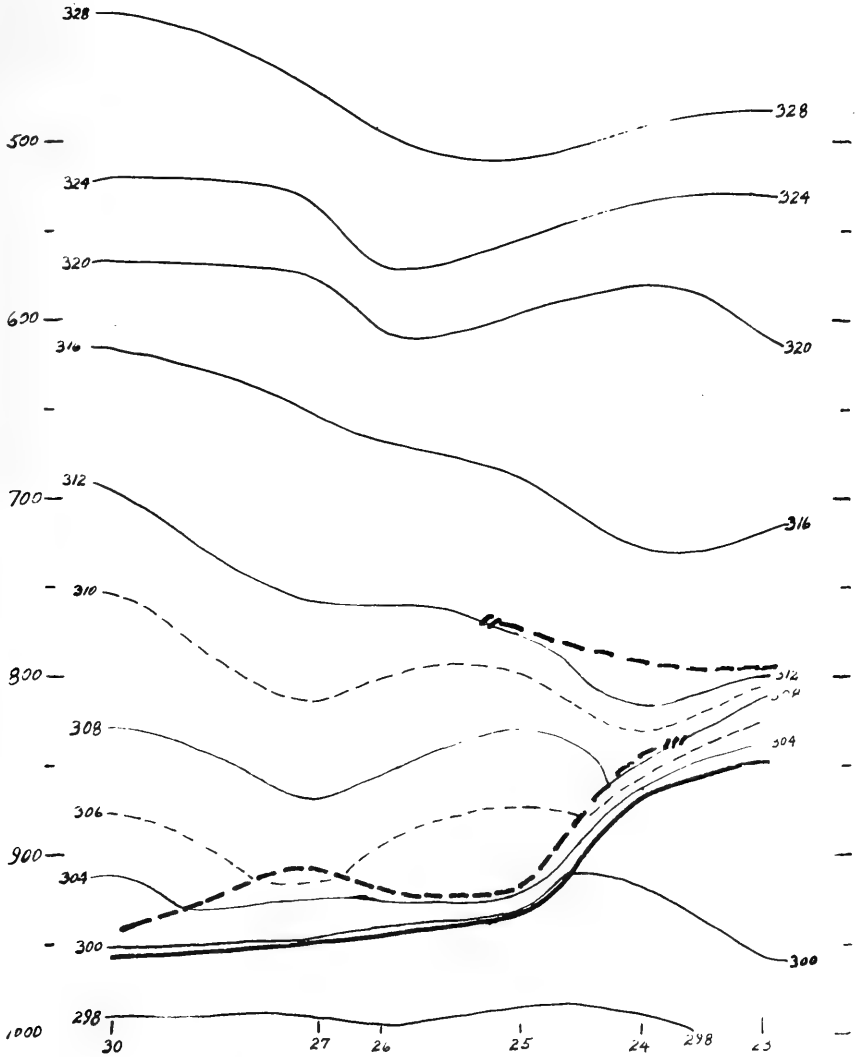

Figure 5. Potential temperature (^{o}K) cross section for section described in Figure 4.

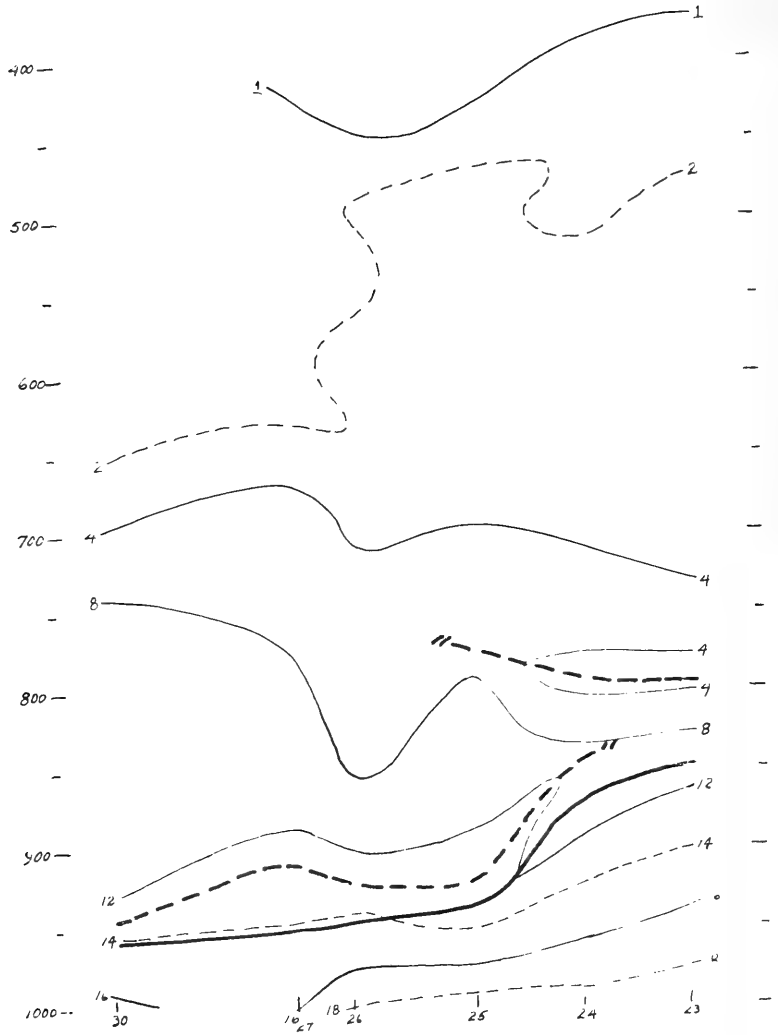

Figure 6. Moisture cross section (gm kg^{-1}) for section described in Figure 4.

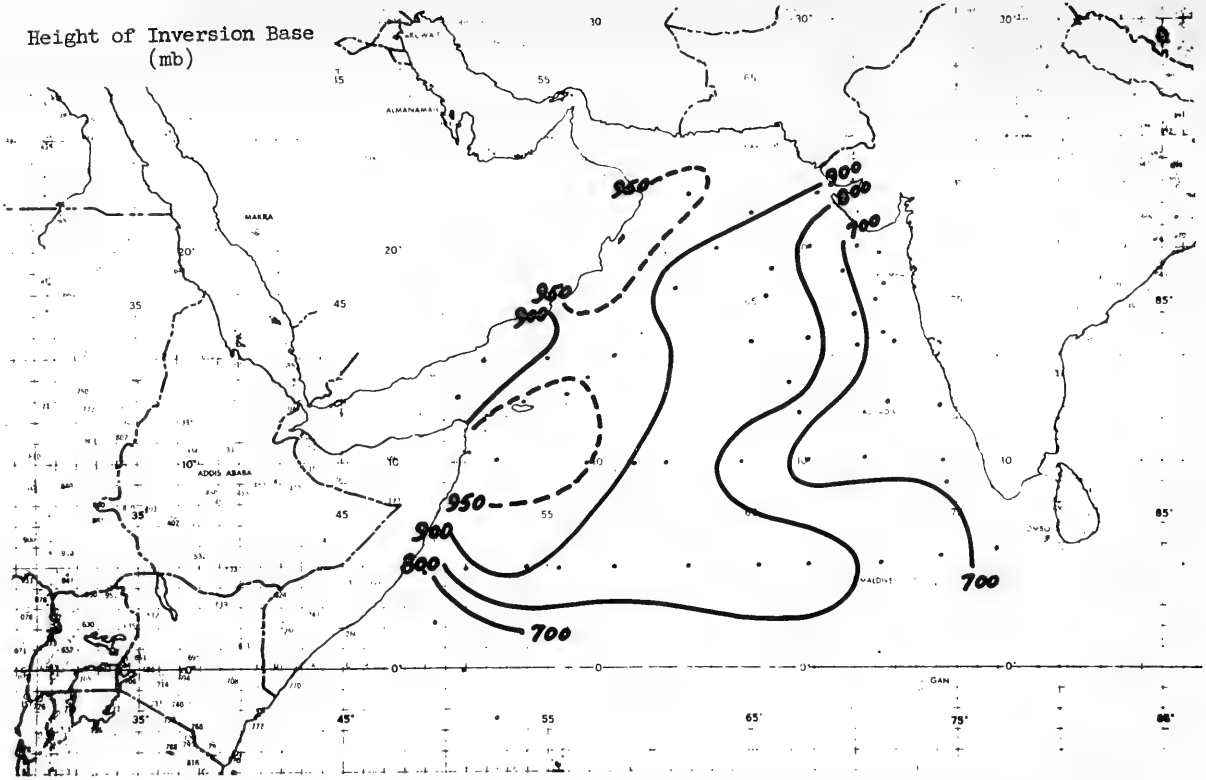

Figure 7. Distribution of the Height (mb) of the Base of the Monsoon Inversion Over the Arabian Sea. Black Dots Indicate Position of Available Data.

cross section taken along latitude 5°N, showed the presence of the inversion in most of the soundings, generally higher in the eastern section. In this cross section and also in the one taken along latitude 10°N, the presence of a second inversion near 600 mb was noticed in most of the soundings.

In the western equatorial region near the coast of Africa conditions were more variable. Generally, more unstable conditions prevailed there. Most of the soundings in that area showed moisture extending to high levels. A few soundings obtained from the research aircraft earlier in the season showed tendency for an inversion near 850 mb.

In general, the distribution showed a pronounced low inversion over the cool waters in the upwelling areas near the coasts of Somali and Arabia, a general rise in the inversion downstream toward the coast of India and a pronounced tendency for sudden and violent overturning with disturbed weather in the coastal area just west of the Indian coast. The disturbed weather zone along the east coast extended south from about latitude 20°N; north of this latitude more stable and drier conditions were prevalent, which is of course reflected in the presence of the desert-like conditions of northwest India and west Pakistan.

SUMMARY AND CONCLUSIONS

Some remarks should be made concerning the basic assumption behind the method of analysis used. The data were all obtained from a moving platform and in the case of ATLANTIS data covered a period of 7 weeks. The aircraft data mentioned was obtained about a month and a half earlier. They were analyzed to show variations in space, under the assumption that the variations in time were negligible compared to those in space. On the basis of the experience during the 1963 season, we think that this principle holds well. Of course, not all of the details shown by the data can be considered indicative of space variations exclusively. The gross features emphasized above are unquestionably evidence of space variations. The validity of this approach is supported by the fact that the picture derived from the analysis is quite close to the one to be expected considering the factors operating over that area.

The picture can be summarized as follows: The establishment of the monsoon circulation near the surface over the Arabian Sea in the characteristic manner illustrated in Figure 1 and in reference to the land masses of Africa and Arabia influences greatly the distribution of water temperatures over the Arabian Sea mainly through the processes of upwelling in the western side of the sea. At the same time the oceanic influence on the air mass in the surface layer combined with a continental air mass that moves eastward in the levels upward from about the 900 mb level results in stabilizing the thermal stratification in the western zone of the sea. We have thus a relatively cool moist shallow air mass below and a dry warm mass aloft separated by a thermal inversion and moisture discontinuity. These

stability conditions in the west central Arabian Sea seem to persist with a minimum of variation throughout the monsoon season.

As the monsoon current moves northeastward over the sea, flux from the sea surface, mixing enhanced by the relatively strong flow near the surface, and adiabatic ascent imposed by the field of motion act to increase the heat and moisture content of the monsoon air and to increase upward the depth of the moist layer. The flux of heat from the sea to the ocean in this area has been computed as close to 600-700 cal cm^{-2} day^{-1}. At the same time sinking motion in the warm air mass aloft contributes also to vertical mixing with the moist mass below.

In the western two-thirds of the sea the properties of the monsoon current appear to be influenced almost exclusively by the process of air-sea property exchange. In the eastern third of the oceanic mass, closer to the Indian coast, the prevailing tendency is for dissolution of the inversion, violent vertical mixing leading to generally unstable conditions with considerable layered cloudiness and convection. The prevalence of unsettled weather in that area throughout the monsoon season is very well supported by the mean weather distribution charts. The destruction of the inversion cannot be ascribed to purely air-sea interaction processes; it is apparently due to developments in the synoptic scale. Conditions in the area to the west of Bombay suffer significant interdiurnal variations and periods of relatively good weather alternate with periods of more violent and widespread rain activity. Periods of so-called breaks in the monsoon over the west coastal sector of India seem to be associated with conditions over the Arabian Sea such that the relatively stable conditions over the ocean are extended eastward into the Indian coast. Our studies in Bombay indicated synoptic developments at 500 mb as being largely responsible for weather variations along the west coast of India; the low level flow showed little evidence of the synoptic systems.

The conditions of flow and the distribution of the water and land masses are such that the air that penetrates the west coast of India properly has had considerable oceanic influence and has great rain producing potential. On the other hand on account of the decrease of the water mass northward and associated increase in the influence of the Arabian land mass, the air mass moving into west Pakistan and northwest India, even at the height of the monsoon season, has a minimum of oceanic influence. This is an important contributing factor to the heat and dryness that prevails in that area.

As mentioned at the beginning, the Arabian Sea during the southwest monsoon season offers many interesting examples of air-sea interactions, and every corner of the ocean exhibits conditions that differ significantly from the others. There is no question that the processes of air-sea interaction play a major role on rain-producing processes over the Indian Subcontinent.

REFERENCES

Colón, José A. 1964 On Interactions between the Southwest Monsoon Current and the Sea Surface Over the Arabian Sea; Indian Journal of Meteorology and Geophysics, 15, 183-200.

A LOW LEVEL JET PRODUCED BY AIR, SEA AND LAND INTERACTIONS

Andrew F. Bunker
Woods Hole Oceanographic Institution
Woods Hole, Massachusetts

ABSTRACT

The summer monsoon blowing from the southwest over the Arabian Sea produces upwelling of very cold water off the coasts of Somalia and Arabia. Aircraft meteorological observations show that a narrow, 25 m sec^{-1} jet exists at about 600 m over the cold water off Somalia. Analysis of data available at the moment indicates that this jet results from the combination of reduced frictional drag of warm air over cold water and the thermal wind shears produced by the cooling of the lower air by the water.

ABSTRACT

As the southwest monsoon develops over the Arabian Sea, a sequence of sea, air, and land interactions occurs that culminates in the production of a 25 m sec^{-1} low level jet at 600 to 1000 meters blowing off the coast of Somalia. Aircraft and surface observations are presented which describe the jet, the thermal structure of the atmosphere, the sea surface temperatures, and the surface pressures. From these data and climatological data it is shown that the jet results from a sequence of two complete cycles of thermal reactions of the air to sea and land temperatures and kinetic reactions of the water to atmospheric wind stress. These cycles occur on decreasing size scales but with increasing intensities thereby producing an intense local jet. The geographical location of the jet is fixed by the configuration of the land masses and proximity to the equator. The existence, general shape, magnitude, and geographical position of the jet are explained as resulting from (a) a large land mass north of the Indian Ocean, (b) a land mass to the west of the Ocean, (c) strong heating of the land which intensifies the pressure gradient, (d) a small value of the Coriolis force, and (e) air-sea interactions which produce through upwelling of cold water and cooling of the air thermal winds and a low frictional drag of the air over the water.

INTRODUCTION

As part of the International Indian Ocean Expedition, meteorological studies were carried out over the Arabian Sea using a C-54Q aircraft. This airplane was equipped with instruments designed to measure temperatures, winds, humidities, clouds, radiation, and turbulence. On August 30, 1964, a flight was made from Aden cutting perpendicularly across the wind blowing from the SW off the coast of Somalia. The track outbound was flown at 100 to 600 meters. A climb was made to 4500 m at 4° N, 56° E. The return flight to Aden was made at 4500 m and 5 radiosondes were released enroute. On September 1, 1964, a track was flown from Aden to Bombay cutting the Somali jet again. The portion of the track from Aden to 11° N, 58° E was flown at low levels while the remainder was flown at 4500 meters. From these observations it becomes clear that the strong winds take the form of a low-level jet with a maximum speed of about 25 m sec^{-1}.

DESCRIPTION OF THE JET

Figures 1 and 2 are presented to show the main characteristics of the wind system as it existed on the 2 days, August 30 and September 1, 1964. The wind speed - height curve, Figure 1, was drafted from the Doppler radar winds observed during the aircraft's ascent at about 11° N, 58° E. It is seen that a large wind shear exists in the 500 to 1000 meter region, that a rather broad maximum exists in the 1000 to 1500 meter range, and a steep negative gradient exists above this level.

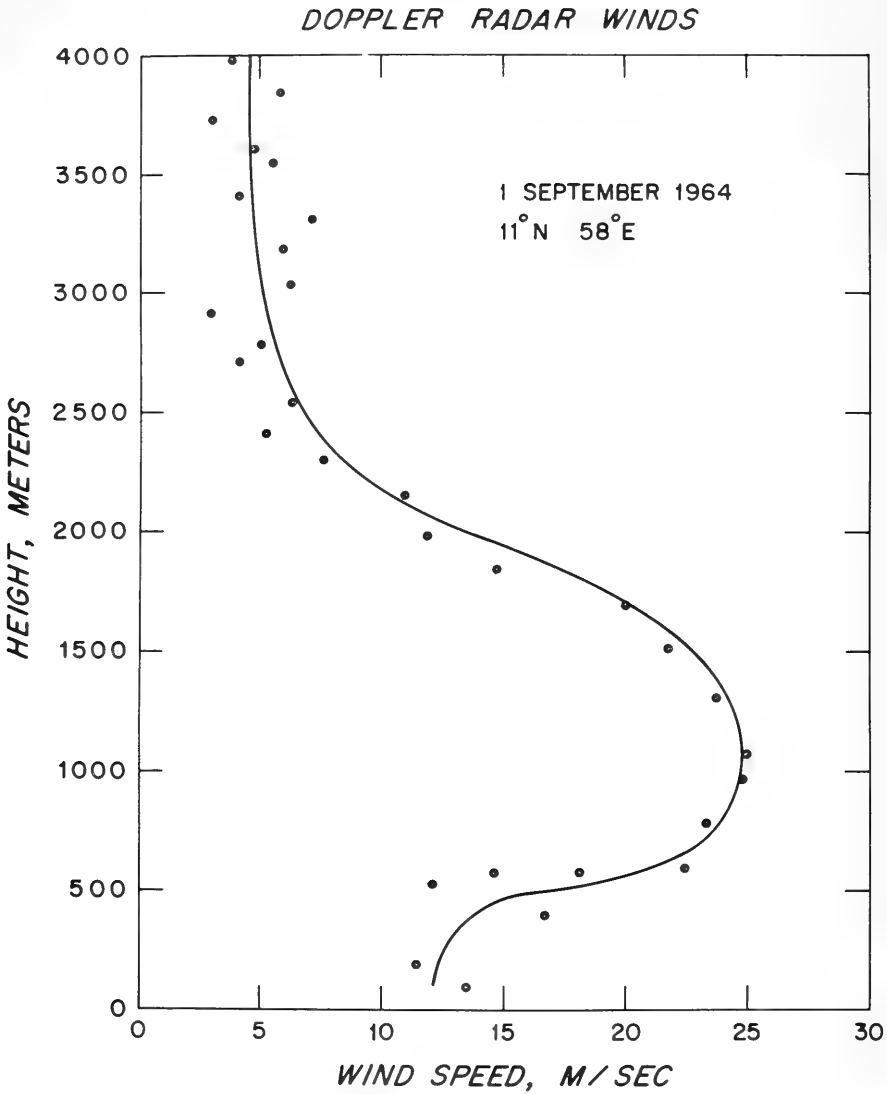

Figure 1. Doppler radar winds obtained from the C-54Q aircraft are plotted against height.

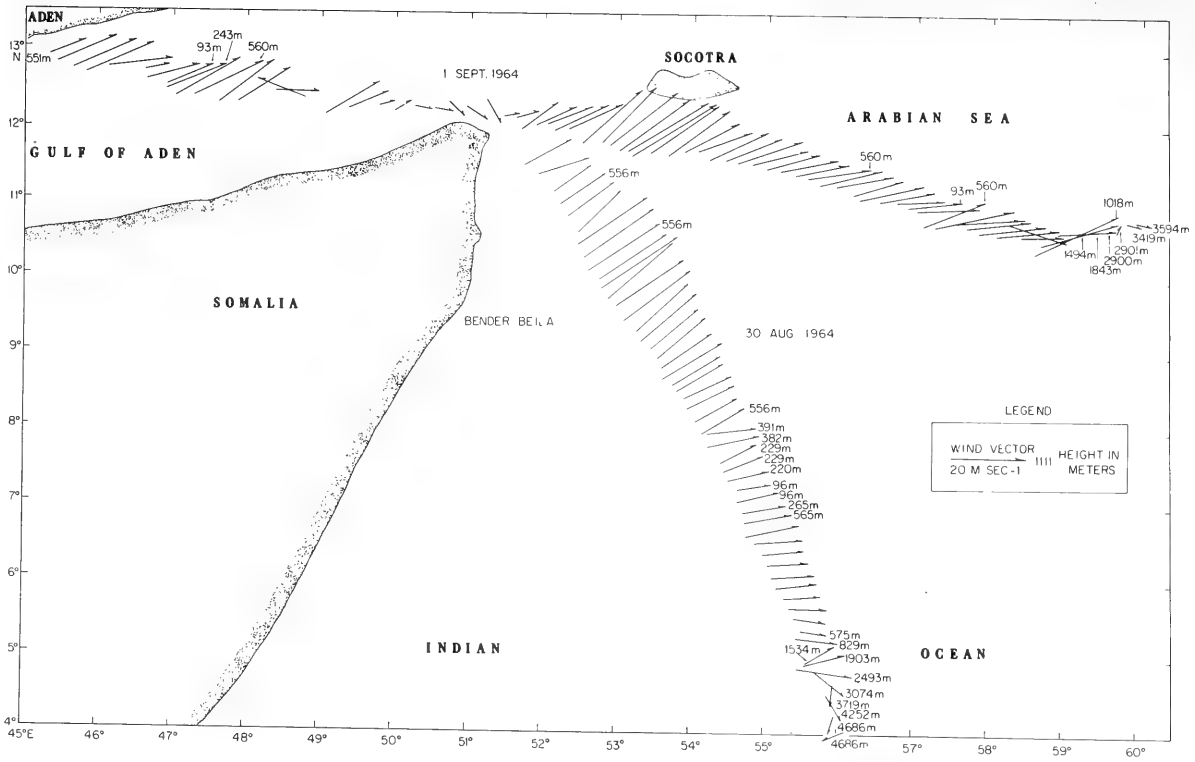

Figure 2. Chart of Doppler radar wind vectors obtained from C-54Q flights on two days. Values at head of vectors give the height of observation in meters.

Figure 2 presents the horizontal distribution of the observed wind vectors on the same 2 days. On August 30, the aircraft crossed the axis of the jet at 10° N, 53° E at 550 meters. At this point the velocity was about 25 m sec^{-1}. One hundred km either side of the axis the velocity drops to about 15 m sec^{-1} indicating a rather sharp narrow jet.

On September 1, 1964, a track about 45° to the wind was flown. The plot of this flight shows that a strong narrow jet with 27 m sec^{-1} winds was encountered in the vicinity of 12° N, 53° E. Beyond this area the wind dropped off to speeds of about 16 m sec^{-1}. As the ascent was made at 11° N, 58° E, the aircraft passed through a jet at 1000 meters, with 25 m sec^{-1} speeds. One would like to know whether this is the same jet that was encountered at 12° N 53° E at a height of 560 m. It is possible that it is a broad jet extending from 12° N, 53° E to 11° N 58° E with a level of the maximum wind that rises in the southeasterly direction. High values of the turbulence encountered along this track suggest that the aircraft probably was flying underneath a wind maximum. This point will be discussed later after the presentation of the turbulence data.

It should be stated at this point that the jet is not a transient phenomenon that happened to exist in the area on the days that the flights were made. Rather, the intense winds in this area are a persistent feature of the southwest monsoon, as a casual inspection of weather charts of the area will reveal. Ship reports show relatively minor variations in strength and position from day to day.

THE SEQUENCE OF INTERACTIONS BETWEEN AIR, SEA, AND LAND AND THE DEVELOPMENT OF THE SOMALI JET

(1) Global-Scale interactions. The first phase in the development of the wind system occurs in the northern hemisphere in the spring on a scale involving the entire continent of Asia and the Indian Ocean. With the return of the sun to the hemisphere the land masses of Asia and North Africa are warmed. The land in turn warms the atmosphere and gradually changes the cold highs to warm lows. During this same time interval the temperature of the Indian Ocean south of the equator remains about the same or cools a small amount. The maintenance of the water temperature keeps the air temperature about the same and hence the surface pressure remains the same or increases a bit. By May the pressure in the north has been reduced to about 1005 millibars while the pressures in the south have increased to about 1022 mb. This pressure gradient accelerates the air mass northward across the equator and northeasterly across the Arabian Sea.

(2) Oceanic-Scale interactions. The reaction of the sea water to this moderate air flow from the south is the movement of the surface water to the east away from the coast of Africa. The presence of the African Continent prevents replacement of the water except by upwelling of deeper cool water. As a result of this replacement, the waters from the Mozambique Channel to north of the equator become a few degrees cooler than the water 2000 kilometers

to the eastward. The effect of this cool water is to cool the lower atmosphere and thereby increase the surface pressure. Normally at this season a belt of high pressure lies along the 10° S latitude line at 500 millibars. With the cooling of the lower air below and to the north of this belt, the surface high develops a weak ridge extending northward along the African Coastal waters to about 10° N. The characteristics and semi-permanent nature of this ridge of high pressure are clearly shown on the IGY Tropical Zone Weather Maps published by the Seewetteramt, Deutscher Wetterdienst, Hamburg. Study of the maps for July, August, and September 1957, shows the ridge to be present on all maps with minor variations in amplitude and position. Adjacent to this ridge is a trough of low pressure lying to the west over East Africa. This trough is caused by the intense solar heating of the land and air. Its effect is to greatly increase the pressure gradient in the region around 10° N, 50° E. The surface pressure map for August 30, 1964, has been drawn from data made available by the International Meteorological Center, Bombay, and presented as Figure 3.

(3) Local interactions. As a result of the steep pressure gradient developed along the coast of northeast Africa, the air that has moved slowly across the equator into the regions begins to accelerate and quickly attains higher velocities. Once the air has attained relatively high velocities north of about 5° N, the transport imposed upon the surface water is greatly increased. With this increase in transport the upwelling of bottom water is greatly increased and the surface temperatures drop many degrees over an area of more than 100 square degrees. Figure 4 presents a chart of surface water temperatures drawn by H. Stommel and B. Warren of W.H.O.I. The data were obtained from the research vessels, ARGO, of Scripps Institute of Oceanography and DISCOVERY, of the National Institute of Oceanography during their cruises in August 1964, to the Somali Current region. It is seen that immediately off the coast at 9° N, exceedingly cold water with temperatures down to 13° C. was observed.

This colder water continues the interaction cycle by cooling the air at a greatly accelerated rate. The intensity of this cooling is shown in Figure 5 which presents dropsonde and psychrograph data obtained from the C-54 aircraft on August 30, 1964. The figure is a cross section of the atmosphere from the Gulf of Aden to 4° N, 56° E. Potential temperatures were plotted on the diagram and isentropes drawn from the data points. The cooling of the air by the water about 200 kilometers southeast of the mouth of the Gulf of Aden is very apparent. This highly localized cooling is superimposed upon the pattern of a general warming of the air from south to north.

To explain the increase in wind speed with height to the jet maximum and its subsequent decrease above this level, the temperature cross section made on August 30, 1964, must be studied. It will be noted that the temperature increases to the right of the wind, indicating that the wind will increase with height. Above the 900 mb level or the level of the jet maximum, the air temperature decreases to the right of the wind and hence the wind should decrease with height. Measurement of the horizontal temperature gradient and application of the thermal wind shows that the wind should

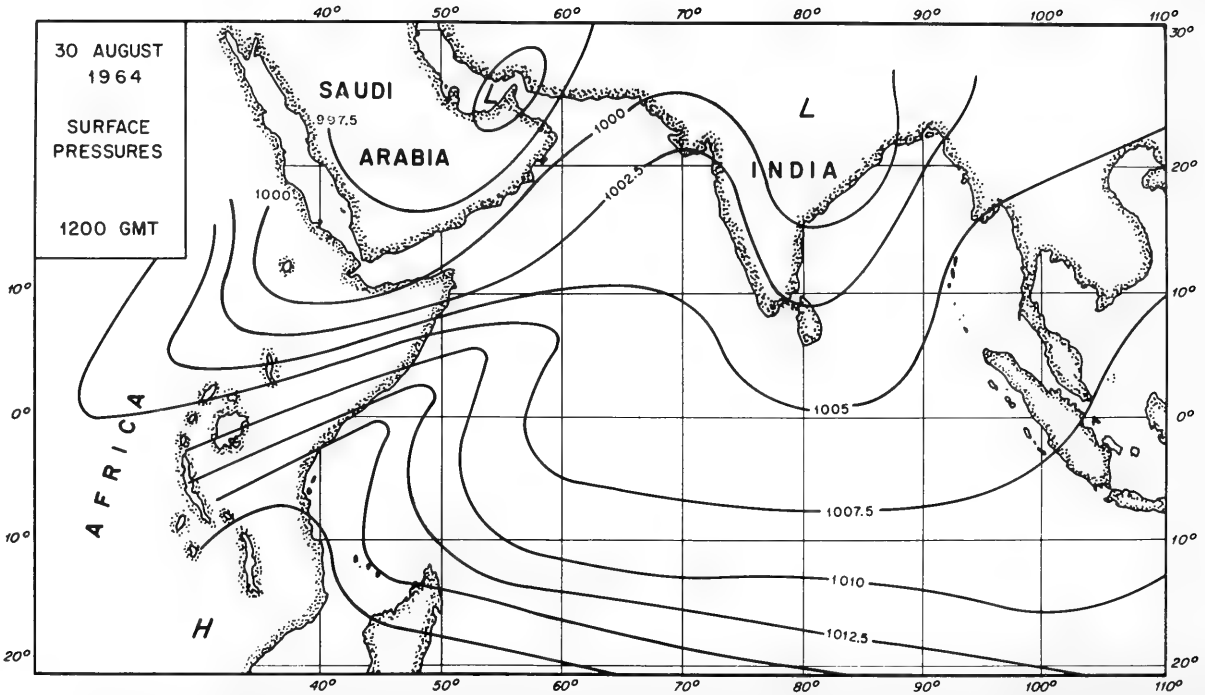

Figure 3. Surface pressure chart drawn from data obtained by the International Meteorological Center, Bombay.

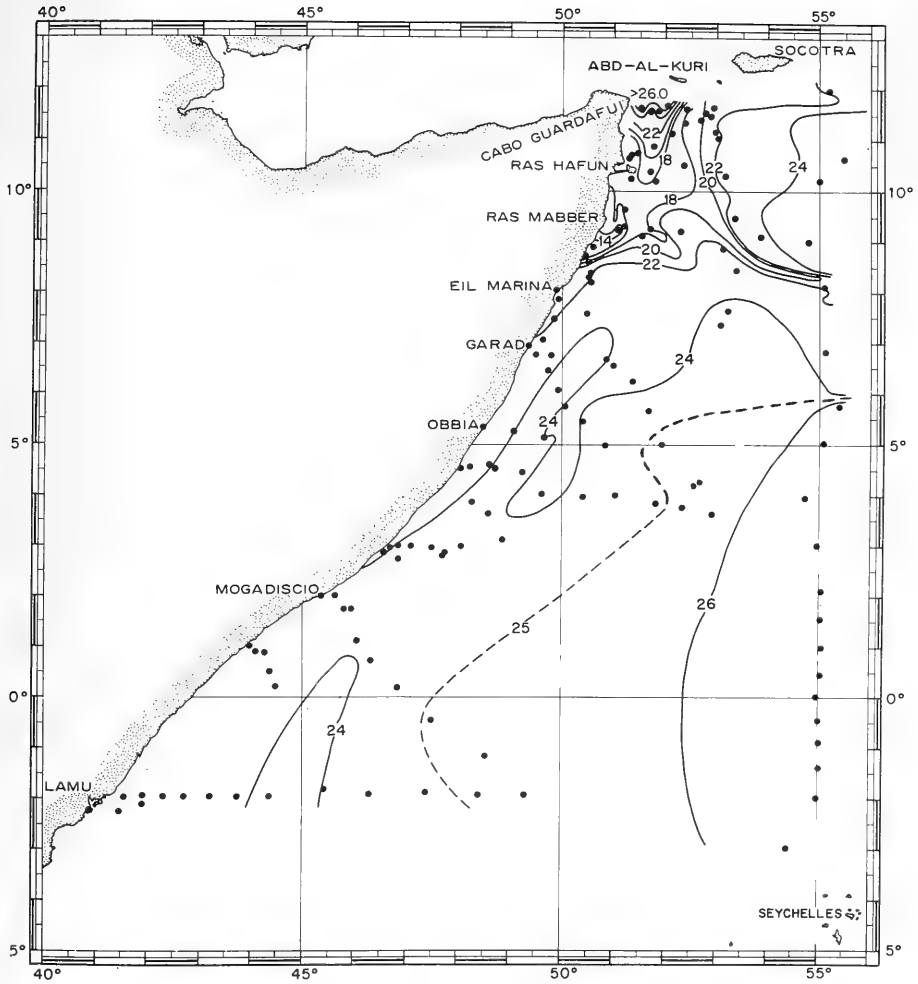

Figure 4. Surface water temperature chart constructed from ARGO and DISCOVERY data by Stommel and Warren.

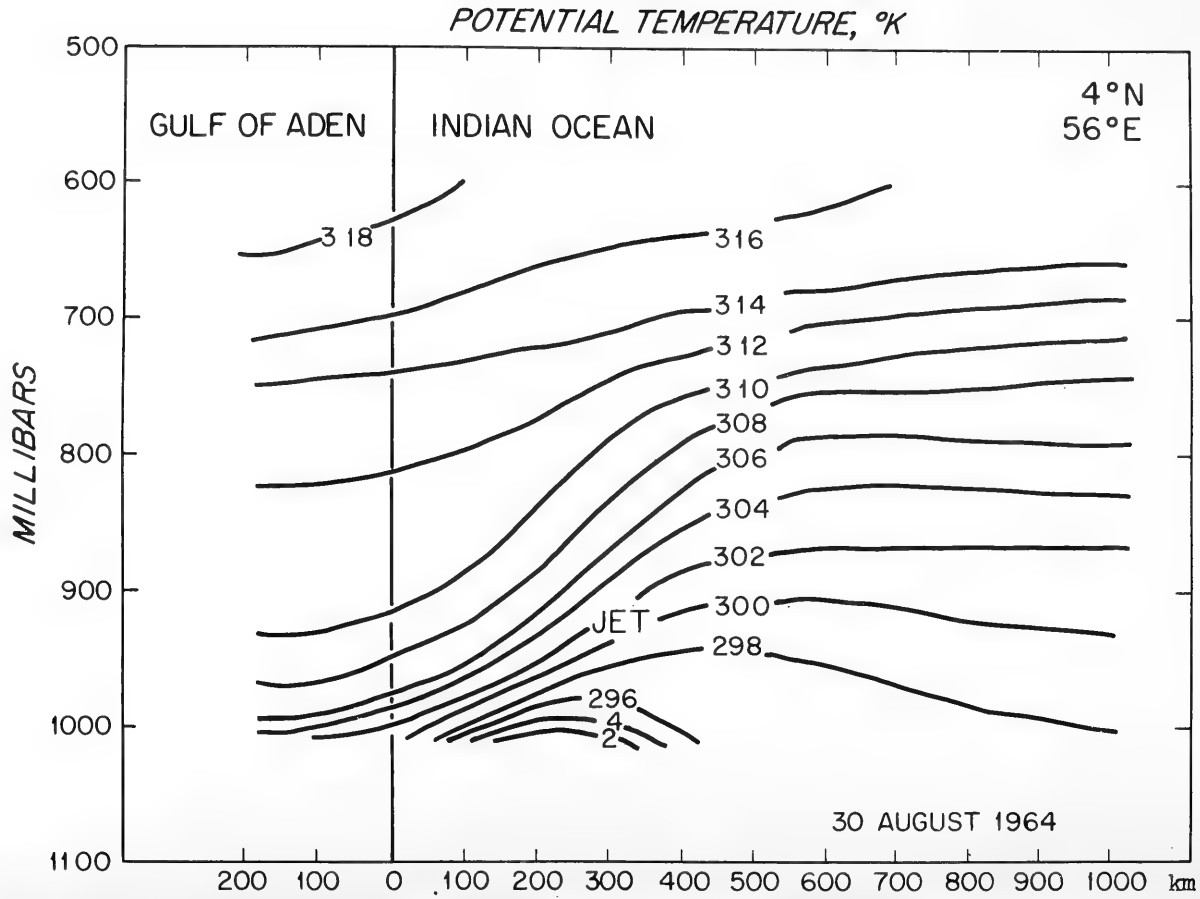

igure 5. Potential temperature cross-section of atmosphere across the Somali jet.

increase about 10 m sec^{-1} through the lowest 600 meters. As this situation is one in which the Coriolis and pressure gradient terms of the equation of motion are not balanced, the increase in wind with height probably does not attain the full geostrophic value. The wind speed increase from 100 m to 1000 m on September 1, 1964, was about 12 m sec^{-1} which is in fair agreement with the computed thermal wind increase.

One additional bit of information is now presented that will aid in the analysis of the generation of the low level jet. The magnitudes of the root-mean-square turbulent vertical velocities of the air have been measured from the aircraft's accelerometer according to the method of Bunker (1955) and expressed in cm sec^{-1}. The observations were made on September 1, 1964, around 11° N, 57° E. Also plotted on the height-vertical velocity diagram, Figure 6, are values of the turbulent velocities observed in other regions of the world. Several features of these data are very unusual and significant. First, it is noted that the turbulent velocities at the lowest level are about the same as the turbulent velocities measured in the trade winds of the North Atlantic Ocean by Bunker (1955). From this observation of weak turbulence it is concluded that the frictional drag of the water on the air is nearly the same as the drag found under the lighter (5 m sec^{-1}) trade wind situation and is therefore many times smaller than would be expected for high winds of 15 to 20 m sec^{-1}.

The small frictional force coupled with the small Coriolis force, due to the small Coriolis paramater near the equator, cannot balance the pressure gradient force and hence the air particles are accelerated rapidly across the isobars. In the region of the strongest winds, it appears that geostrophic balance is never attained. Down wind of the jet the pressure gradient decreases and the wind becomes geostrophic. To understand and prove these relationships in this region a much more detailed and quantitative study of the terms of the equation of motion must be made.

The second noteworthy feature of Figure 6, is the high turbulent velocities observed at the 600 meter level. For comparison, observations made at various heights in a strong wind (20 m sec^{-1}) situation over the North Atlantic Ocean by Bunker (1960) are plotted on the diagram. It is seen that after a rapid increase in turbulence in the lowest layers the turbulence decreases rapidly with height. Such a turbulence-height curve is characteristic of a situation in which the turbulence is generated by the flow of air over a surface and decays aloft. In the present case it appears that only a small amount of turbulence is generated by the flow of the stable air over the water and that a greater amount is generated at a higher level where the air is not as stable. It is concluded from this trace that the turbulence must be generated by high wind shears and that the aircraft was flying below the level of the maximum winds. If this is true then the jet observed at 12° N, 53° E, at 500 m probably extends to 11° N, 58° E, where it was observed at 1000 meters.

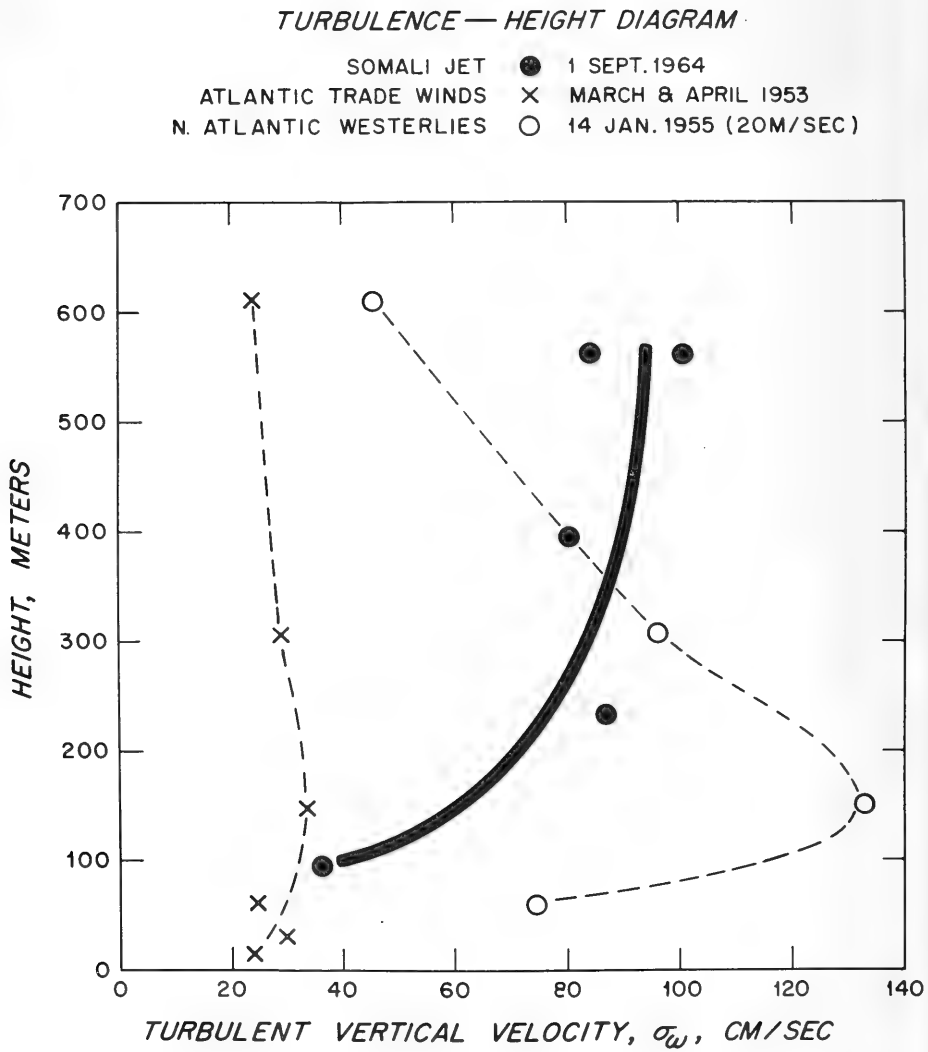

Figure 6. Turbulent vertical velocity values plotted against height.

SUMMARY

The observations made off the coast of Somalia describe the low level jet system. One question is left open concerning its geographical limits. It is possible that the system consists of a single jet broadening downwind and varying in height across stream. Another possibility is that the system consists of more than one jet.

Interpretation of the observations leads to the conclusion that the jet is formed by a series of interactions between the land. sea. and air. Also it is evident that the jet depends upon the configuration of the land masses and their proximity to the equator. It is this dependence on position and configuration that restricts the jet to a relatively small area off the coast of Somalia and makes it a semi-permanent feature of the southwest monsoon.

Acknowledgement -
The research described in this paper was supported by National Science Foundation Grant 22389. The C-54Q aircraft was bailed to the Woods Hole Oceanographic Institution by the U. S. Navy through the Office of Naval Research.

REFERENCES

Bunker, A.F. 1955 - Turbulence and shearing stresses measured over the North Atlantic Ocean by an airplane-acceleration technique. Journ. Meteor., Vol. 12, 445-455.

Bunker, A.F. 1960 - Heat and water vapor fluxes in air flowing southward over the western North Atlantic Ocean. Journ. Meteor., Vol. 17, 52-63.

U. S. FLEET NUMERICAL WEATHER FACILITY ACTIVITIES RELATING TO SEA-AIR INTERACTIONS ON A SYNOPTIC SCALE

Cdr. W. E. Hubert, USN
Fleet Numerical Weather Facility
Monterey, California

"The opinions presented in this paper are those of the author and do not necessarily represent the official views of the Navy Department at large."

ABSTRACT

The mission of the Fleet Numerical Weather Facility is to provide numerical weather products on an operational basis peculiar to the needs of the Naval Establishment and to develop and test numerical techniques in meteorology and oceanography applicable to Naval Weather Service analysis and forecasting problems. At Monterey the method of approach to these assignments has been to treat the atmosphere and the oceans as one environment with particular attention being directed toward interactions between the two media which constitute this environment.

The purpose of this paper is to summarize the various analysis and forecast programs currently utilized at Fleet Numerical Weather Facility Monterey and to outline future plans. Those programs which depend more heavily on quantitative computations of air-sea interaction or on strictly maritime meteorological observations are discussed in more detail. These include: sea surface temperature analyses (and their scale and pattern separation), sea and swell analyses and forecasts, and synoptic current analyses (and their use in estimation of convergence in the sea and their effects on thermal structure).

Finally, a description will be given of the master scheme which is being developed for numerical analysis and prediction of oceanographic elements.

INTRODUCTION

One of the assigned missions of the U. S. Fleet Numerical Weather Facility (FNWF) at Monterey, California, is to prepare meteorological and oceanographic analyses and forecasts in support of fleet and other operations throughout the Navy. As the activity's title implies, these products are prepared numerically using the latest high-speed electronic computers. The approach used at FNWF has been to apply a combination of dynamic theory and empirical experience to problem solving by computer. In general, only problems which have direct Navy application and which show promise of operational usefulness within 1-year's time are undertaken at FNWF. In this sense, the developmental efforts at the facility should be called "applied" rather than "basic research."

While early efforts at Monterey were concentrated on atmospheric analysis and forecasting, emphasis has been shifting more and more in the last 2 years to oceanographic problems and, in particular, to sea-air interactions. The atmosphere and the oceans are considered to be one environment as far as naval operations are concerned. Each of the media affects conditions in the other and their behavior should not, and cannot, be treated independently. The development of improved environmental analyses and forecasts on a synoptic basis demands that we account for, in a quantitative manner, the energy exchanged between sea and the atmosphere.

NAVY PROBLEM AREAS INVOLVING SEA-AIR INTERACTION

While the entire problem of sea-air interaction involves the transport of some property (momentum, heat, moisture, etc.) between the two media, the principal effects now being studied at Monterey can be broken down into subareas. One general class of programs involves the transfer of atmospheric momentum to the sea (generation of sea, swell and surface currents), and the other primarily deals with heat exchange at the air-sea interface.

Heat exchange obviously works in both directions. Transfer to and from the atmosphere must be included in atmospheric forecast models. The relationships between synoptic scale heat exchange and weather now under investigation at FNWF will be covered by Dr. Laevastu (1965) later in this conference. The exchanges which influence sea surface temperatures (and consequently subsurface thermal structure) are of primary interest in Anti-Submarine Warfare (ASW) applications and will be covered in further detail herein.

Wind-driven waves (and swell) are important from several viewpoints. They not only affect day-to-day operations but can be critical in underway replenishment, launch and recovery from a carrier, optimum ship routing, amphibious operations, etc. In ASW problems they influence sea surface temperature, layer depth and thermocline intensity through mechanical mixing.

Wind-driven and thermal currents are of minor importance to naviation, search and rescue but play a major role in modification of layer depth through large-scale mass convergence/divergence in the surface layers of the oceans. In the eastern North Pacific, convergence/divergence considerations have frequently been found to outweigh all other terms contributing to changes in layer depth.

Heat transfer is of primary interest to ASW operations in that surface cooling causes convective mixing (resulting in a deepening of the mixed layer and intensification of thermocline gradient) while surface heating forms a shallow, transient surface thermocline (in the absence of mechanical mixing through wave action).

All of the above processes of interaction either contribute to sea "noise" or modify surface and subsurface temperature structure, and therefore influence sound propagation in the oceans. An accurate analysis and/or forecast of the state of the total environment as influenced by sea-air interaction is the key to successful naval operations in general and to the Anti-Submarine Warfare Environmental Prediction System (ASWEPS) in particular.

The following table summarizes the principal environmental inputs to ASWEPS; there are others, such as bottom effects, but those listed here are the problem areas under attack at Monterey(see Table I).

THE FNWF MASTER SCHEME FOR OCEANOGRAPHIC ANALYSIS AND PREDICTION

Figure 1 outlines the master scheme developed at Monterey for numerical analysis and prediction of oceanographic elements and processes (see FNWF Tech. Memo No. 5). If nothing else, the figure shows the complexity of the numerical program being undertaken by FNWF in the general field of interest to this conference.

Looking first at the column headed Basic Data, one can see that a large part of the input data to this program is derived from meteorological observations. Since the number of BT observations is insufficient for truly synoptic oceanographic analyses (except perhaps in limited areas), we are forced to derive the maximum information from meteorological reports at the ocean surface. The basic approach at FNWF has been to obtain the first estimate of oceanic thermal structure from purely exchange considerations and then to modify this "guess" with BT data where available.

The various computations involved in this method of oceanographic analysis and prediction are summarized in the middle of Figure 1 under the column headed Computed Quantitites and Processes. The flow diagramming leading to and resulting from these computations serves to emphasize the entire concept of sea/air exchange utilized in the FNWF oceanographic scheme. Details of some of the more important components of this overall plan will be covered herein or by Dr. Laevastu.

TABLE 1. FNWF ENVIRONMENTAL INPUTS TO ASWEPS

PROGRAM AREA	
SEA STATE	- DERIVED FROM GEOSTROPHIC SURFACE WINDS CORRECTED FOR LOW-LEVEL STABILITY. INFLUENCE ASWEPS THROUGH NOISE AND MECHANICAL MIXING.
SURFACE CURRENTS	- DERIVED FROM SURFACE WINDS AND OCEAN THERMAL STRUCTURE. INFLUENCE ASWEPS THROUGH ADVECTION OF SST AND BY CONVERGENCE/DIVERGENCE.
SEA SURFACE TEMP. (SST)	- ANALYZED FROM SHIP REPORTS. FORECAST FROM ADVECTION AND HEAT FLUX CONSIDERATIONS. USED AS ANCHOR POINT FOR THERMAL STRUCTURE WORK.
HEAT TRANSFER	- COMPUTED FROM HEAT EXCHANGE FORMULAE INVOLVING PRIMARILY METEOROLOGICAL PARAMETERS. INFLUENCES ASWEPS THROUGH TRANSIENTS AND CONVECTIVE MIXING.
LAYER DEPTH & THERMOCLINE INTENSITY	- DERIVED FROM MECHANICAL AND CONVECTIVE MIXING PLUS CONVERGENCE/ DIVERGENCE. IMPORTANT TO SOUND PROPAGATION.

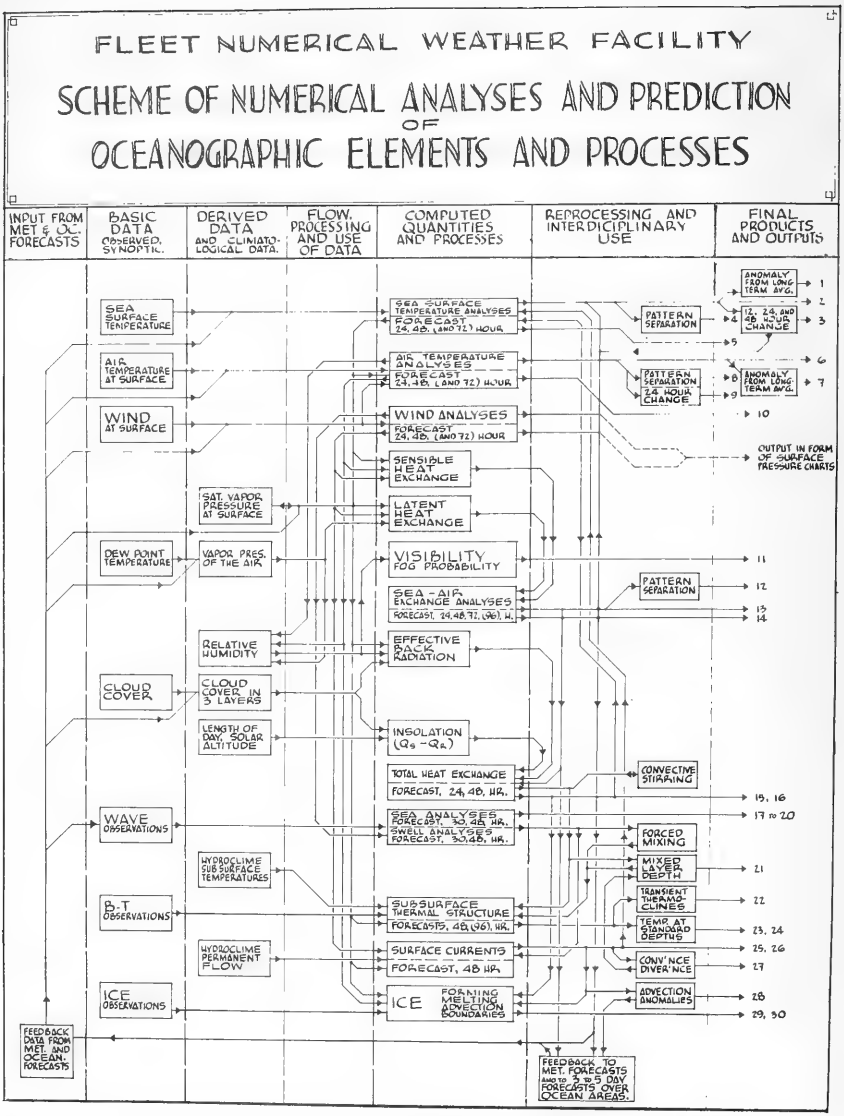

Figure 1. Fleet Numerical Weather Facility, Monterey Master Scheme of Numerical Analysis and Prediction of Oceanographic Elements and Processes.

EXAMPLE OF FNWF OCEANOGRAPHIC PRODUCTS

A. SEA SURFACE TEMPERATURE

The FNWF Sea Surface Temperature (SST) analysis program uses as input data all ship injection temperature reports from the previous 3 1/2 days. A median seeking technique is utilized to reduce the influence of erroneous reports. All observations within 0.7 mesh lengths (about 150 miles) of each grid point are compared with the previously analyzed value at each ship's position. If a new observation is warmer than the previous analysis, the value at the nearest grid point is raised a fixed amount (0.1C); similarly, the value is lowered the same amount if the observation is colder. Areas of no data are modified only by relaxation and smoothing.

Figure 2 is an example of a numerical analysis of this parameter. Details of this program and error distributions of SST observations have been described by Wolff (1964). The SST analyses made at FNWF, Monterey are routinely decomposed into large and small scale patterns (Holl, 1963) to clarify the results of large-scale circulation changes, fluctuations in upwelling, etc. The large-scale SST pattern derived from Figure 2 is shown in Figure 3. Its similarity to ocean current systems will be pointed out later.

B. SEA AND SWELL

The analysis and forecast program for wind waves uses a singular technique to obtain significant wave height and period. Surface geostrophic winds at 3-hourly intervals are the basic input. Duration is determined to the nearest 3 hours and fetch corrections are made in regions of offshore flow. The formulae for wave height and period as functions of duration D_f and geostrophic wind speed U_g used at FNWF are

$$H_{1/3} = a(U_g)^2 D_f + bUg$$

$$H_{1/3} = (c + dD_f)\, Ug + e$$

A sample wave analysis is shown in Figure 4.

Swell is defined as waves which have traveled more than 24 hours from a generating area. Based on a history tape of wave heights, periods and directions at 12-hourly intervals; travel distance, swell height and swell period are computed from the following equations:

$$D = a_1 T_f \bar{m} t$$

$$T_d = \left(T_f^2 + \frac{b_1 D}{\bar{m}} \right)^{\frac{1}{2}}$$

$$H_d = H_f \left(\frac{T_d}{T_f} \right)^{-2.65}$$

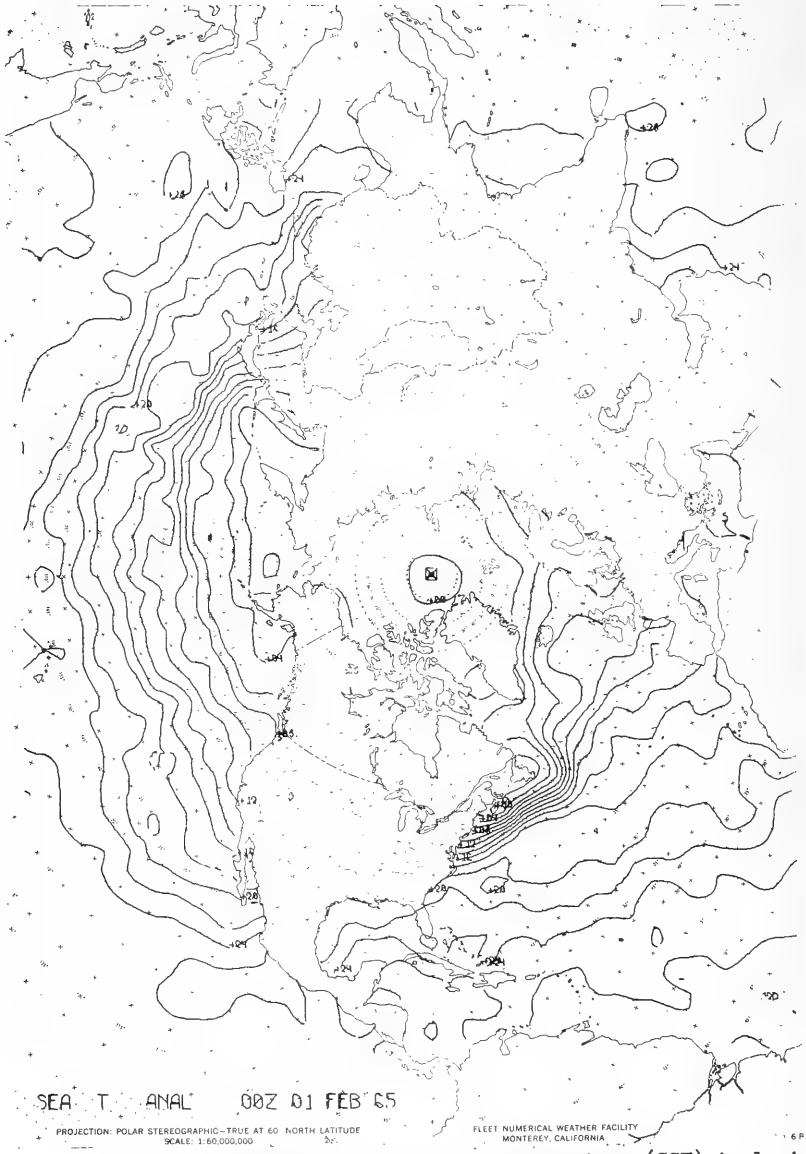

Figure 2. Operational Sea Surface Temperature (SST) Analysis for 00 GMT 1 February 1965. Degree C.

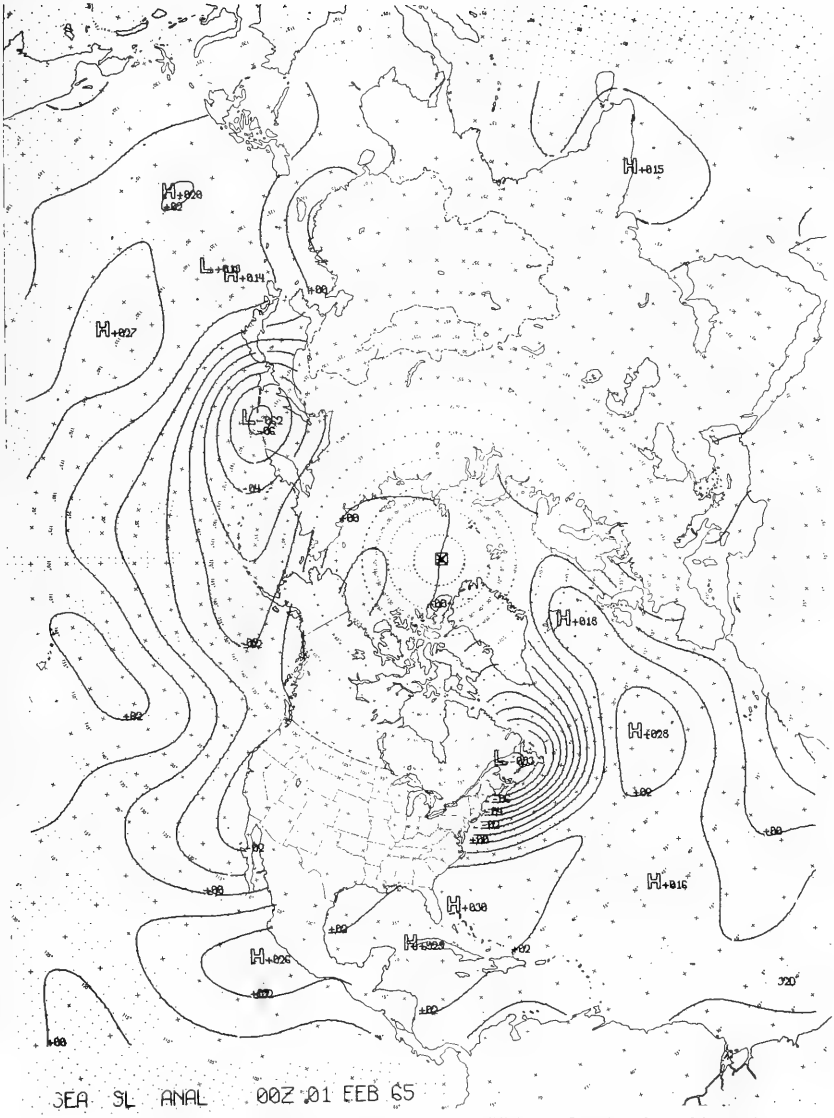

Figure 3. Large Scale Part of SST Analysis for 00 GMT 1 February 1965. Result of Scale and Pattern Separation.

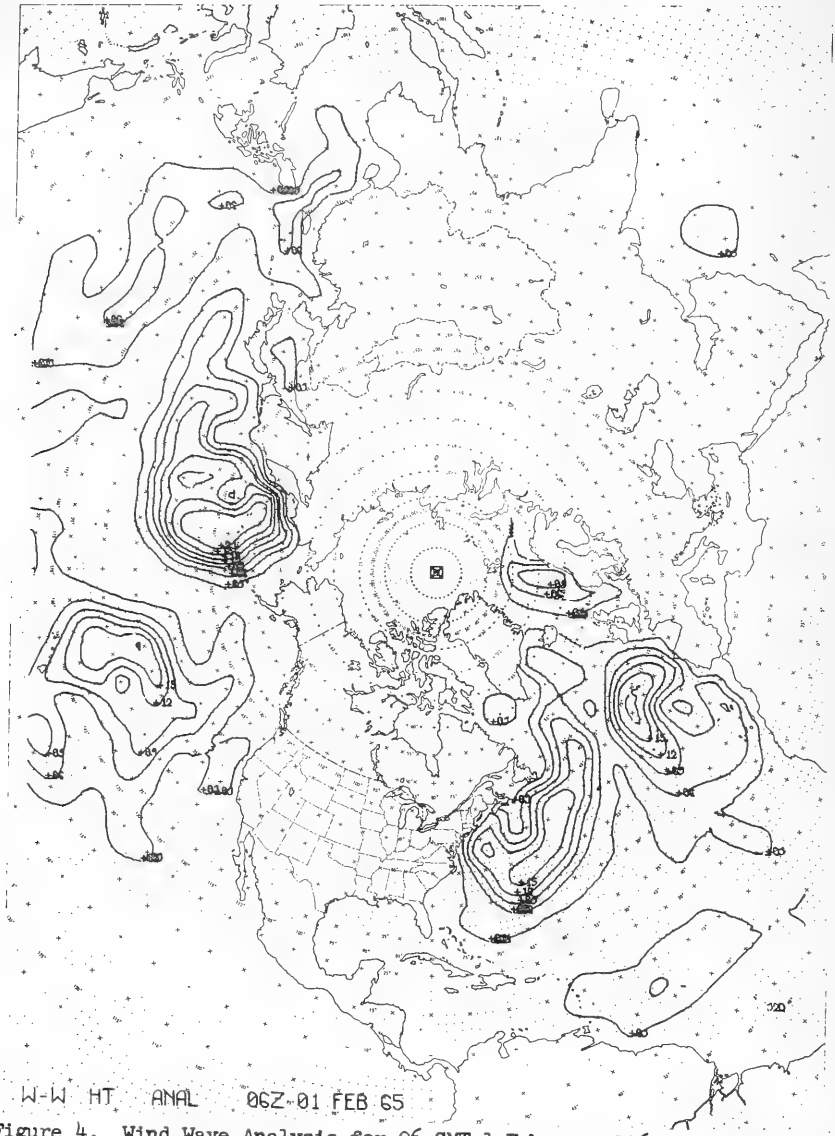

Figure 4. Wind Wave Analysis for 06 GMT 1 February 1965. Significant Heights in Feet.

where D is travel distance, T_f is the period at the end of fetch, $\bar{m}$ is the mean map factor, t is decay time, T_s is the swell period, H_d the swell height. H_f the height at end of fetch, and a_1 and b_1 are constants. Swell analyses and forecasts are plotted in the same manner as the waves in Figure 4.

OCEAN CURRENTS

The details of this program have been described earlier by the author (Hubert, 1964). Essentially, the computational procedure accounts for two principal current components -- (1) the "characteristic" or thermohaline flow and (2) the mass transport due to wind and waves.

Assuming a level of zero current velocity at some depth (Δz), the geostrophic thermal current at the surface is computed from the mean temperature, $\bar{T}$, in the layer

$$\vec{V}_c = - \frac{g \, \Delta Z}{f \, \bar{T}} \nabla \bar{T} \times \vec{K}$$

In practice, the mean temperature is obtained from a weighted combination of a climatological temperature field at 200 meters and the synoptic SST Analysis described earlier.

The wind-driven current as determined by Witting (1909) is obtained from

$$\vec{V}_w = K_3 \left(\vec{\bar{V}}_g \right)^{1/2}$$

where $\vec{\bar{V}}_g$ is the mean geostrophic wind speed for a 36-hour period.

Figure 5 is an example of a current transport chart (in nautical miles per day) obtained at FNWF on a synoptic basis. As can be seen from this figure, well-known features such as the Gulf Stream, Kuroshio, Equatorial Counter Current, etc., are quite well defined by this procedure. Since the computations are carried out in component (u,v) form, directional fields are also available.

In order to obtain a single continuous field displaying both direction and speed of the computed currents, a stream function (ψ) analysis is made using methods similar to those employed by Bedient and Vederman (1964) to represent atmospheric flow in the tropics. The vorticity of the current flow is determined from the (u,v) component fields and the Poisson equation

$$\nabla^2 \psi = \frac{\partial v}{\partial x} - \frac{\partial u}{\partial y}$$

is solved for ψ using relaxation techniques.

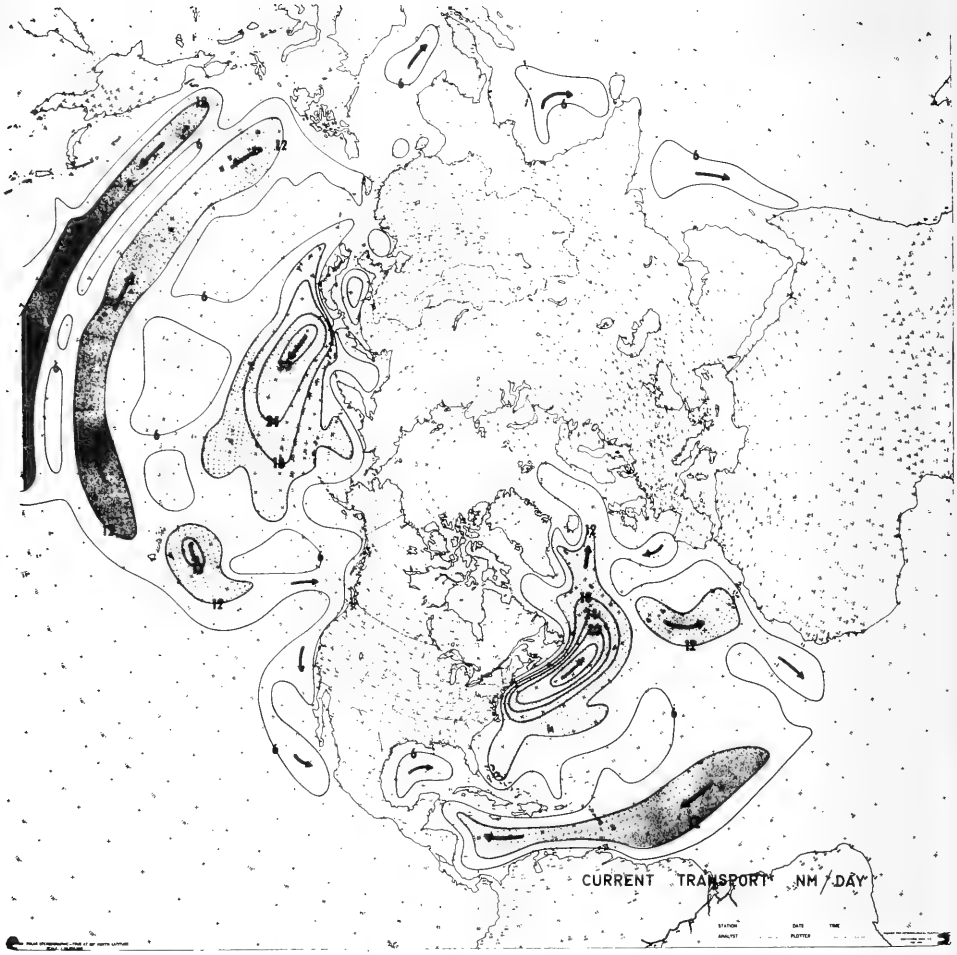

Figure 5. Current Transport Computation at 06 GMT 1 February 1965. Transport in Nautical Miles/Day. Transport Over 12 n.mi./day Stippled.

The stream function field which corresponds to the current transport chart in Figure 5 (06 GMT 1 February 1965) is shown in Figure 6. Current vectors have been plotted at selected gird points to show the degree of fit. The fact that the derived stream function is nondivergent while there is divergence in the initial velocity field explains some of the cross-contour flow. In general, however, this appears to be small in most places, and the stream field provides a good representation of the current pattern.

It is interesting to note that the stream function analysis shows close correlation to the large-scale SST analysis shown in Figure 3. As one should expect, thermohaline considerations (as influenced by the semipermanent circulation of the atmosphere) determine the large-scale current pattern while mass transport by wind and waves contributes toward smaller scale details.

A good example of the latter effect can be seen to the northeast of Hawaii. A strong, quasi-stationary cyclone has completely disrupted the normal west-east extension of the Japanese current. To a lesser degree, the same thing is happening off the west coast of France; the typical northwesterly current has been replaced by flow from the southeast.

D. ADVECTIVE TEMPERATURE CHANGES

From the computed currents one can determine the change in SST which would be due to advection alone. Since the "permanent" or thermohaline component would be nearly along the sea surface isotherms, the advective patterns should result primarily from atmospheric driving forces of synoptic scale. Figure 7a shows the results of advecting the SST pattern with the current field shown in Figures 5 and 6. Areas of cold advection are stippled with heavier shading used to denote advection of greater than about 0.1F per 24 hours. Weak warm advection is indicated by lack of shading while warm advection stronger than 0.1F per 24 hours is shown by cross-hatching.

Figure 7b represents the actual difference between the SST analyses from 12 GMT 1 February and 12 GMT 31 January 1965. As can be seen, the correspondence in some parts (particularly in the vicinity of strong storms near Hawaii, Newfoundland and the Azores) is fairly good. In other areas the signs are clearly opposite. One can only conclude that advection plays an important role in some areas and is completely outweighed by heat exchange effects in other areas. Namaias (1959) and Eber (1961) came to about the same conclusion. The maximum advection computed in this case was 0.85°F per 24 hours which agrees with earlier findings of Laevastu (1960).

5. THE FNWF SCHEME FOR SUBSURFACE THERMAL STRUCTURE ANALYSIS AND PREDICTION

Figure 8 is a further breakdown of the master scheme discussed in section 3. As can be seen, all of the computational programs described in the preceding section enter into the determination of thermal structure with

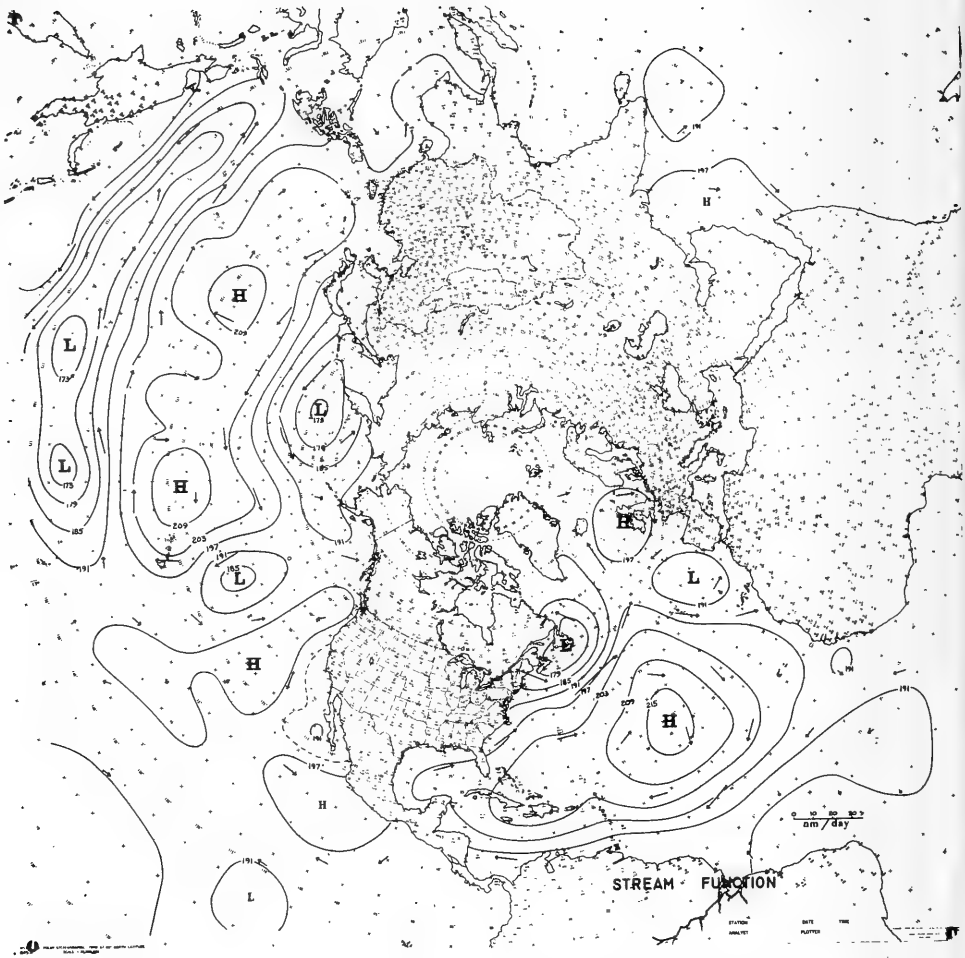

Figure 6. Current Stream Function Analysis for 06 GMT 1 February 1965. Units 10^7 sec^{-1}. Current Arrows to Scale Plotted at Selected Grid Points.

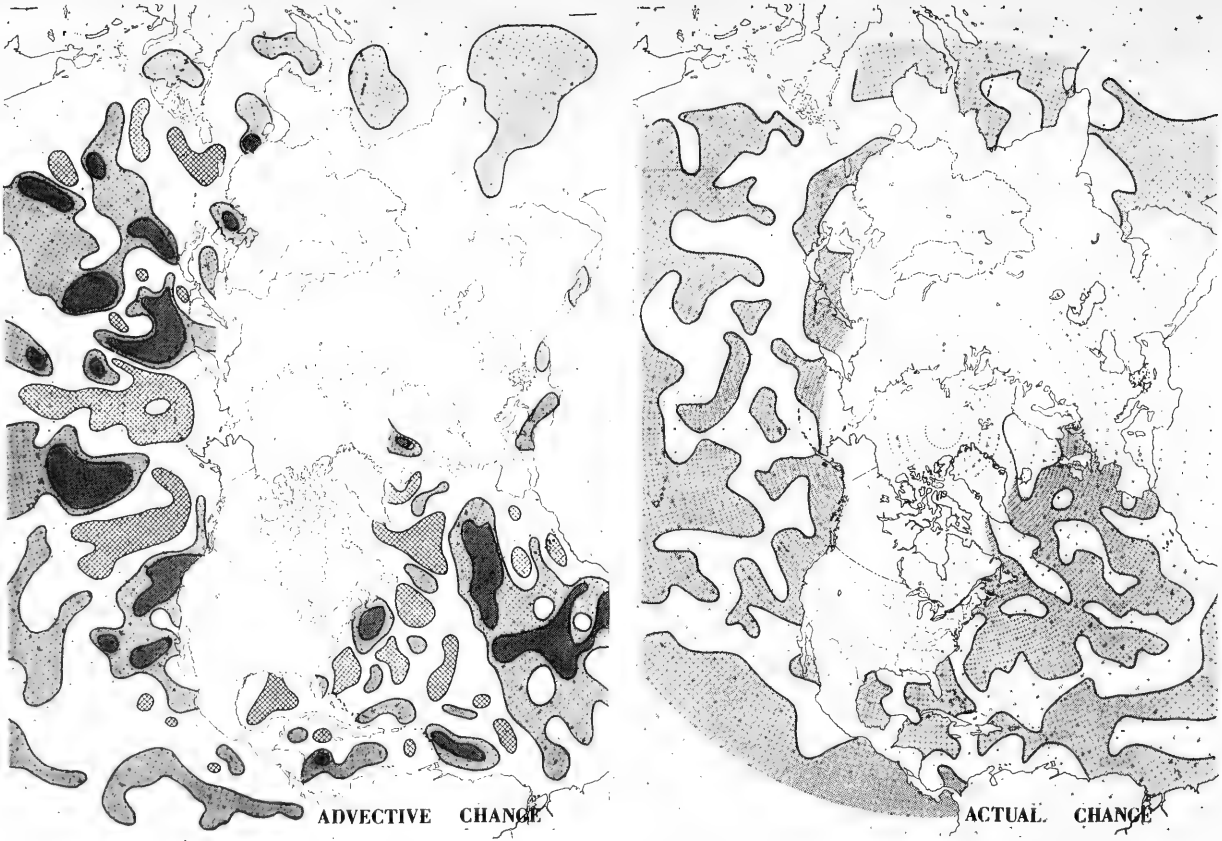

Figure 7. (a) Computed advective change of SST at 06 GMT 1 February 1965. Cold advection stippled; heavy stippling greater than 0.1°F/24 hrs. Warm advection greater than 0.1°F/24 hrs is cross-hatched. (b) Actual SST change 24 hours prior to 12 GMT 1 February 1965. Cooler areas stippled.

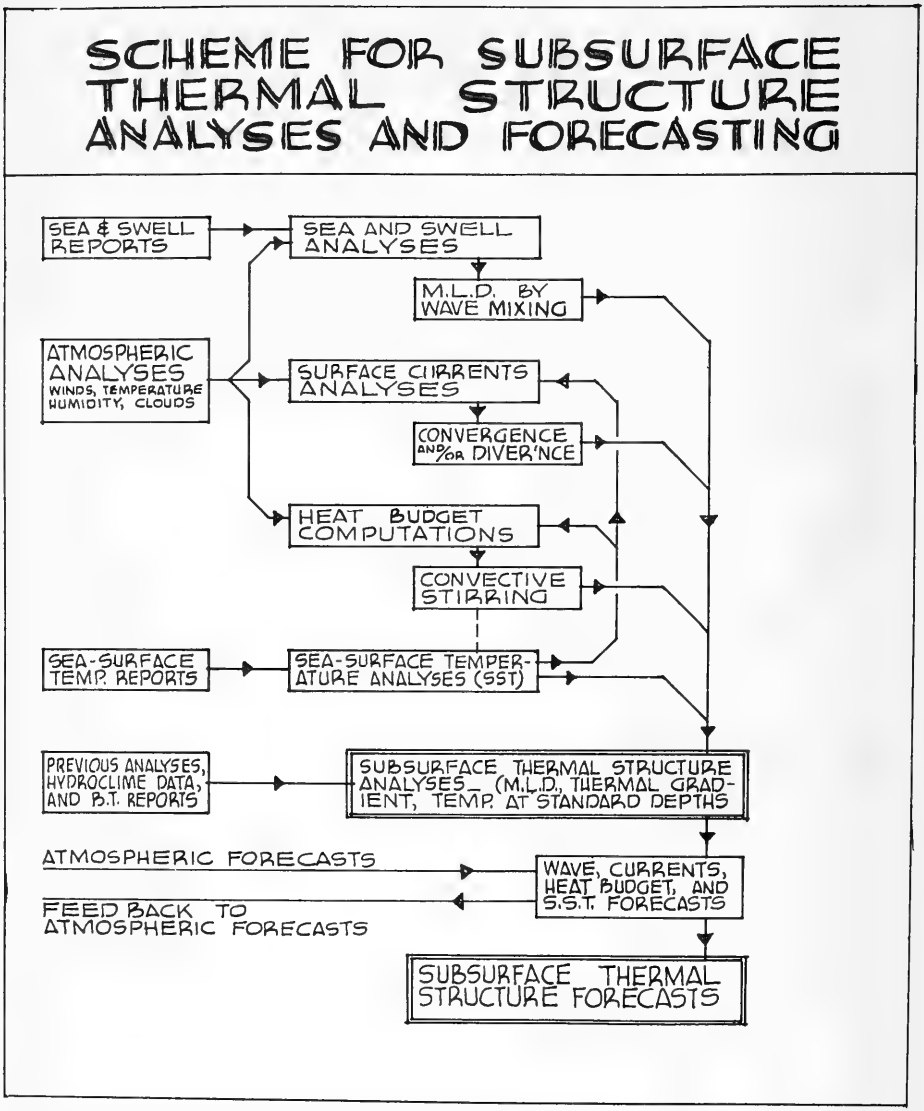

Figure 8. Fleet Numerical Weather Facility, Monterey Scheme for Subsurface Thermal Structure Analyses and Forecasting.

depth. The analyses will be built downward from the surface (where the most reports are available).

The previous day's analysis will first be modified by mechanical and convective mixing, where applicable, and large-scale convergence and divergence in the surface layers. Climatological (hydroclime) restraints will be used to keep computed changes within reasonable limits. Finally, BT observations will be introduced by means of a median seeking technique such as used in the SST analysis program.

Most of the components needed to assemble the complete subsurface analysis and prediction package have been programmed for numerical solution. The first major portion to be completed is expected to be a hemispheric analysis and prediction of mixed-layer depth.

REFERENCES

Bedient, H.A. and Vederman, J. 1964: Computer analysis and forecasting in the tropics. Monthly Weather Review, Vol. 92, No. 12, pp 565-577.

Eber, L.E. 1961: Effects of wind-induced advection on sea surface temperature. J. Geophys. Res., 66, pp 839-844.

Holl, M.M. 1963: Scale-and-pattern spectra and decompositions, Tech. Memo No. 3, Meteorology International, Monterey, Calif.

Hubert, W.E. 1964: Computer produced synoptic analyses of surface currents and their application for navigation. Presented 1964 National Marine Navigation Meeting, San Francisco, Dec 1964.

Laevastu, T. 1960: Factors affecting the temperature of the surface layer of the sea. Merentutkimuslaitoksen Julkaisu, 167, pp 131.

_____ 1965: Synoptic scale heat exchange and its relation to weather. FNWF, Monterey Tech Note No. 7, Feb 1965.

Namias, J. 1959: Recent seasonal interactions between North Pacific waters and the overlying atmospheric circulation, J. Geophys. Res., 61, pp 631-646.

Witting, R. 1909: Zur Kenntriss des vom Winde erzengten Oberflackenstromes. Ann. Hydrogr. Marit. Met, 73:193.

Wolff, P.M. 1964: Operational analyses and forecasting of ocean temperature structure. (Rpt Fleet Numerical Weather Facility)

SYNOPTIC SCALE HEAT EXCHANGE AND ITS RELATIONS TO WEATHER

Taivo Laevastu
U. S. Fleet Numerical Weather Facility
Monterey, California

"The opinions presented in this paper are those of the author and do not necessarily represent the official views of the Navy Department at large."

ABSTRACT

The present study was undertaken to learn about the contribution to heat exchange contrasts through sea-air heat exchange and to contribute therewith to the understanding of the feedback of energy between the sea and the atmosphere on a synoptic scale.

The formulas and procedures for computation and forecasting of the heat exchange components are given and reference is made to the studies of their accuracy and sources of errors. The disadvantages of the monthly and seasonal computations, as compared to synoptic ones, are briefly discussed.

Examples of the synoptic distribution of heat exchange components during given days over the North Pacific Ocean are presented. Graphical and descriptive models of the heat exchange patterns in relation to anticyclones and different developmental stages of cyclones are constructed. Based on these models, the effects of the energy change on the ocean surface properties are explained and verification demonstrated with synoptic analyses of the short-term changes and anomalies of sea surface temperature. The return effects of these anomalies to the surface weather are postulated and the numerical tests of the use of "correction factors," indirectly derived from the present study, are briefly indicated.

A hypothetical model of the coupling of the heat exchange model with the 500-mb SD patterns is given, its use for deriving surface pressure patterns is demonstrated, and the possible use of this approach is shown by verification of forecasting attempts over 48 and 72 hours.

Though some principal aspects of the presented feedback models have been tested and found to contribute toward improving the present forecasting models, they are still experimental in nature. However, they increase the prospects of preparing numerical 3 to 5 day forecasts in the not too distant future. The primary use of heat exchange computations at Fleet Numerical Weather Facility is in synoptic oceanographic analysis and forecasting.

INTRODUCTION

The development of truly synoptic oceanographic analysis and forecasting emphasizes thermal structure in the sea and therefore requires the quantitative knowledge of energy exchanged between the sea and the atmosphere. It can be postulated that temperature in oceanographic analyses has the same importance as atmospheric pressure in meteorological analyses. Furthermore, oceanographic analysis and forecasting must be based mainly on synoptic weather observations by ships, as truly synoptic subsurface oceanographic observations are scarce indeed and would be too time consuming and expensive to make on a worldwide synoptic scale.

A number of meteorologists, especially those from the so-called Bergen School and a few others, have left no doubt that there is also a need to include heat exchange effects into successful weather forecasting models. Therefore, the synoptic study of heat exchange finds application also in meteorology.

A number of heat exchange studies have been done in the past on a seasonal and monthly basis; however, synoptic studies have been scarce. The most extensive of the latter are by Petterssen, Bradbury and Pedersen (1962) and by the present author (Laevastu, 1963).

Among the objectives of the present study, reported herein, were:

(1) To investigate the feasibility of synoptic computations of heat exchange components and to study their accuracy and possible sources of errors.

(2) To study the day to day variability of heat exchange patterns at the surface and their relations to surface weather and upper air patterns.

(3) To study the effects of heat exchange on the ocean. This report presents mainly the results of objective (2) above; other objectives are dealt with briefly. In addition, a hypothetical model of energy exchange and feedback between the ocean and atmosphere is given, and its possible application is explored. This study was carried out with the support of NSF Grants Nos. GP-353 and GP-2459 and with support from Fleet Numerical Weather Facility. The author wishes to express his sincere thanks to Commander Hubert and Mr. Carstensen for valuable advice and help in the preparation of this paper.

FORMULAS FOR HEAT EXCHANGE COMPUTATION AND ACCURACY AND SOURCES OF ERRORS

The formulas used for heat exchange computations are summarized in Table 1. The validity and accuracy of these formulas have been described earlier by the present author (Laevastu, 1960). The heat exchange

TABLE 1a.

Formulas for synoptic computation of heat exchange between the sea and the atmosphere

All units of in g cal cm^{-2} 24 h^{-1}

(1) Insolation (Q_S) = $0.014A_n t_d (1 - 0.006 C^3)$

(2) Albedo (Q_r) = $0.15 Q_S - (0.01 Q_s)^2$

(3) Effective back radiation (Q_b) = $(297 - 1.86T_w - 0.95U_o)(1-0.0765 C)$

(4) Latent heat transfer

$e_w - e_a$ pos. $Q_e = (0.26 + 0.077 V)(0.98 e_w - e_a)$

$e_w - e_a$ neg. $Q_e = 0.077 V (0.98 e_w - e_a)$

(5) Sensible heat transfer

$T_w - T_a$ pos. $Q_h = 39 (0.26 + 0.77 V)(T_W - T_a)$

$T_w - T_a$ neg. $Q_h = 3 V(T_w - T_a)$

(6) Total heat exchange (Q_e) = $Q_s - Q_r - Q_b - Q_e - Q_h$

TABLE 1b.
List of notations used in Table 1a

A_n - noon altitude of the sun ($^\circ$).

C - cloud cover (in 1/10 of the sky)

e_a - water vapor pressure of the air (mb)

e_w - saturation vapor pressure of the sea surface (mb)

L_t - latent heat of vaporization (g cal g^{-1})

Q_b - effective back radiation $\lceil$g cal $(24h)^{-1}\rfloor$

Q_e - latent heat transfer

Q_h - sensible heat transfer

Q_r - reflected heat (albedo)

Q_s - insolation

t_d - length of the daylight (min)

T_a - air temperature ($^\circ$C)

T_w - sea surface temperature ($^\circ$C)

U - relative humidity (%)

V - wind speed (m sec^{-1})

computations, which form the basis for the present study, were made manually. The computational procedure has been described in technical reports (Laevastu, 1963), where also nomographs are given. Before averaging the meteorological elements (reported by observing ships) by areas (e.g., 2 1/2° or 5° squares), a subjective contouring of the distributions is necessary. This subjectivity will be eliminated in computer programs of synoptic heat exchange now in preparation at Fleet Numerical Weather Facility, Monterey.

Detailed discussions of the sources and magnitudes of errors are given in the aforementioned technical reports. It has been concluded that the plausibility of the results obtained depends largely on the density of meteorological elements reported over the ocean and on their analysis because not the absolute values of the elements, but rather the differences between the properties at the sea surface and some higher observation level (e.g., 8 to 10 meters), are used in most cases. Other difficulties, such as the analysis of distribution of cloud cover, estimation of wind speed over the sea, etc., are well known.

In the evaluation and use of the computed results one must also be conscious of the possible effects of short-term (diurnal and interdiurnal) variability of meteorological elements. However, as will be shown later, the patterns of heat exchange components are usually larger in scale and relatively persistent from day to day, changing in intensity and position in relation to the change of corresponding surface pressure patterns, thus eliminating partly the effect of short-term variations. The effects of diurnal fluctuations of meteorological elements on computed heat exchange are discussed by the present author elsewhere (Laevastu, 1960, 1963).

Considering that rather large variability in meteorological conditions occurs from day to day, that many of the heat exchange formulas use the differences between the sea surface and the surface air properties, that the relations of the influence of the elements in these formulas are often non-linear, and that the formulas have mostly been worked out for and verified on short-period (e.g., 24 hours) measurements and computations, it becomes obvious that synoptic computations of heat exchange are usually not comparable to heat exchange patterns computed with monthly or seasonal averages. The above described condition is numerically illustrated in Table 2. Four values of sea-air temperature and water vapor pressure are arbitrarily selected. Furthermore, four values of wind speeds are taken in two different sequences, which give two different values of sea-air exchange (Q_a) in the last two columns. The average values of meteorological elements as well as the averages of the computed sea-air exchange are given on the sixth line. The averaged Q_a values are 59.3 and 182.5 g cal cm^{-2} $24h^{-1}$ and illustrate the differences in results caused by a difference in the sequence of wind speeds used, even though the average wind speed is 6.25 m sec^{-1} in both cases. The seventh line gives the Q_a value (104) computed with the averaged values of meteorological elements. It can be concluded from Table 2 and from a knowledge of the variability of meteorological conditions that monthly and seasonal computations can be expected to yield only an approximate distribution of heat exchange patterns and their relative numerical values. To

Table 2

Examples of Sea-Air Heat Exchange (Q_a), Computed With Assumed Synoptic Values and With Subsequently Averaged Same Values of Meteorological Elements.

	V_1 m sec^{-1}	V_2 m sec^{-1}	$T_w - T_a$ °C	$e_w - e_a$ mb	Q_{e1}	Q_{e2}	Q_{h1}	Q_{h2}	Q_{a1}	Q_{a2}
					g cm^{-2} 24h^{-1}		cal cm^{-2} 24h^{-1}			
1	2.5	10	4	6	159	363	70	160	229	523
2	5	7.5	2	3	113	147	50	64	163	211
3	7.5	5	0.6	1	49	38	19	15	68	53
4	10	2.5	-2	-3.6	-163	-42	-60	-15	-223	-57
Sum	25	25	4.5	6.4	158	506	79	224	237	730
Av.	6.25	6.25	1.15	1.6	39.5	126.5	19.8	56	59.3	182.5
Q_e, Q_h and Q_a computed with above averaged meteorological elements					71		33		104	
Differences between averaged values and values computed with averaged meteorological elements					-31.5	55.5	-13.2	23	-44.7	78.5

arrive at realistic monthly or seasonal average heat exchange values the synoptic heat exchange must be computed with synoptic meteorological elements and summed and averaged after these computations have been performed.

EXAMPLES OF SYNOPTIC DISTRIBUTION OF HEAT EXCHANGE COMPONENTS

Some examples of the distributions of heat exchange components are shown in Figures 1 to 7. The variations in insolation are largely determined by the time of year, latitude and cloud cover (Figure 1). The effective back radiation is also affected by cloudiness, the relative humidity and the sea surface temperature (Figure 2). The transfer of latent heat and sensible heat transfer are most directly connected to surface weather systems (Figures 3 and 4). These two components are summed together and the quantity called sea-air exchange (Q_a). Two consecutive days of Q_a distribution over the North Pacific are shown in Figures 6 and 7 together with the surface weather charts and the total heat exchange (Q_ℓ). These figures indicate that the patterns of Q_a are large in scale, corresponding to surface weather patterns, and that they change from day to day in the same manner as the weather patterns. In lower latitudes, below 20° North, a number of smaller centers of Q_a are apparent. This is partly in agreement with the surface pressure distribution as shown by synoptic analyses. Furthermore, there are some uncertainties involved in the computations in this area, as the ship reports south of about 20°N, as well as north of about 55°N, are sparse. The higher values of Q_a are usually found on the cold air side of cyclones. Low or negative values of Q_a are found, on the other hand, in the warm sectors of cyclones. Relatively high Q_a gradients can be found along the cold fronts. The relations of the Q_a fields to cyclones change slightly with the age of the cyclone itself.

In some cases pronounced Q_a contrasts have been observed in areas and places where cyclogenesis would be expected and does, in fact, occur 1 to 2 days later. In the eastern parts of the ocean the Q_a contrasts are much less pronounced than in the western parts. The disappearance of Q_a contrast within a cyclone area usually precedes the dissipation of the cyclone, and might be useful in forecasting the filling of a system. Physically, it can be explained that the energy sources and sinks for the cyclones at the sea surface are cut off due to the exchange processes at the surface. These tend to diminish the gradients of properties between the sea surface and the lower layers of the atmosphere and consequently to dissipate the cyclone because it has been cut off from any new sources of energy.

The relations between anticyclones and heat exchange patterns are less distinct than in the case of cyclones. However, there is usually a higher Q_a in the eastern part of an anticyclone and lower Q_a pattern in the western part of it. Most of the well defined high and/or low Q_a patterns are related both to the cyclone and the adjacent anticyclone (see further Figure 9).

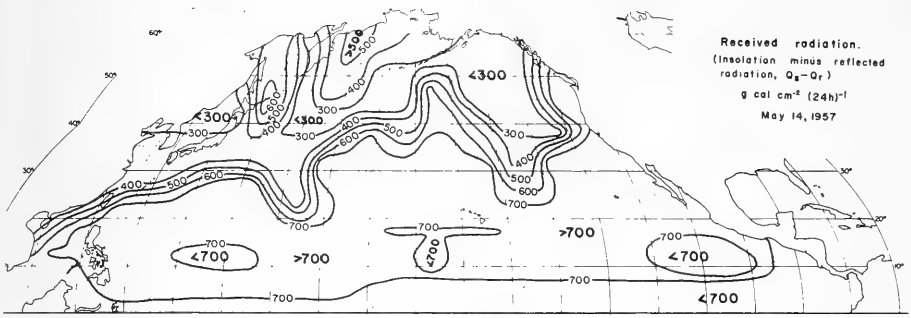

Figure 1. Received radiation on 14 May 1957

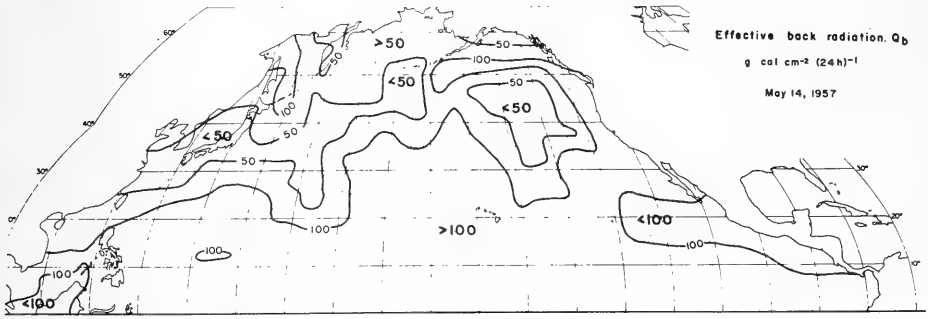

Figure 2. Effective back radiation on 14 May 1957

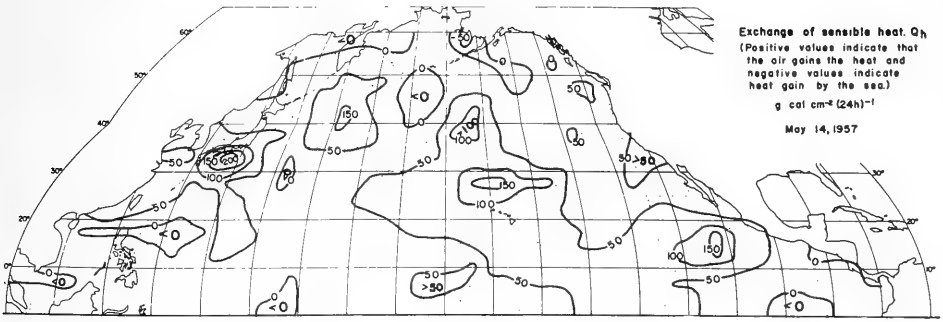

Figure 3. Transfer of sensible heat on 14 May 1957

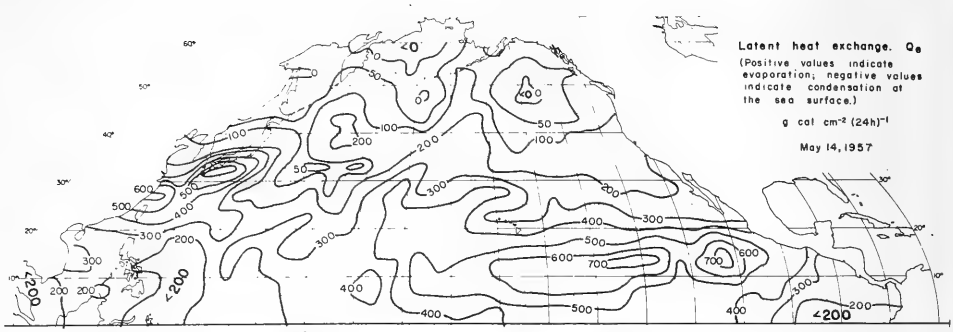

Figure 4. Transfer of latent heat on 14 May 1957

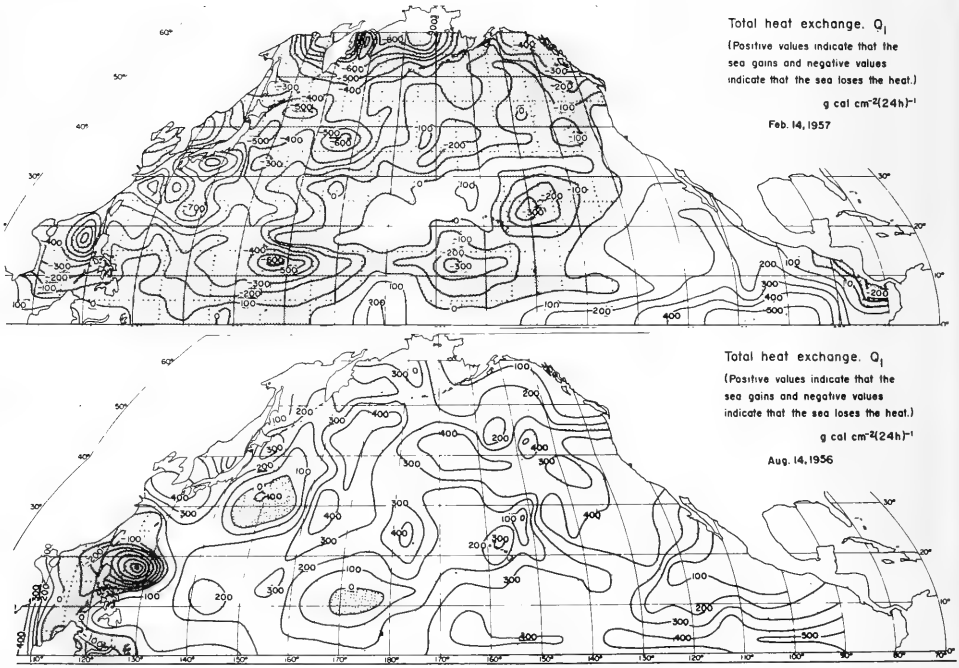

Figure 5. Total heat exchange on 14 February 1957 and 14 August 1956

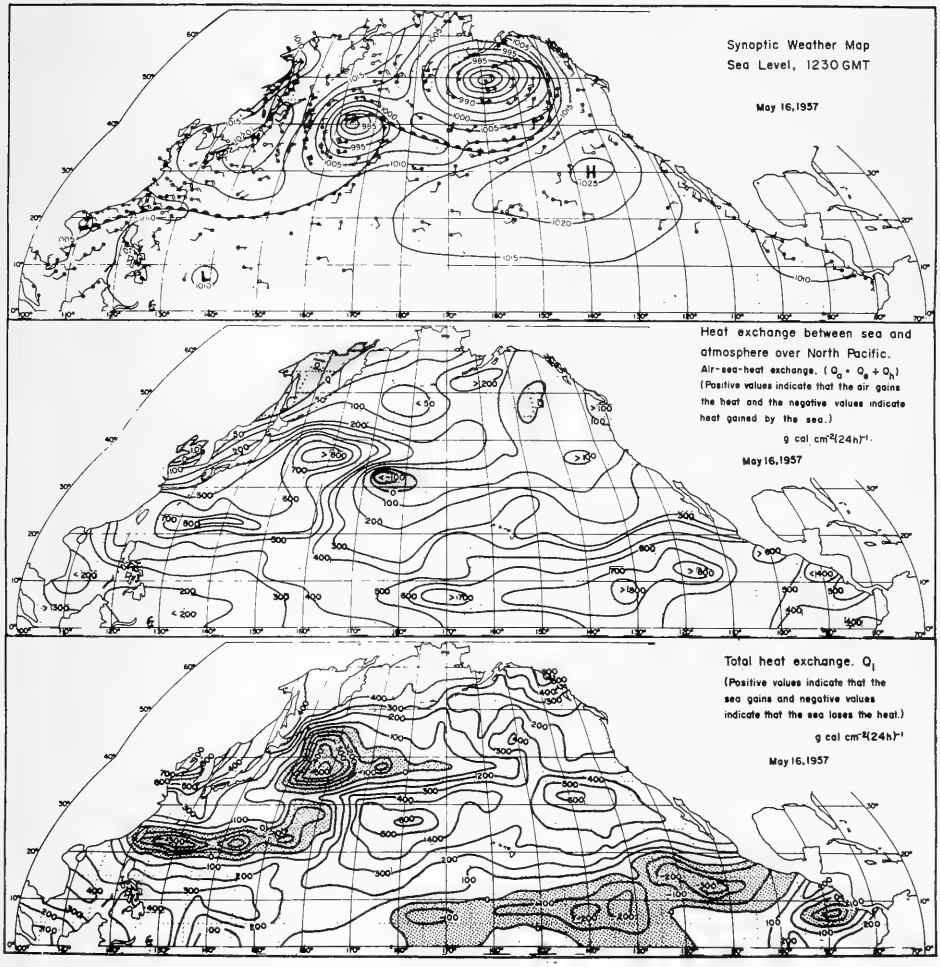

Figure 6. Surface pressure, sea-air exchange and total heat exchange on 16 May 1957.

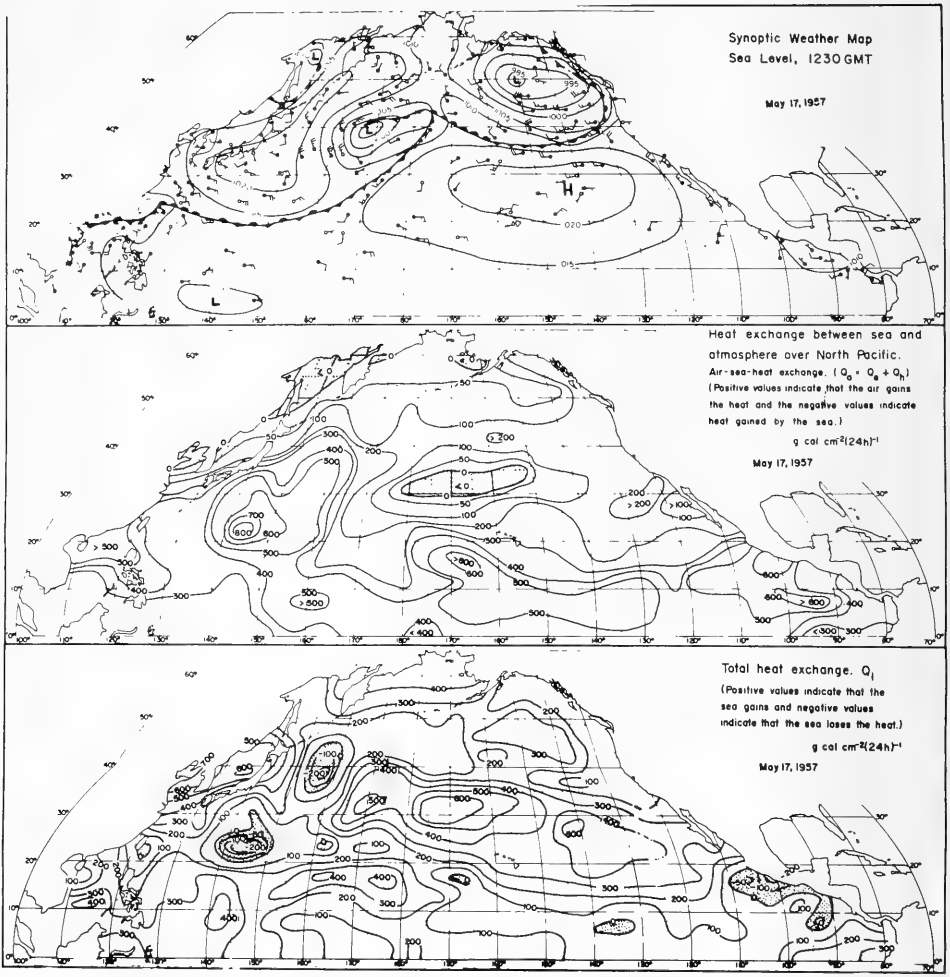

Figure 7. Surface pressure, sea-air exchange and total heat exchange on 17 May 1957.

The total heat exchange Q_ℓ indicates the amount of heat gained or lost by the sea in 24 hours. Figure 5 shows the total heat exchange distribution at 2 given days in the winter and summer, respectively. High loss of heat along the east coast of Asia can be observed during the winter over an area which reaches to a relatively low latitude (ca. 20°N) and a considerable distance out from the coast (to ca. 165°E). Eastern and southeastern parts of the ocean show relatively low loss or gain of heat during the same date.

The distribution of Q_ℓ in summer is more latitudinal and is affected by meteorological conditions as shown by Figures 5, 6, and 7.

SIMPLIFIED PHYSICAL MODEL RELATING HEAT EXCHANGE PATTERNS TO CYCLONES AND ANTICYCLONES

Based on the examination of a number of synoptic heat exchange computations over the North Pacific a simplified physical model, relating the heat exchange patterns to cyclones and anticyclones, is presented in Figure 8. This model is largely self-explanatory. It shows the location of the heat exchange patterns with the developmental stages of the cyclone as well as in the vicinity of the surrounding anticyclones. The adjacent cyclones and anticyclones are connected to each other through "common" heat exchange patterns, as schematically shown in Figure 9. Figure 10 presents a hypothetical vertical E-W section of a cyclone as it might be related to the heat exchange processes. Figure 11 gives a scheme of heat exchange, flow patterns and upper level topography of a warm sector cyclone. Whether the simplified models in Figures 8 to 11, derived from an examination of 30 synoptic Q_a charts, correspond exactly to the processes in nature or need further testing and improvement is not subject to discussion here; their importance lies in the fact that they fit without serious discrepancies and lead to the consideration that the sea-air heat exchange patterns might be related to upper air patterns. In fact, a study of the 500-mb small scale (SD) patterns shows a remarkable similarity to the heat exchange patterns, especially with regard to position. Tests were made, therefore, using the 500-mb SD patterns for analysis as well as forecasting of surface pressure distribution. (The pattern separation procedure has been described by Holl, 1963). The construction of surface flow patterns from 500-mb SD patterns is shown in Figure 12. The positions of surface lows and highs and their central pressures are also indicated, using preliminary relations between SD central values and central pressures at the surface (Figure 13). The results of another preliminary study show that cyclone centers should be sloped about 4° latitude ENE of SD centers and anticyclone centers about 5° toward 120°. As the 500-mb forecasts usually show somewhat better skill over longer forecasting periods (48 to 72 hours), this model has led to a possible auxiliary surface forecasting procedure. Some numerical results of verification and comparison tests of this model for 48 and 72 hours compared with the operational Fleet Numerical Weather Facility surface model are shown in Table 3. A report on the incorporation of the above results in extended numerical forecasts (3 days) is in preparation at Fleet Numerical Weather Facility.

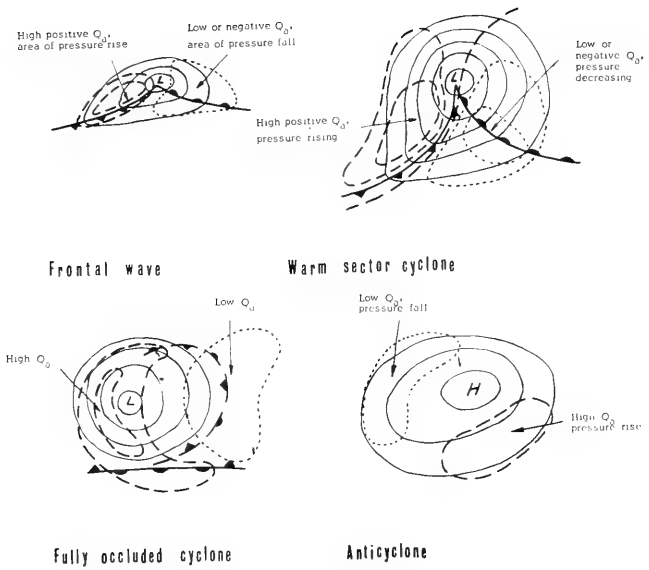

Figure 8. Simplified model on the relations between sea-air heat exchange and cyclones and anticyclones

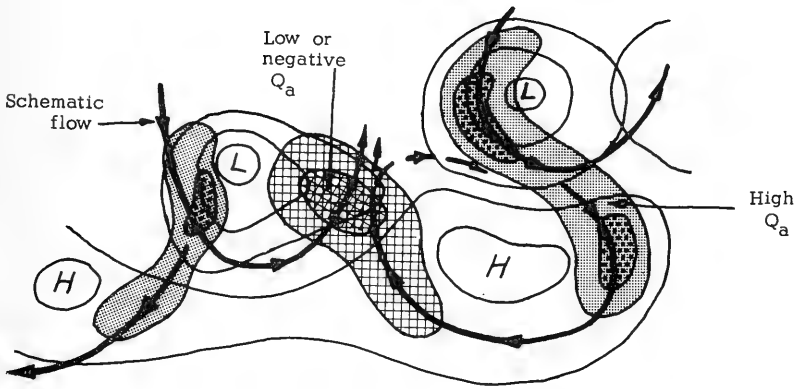

Figure 9. Scheme of Q_a patterns common in adjacent cyclones and anticyclones.

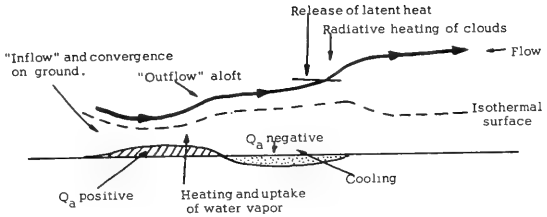

Figure 10.

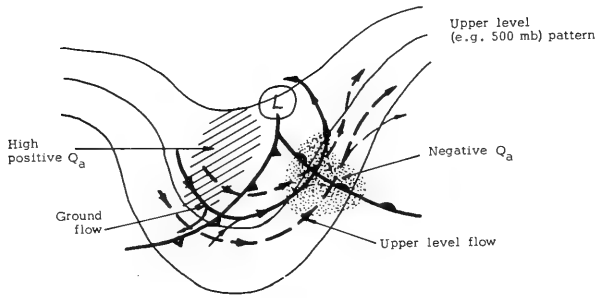

Figure 11.

Figure 10. Schematic Vertical E-W Section Through a Warm Sector Cyclone With Assumed Model on the Relation to Heat Exchange.

Figure 11. Scheme of Heat Exchange, Flow Patterns and Upper Level Topography of a Warm Sector Cyclone.

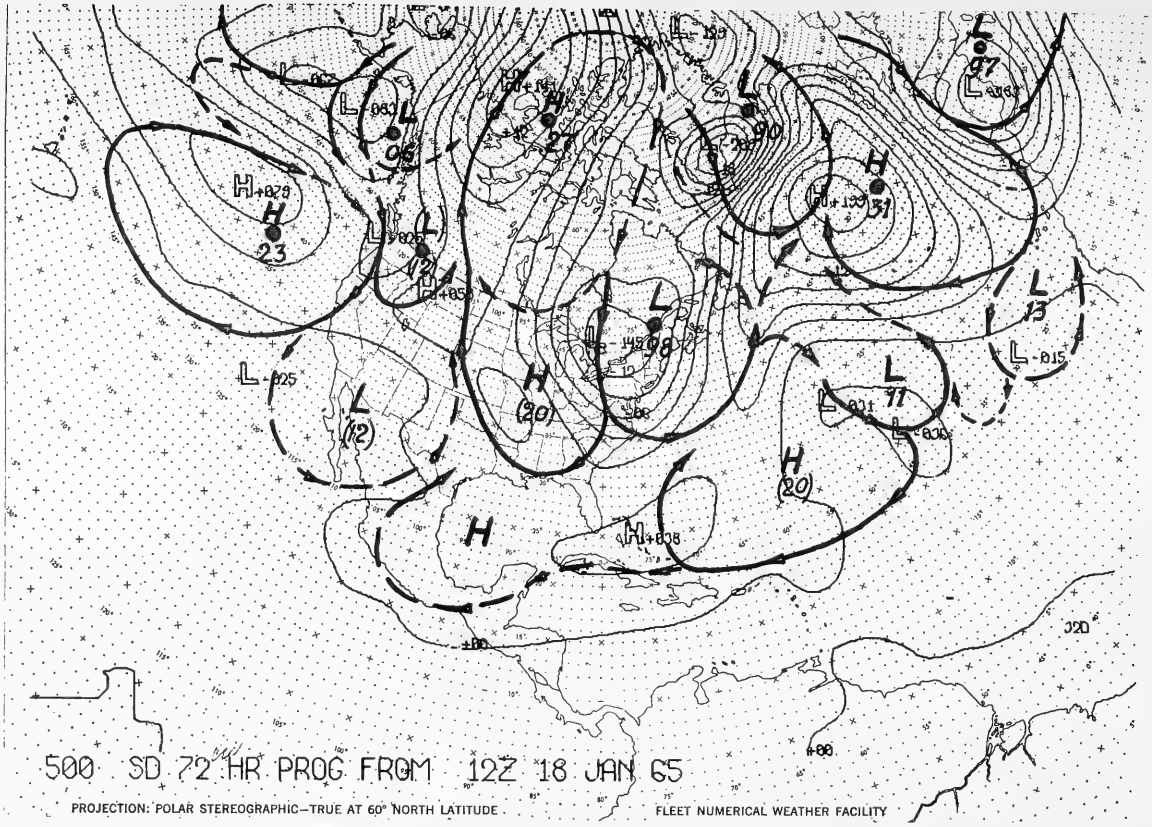

Figure 12. Relations between 500-mb patterns and surface flow patterns. (The forecasted positions and central pressures of lows and highs are indicated with fat characters.)

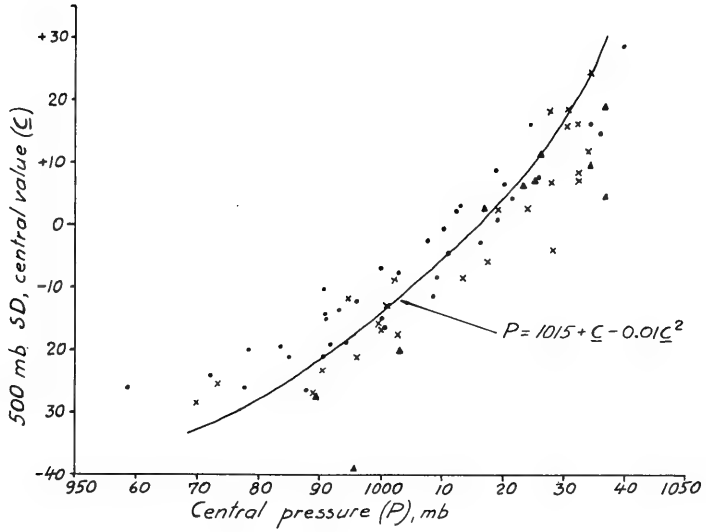

Figure 13. Relations between central values of 500-mb SD patterns and central pressures of cyclones and anticyclones.

Table 3. Comparison of errors in surface forecast (SF Prog.) with the errors in forecast derived from 500-mb SD patterns (preliminary results).

	48 h. SF Prog.	48 h. Prog. from 500-mb SD	36 h. SF Prog.	72 h. Prog. from 500-mb SD
(1) Number of highs (H) and lows (L) considered.	22	22	21	21
(2) Average differences of central pressures of H's and L's from verifying analysis (mb).	8.6	7.0	8.9	9.4
(3) Average differences of the positions of centers of H's and L's from verifying positions (^{o}Lat.)	8.4	6.5	6.5	7.3

SIMPLIFIED FEEDBACK BETWEEN THE SEA AND THE ATMOSPHERE

The ocean/atmosphere feedback has been described in general terms in a few publications in the past (e.g., Bjerknes, 1960), but a complete description in terms of energy exchange is not available. In this chapter an attempt is made to describe the synoptic feedback between the sea and the atmosphere, based upon the results of previous chapters.

An essentially diabatic simplified model is considered herewith, with the conversion of energy in the atmosphere itself being largely neglected, as it has been described by several authors earlier. Some existing numerical meteorological models permit heat exchange input without extensive changes. Tests with these models will clarify further the quantitative relations between energy exchange and weather processes and will indicate the usefulness of the inclusion of heat exchange parameters.

The feedback system can easily be derived from Figures 8 to 11, a simplified description of which is given below. In this description it is assumed that the sea surface isotherms are essentially latitudinal and equidistant at the initial stage. Compass directions, rather than descriptive terms of the sectors of cyclones and anticyclones, are used.

Anticyclonic circulation:

Atmospheric circulation in relation to heat exchange. In the N part of the anticyclone the eastward flow is approximately parallel to the sea surface isotherms and would not result in appreciable sea-air exchange. In the NE part of the anticyclone the air flow has a southerly component, which brings colder air over warmer water. This factor can increase progressively in the E and SE parts of the anticyclone. A slight pressure rise is usually observable in the SE part of the anticyclone in the following days which gives an apparent movement of the anticyclone to the SE, and an apparent location of anticyclone center towards areas with negative sea-surface temperature anomalies.

The energy gain of the air in S and SW part of the anticyclone decreases, and low or negative Q_a values are found in the NW sector due to the northward component of the air across sea surface isotherms. In this area pressure fall occurs.

Changes in the ocean, caused by advection and heat exchange. If the heat exchange and advectional effects in the sea and in the atmosphere were perfectly balanced, few disturbances would result. However, due to local inequalities of heat exchange processes and to advectional changes sea surface temperature anomalies are caused, which in turn may affect the heat exchange processes.

In some cases advectional effects might account for the greater part of the anomalies in the oceans. In the W and NW part of the anticyclone, warmer weather is advected towards N and NE. In the NE and E part colder water is advected towards south. Further cooling of the ocean in the SE sector can be effected by intensive sea-air exchange in this area. In the S and SW part

of the anticyclone, slight warming of the sea surface is expected partly due to latitudinal warm advection and partly due to low sea-air exchange and high insolation.

Subsequent changes in the atmosphere. Assuming that the advectional and local heating effects, described above, are not in equilibrium with the cooling and heating processes and advectional anomalies result, the following further changes could be expected in the atmosphere:

In the W and NW part of an anticyclone the warm advection would counteract the heat loss of the air by decreasing sea-air temperature difference, and the expected pressure fall would be slowed down with time. If the warm water advection is especially strong, a pressure rise in the N part of the anticyclone could be observed in a few days, resulting in an apparent slight northward movement of the high.

In the NE and E part, the cold water advection would diminish and/or counteract the increase of sea-air exchange. The same effect occurs in the E and SE part, thus counteracting the prospective accompanying pressure rise and eastward movement of the high. This mechanism might explain the quasi-stationary nature of highs in the lower latitudes over the oceans.

Cyclonic circulation:

Atmospheric circulation in relation to the heat exchange. In the W and SW part of a cyclone, high positive sea-air exchange is taking place, due to the southward component of cool, drier air across the sea surface isotherms. This cool air is usually accompanied by subsidence which results in clear, cloudless skies. The high sea-air exchange is accompanied by relatively rapid pressure rises in this sector.

In the S part of a cyclone, the air flow is nearly parallel to the sea surface isotherms or with a slight northerly component, which increases in the SE part of the cyclone and results in heat and moisture loss by the air, accompanied by pressure falls.

In the E and NE part the flow is towards colder sea surface temperatures. The heat loss by air is, however, decreasing rapidly, because of cooling of the lower layers of the air and creation of stable conditions.

In the N part of the cyclone the curvature is usually relatively sharp and in the NW part the heating of the air starts again due to a slight southerly component.

Changes in the ocean caused by advection and heat exchange. In the W and SW part of a cyclone, cool sea surface advection takes place. This cooling is further aggravated by deep mixing in the sea due to heavy winds and waves and by heat loss from the sea through sea-air exchange.

In the S and SE part an E to NE advection of warmer water occurs, which is accompanied by low heat loss or occasionally heat gain through sea-air

exchange (diminished by low insolation due to heavy cloudiness behind a warm front).

In the NE and N part this advection turns to cold advection from the NE. Slight upwelling can be expected in the center of a cyclone due to divergence in the surface layers.

Subsequent changes in the atmosphere. In the W and SW part of the cyclone, the cool advection counteracts the normally large sea-air exchange and warming of the air, which results in further SE movement of the cold front.

In the S and SE part the warm advection would extend the area of heat loss toward the NE, accompanied by a pressure fall in the same direction. It is thus apparent that the advective and local changes cause a kind of twisting movement around a cyclone giving a force in the NE direction. The model of occluded cyclones together with the description above also gives partial explanation why occluded cyclones tend to move more to the left. The above model also explains partly the tendency of cyclone centers (and the W parts of them) to locate over areas with positive sea surface temperature anomalies.

This description of the feedback model should not be considered as a final one, but rather as a framework, subject to further refinement. The observed pressure tendency anomalies, empirically related to sea-air exchange, remain unexplained in detail in these models.

The above described model should be thought of as entirely auxiliary to existing operational models of atmospheric behavior, providing an additional "correctional" factor only.

Partial verification of the above described feedback model has been sought and indeed found. The effects on the ocean are demonstrated in Figures 14 to 16. Figures 14 and 15 show surface pressure distribution and the positions of sea surface isotherms on 10 and 13 December 1964. Figure 16 shows the sea surface temperature changes at four selected grid points in this area and period, taken from Fleet Numerical Weather Facility's synoptic analysis of sea surface temperature (Wolff, 1964). Positions of these grid points are indicated on Figure 14. An examination of Figures 13 to 15 indicates that the observed short-term sea surface temperature changes are partly advectional and correspond to the changes described and expected in the above simplified feedback model. The partially advective nature of the short-term sea surface temperature changes is furthermore substantiated by the synoptic analyses of surface currents (Hubert, 1964). Furthermore the change of sea surface isotherms between 12 and 14 December 1964 (Figure 17) also indicates that the sea surface temperature change patterns are large in scale and correspond to expected advectional patterns, as shown by a comparison to surface pressure analysis charts for this period.

The preliminary verification tests of the atmospheric part of the feedback model, utilizing the short-term sea surface temperature anomalies, was done subjectively for a number of forecasting periods. The results indicated

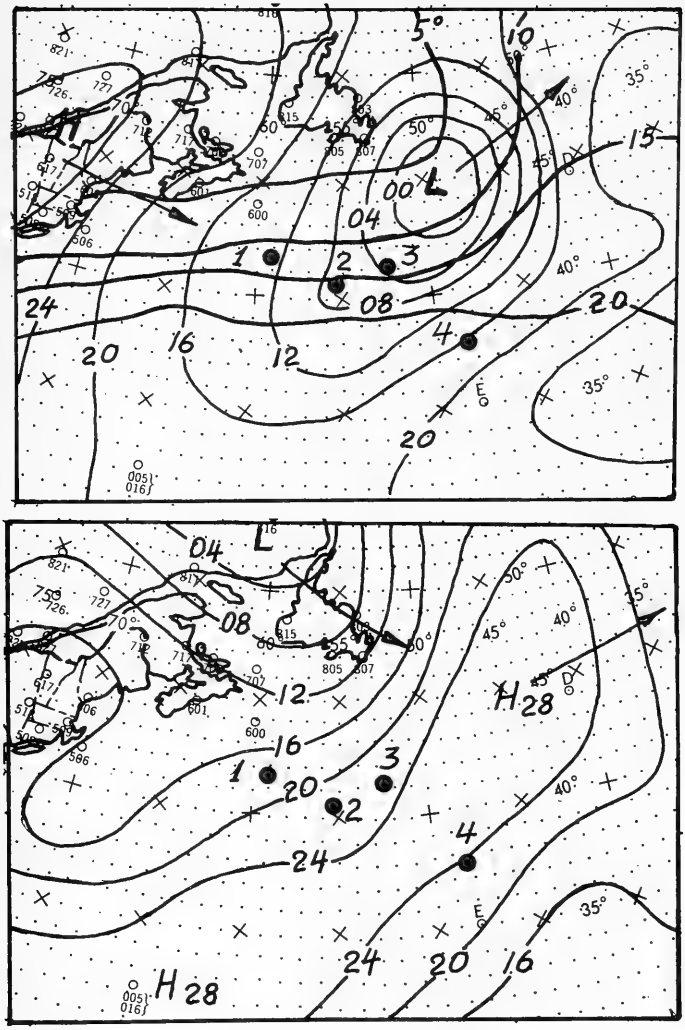

Figure 14. Surface pressure and sea surface isotherms in the NT Atlantic on 10 December 00Z 1964. The subsequent movement of cyclone and anticyclone centers is shown with arrows.

Figure 15. Surface pressure in the NW Atlantic on 13 December 00Z 1964.

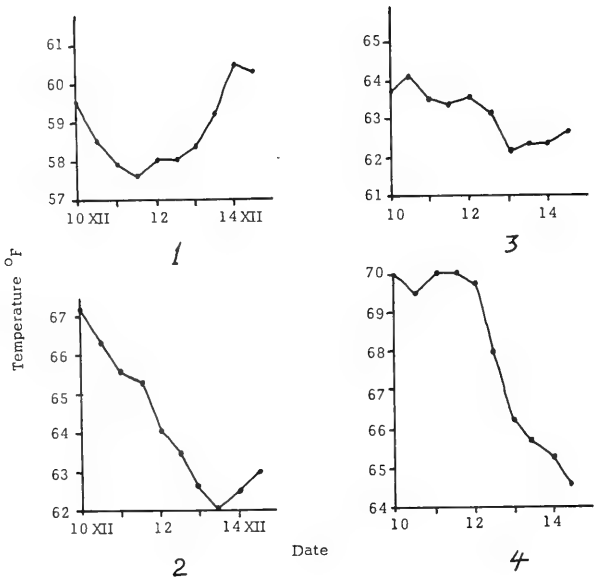

Figure 16. Change of sea surface temperature at four selected grid points in the NW Atlantic from 10 to 14 December 1964. (Positions of the selected grid points see Figure 14.)

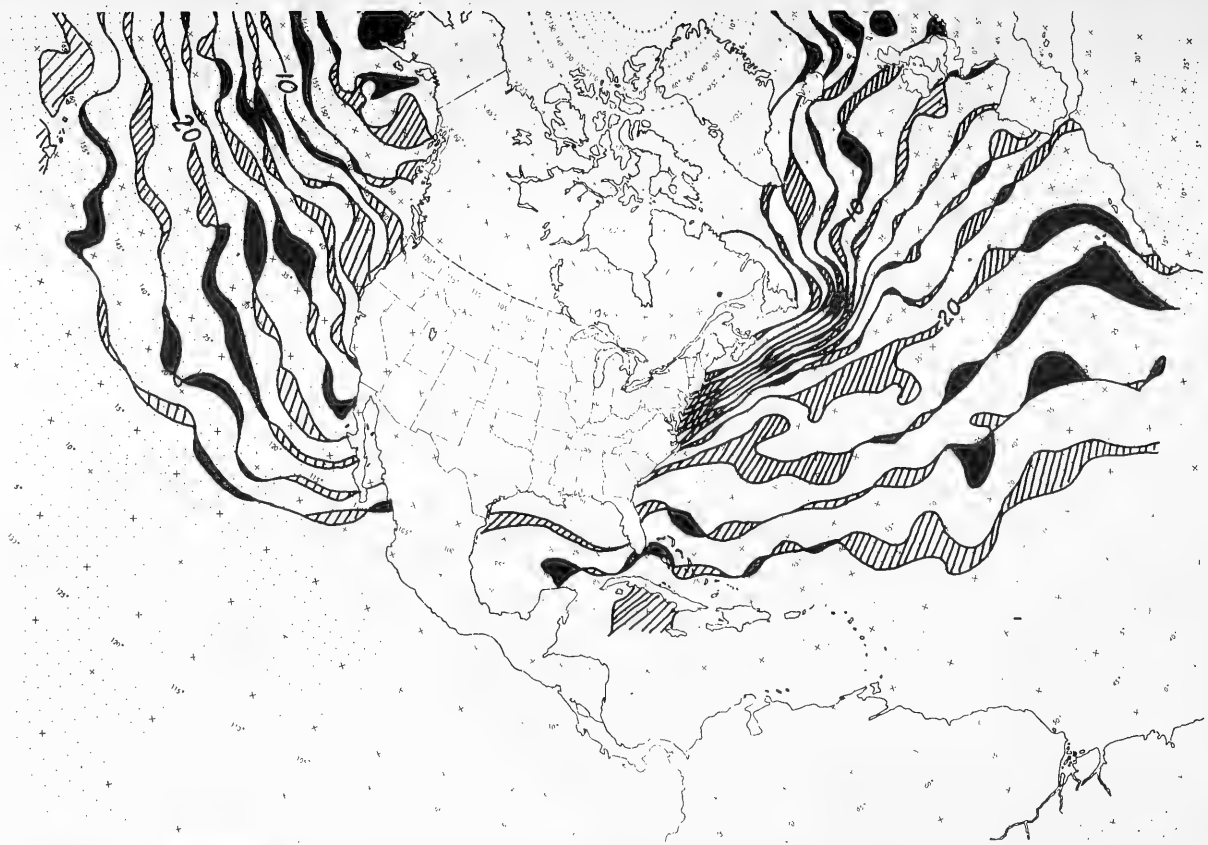

Figure 17. Change of sea surface isotherms between 12 and 14 December 1964.
increase of SST ////////// decrease of SST

some skill. Consequently some slightly different "correction factors were programmed at Fleet Numerical Weather Facility for numerical testing in connection with operational numerical surface forecasting models. These tests and developments, promising minor improvement to existing models, are in progress and will be reported at a later date.

Although the synoptic energy feedback from the sea to atmosphere promises some use and improvement, the principal use of synoptic energy exchange computations at Fleet Numerical Weather Facility is in oceanographic analysis and forecasting, as demonstrated by Commander Hubert at this conference (Humbert, 1965).

REFERENCES

Bjerknes, J. 1960 Ocean temperatures and atmospheric circulation. WMO Bull. 9(3):151-7.

Holl, M. 1963 Scale-and-pattern spectra and decomposition. Met. Int. Inc., Monterey, Techn. Memo 3.

Hubert, W.E. 1965 U.S. Fleet Numerical Weather Facility activities relating to sea-air interactions on a synoptic scale. FNWF Techn. Note No. 5.

Hubert, W.E. 1964 Computer produced synoptic analyses of surface currents and their application for navigation. Presented at the 1964 National Marine Navigation Meeting, Institute of Navigation, Dec. 7-8, 1964, San Francisco.

Laevastu, T. 1960 Factors affecting the temperature of the surface layer of the sea. Soc. Scient. Fennica, Comment. Physico-Mathem. 25(1):1-136.

Laevastu, T. 1963 Energy exchange in the North Pacific; its relations to weather and its oceanographic consequences. Parts I, II and III. Hawaii Inst. Geophys. Rpts Nos. 29, 30 and 31 (Rev.).

Petterssen, S.; D. L. Bradbury and K. Pedersen 1962 The Norwegian cyclone models in relation to heat and cold sources. Geofys. Publ. (Geophys. Norv.) 24(9):249-280.

1965 U.S. Fleet Numerical Weather Facility; The use of 500-mb SD pattern forecasts for derivation of surface forecasts, and the accuracy of 3-day forecast based on 500-mb SD patterns. FNWF Techn. Note(in preparation).

Wolff, P.M. 1964 Operational analyses and forecasting of ocean temperature structure. 1st U.S. Navy Symp. on Military Oceanogr., Proc., 171-195

LABORATORY STUDIES OF WIND ACTION ON WATER STANDING IN A CHANNEL

G. M. Hidy
National Center for Atmospheric Research
Boulder, Colorado

and

E. J. Plate
Colorado State University
Fort Collins, Colorado

ABSTRACT

The processes of wave and current development resulting from wind action on initially standing water have been investigated in a wind-water tunnel. The mean air flow over wavy water was examined along with the variation of several properties of the water motion with fetch, water depth, and wind speed. Measurements of phase speed and length of significant waves, the standard deviation of the water surface, the average surface drift, the autocorrelation of surface displacement and the frequency spectra are reported. The experimental results indicate that (a) the air motion in the channel follows a three dimensional pattern characteristic of wind tunnels of rectangular cross-section; (b) wind waves generated in the channel travel downstream at approximately the same speed as gravity waves of small amplitude, provided the effect of the drift current is taken into account; (c) the average drag coefficients for the action of the wind on the water surface increase with increasing wind speed, and these data are reasonably consistent with results of previous investigators; (d) the autocorrelations and frequency spectra indicate that the wind waves in the channel consist of nearly regular primary waves on which are superimposed smaller ripples; (e) energy in the high frequency range in the spectra tends to approach an equilibrium distribution while the lower frequency components continue to grow with increasing fetch; and (f) a similarity shape for the frequency spectra develops. The experiments in this study were not intended to model the processes of interaction between the ocean and the atmosphere. Nevertheless, the small waves generated in the channel appear to be at least qualitatively related to the development of waves on much larger bodies of water.

I. INTRODUCTION

In spite of a long history of effort devoted to the air-water interaction problem, the basic knowledge of the mechanisms for transport processes near the boundary between these two fluids has developed rather slowly. A variety of theoretical and experimental studies have been reported in the literature, but, because of the complexities of the physical processes involved, the detailed nature of the interaction remains inadequately understood.

Most of the experimental studies of air-water interaction have been undertaken on lakes or on the ocean where the conditions of the fluids are highly variable in time and space. These investigations have contributed significantly to the knowledge of the atmosphere and the sea. However, their usefulness in elucidating the fundamental physics of the exchange processes occurring between the two fluids is limited. Therefore, more studies should be carried out under controlled conditions in the laboratory to gain new insights into the mechanisms of transport across the air-water boundary.

Ursell (1956) has reviewed the fundamental laboratory experiments dealing with air-water interaction that were undertaken before 1954. Since the publication of Ursell's paper, a number of new investigations have been reported which included those of Sibul (1955), Cox (1958), Fitzgerald (1963), Schooley (1963) and Hanratty and coworkers (e.g., Cohen and Hanratty (1965)). With the exception of Cohen and Hanratty's work, the experiments performed by these investigators were not designed specifically to verify recent theoretical conclusions, or to serve as a starting point for developing refined ideas about the nature of air-water interaction. With this background in mind, a detailed experimental program has been initiated at NCAR and at CSU to study the relationship between the turbulent flow of air and water in a channel.

Properties of the Fluid Motion

When air moves at moderate velocities over water, a drift current develops, and small waves are generated on the liquid surface. A schematic picture of the development of combined air and water motion along with the growth of waves in a channel is shown in Figure 1. The properties of fluid motion examined in this study are indicated in this drawing. The coordinate system is indicated so that x is the distance downstream, and z is the vertical direction. The mean water surface is given by $z = d$ while the surface displacement from this level is denoted as ξ. The fetch F denotes the distance from the leading edge of the water to a particular point somewhere downstream. In terms of a two dimensional model, the velocity distribution in the water is $u(z)$, and the drift as the water surface is u_o. The air flow is given by $U(z')$, where U_∞ denotes the air velocity at approximately 20 cm above the mean water surface, and $z' = (z - d)$. The wave length $\bar{\lambda}$ and the phase speed $\bar{c}$ denote properties of significant waves.

For the purpose of this study, significant waves will refer to the

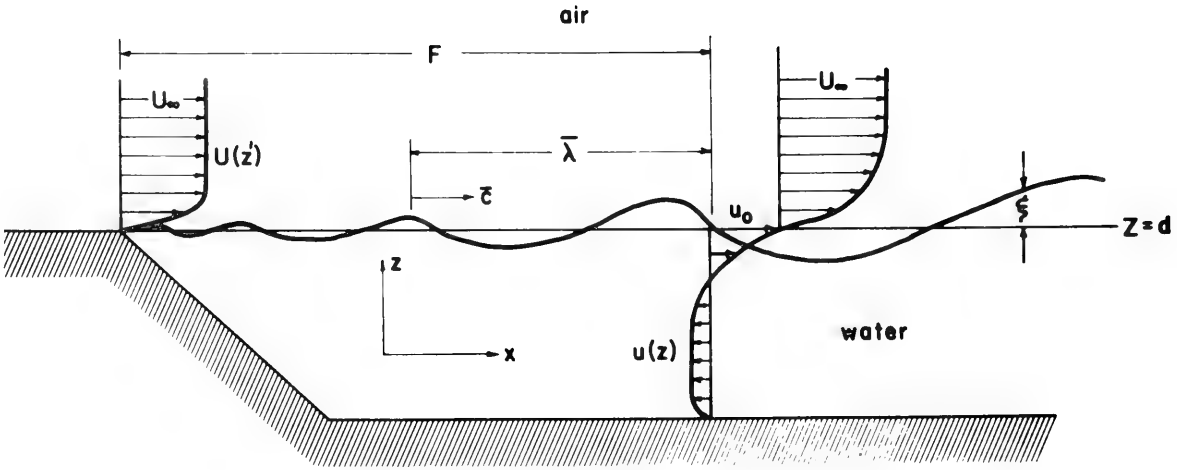

Figure 1. A schematic drawing of air and water motion associated with growing waves on a water surface.

larger regular waves observed at a given fetch. In general, smaller ripples are superimposed on the larger disturbances.

In this paper, a number of experimental results are discussed which refer to the mean air and water motion as indicated in Figure 1. Measurements of the statistical properties of the wind generated waves, including the autocorrelation and spectral density functions, are examined in the light of other properties of the fluid motion. There has been no attempt to model the ocean-atmosphere interaction with the laboratory equipment. However, it will be seen that a number of experiments for fluid flow in the channel are at least qualitatively related to the observed small scale interaction between the sea and the atmosphere.

II. EXPERIMENTAL EQUIPMENT AND PROCEDURE

The experiments were conducted in the wind-water tunnel at Colorado State University. This facility, shown schematically in Figure 2 consists of a tunnel or a closed channel 0.61 m wide by 0.76 m high whose plexiglass test section has a length of about 12 m. During operation, the maximum depth of water is approximately 15 cm. Air is sucked through the tunnel at velocities up to 18 mps by a large axial fan at the outlet. The inlet cone is designed to give a 4/1 contraction ratio. Two fine mesh screens are placed in the inlet cone. Honeycombs are placed just upstream of the outlet diffuser to minimize the axial rotation in the air induced by the fan. Sloping beaches are placed at the inlet and the outlet to prevent the reflection of waves. The "beaches" are constructed of aluminum honeycomb. The inclines are shaped in such a way that as smooth as possible a transition can be effected in the air-water flow. In this study, the bottom of the tunnel was smooth.

The air flow through the tunnel was measured by a pitot-static tube placed on a carriage in conjunction with a capacitative pressure transducer. The probe could be positioned anywhere in the section of the tunnel from the bottom to a level about 10 cm from the top.

The pressure gradient of the air and the depth of the water were measured every 4 feet down the tunnel with piezometer taps connected to a set of manometers.

Phase speeds and lengths of waves were determined from photographs taken with a movie camera. The length for successive waves was measured from the movies by comparing the distance between crests with a ruler in the picture. The phase velocities of waves referred to a fixed point were estimated by measuring from adjacent frames the distance traveled by a given crest during the time between successive frames. Time intervals between frames were read off a timer that was shown in the film.

To measure the change in the height of the water, a capacitance probe was used which is similar to Tucker and Charnock's (1955). This probe consisted of a 34 gauge magnet wire stretched vertically along the center

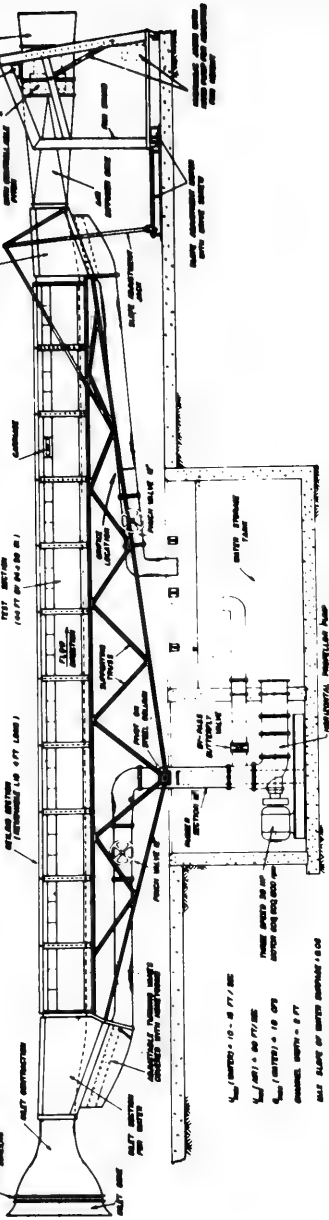

Figure 2. A general view of the wind-water tunnel.

line of the cross-section of the tunnel. These wires were placed at 1.2 m intervals downstream from the inlet of the tunnel. The wire itself and the water serve as the two plates of a condenser, and the insulation material (Nyclad) on the wire provides the dielectric medium. The capacitance between the wire and the water was measured with an AC excited bridge; the unbalance voltage from the bridge was linearized, amplified and rectified so that a DC output voltage was obtained which was directly proportional to the water depth. The output signal was fed to an oscillograph where the gauge response was continuously recorded during a run. The capacitance bridge-oscillograph combination was calibrated to give a recorded amplitude linearly proportional to the (varying) water depth with a flat response to frequency (±1%) up to approximately 30 cps.

From the continuous records of the surface displacement, data were read off at equal intervals of 0.025 sec. These data were used for obtaining values of standard deviation σ of the surface displacement, the autocorrelations $R(\tau)$ of the surface displacement, and the spectral density function $\phi(f)$. The computations were carried out on the NCAR-CDC 3600 computer.

It was not possible to obtain the vertical velocity distribution in the water. However, the surface velocity of the water u_o was measured by placing a small slightly buoyant particle on the water and observing the time required for it to move past fixed stations downstream. Values of the surface velocity could then be calculated from the intervals of distance of travel and the time of passage.

In this study, attention was centered on the measurement of the properties of water waves under conditions of steady (mean) air motion. In order to attain steady conditions in the air flow, the wave development, and the set up of water in the tunnel, the fan was started about 15-20 minutes before the photographs, the pitot tube measurements, and the wave amplitude data were taken at a particular location in the tunnel. In cases where wave data were being measured, a sample of a wave train corresponding to the passage of 100-200 waves was taken for a given run.

Samples of wave development were taken for several different conditions. For the condition of water initially standing on a smooth bottom, air velocities taken 20 cm above the water surface, were varied from 0 to 17 mps, and the depth of water was changed from 2.5 to 10 cm. The properties of fluid motion in these cases were observed at distances of approximately 1.8 m to 12 m from the leading edge of the water.

III. THE AIR FLOW OVER THE WATER

Since the air is forced by the fan through the wind tunnel of approximately constant cross section, a pressure gradient develops in the downstream direction. The pressure in the air p_a was found to vary approximately linearly with fetch through the channel. Typical values of the pressure gradient $\frac{1}{\rho w g}\frac{\partial P_a}{\partial x}$ (cm water per cm) as measured in the last 6 m of the

channel are shown in Figure 3. The pressure gradient was found to increase with wind speed, and with depth of the water.

Velocity Distribution in the Air

Measurements of the mean horizontal air motion in the vertical direction and across the channel were taken at several sections for U_{∞} from 6 mps to about 14 mps. Typical data for vertical profiles along the center section of the channel are shown in Figure 4A. The vertical profiles of $U(z')$ indicate that the air flow generally develops a behavior characteristic of turbulent flow in a boundary layer over roughened surfaces. In a few cases, a small kink in the distribution of $U(z')$ was observed which usually appeared at ~5 cm height above the mean water level. Using pitot tube measurements, Francis (1951) also observed these kinks. Schooley (1963) was able to find the kinks by tracing mean trajectories of bubbles over the waves. However, their measurements indicated that the kinks appeared somewhat closer to the water surface, $z' = 2\text{-}3$ cm. The existence of the kinks in the profiles of air velocity indicate that a jet of high velocity air may sometimes develop over wavy water in channel flows. To the authors' knowledge, however, with the possible exception of Sheppard (1952), this phenomenon has not been observed with any measurements over water in the atmosphere.

Typical measurements of the horizontal distribution of velocity are shown in Figure 4B. These data are representative of flow in wind tunnels of rectangular cross-section. It is interesting to note that the boundary layers associated with the side walls can become rather thick. This thickening had no apparent effect, however, on the development of significant waves in the channel. The waves still exhibited a nearly linear crest moving approximately normal to the mean wind direction.

The lines of constant air velocity plotted for a given cross-section reveal an interesting feature of the channel flow as shown in Figure 5. Because of a secondary circulation in the tunnel, the lines of constant velocity are squeezed down in the corners of the cross-section. This has been observed previously for flow in rectangular ducts (e.g., Schlichting (1960)). However, the effect appears to become somewhat more pronounced when fluid flows over a moving boundary in the CSU channel.

The three dimensional structure of the air flow does not visibly affect the waves generated on the water surface. However, the pressing of the air moving at higher speeds down along the walls seems to be transmitted to the horizontal velocity in the water. Measurements of the horizontal distribution of velocity in moving water show two maxima developing just underneath the "ears" of the constant velocity curves drawn in Figure 5. Hence, strictly speaking, the velocity in the air and in water should be written as $U(y,z')$, and $u(y,z)$, instead of $U(z')$, and $u(z)$. However, for the purposes of this discussion the motion of the air and the water will be treated as two dimensional.

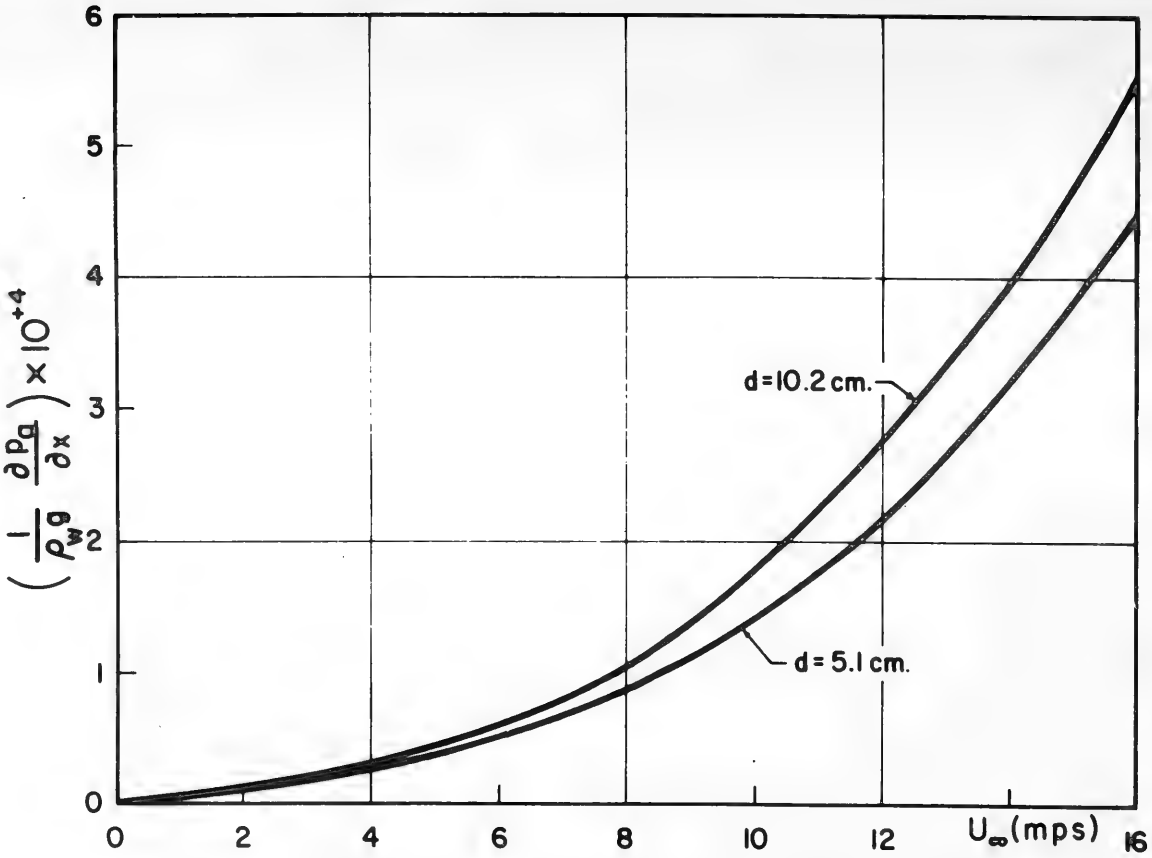

Figure 3. Variation in the pressure gradient in air with air speed in the wind-water tunnel. The pressure gradient is given in terms of length of water per length of channel.

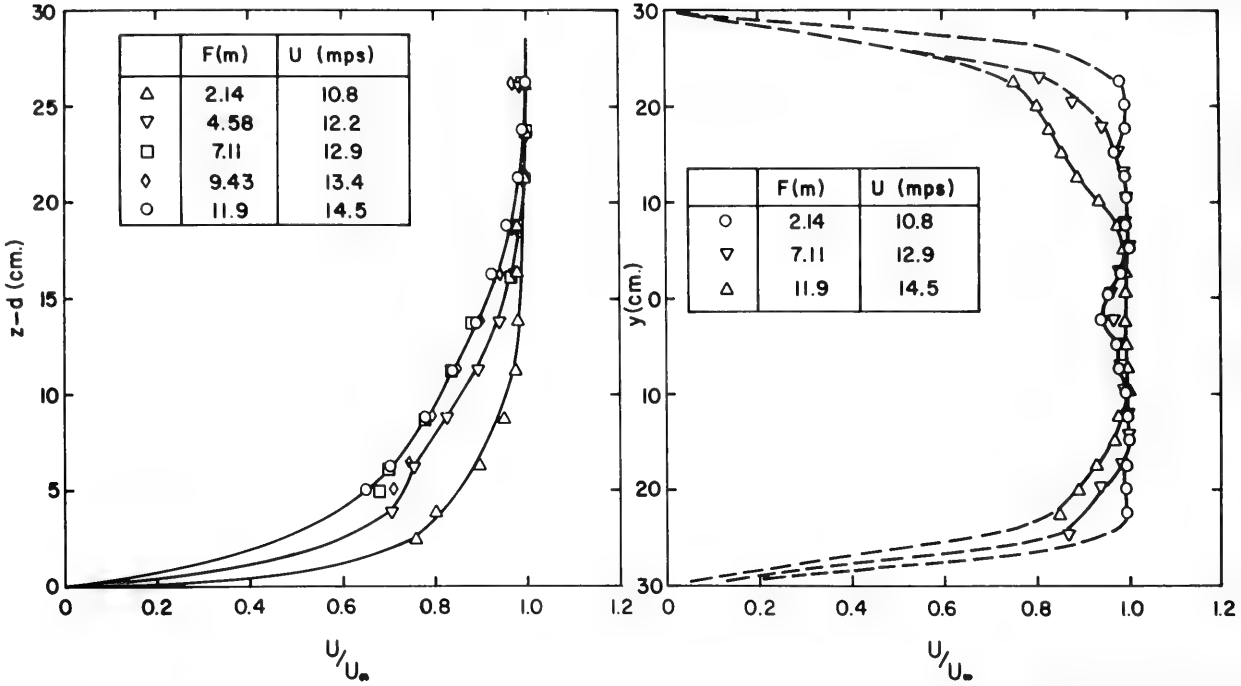

Figure 4. Typical distributions of air flow in the wind-water tunnel.
A. Vertical profiles taken along the center section, and
B. Horizontal profiles taken at (z-d) ≈ 20 cm.

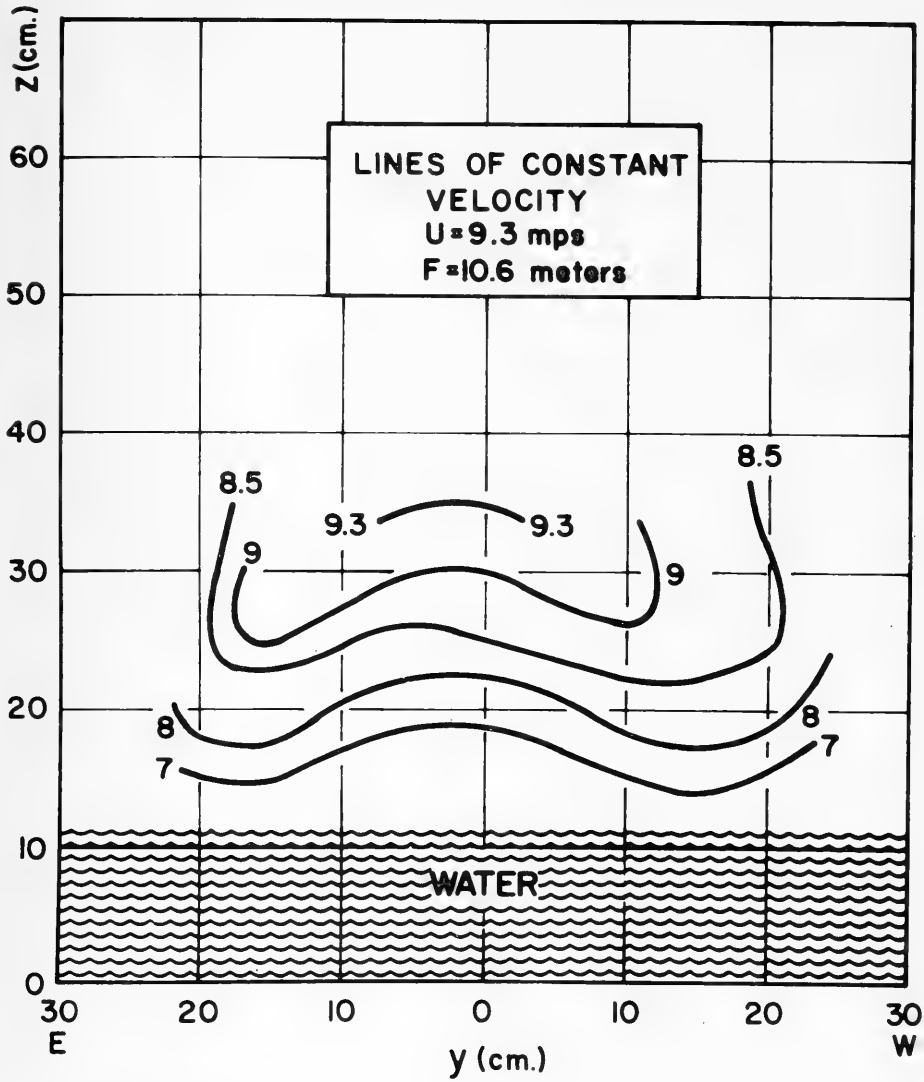

Figure 5. Distribution of air velocity at a given cross-section in the channel.

The vertical profiles for air velocity taken for increasing F along the center line of the tunnel were found to fit the form:

$$\frac{U}{U_\infty} = \left(\frac{z - d}{\delta}\right)^{1/n}$$

where δ is the thickness of the boundary layer as defined by the value of z' where $U(z') = 0.99U_\infty$. Over a wide range of fetch, and for $6.1 < U_\infty < 13.6$ mps the data taken in the channel fit Eq. (1) where $n = 4.5$. This similarity distribution is shown in Figure 6. Several typical values of δ are given in Table I. The shape corresponding to Eq. (1) with $n = 4.5$ is frequently found in wind tunnel data for flow over moderately rough surfaces.

Air Flow Close to the Waves

One of the purposes of this study is to examine the nature of the air flow close to the water boundary. A key problem in this work centers around the question of separation of flow to the leeward of the wave crests (Ursell (1956)). Furthermore, recent theories for energy transfer to the waves from the air place strong emphasis on the behavior of the region where air velocity equals the phase speed of waves. For waves generated in the tunnel, this zone is very close to the water surface, much closer than can be reached with a fixed probe. That is, the present equipment can only measure average velocities in the air within about 1 cm of the crests of the highest waves. To observe the nature of the air motion near $U = \bar{c}$, and to trace the presence of separation, the probe must be placed much closer to the oscillating water surface than the fixed probe will permit. Therefore, a moving probe has been designed which will follow the significant waves and maintain approximately a constant level above the water surface. The schematic picture of the design, worked out by one of the authors, is shown in Figure 7. The probe is maintained at a constant level above the water by a servo-driven mechanism activated by the depth gauges. This system is currently under construction, and we expect to begin obtaining data from it sometime next year.

IV. PROPERTIES OF THE WAVES

Over a wide range of air flow which follows the patterns described in sec. III, only small gravity waves and capillary ripples were generated on the water standing in the channel. Although the air reached speeds greater than 12 mps, breaking of waves, in the sense of forming white caps, was not observed. At high air velocities droplets of spray were observed being shed from crests of the larger waves, but the waves did not become sharp crested as seen in "fully developed" seas.

Up to wind speeds of about 3 mps, taken about 20 cm above the water, no waves appeared on the water surface. However, very small oscillations of the entire water surface could be observed in this range of air flow by watching variations in reflected light on the water. Above 3 mps, ripples began to form near the leading edge of the water. These small disturbances

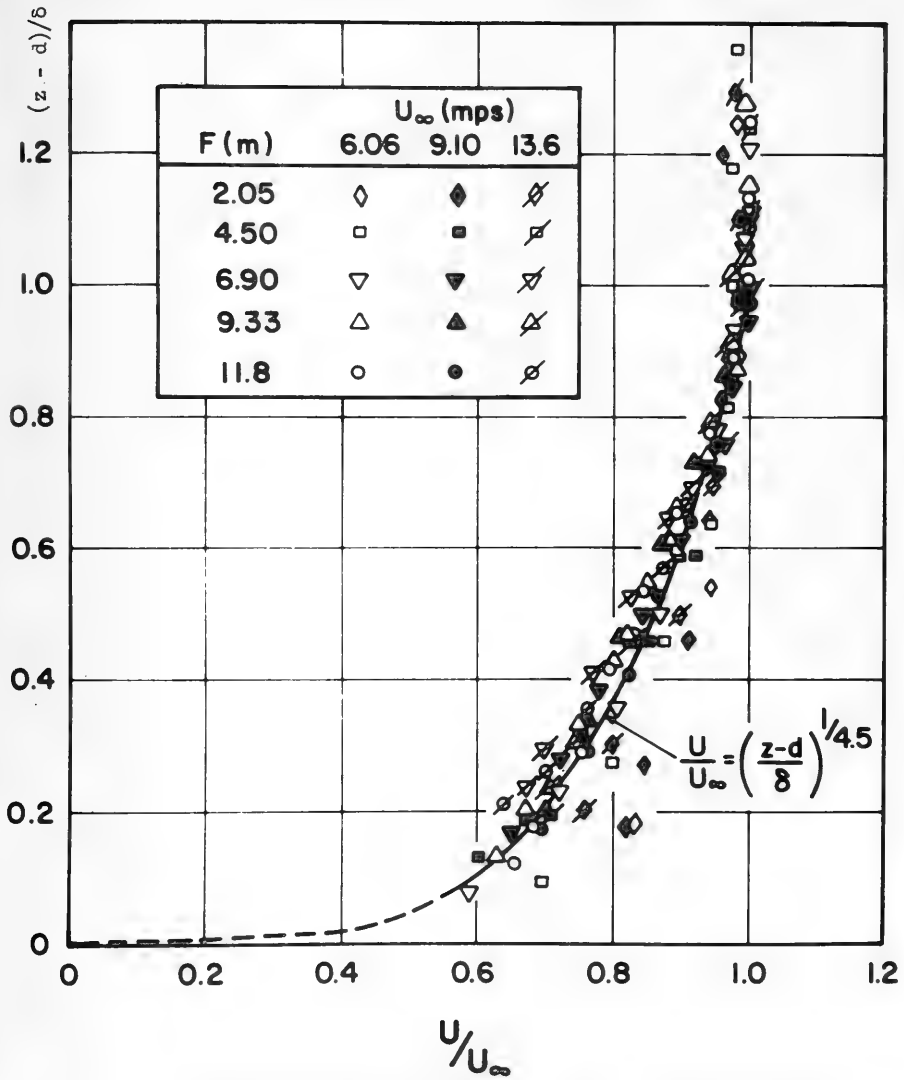

Figure 6. A similarity distribution for the air velocities along the center section of the tunnel.

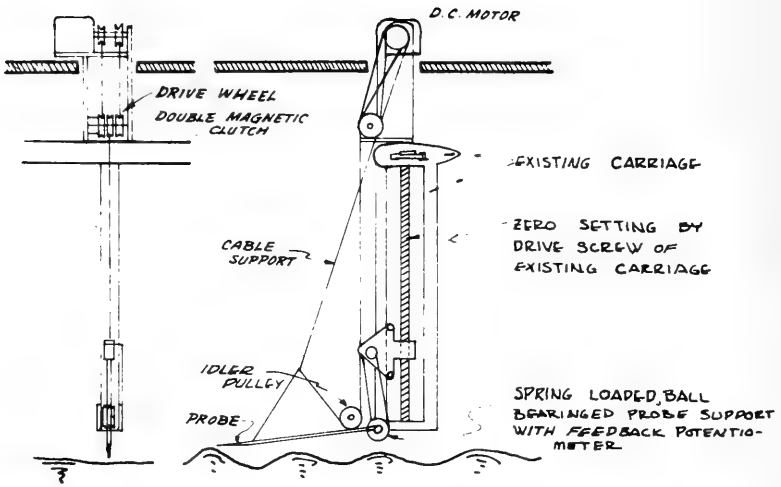

SCHEMATIC DESIGN OF MECHANICAL SYSTEM

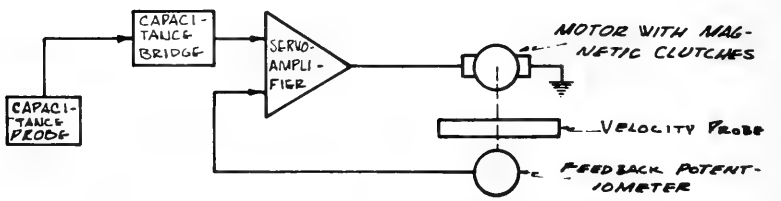

SCHEMATIC DESIGN OF ELECTRICAL SYSTEM

Figure 7. The design of the system for positioning instrument probes near the water surface.

had wave lengths of 1 - 3 cm. Their direction of propagation was primarily normal to the wind direction. As the wind speed increased, the ripples initially present became larger in amplitude and height. Under the action of the steady air motion, the waves traveled downstream at an increasing speed, growing in amplitude and length. For wind speeds in the range U_{oo} = 3-6 mps, significant waves were observed to run with crests approximately normal to the wind direction, with smooth windward surfaces, and rippled leeward surfaces. Above 6 mps, capillary ripples were noted on both the windward and the leeward sides of the significant waves. At any given point downstream from the inlet, groups of 5-20 small gravity waves of nearly the same period passed by. These groups were separated by relatively calm regions of small ripples having varied periods. The existence of groups of waves separated by relatively calm water is probably related to interference between different components of the wave train, giving an appearance of "beats."

The growth with fetch of waves in the channel is reflected in two characteristic lengths, the standard deviation σ and the wave length $\bar{\lambda}$. The increase with F and U_{oo} of σ and $\bar{\lambda}$ is shown in Figure 8. The effect of depth is also shown in the drawing. Decrease in depth tends to reduce the wave length, and the standard deviation of the (larger) waves generated at higher wind speeds. Our data for σ and λ were compared to those reported by Sibul (1955). For a given value of U_{oo} and d, the results of both these studies appeared to be essentially the same.

Two characteristic velocities are associated with the water motion. These are the surface velocity u_o, and the phase speed of significant waves $\bar{c}_e$. The change with F, U_{oo} and d of these properties is shown in Figure 9. For a given wind speed, the surface drift remains nearly constant over the range of d shown, except near the ends of the channel. The wave speed c_e is approximately independent of depth down to 5.1 cm, but it increases with both U_{oo} and F.

Keulegan (1951) found that the ratio of the drift velocity u_o to the wind speed could be correlated with the Reynolds number $Re_d = u_o d/\nu_w$, where ν_w is the viscosity of the water. In his calculations, Keulegan used an air speed averaged over the cross section of his channel, U_{avg}. Goodwin (1965) found that $U_{avg} = 0.85\ U_{oo}$ for the data in the CSU channel. Using this relation, the values of u_o have been plotted with Re_d as shown in Figure 10. The drift velocities found in this study are correlated satisfactorily in terms of Re_d. Our data fall about 30 percent lower than Keulegan's curve for wavy water. The difference between these two studies may be accounted for in three ways. First, if it is assumed that the mass flow of water and air are related to each other and not the velocities, the momentum ratio, $\rho_w u_o/\rho_a U_{avg}$ should be used in this correlation. Keulegan's data were taken at sea level while the CSU measurements were made at nearly 1800 m altitude. If our data are corrected for the decrease in air density with altitude, they will fall about 12 percent below Keulegan's curve. The remainder of the difference between these experiments may be related to (a) the effect of non-uniformities in u_o in the y-direction resulting from the nature of the air flow shown in Figure 5, and (b) the fact that Keulegan used a value of u_o averaged over the length of his channel while our values of u_o are taken locally. The effect of (b) should be small, however, since u_o varies little with fetch.

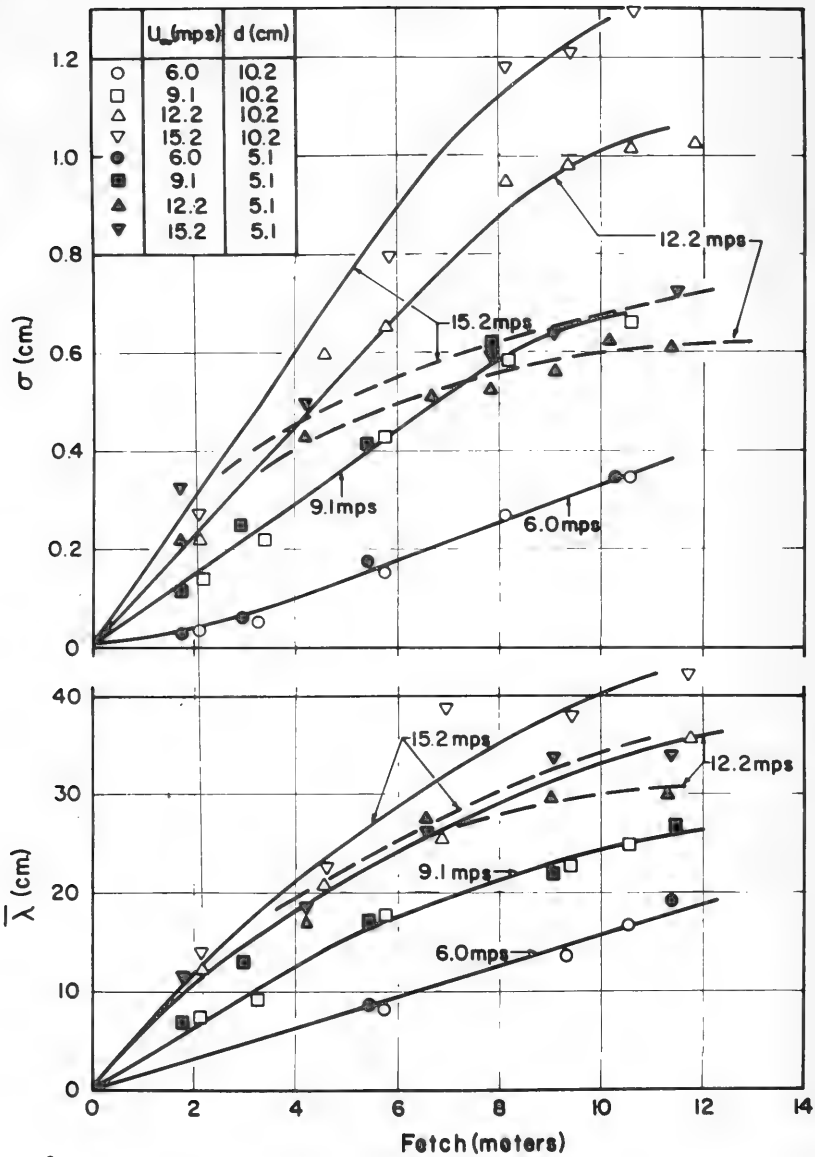

Figure 8. Variation in characteristic lengths of surface waves with fetch and water depth.

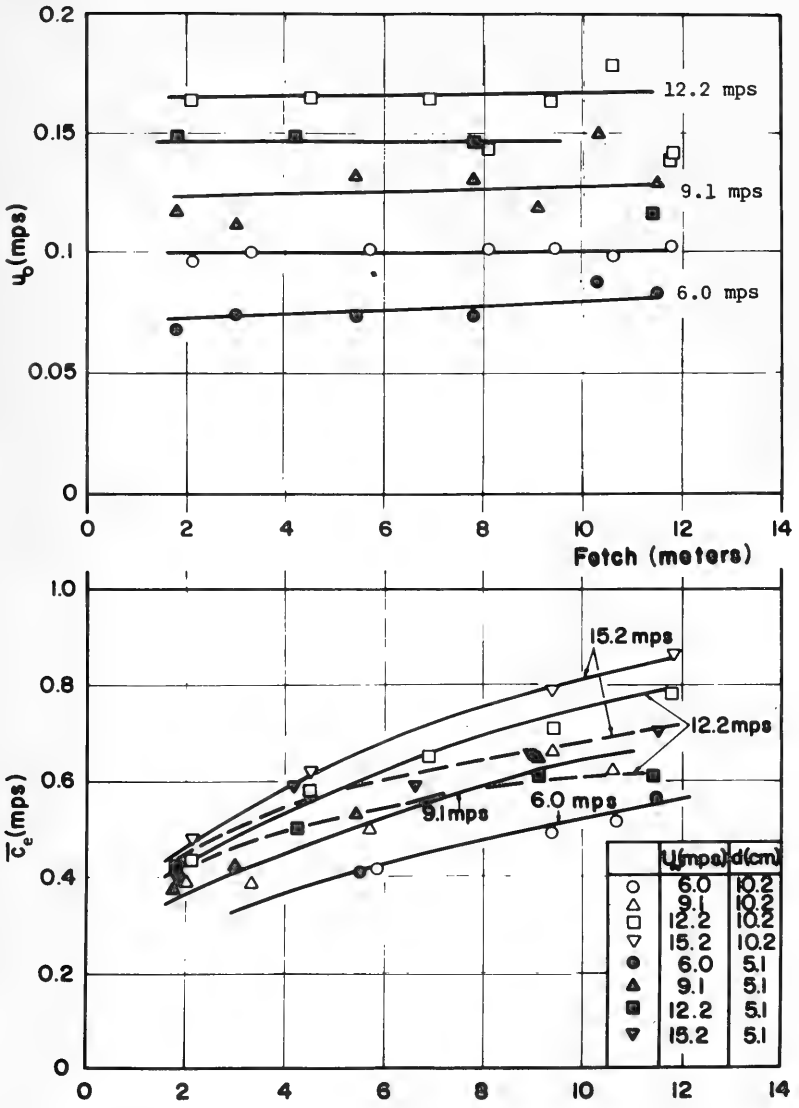

Figure 9. Variation in characteristic water velocities with fetch and depth.

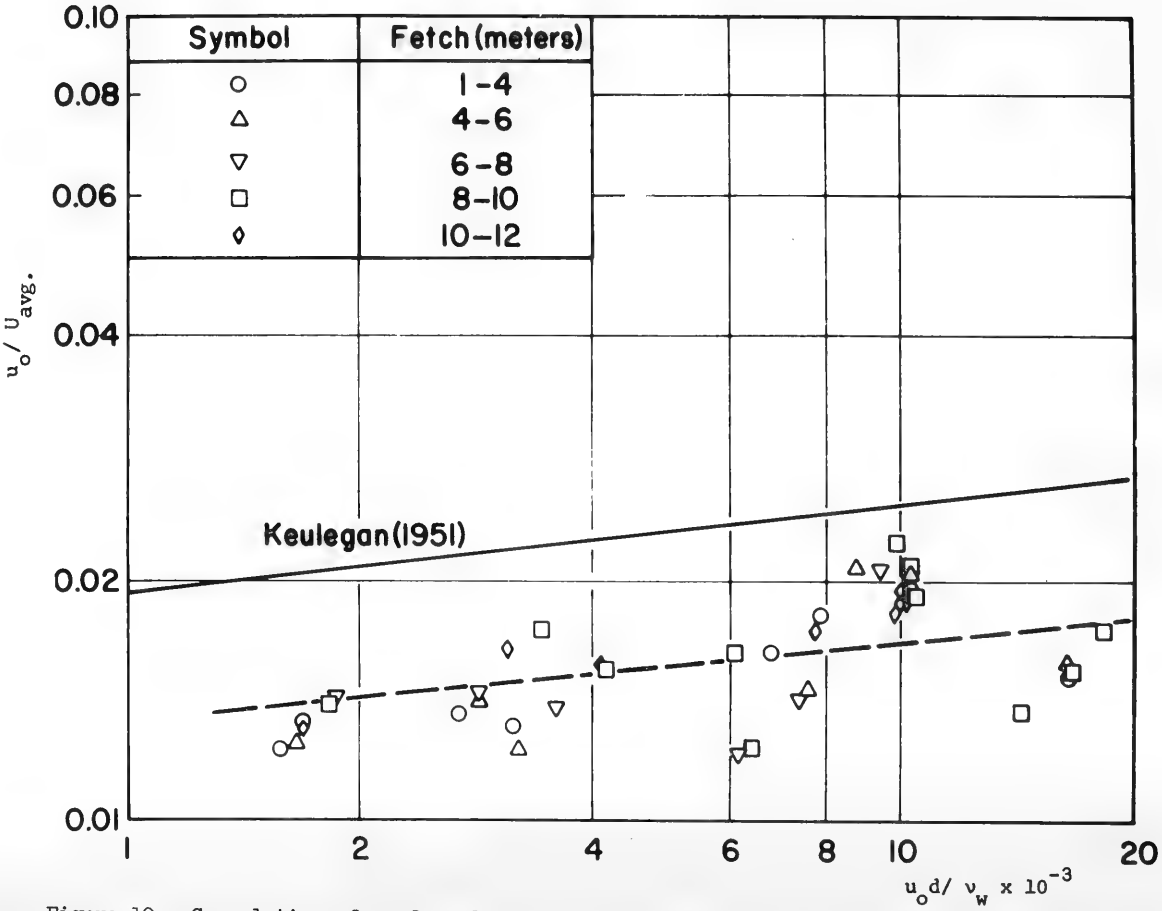

Figure 10. Correlation of surface drift with Reynolds number, Re_d, after Keulegan (1951).

The Phase Speed and the Drift Current

The phase speed of significant waves $\bar{c}_e$ as measured with respect to a fixed point was compared with values calculated from the theory for small amplitude gravity waves. The theoretical phase speed is:

$$c_o = \left[g\bar{k}^{-1} \tanh(\bar{k}d) \right]^{\frac{1}{2}} \qquad (2)$$

where $\bar{k} = 2\pi/\bar{\lambda}$. In all cases, the values of $\bar{c}_e$ were larger than values calculated by Eq. (2). This effect has also been observed by Francis (1951) and Cox (1958). Francis qualitatively accounted for the deviation by considering an increase in wave velocity associated with the surface drift, and the fact that the waves are finite in amplitude. Cox, on the other hand, attributed the difference to the combined effects of finite amplitude, orbital velocity of low-frequency wavelets, drift currents, and dynamic effects of the wind. Cox only analyzed in detail the finite amplitude effect as calculated by Sekerzh-Zenkovich (1956). Cox found that the finite amplitude effect could only explain his observed increase in phase velocity for waves larger than $\bar{\lambda} \simeq 7$ cm. The observed differences in phase speed for wavelets of length smaller than ~ 7 cm could not be accounted for by the influence of finite amplitudes alone.

For strict comparison to $\bar{c}_e$, c_o should be corrected for the mean motion of the water and not the surface drift since c_o should be measured relative to an average transport in the water. Because the orbital movement of water particles associated with the waves extends downward to some depth, the surface drift u_o is not the proper correction factor. The correction should be proportional to a weighted average water velocity over some depth below the surface.

Lilly (1964) has proposed a drift correction for waves traveling on water at finite depth. Assuming that the vertical profile of the drift current is parabolic (laminar flow), and that the waves have infinitesimal amplitudes, Lilly found that

$$\bar{c}_T = c_o \left\{ 1 + \frac{u_o}{c_o} \left[1 + \frac{3}{2(\bar{k}d)^2} - \left(\frac{1 + 2\cosh(2\bar{k}d)}{(\bar{k}d)\sinh(2\bar{k}d)} \right) \right] \right\} \qquad (3)$$

For deep water, $\bar{k}d \to \infty$ and Equation (2) implies that the waves travel with the surface flow only (i.e., $\bar{c}_T = c_o + u_o$). However, for shallow water, $\bar{k}d \to 0$, and Eq. (3) predicts, as expected, that $\bar{c}_T \to c_o$.

The values of $\bar{c}_T$ as calculated by Eq. (3) were compared to the corresponding experimental data, and the results are shown in Figure 11. Experiment and theory agree within $\pm$ 15 percent. This error is approximately that expected on the basis of experimental errors in estimation of $\bar{c}_e$, and $\bar{c}_T$ using $\bar{\lambda}$ and u_o.

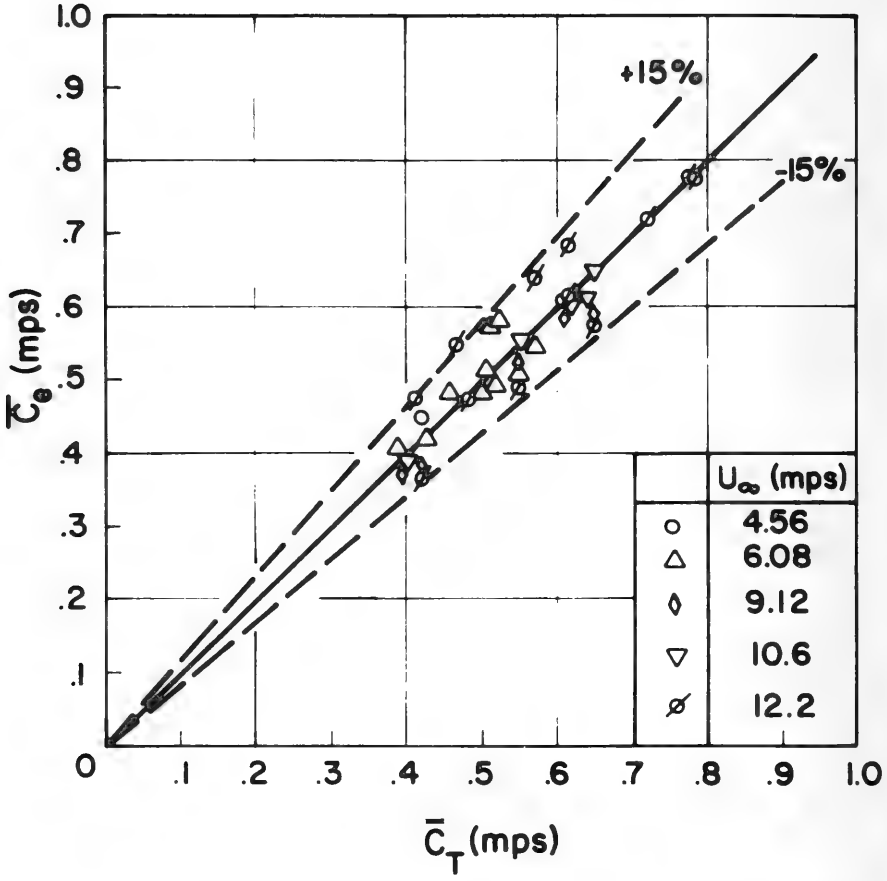

Figure 11. Comparison between experimental values of the phase speed of significant waves and values calculated by Lilly's theory.

Systematic deviations between $\bar{c}_e$ and $\bar{c}_T$ might be expected since both the effect of surface tension and of finite wave amplitude were not considered in deriving Eq. (3). The correction in $\bar{c}_T$ for surface tension in deep water waves was found to be negligible for the experimental observations. However, the Stokes correction of c_T for gravity waves of finite amplitude (e.g., Lamb (1932)) could vary from 1 percent to 11 percent (increase) if it is assumed that the amplitude of significant waves is $3.0\ \sigma$ (e.g., Sibul 1955)). Thus, Lilly's equation would give values of $\bar{c}_T$ somewhat larger on the average than the experimental data.

The effect of finite amplitudes in the wind waves may be offset partially by the influence of turbulence in the water. Dye traces of the motion in the water indicate that the water flow was turbulent and not laminar. The use of a turbulent velocity profile having a steeper gradient near the surface than the parabolic curve but having the same drift velocity at the surface would result in a smaller correction factor for drift than predicted by Eq. (3).

These results indicate that the significant wind waves on the water in the channel travel relative to a mean drift approximately as gravity waves of small amplitude. The waves tend to propagate in this way in spite of the steady pushing of the moving air.

Shearing Stress on the Water

An important parameter for measuring the action of the wind on the water is the shearing stress on the water surface, τ_s. This is often calculated in terms of the drag coefficient

$$C_s = \tau_s / \rho_a U^2 \quad , \tag{4}$$

where ρ_a is the density of the air. An average value of the shearing stress at the surface $\bar{\tau}_s$ can be estimated for the data of the present study by taking a force balance on the body of air, or the body of water in the channel at a given time. The shearing stress on the (smooth) walls, on the top of the tunnel and on the bottom can be estimated in well known ways (e.g., Schlicting (1960)). Then the stress $\bar{\tau}_s$ can be calculated from differences between the pressure gradient (on the set up of water), and the shear forces on the walls, bottom and the top. This has been done for our data by Goodwin (1965). His results are expressed as the average drag coefficient based on the average air velocity in the tunnel as defined by:

$$\bar{C}_s = \bar{\tau}_s / \rho_a U_{avg}^2 \tag{5}$$

Estimates of $\bar{C}_s$ as they vary with U_{avg} are shown for two different depths in Figure 12. For comparison, the data of other investigators, Francis (1951), Keulegan (1951), and Fitzgerald (1962) are also indicated. Goodwin's calculations by the force balance technique as applied to the water and the

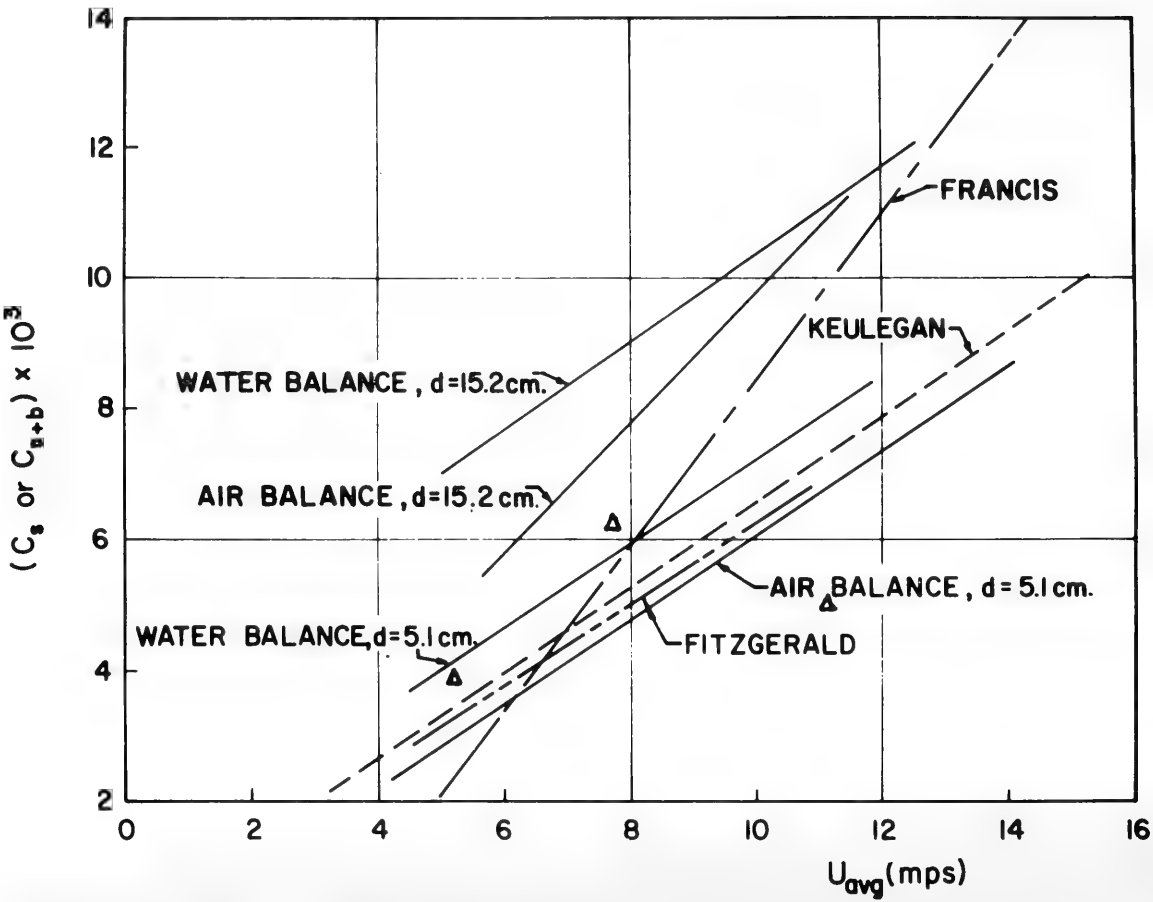

Figure 12. Mean drag coefficients on the water surface. The triangular points refer to averaged local coefficients as calculated from Eq. (7).

air are not the same, but some differences are expected, which will result from estimations of the stresses on the walls of the tunnel. The data for d = 5.1 cm appear to be in reasonably good agreement with the results of Keulegan and Fitzgerald. However, Francis' results show a steeper increase in $\overline{C}_s$ with U_{avg}.

It is worth noting here that all of the values of $\overline{C}_s$ correspond to the case where the channel bottom is smooth. Fracis' calculation includes the effect of the average bottom shear $\overline{\tau}_b$ as well as the surface shear in his value of the drag coefficient (i.e. $\overline{C}_{s+b} = (\overline{\tau}_s + \overline{\tau}_b)/\rho_a U_{avg}^2$). This is equivalent to assuming that the ratio $\overline{\tau}_b/\overline{\tau}_s$ is zero for turbulent flow in the water. Fitzgerald based his data on the same assumption. However, Keulegan took $\overline{\tau}_b/\overline{\tau}_s = 0.25$ in estimating $\overline{C}_s$ only. In view of this, it is not clear why Fitzgerald's data for $\overline{C}_{s+b}$ show close agreement with the results of Keulegan and Goodwin for $\overline{C}_s$ while Francis' results display a considerably larger variation of $\overline{C}_{s+b}$ with U_{avg}. It is also difficult to understand why Goodwin found such a large change in $\overline{C}_s$ with depth of the water. At present, this conclusion cannot be checked with the findings of other investigators because their results apply to one water depth only.

Local values of the drag coefficient ($C_s' = \tau_s/\rho_a U_\infty^2$) can also be estimated from our data. Although evaluation using the assumption of the logarithmic profile cannot be applied, the momentum integral technique can be used (e.g., Schlichting (1960)). The relation for C_s' by this method is:

$$C_s' = \frac{1}{U_\infty^2}\left[\frac{d(U_\infty^2\theta)}{dx} - \frac{\delta^*}{\rho_a}\left(\frac{dp_A}{dx}\right)\right] \tag{6}$$

where δ^* is the displacement thickness:

$$\delta^* = \frac{1}{U_\infty}\int_d^{z''}(U_\infty - U)\,dz' \quad , \tag{7}$$

θ is the momentum thickness:

$$\theta = \frac{1}{U_\infty^2}\int_d^{z''}U(U_\infty - U)dz' \quad , \tag{8}$$

and z" is the value of (z-d) where $U = U_{\infty}$.

To accurately obtain values of C_s' from Eq. (6), the slope of U_∞ and values of δ^* must be well established. The contribution of $(U_\infty - U)$ to the integrals in Eqs. (7) and (8) depends strongly on the region of the

vertical profile where the curvature is greatest. In our measurements, this is poorly defined because the curving portion of $U(z')$ lies too close to the water for accurate measurement with the fixed probe. Thus, the use of Eq. (6) with Eqs. (7) and (8) can be expected to give only an order of magnitude estimate of C_s'.

In addition to the problem of using the experimental data in Eqs. (7-9), the application of a definition for proper air velocity must be considered. Eqs. (7-9) apply to flow over a solid boundary. When the boundary is moving and waves are superimposed on this motion, the air speed relative to fixed coordinates may be an incorrect estimate for $U(z')$. Two other systems of velocity coordinates can be used. The air velocity relative to the surface drift may be a better system, or as Benjamin (1959) has noted, the motion relative to the phase speed c may be better than the fixed system of reference. Introduction of either one of these reference velocities will affect the definitions of δ^* , θ , δ , and C_s'.

In spite of these difficulties, it is useful as a first approximation to apply Eqs. (7-9) for evaluating C_s'. Calculations of the local drag coefficients based on the data for $U(z')$ were made, and some typical results for δ^* , θ , and C_s' are shown in Table I. These results indicate that C_s' decreases somewhat with fetch, but tends to increase with wind speed. The decrease with fetch is typical of the variation in C_s' in the context of a growing boundary layer over a solid surface.

TABLE I

F(meters)	Nominal Average Air Speed (mps)	U_∞ (mps)	δ (cm)	δ^* (cm)	θ (cm)	$C_s' \times 10^3$
2.14	5.2	4.76	7.12	2.00	0.682	3.39
4.58		5.20	14.0	2.80	1.23	2.65
7.03		5.48	17.8	4.04	2.08	2.33
2.14	7.7	7.20	13.7	2.97	1.44	5.66
4.58		7.95	19.6	4.60	2.28	4.32
7.03		8.80	22.8	5.43	2.82	3.31
2.14	11.6	10.8	12.7	3.18	1.40	5.31
4.58		12.1	19.3	4.90	2.35	3.75
7.03		12.8	21.6	5.68	2.74	2.50

Using the nominal average velocity ($0.85\ U_\infty$ measured at large fetch), estimates of $\overline{C}_s$ were calculated by averaging each set of three values of C_s' for the ranges of U_∞ in Table I. As a comparison to Goodwin's results, the three estimates of $\overline{C}_s$ by this method are plotted as triangular points in Figure 12. The data for $\overline{C}_s$ by two different calculations check reasonably well for the 5.1 cm depth of water.

The velocity profiles for air were taken primarily at 15.2 cm water depth, but there should be little change in air flow at 5.1 cm. One should bear in mind, however, that $\overline{C}_s$ calculated from the data in Table I represents $\overline{\tau}_s$ in a narrow slice along the center section of the channel. Strictly speaking, Goodwin's estimates of $\overline{\tau}_s$ include the variation of C_s' in the y direction. From Figure 5, it is clear that the shear on the water surface near the maxima in the cross-sectional distribution of air velocity will be larger than that at the center section. This may account for the differences between values of $\overline{C}_s$ at d = 15.2 cm as estimated by Goodwin's method and the momentum integral technique.

V. WAVE SPECTRA

Autocorrelation Functions and the Frequency Spectra

The time correlations between displacements of the water surface were calculated from the digitized depth gauge data. The autocorrelation function $R(\tau)$ is defined as:

$$R(\tau) = \overline{\xi(t_1)\,\xi(t_2)}\,, \qquad \tau = t_2 - t_1 \tag{10}$$

where $\xi(t_1)$ and $\xi(t_2)$ are surface displacements taken at the same point for two different times, t_1 and t_2. The averaging technique in Eq. (10) was carried out after the method given in Blackman and Tukey (1958).

The function $R(\tau)$ for waves in the channel was found to exhibit certain interesting features. A typical example is shown in Figure 13. $R(\tau)$ was generally found to oscillate regularly about the $R(\tau) = 0$ line with increasing τ. Its amplitude decreased sharply initially, but it became fairly steady at higher values of τ, though sometimes it varied slowly as if a lower harmonic was present. The behavior of $R(\tau)$ suggests that there is a tendency for the mutual action of the two fluids to force a nearly periodic, regular disturbance to develop on the water at a given fetch in the channel. On the regular waves are superimposed small, random disturbances which are related to the larger values of $R(\tau)$ for small τ. This, of course, is precisely the physical picture which developed from visual observations of the development of the significant waves.

It is well known that the autocorrelation of a periodic function of period P is another periodic function with period P and a zero mean. Hence, the period of the significant waves can be estimated from the zero crossings of the autocorrelation function at large values of τ where the effects of the random component are small. As seen in Figure 13, the components of "noise" tend to damp out rapidly, so that the period of the significant waves also can be calculated approximately from zero crossings of $R(\tau)$ over the whole range of τ. Typical values of $1/P$ found in this manner are listed in Table II.

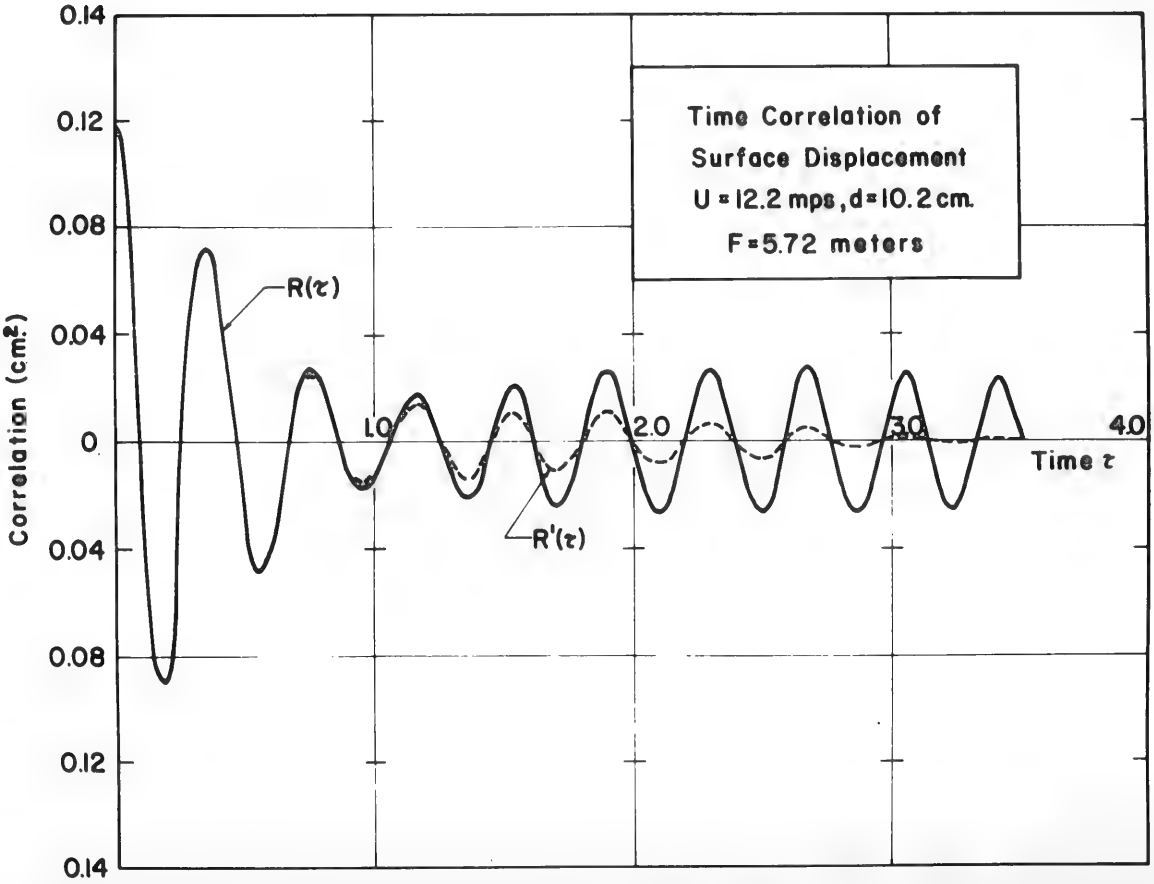

Figure 13. Typical unfaded and faded autocorrelation functions for the displacement of the water surface.

TABLE II

Case	$\bar{c}_e / \bar{\lambda}$	1/P	f_m
21	2.74	2.87	2.91
79	4.62	4.83	4.74
100	5.61	5.71	5.65
113	2.91	2.85	2.76
169	3.24	3.31	3.26

The energy spectra were calculated by means of the following relation:

$$\Phi(f) = \int_0^\infty R(\tau) \cos 2\pi f t \, dt \, . \qquad (11)$$

The scheme for evaluating the integral in Eq. (11) for a finite record is given by Blackman and Tukey, (1958). However, instead of the usual technique of "hanning," it was preferred to obtain a suitable lag window by multiplying the function $R(\tau)$ by:

$$g(\tau) = (1 + \cos \frac{\pi \tau}{T_m}) \, , \qquad (12)$$

where T_m for our data is 3.5. The fading function $g(\tau)$ has the advantage of suppressing the periodic component in the autocorrelation function at large lags without removing any information at short lags. An example of the faded autocorrelation $R'(\tau)$ (=Rg) corresponding to the curve of $R(\tau)$ is shown in Figure 13.

The spectrum corresponding to the faded autocorrelation $R'(\tau)$ in Figure 13 is shown in Figure 14. Note that the tendency toward periodicity in the wave train also is indicated in this spectrum. Higher harmonics of the frequency f_m for which the energy is maximum appear as indicated in this Figure. If the waves were perfectly periodic, the idealized spectrum based on the $R(\tau)$ curve would develop as spikes of infinite height at n multiples of f_m. However, because the waves are not truly periodic, and because of the random components which exist in the signal, the spectrum actually takes the bumpy shape indicated in Figure 14.

Typical values of f_m are shown with corresponding values of 1/P and $\bar{c}_e/\bar{\lambda}$ in Table II. Because of the narrowness of the region containing most of the energy in the spectra for wind generated waves in the channel, these three frequencies are approximately equal. Thus, for practical

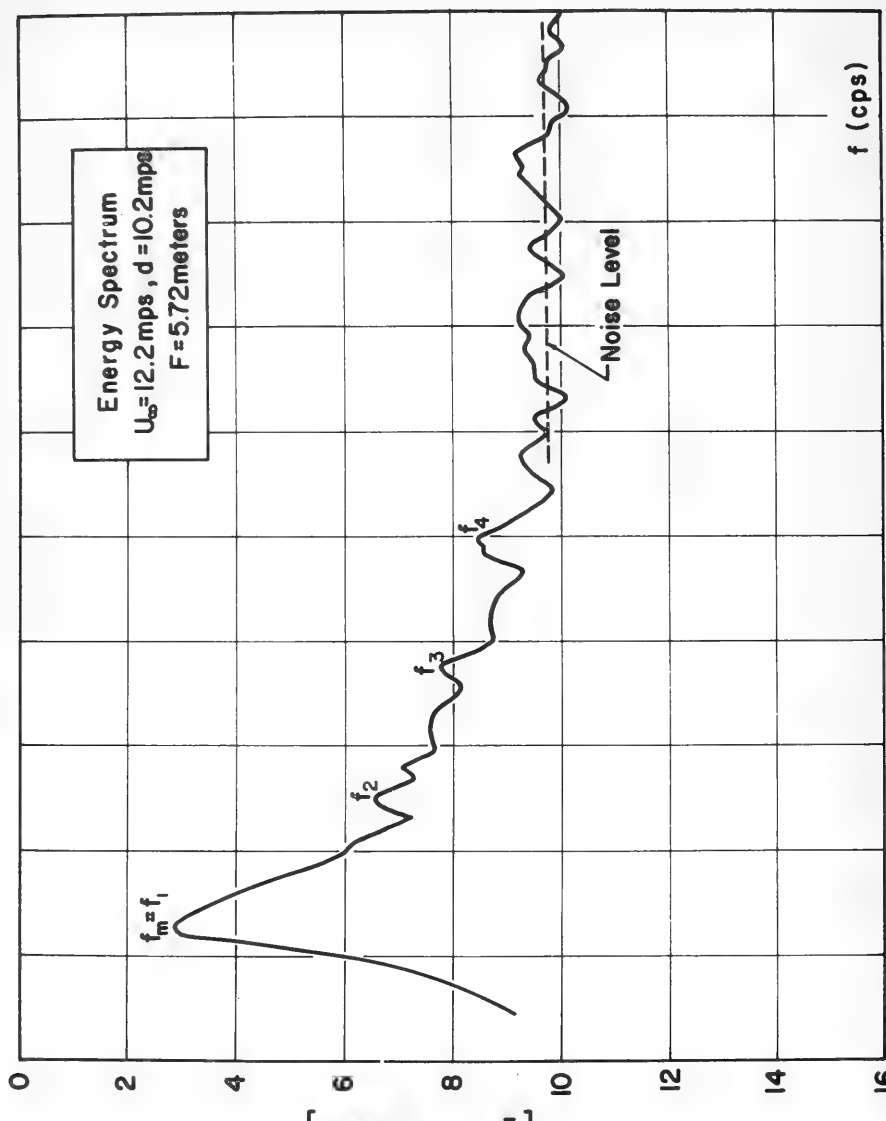

Figure 14. The energy spectrum corresponding to the faded autocorrelation in Figure 13.

purposes, the waves in the channel may be characterized essentially by the properties associated with the significant waves.

The Growth of Waves in the Channel

The frequency spectra calculated at different fetches for the same air velocity indicate how the waves grow as they move downstream along the channel. A typical set of spectra for increasing fetch is shown in Figure 15. These curves have been corrected by subtracting out the noise level, and have been smoothed by a method similar to that discussed by Hidy and Plate (1965). Near the leading edge of the water (small fetch), the observed spectrum contains little total energy and is rather sharp. As the waves travel downstream, the magnitude of the spectral density function increases, the primary peaks broaden at first, then tend to sharpen up while the values of f_m decrease.

The growth of waves in the range of higher frequencies tends to be limited as indicated in Figure 15. The complete mechanism for restraining the growth of the high frequency components is not known. However, it can be seen that the limitation in growth, in part, can be the result of attaining a balance between gains in energy input from the air and losses by dissipation. The dissipation of energy in small gravity-capillary waves is probably related to the action of viscosity and surface tension. The loss by viscous forces in waves is proportional to $(ak)^2$ (Lamb (1932)) where a is the amplitude of a wave. As proposed by Longuet-Higgins (1962a), the loss resulting from surface tension can be related to the drain of energy from larger waves when capillary ripples are formed near the crests of the larger components. This particular mechanism indicates that the energy loss is proportional to $(a_c^2 k_c^3)$. The subscript c refers to the capillary ripple on the crest of a larger wave. If the interaction between components in the wave train is a second or higher order effect (e.g., Phillips (1963)), the action of dissipative processes should balance the input of energy from the air motion in such a way that the net energy at equilibrium is smaller the higher the frequency range. This seems to be suggested in the behavior of the spectra shown in Figure 15.

It is interesting to note that the growth of components in the lower frequency range, say $f \leq 3.5$ cps in Figure 15, is approximately exponential. Qualitatively, this type of growth has been predicted in the recent shearing flow theories of Miles (see, for example, Miles (1960)).

Similarity Shape of the Spectrum

An important feature which was also exhibited by many of the spectra for the channel waves was the tendency for growth in such a way that a similarity shape in the spectral density function is maintained. The frequency spectrum can be expressed, with Eq. (11) in normalized form, as:

(12)

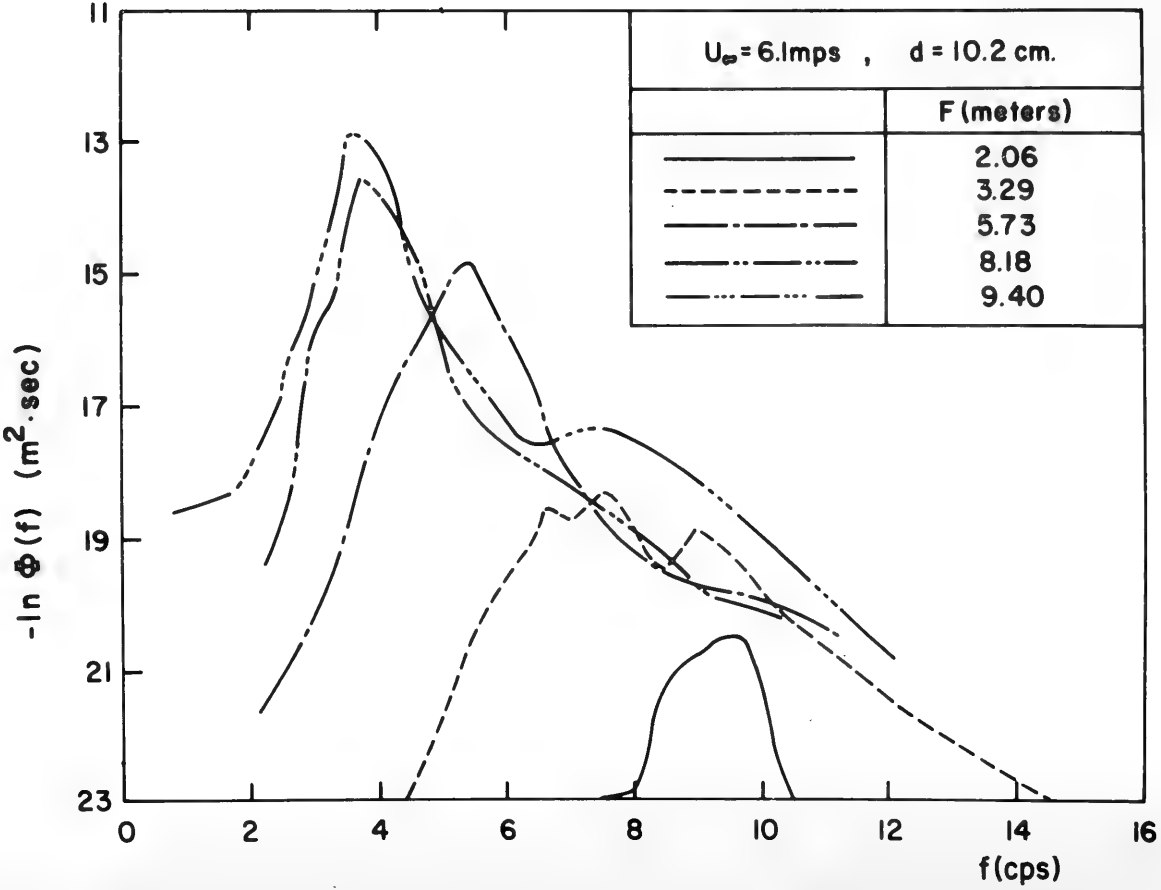

Figure 15. Growth of waves in the channel as indicated by the changes in frequency spectra with fetch.

$$\frac{\Phi f_m}{\sigma^2} = \psi(f/f_m) \qquad (13)$$

where ψ denotes a dimensionless quantity representing a "universal" spectral density function.

Typical smoothed spectra which have been smoothed and corrected for noise level after Hidy and Plate (1965) are plotted in a form corresponding to Eq. (12) in Figure 16. The spectra in Figure 16 serve to define the similarity function ψ quite well. The conditions of U_∞, F and d for these spectra are shown in Table III along with the values of σ, f_m and Φ_m. In general, it was found that the channel data followed ψ quite satisfactorily for the range $6 < U < 15$ mps, and for $3 < F < 12$ meters.

TABLE III

Case	d(meters)	U_∞ (mps)	F(meters)	$\sigma \times 10^2$ (meters)	f_m(cps)	Φ_m
163	0.0254	6.10	5.24	0.131	4.83	2.90×10^{-4}
175	0.102	10.7	10.7	0.767	2.36	7.99×10^{-3}
188	0.102	17.4	8.16	1.36	1.93	2.97×10^{-2}
192	0.0508	10.7	11.5	0.538	2.33	5.53×10^{-3}
208	0.0508	9.15	7.86	0.614	2.48	8.65×10^{-3}
212	0.102	10.7	5.74	0.457	3.17	4.15×10^{-3}

According to Phillips (1958a), on dimensional grounds, the equilibrium or saturation region in the high frequency region of the spectra for gravity waves should follow the f^{-5} rule. In contrast, it has been suggested by Hicks (see, for example, Phillips (1958b)) that the pure capillary spectrum should follow an $f^{-7/3}$ rule. As indicated in Figure 16, the dimensionless spectra for waves in the channel tend to follow the f^{-5} rule over approximately two decades in the high frequency range. In the highest frequency ratios, there is a tendency for some of the spectra to develop a slope less than -5. Capillary wave behavior should begin to appear above f = 13 cps in the frequency spectra. Only two cases, numbers 163 and 188 as shown in Figure 16, actually reach this range. For case 163, capillary waves should appear for $f/f_m = 2.7$ to 3.0, while, for case 188, $f/f_m = 6.8$ to 7.0. Thus, in Figure 16, these two examples may display the beginnings of a transition to the $f^{-7/3}$ range.

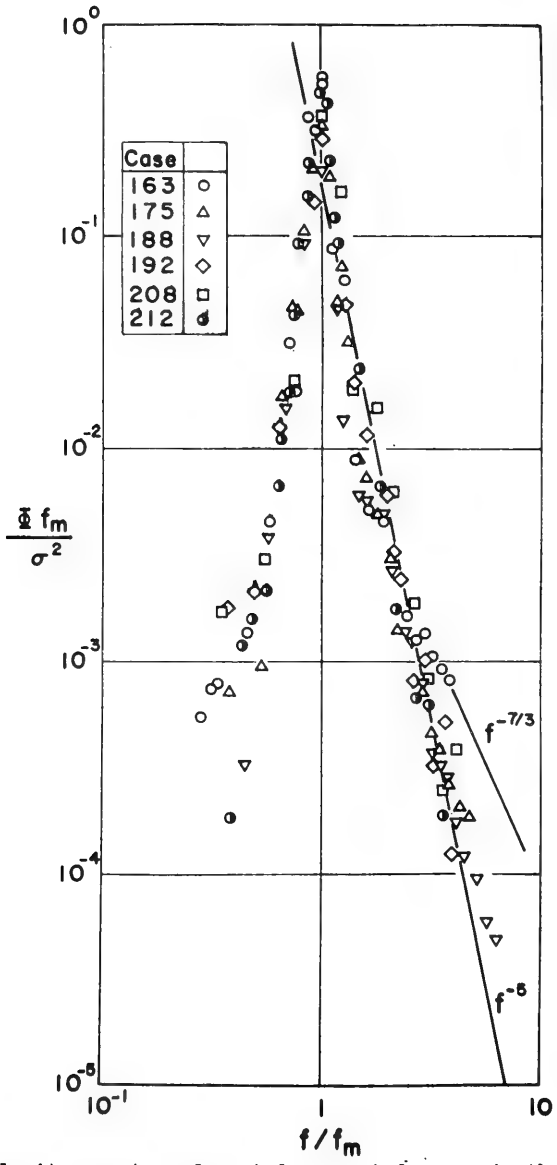

Figure 16. The similarity spectrum for wind generated waves in the channel. After Hidy and Plate (1965).

Unfortunately, the existence of the $f^{-7/3}$ rule cannot be verified generally in these results because the highest frequencies which can be resolved with some accuracy in the computation scheme used, lie around 15 cps. Therefore, these data cannot provide conclusive evidence for the existence of an equilibrium range in capillary waves.

VI. SOME COMPARISONS BETWEEN WAVES IN THE CHANNEL AND OCEAN WAVES

This study was not intended specifically to model waves at sea. Nevertheless, it is worthwhile to see where the data taken for the channel waves fit into the overall picture of wind generated waves.

The properties of the wind waves generated in the channel easily can be placed in perspective with much larger scale conditions by using well known pictures of wave behavior. As an illustration, the channel data have been plotted schematically in two "scaling" drawings of Hicks (1963), as shown in Figures 17A and B. In Figure 17A, the logarithm of the standard deviation is plotted against the logarithm of fetch. The numbers near curves or points refer to wind speeds taken in the field at somewhat different anemometer heights. The values of wind speed for our data correspond to U_{∞}. Our data for waves in the channel fit nicely into the extreme region of short fetch of this figure. Similarly, Figure 17B shows the variation in f_m with fetch. Again our results for small waves correspond to field data taken at very small fetch.

Another way of illustrating where the wave data for the channel fit into the geophysical picture comes from the correlation curves of Wiegel (1963). On dimensional grounds, the mean properties of wind generated waves (on deep water) should be related to a Froude parameter with the characteristic length being the fetch. This correlation shows essentially the variation in standard deviation, length of significant waves, and frequently with fetch.

Wiegel's results include data taken over an extremely wide range of conditions, which include results of some laboratory experiments and field studies on lakes and on the ocean.

A plot of a number of values of σ, $\bar{\lambda}$, and f_m for the waves in the CSU channel is shown in Figure 18 along with average curves estimated from Wiegel's Figure 6-5-7. The averaged curve for the correlation of standard deviation (or 0.33 times the significant wave height $H_{1/3}$) falls approximately along the mean of the data from this study. Furthermore, the lines of maxima and minima in σ, as estimated from Wiegel's correlation, encompass all of our values. It is interesting to note, however, that there is a systematic deviation with U_{∞} for the parameter $g\sigma/U_{\infty}^2$ in Figure 18. This indicates that the Froude criterion gF/U_{∞}^2 cannot be the only parameter for modeling the mean displacement of the water surface. Furthermore, it is clear from the data in Figure 8 and the points for high wind velocity in Figure 18 that the water depth should be included in correlating heights for waves moving at finite depth in channels.

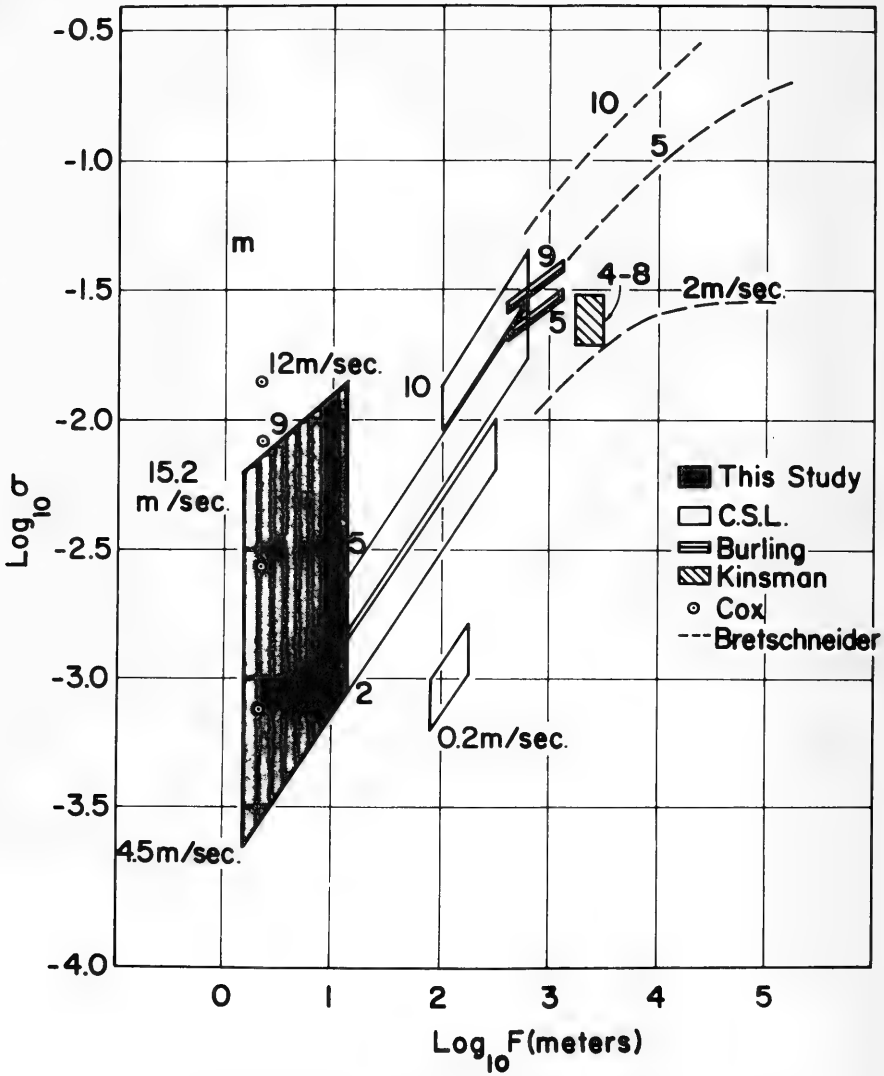

Figure 17A. Properties of small wind waves. Standard deviation. After Hicks (1963).

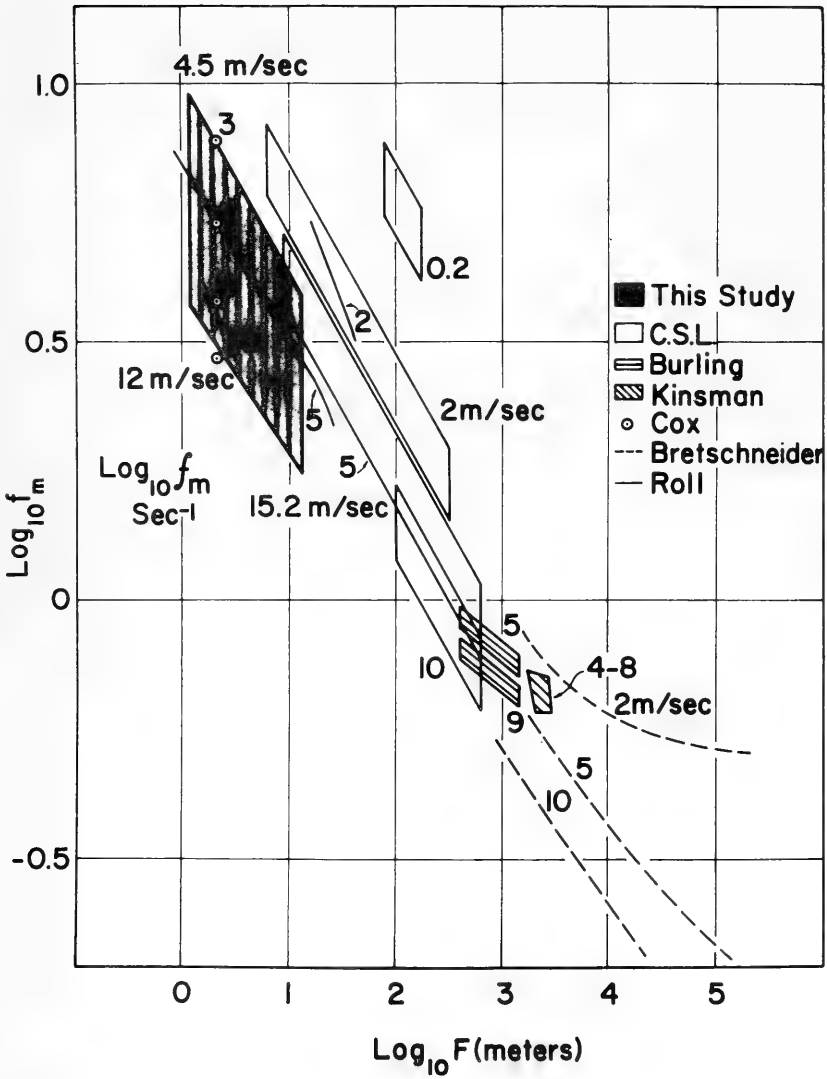

17B. Properties of small wind waves. Frequency of significant waves. After Hicks (1963).

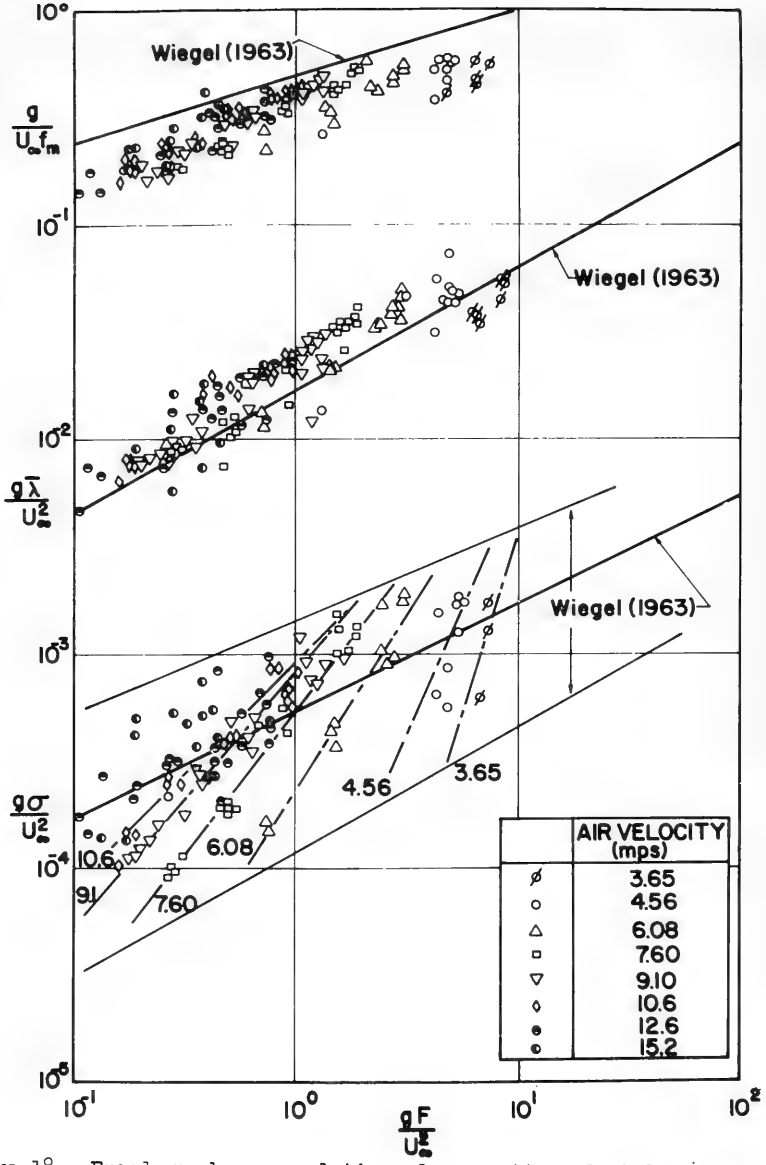

Figure 18. Froude number correlation of properties of wind waves. After Wiegel (1963).

The data for the dimensionless wave length of significant waves in the channel fit Wiegel's correlation curve satisfactorily. There is a tendency, however, for our points to lie somewhat above the estimate of Wiegel's line.

A plot of the wind tunnel data for f_m indicates that Wiegel's curve is again approached. However, in this case, our data lie somewhat below the estimated correlation curve. This is somewhat misleading, however, since comparatively little data is presented for this value (in terms of P) in Wiegel's paper.

The dimensionless energy spectrum derived by Eq. (12) can be compared to the dimensionless form discussed by Bretschneider (1963a and 1963b), provided that it is assumed that σ^2/f_m is approximately equal to $0.34\ \Phi_m$ where Φ_m is the maximum value of the spectral density function (see, for examples, the values in Table III). This has been done and the comparison is shown in Figure 19. Bretschneider's estimate for the Neumann spectrum corresponding to fully developed sea is shown along with our dimensionless spectrum. For further comparison, typical data of Burling as calculated by Bretschneider are shown in Figure 19. As might be expected, the dimensionless spectrum for waves at very short fetch in the channel is narrower than Burling's data taken at $F \approx 1000$ meters and the Neumann spectrum for nearly infinite fetch. The three dimensional character of waves developing on the surface of the oceans or lakes, of course, cannot be reproduced in the channel.

Acknowledgement

The wind-water tunnel at Colorado State University was constructed under a matching grant from the National Science Foundation. This work was supported by the National Science Foundation in connection with its grant to Colorado State University, and its contract with the National Center for Atmospheric Research. The authors are grateful to R. Biro, C. Goodwin, Hosein Shokouh, C. Yang and many others for their efforts in carrying out the experimental program and analyzing the extensive data of this study.

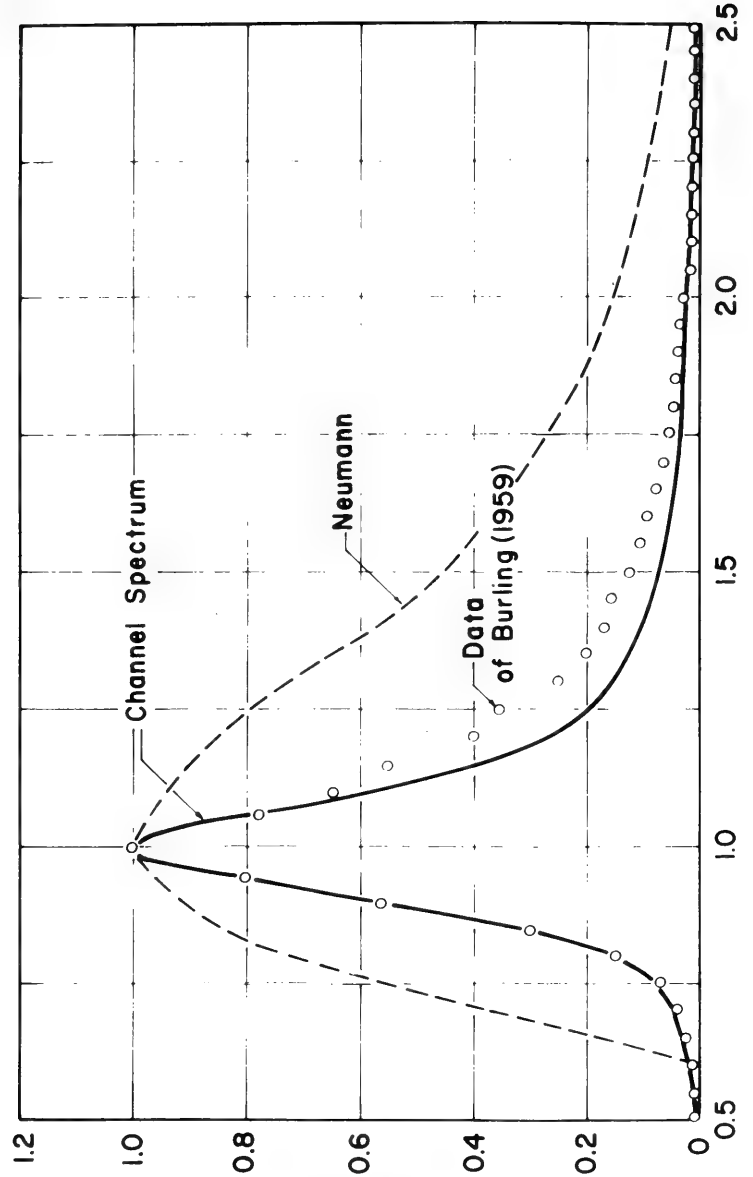

Figure 19. Comparison between dimensionless spectra for wind waves and the data of Burling for short fetch.

REFERENCES

Benjamin, T. B. 1959: Shearing flow over a wavy boundary. J. Fluid Mech. 6: 161-205.

Blackman, R.B. and J. W. Tukey 1958: The measurement of power spectra. Dover Publications, New York, 190 pp.

Bretschneider, C. L. 1963a: A one-dimensional gravity wave spectrum, in Ocean Wave Spectra. Prentice Hall, Inc., Englewood Cliffs, N. J., 357 pp.

1963b: Discussion of H. Walden's Comparison of one-dimensional wave spectra recorded in the German Bight with various "theoretical" spectra, in Ocean Wave Spectra. Prentice-Hall, Inc., Englewood Cliffs, N.J., 357 pp.

Cohen, L. S. and T. J. Hanratty 1965: Generation of waves in the co-current flow of air and a liquid. A.I.Ch.E. Journal, 11: 138-144.

Cox, Charles 1958: Measurements of slopes of high frequency wind waves. J. Mar. Res., 16: 199-225.

Fitzgerald, L. M. 1963: Wind-induced stresses on water surfaces; a wind tunnel study. Aust. J. Phys., 16: 475-489.

Francis, J. R. D. 1951: The aerodynamic drag of a free water surface. Proc. Roy. Soc. (London), A 206: 387-406.

Goodwin, C. R. 1965: The effect of wind drag on open-channel flow. Unpublished M. S. thesis, Colorado State University, Fort Collins, Colo., 93 pp.

Hicks, B. L. 1963: Estimation of the spectrum function for small wind waves, in Ocean Wave Spectra, Prentice-Hall, Inc. Englewood Cliffs, N. J. 357 pp.

Hidy, G. M. and E. J. Plate 1965: On the frequency spectrum of wind generated waves, to be published in Phys. of Fluids.

Keulegan, G. H. 1951: Wind tides in small closed channels. J. Res. Nat. Bur. Stand., 46: 358-381.

Lamb, H. 1932: Hydrodynamics. Dover Publications, New York. 738 pp.

Lilly, D. K. 1964: Personal communication.

Longuet-Higgins, M. S. 1962a: The generation of capillary waves by steep gravity waves. J. Fluid Mech., 16: 138-159.

1962b: The directional spectrum of ocean waves, and processes of wave generation. Proc. Roy Soc. (London), 265A:286-317.

Miles, J. W. 1960: On the generation of surface waves by turbulent shear flows. J. Fluid Mech., 7: 469-478.

Phillips, O. M. 1958a: The equilibrium range in the spectrum of wind generated waves. J. Fluid Mech., 4: 426-433.

1958b: Comments on Dr. Cox's paper. J. Mar. Res., 16: 226-230.

1963: The dynamics of random finite amplitude gravity waves, in Ocean Wave Spectra, Prentice-Hall, Inc., Englewood Cliffs, N. J.,357 pp.

Schlichting, H. 1960: Boundary layer theory. 4th Ed., McGraw Hill Book Co., Inc., New York, 647 pp.

Schooley, A. H. 1963: Simple tools for measuring wind fields above wind-generated water waves. J. Geophys. Res., 68:5497-5504.

Sekerzh-Zenkovich, Y. I. 1956: On the theory of stationary capillary waves of finite amplitude on the surface of a heavy fluid. Dokl. Akad. Nauk SSSR, 109:913-918.

Sheppard, P. A. 1952: Current research at Imperial College, London on the structure of turbulent flow, in Geophysical Research Directorate papers No. 19, USAF Cambridge Res. Center, Cambridge, Mass., 528 pp.

Sibul, O. 1955: Laboratory study of wind waves in shallow water. U.S. Army Corps of Engineers, Beach Erosion Board, Tech. Memo, No. 72, 35 pp.

Tucker, J. J., and H. Charnock 1955: A capacitance-wire recorder for small waves, in Proc. of the 5th Conference on Coastal Engineering, Council of Wave Research, University of California, Berkeley, California.

Wiegel, R. L. 1963: Some engineering aspects of wave spectra, in Ocean Wave Spectra. Prentice-Hall, Inc., Englewood Cliffs, N. J., 357 pp.

Ursell, F. 1956: Wave generation by wind, in Surveys in Mechanics. Cambridge University Press, 475 pp.

ON THE INSTABILITY OF EKMAN BOUNDARY FLOW

Douglas K. Lilly
National Center for Atmospheric Research
Boulder, Colorado

Note: The full text of this address has been submitted for publication in the Journal of the Atmospheric Sciences.

ABSTRACT

Experiments by Faller (1963) revealed the existence and nature of a shearing instability in laminar Ekman boundary flow. Barcilon (1964) formulated the appropriate linear stability equations and obtained partial and approximate solutions, based on the large Reynolds number methods appropriate to other related problems. Numerical solutions of the perturbation differential equations have been obtained for a large number of variations of the three variable parameters, α , the dimensionless wave number, ε , the angle of the instability bands relative to the geostrophic flow, and R, the Reynolds number. Solutions are presented for the eigenvalues, the real and imaginary velocity components, and for the eigenvectors, the actual modes of the normal, parallel, and vertical velocity components.

Two essentially different unstable modes are found, only one of which corresponds to Faller's measured results. This solution, which we call the normal mode, derives its energy from the mean flow component normal to the bands. It is characterized by a band orientation lying between the geostrophic and surface flow directions, i.e. ε is positive and less than 45°. The critical Reynolds number is about 110, compared to Faller's measured value of 125, and the critical values of α , ε and the small real wave velocity are in good agreement with the experiments. This instability is adequately explained (Faller, 1963, also see Stuart, 1955, for a related problem) by inviscid theory, and is associated with the principal point of inflection in the normal mean velocity profile.

The other instability mode obtains its energy from the mean flow shear component parallel to the instability bands, and we therefore denote it as the parallel mode. At the critical point the bands have an angle $\varepsilon < 0$, that is a direction outward from the geostrophic flow, and a wave length about double that of the normal mode bands. The critical Reynolds number is about 60, thus in the experimental realizations the parallel mode should be present before and together with the normal mode. Faller apparently observed this instability qualitatively but erratically. His dye visualization method was probably most responsive to nearly stationary bands, while the parallel mode bands have a large inward real wave velocity.

Further analysis of the dynamics of the parallel mode reveal similarities and differences with other types of hydrodynamic instability. Rotation is of critical importance, as can be determined by comparison of numerical solutions or the perturbation equations with and without the Coriolis terms. Analytic solutions can be obtained from a simplified version of the perturbation equations, which compare fairly closely with the complete numerical solutions. A similarity can be seen to exist with baroclinic instability for cases of short wave length and neutral static stability.

Comparisons between the instabilities present in laminar boundary flow with the finite amplitude disturbances existing in a real turbulent boundary layer are at best qualitative. It may be postulated, however, that either or both of the modes of energy transfer described here could form the principal energy-containing eddies of the atmospheric planetary boundary layer.

FEDERAL RESEARCH PROGRAMS IN AIR SEA INTERACTION

Feodor Ostapoff
U. S. Weather Bureau
Washington, D. C.

The conclusion of a conference of this sort may be an appropriate time to discuss the role of the Federal Government in air-sea interaction research, since, as you know, considerable government attention is now directed to this topic.

Let me say first, that, not long ago, air-sea interaction research had not been identified as such, but was carried out under either the National Atmospheric Science Program or the National Oceanography Program. As a matter of fact, this was the first year that an item named "air-sea interaction research" has been carried in the Atmospheric Science Program.

Why this recent burst of activities and special emphasis? For a long time man concerned himself with problems of the sea. Obviously, phenomena at the sea surface were always of greatest interest, and these are problems which, in one way or another, are the direct result of meteorological events. For example, water waves aroused the interest of the most brilliant minds of the last 200 years. Names like Lagrange, Cauchy, Poisson, Airy, Stokes, Kelvin, Euler, and others come to mind. Today, waves are still subjects of intense investigations. Other examples could be cited such as concepts of the oceanic circulation. As early as 1686, reference was made by Halley that the surface circulation of the ocean is wind-driven. It is most difficult to conceive for the ocean such a simple model of meridional circulation such as the Hadley cell in the atmosphere. For the ocean is heated and cooled at the surface, or, in other words its heat sources and sinks are essentially at the same geopotential. Meridional convection processes seem to be rather inefficient. On the other hand, when about 80 years ago the first deep-sea temperatures were taken in the tropical ocean by the Challenger Expedition and very low temperatures were observed at great depth, it was immediately reasoned that this water is of polar origin and must have descended to a great depth due to cooling at the surface. The thermohaline circulation, which for a number of years was subject to little attention, is now being restudied, for example by Dr.K . Bryan.

This merely illustrates the difficulties we face in defining air-sea interaction research. It is quite possible -- and this has been done -- to include in such a category almost all of meteorology and oceanography. However, for the purpose of this discussion we like to narrow the definition of air-sea interaction because we, in the government, find it most advantageous for administrative purposes to consider in a program only the direct aspects of air-sea interactions. Of course, conferences such as this should not adopt this narrow parochial view and should discuss broad problem areas.

Historically, the Second World War had a profound impact on both oceanography and meteorology. Meteorology then advanced with the help of modern high-speed computers to such an extent that realistic models of the general circulation could be developed and tested and the entire prediction service operated on a more objective basis. The degree of sophistication incorporated in these models increased to a level that soon effects of the

underlying surface become important. Increased numbers of observations and entire new systems were introduced. And again, high-speed computers made it possible to digest the wealth of information. Thus, theory and observation began to exist on an equal footing. Indeed, it is now realized that a new approach to the observational program is in order.

One of the problems facing us, an urgent one in meteorology, is how to obtain new and more accurate information on energy exchanges between the ocean and the atmosphere and vice versa. This problem was investigated in the early 1960's by a joint panel on air-sea interaction of the National Academy of Sciences Committee on Oceanography and the National Academy of Sciences Committee on Atmospheric Sciences. The Chairman of this Panel is Dr. Benton. The work of the Panel culminated in National Academy of Science's Publication No. 983, 1962. This report outlined eloquently the problem areas of air-sea interaction and formulated six recommendations which, if implemented, will lead (in the Academy's opinion) to a new approach to the general problem. Today I would like to stress only one of the six recommendations which introduces the concept of "area studies."

An area study is in effect what meteorologists would call a synoptic scale investigation over a suitable and carefully selected oceanic area where a number of observational techniques can be employed and intercompared. The problem of energy exchanges is considered of such complex nature, and the available methods still not completely adequate (perhaps with the exception of direct Reynolds stress measurements and vertical heat flux determinations) that it seems necessary to plan and to conduct a thoroughly redundant experiment in order to gain some confidence in any oneof the existing techniques. The study area will be bounded by a line of meteorological observations at its circumference in order to evaluate line integrals and apply continuity considerations as independent checks on other indirect techniques.

The Federal Government responded to the Academy report when the Interagency Committee on Oceanography and the Interdepartmental Committee on Atmospheric Sciences jointly appointed an Ad Hoc Panel on air-sea interaction chaired by Dr. Jacobs, Director of the National Oceanographic Data Center. In 1963 the Panel made several recommendations one of which has been acted upon by the Interagency Committee on Oceanography and the Interdepartmental Committee on Atmospheric Sciences. Subsequently, the Federal Council for Science and Technology agreed to assign special responsibility for the air-sea interaction research to the Department of Commerce. The following letter records the assigning of this responsibility:

6 March 1964

MEMORANDUM FOR:

J. Herbert Hollomon, Chairman, ICAS
James H. Wakelin, Chairman, ICO
SUBJECT: Air-Sea Interaction Program

At its meeting on February 25, 1964, the Federal Council discussed questions related to the responsibility of the Department of Commerce for

the air-sea interaction program. The Council supported the designation of special responsibility in this area to DOC as an experiment to be reviewed at the end of one year. The Council further agreed to the following specific statement of this responsibility as it appears in the minutes:

"Planning Responsibilities for Interagency Air/Sea Interaction Research

1. The Department of Commerce is responsible for coordinated planning of the Federally-supported air/sea interaction program.

2. This program will be developed in consultation with the participating agencies through their representatives on a joint ICO/ICAS air/sea interaction panel.

3. The program developed by DOC will be submitted jointly to ICO/ICAS for review.

4. These air/sea interaction plans will be submitted to the Federal Council for Science and Technology for endorsement as components of National Programs in Oceanography and Atmospheric Sciences.

5. Agencies are responsible for funding, conducting, and otherwise managing their portions of the program, consistent with their statutory missions. Such portions are those either initially proposed by an agency for support, or added by mutual agreement between the agency, DOC, and the joint panel.

6. DOC will undertake funding needed to fill out the remaining important components of the total program plan consistent with its statutory missions. Area studies of transfer processes represent one such compoment."

The intention of the Council is to stimulate activity and provide effective leadership and coordination of the air/sea interaction program. I am glad to endorse the Council's statement, which should serve to amplify Dr. Wiesner's earlier memoranda on the subject and should clarify the relationship of DOC to the other agencies in this area.

/s/ Don

Donald F. Hornig

The Department of Commerce responded organizationally to the assigned responsibility by establishing a Sea-Air Interaction Laboratory (SAIL) which is operated jointly by the Weather Bureau and Coast & Geodetic Survey. Furthermore, in order to provide a mechanism for coordination of the program

and for consultation in the development of a program a permanent Joint ICO/ ICAS Air-Sea Interaction Panel was established in May 1964.

At that time Dr. Frank Gifford was the Chairman of this Panel. When Dr. J. Spar became Director of Meteorological Research of the Weather Bureau he then assumed the Chairmanship. The members of the Panel are:

Thomas S. Austin - Dept. of Interior, Bureau of Commercial Fisheries
Dr. Woodrow C. Jacobs - National Oceanographic Data Center
Arnold B. Joseph - Atomic Energy Commission
Dr. Donald Martineau - Dept. of Defense
Lcdr. R. M. Morse - Dept. of the Treasury, Coast Guard
Dr. R. V. Thomann - Delaware Estuary Comprehensive Study - Dept. of Health, Education and Welfare
Dr. Fred White - National Science Foundation

In order to proceed with the development of a federal air-sea interaction program, it was first necessary to go through the atmospheric sciences program and the oceanography program in order to identify air-sea interaction research or contributing activities in these programs. Therefore, we attempted to define what we mean by air-sea interaction research. The following definition has been adopted. Research projects must satisfy one or more aspects of the following goals of principal objectives: (1) The development of a sound body of theoretical and empirical knowledge relative to the processes by which energy transfer and transformation occur in the ocean - atmosphere boundary layers across the entire spectrum of time and space scales and, (2) The identification of those processes which are of critical importance in the prediction of the system's future states, with emphasis on understanding those processes which are susceptible to control by artificial means.

There are several ways in which one could further categorize research activities and bring some order into the field. One could discuss air-sea problems in terms of micro-scale, meso-scale, and large-scale problems, which may be arbitrary but convenient. However, these terms do not mean the same thing to everybody. We have prepared an Interim Report on federally-supported air-sea interaction research in FY-64, FY-65, FY-66. This report summarizes the present program. In the report we speak in terms of (1) dynamics of the boundary layer and turbulence, (2) physics and chemistry of air-sea interface, and (3) large-scale field studies. The last category really encompasses elements of the first two. However, special efforts are required to mount such projects. They may require coordination of a special kind because of use of different systems, platforms, and techniques. They may also require interagency coordination and close cooperation with universities and private research institutions.

Category I, the "boundary layer dynamics and turbulence" contains subject matters such as:

- methods to measure vertical eddy fluxes in the turbulent boundary layer
- theories to explain the mechanisms of turbulent flux and its relation to the structure of the boundary layer
- laboratory experiments and mathematical models to study boundary layer processes
- empirical formulae to relate exchange of momentum, sensible heat, and water vapor to the structure of the atmosphere, hydrosphere, and the interface, and
- circulation models of the atmosphere and hydrosphere which include interaction mechanisms

Perhaps there is now a little time available to indicate briefly what is being done in the government in this field, leaving out significant and probably most important contributions from universities. Some results of these studies have been reported in this conference. The main federal support for university work comes from the National Science Foundation and the Office of Naval Research.

Perhaps the Navy's sea-air interaction program is the largest of its kind in the government. One large study considers the generation of ocean waves and its relationship tothe mechanisms of energy transfers from air to sea. Mainly, Reynold's stresses are measured directly under a great variety of conditions. This investigation includes also heat flux measurements. There is a significant study under way to investigate the mechanisms of coupling the air - ice - water system and its relationship to the heat budget of the Arctic Ocean. The objective of the program is to predict or improve the prediction of ice drift, of pressure - ridge formation, of the stability of leads in the ice as well as the formation, growth, deformation and disintegration of sea ice. Computer programs are designed to test statistically and dynamically three-dimensional models of ocean circulation, the application of environmental parameters representing fluxes of the air-sea interface as they relate to macro-scale oceanic processes, and the influence of persistence, climatic, and transient synoptic processes; and frictional and heat energy exchange on the behavior of the ocean. Furthermore, a project deals with the energy budget of an air-water column extending from about 16 meters below to 45 meters above the interface. Micro-scale fluxes of momentum, heat, and humidity are measured at a fixed tower. The results will provide insight into the mechanisms of physical processes on the micro-scale.

The Public Health Service has initiated and is conducting a comprehensive program on water pollution control. This program is carried out over the Great Lakes and encompasses a system of buoys, floats, and surface observations.

The Dept. of the Interior, in particular the Bureau of Commercial Fisheries, is very much interested in air-sea interactions as they relate to heating, cooling, upwelling, advection, convergences and the distribution of fish, in particular the tuna. For this purpose the Bureau is assembling month-by-month historical mean sea-surface charts, is correlating and analyzing sea-level atmospheric pressures, sea-water temperatures, and winds at the 20 stations in the North Pacific and studies the relationship between winds, currents and other vector quantities. Studies are being made of heat exchange at the air-sea interface to develop prediction techniques for eastern pacific temperate tuna.

There are many more projects going on in the Federal Government which deal with this category. However, due to the limitations of time we are not now able to mention them all. It is important to remember that these projects are conducted within the agencies. A large number of projects are contracted with universities and private research institutions.

The following agencies are conducting or supporting research in air-sea interaction:

Department of Defense:

Department of the Army
Department of the Navy

Department of Health, Education and Welfare:

Public Health Service

Department of Interior:

Bureau Commercial Fisheries;
Bureau of Sports Fisheries

Department of the Treasury:

Coast Guard

Atomic Energy Commission

National Science Foundation

Department of Commerce:

Coast & Geodetic Survey
Weather Bureau

Category II, namely, "physics and chemistry at the air-sea interface" is mostly being done outside the government under contract support. Therefore, I will not go into any details of these projects.

Category III which we defined as "large-scale field studies" contains a number of activities. As a matter of fact we could place into this category any major investigation of any geographical area. However, I would like to mention at this point that to our knowledge no study is under way at this time which would satisfy the criterion for an "area study" as defined previously. Of course, in the category of large-scale field studies we would describe the work done during the Indian Ocean Expedition, in particular, its marine meteorological and surface oceanographic activities.

The Navy has a large program in the Arctic which could be considered as a large-scale study. Observations are being obtained from aircraft, satellite, and submarine reconnaisance. The data obtained will reveal time and space distributions of quantities of ice and open water, discrete open water features, and distribution of pressure ridges and ice thickness throughout the Arctic Basin. The data will be used in the development of mathematical models which relate broad scale thermal regimes and motion fields of both media to the ice features.

The Department of Interior has initiated a trade-wind zone program which represents a quantitative study of the seasonal processes as they relate to the Pacific tradewind system, particularly at the air-sea interface. The area of study here is 10 degrees to 30 degrees North and 140 degrees to 180 degrees West. This effort will also attempt to define seasonal displacement of the system and lateral changes of heat fluxes across the air-sea interface and to determine climatic regimes and location and strength of the trade-wind systems.

The Department of Commerce (in addition to Dr. Bryan's work in the theory of ocean circulation, which includes both a wind-driven and thermohaline mode) is mounting now a program along the East Coast which may have some elements of air-sea interaction. Basically an observational program, hydrographic time cross section measurements are planned off South Carolina. The analysis will involve possible meteorological influences on oceanographic parameters. The Weather Bureau increasingly will also make use of its Research Flight Facility, utilizing instrumented aircraft in sampling the atmospheric boundary layer over the ocean in all kinds of meteorological conditions. Further, the Weather Bureau will also continue its storm surge research.

Where do we go from here? It is undeniable that considerable efforts are being made in air-sea interaction research, and at considerable expenditure. Indeed, the Federal Government presently supports this type of research at about a level of $6,000,000 a year. This amount is spent for in-house research activities as well as for contracts and grants to universities and research institutions.

It seems now that we need a comprehensive and coordinated program. We are attempting now to develop a program on scientific technical grounds. The next step is to evaluate the existing program as presently composed of many projects in the various departments and agencies. Finally, the existing program needs to be evaluated in terms of what a program ought to be: missing or weak activities need emphasis and strengthening, and perhaps too much emphasis has been placed in other areas and may represent undesirable duplication. It is also conceivable that we may want to promote "duplication" in some areas in order to provide necessary competition and supplementation.

The Sea-Air Interaction Laboratory is now engaged in the development of the federal program plan. Hopefully, this will be accomplished by the end of this year. In my opinion, this conference contributed significantly in clarifying the research problem areas we face in this important field.

APPENDICES

I. PROGRAM

SEA-AIR INTERACTION CONFERENCE
TALLAHASSEE, FLORIDA
FEBRUARY 23-25, 1965

The conference was sponsored by the Department of Meteorology and the Oceanographic Institute, Florida State University and by the Sea-Air Interaction Laboratory of the Department of Commerce (a joint laboratory of the U. S. Weather Bureau and the U. S. Coast and Geodetic Survey).

SESSION I

3:00 PM, Tuesday, February 23
Room 101, Mathematics-Meteorology Building
Florida State University

Welcome: Dr. Karl Dittmer
Vice President for Academic Affairs
Florida State University

ROLE OF SEA-AIR INTERACTION IN THE ATMOSPHERIC CIRCULATION

Chairman: Dr. N. E. La Seur, Professor of Meteorology, Department of Meteorology, Florida State University.

"Air-Sea Exchange as a Factor in Synoptic-Scale Meteorology in Middle Latitudes." Dr. Jerome Spar, Director, Meteorological Research, U. S. Weather Bureau, Washington, D. C.

"The Three-Dimensional Ocean Circulation Driven by Density Gradients in an Enclosed Basin," by Dr. Kirk Bryan, Geophysical Fluid Dynamics Laboratory, U. S. Weather Bureau, Washington, D. C.

SESSION II

8:30 PM, Tuesday, February 23
Wakulla Springs Hotel

Chairman: Dr. Fred D. White, Program Director for Meteorology, National Science Foundation, Washington, D. C.

"On the Present State of Knowledge in Air-Sea Boundary Layer Problems." Dr. H. U. Roll, NSF Senior Foreign Scientist and Visiting Professor of Meteorology, Florida State University. (Dr. Roll is now President of the German Hydrographic Institute.)

SESSION III

9:00 AM, Wednesday, February 24
Wakulla Springs Hotel

THE ROLE OF SEA-AIR INTERACTION IN TROPICAL METEOROLOGY

Chairman: Dr. Herbert Riehl, Head, Department of Atmospheric Sciences, Colorado State University.

"A Survey of the Role of Sea-Air Interaction in Tropical Meteorology." Dr. Joanne Malkus Simpson, Director of Project STORM FURY, U. S. Weather Bureau, Washington, D.C.

"Sensible and Latent Heat Exchange in Low Latitude Synoptic-Scale Systems." Dr. Michael Garstang, Associate Professor of Meteorology, Oceanographic Institute and Department of Meteorology, Florida State University.

"Intensity of Hurricanes in Relation to Sea Surface Energy Exchange." Irving Perlroth, National Oceanographic Data Center, Washington, D.C.

"The Gulf of Mexico after HILDA (Preliminary Results)." Dr. Dale F. Leipper, Professor of Oceanography, Department of Oceanography and Meteorology, Texas A&M University.

"Evidence of Surface Cooling Due to Typhoons," by Dr. C. L. Jordan, Professor of Meteorology, Department of Meteorology, Florida State University.

"The Modification of Water Temperatures by Hurricane CARLA," by Drs. Robert E. Stevenson, Associate Professor of Meteorology, and Reed S. Armstrong, Graduate Assistant, Oceanographic Institute, Florida State University.

SESSION IV

2:30 PM, Wednesday, February 24
Wakulla Springs Hotel

THE ROLE OF SEA-AIR INTERACTION IN TROPICAL METEOROLOGY (Continued)AND LARGE-SCALE ASPECTS OF AIR-SEA INTERCHANGE

Chairman: Dr. Woodrow C. Jacobs, Director, National Oceanographic Data Center, Washington, D.C.

"On the Low Level Thermal Stratification of the Monsoon Air over the Arabian Sea and its Connection to the Water Temperature Field." Dr. José A. Colón, Meteorologist in Charge, U. S. Weather Bureau, San Juan, P. R.

"A Low-Level Jet produced by Air, Sea, and Land Interactions." Dr. Andrew F. Bunker, Woods Hole Oceanographic Institution.

"U. S. Fleet Numerical Weather Facility Activities Relating to Sea-Air Interactions on a Synoptic Scale." Comdr. W. E. Hubert, U. S. Fleet Numerical Weather Facility, U. S. Naval Postgraduate School, Monterey, California.

"Synoptic Scale Heat Exchange and its Relations to Weather," Dr. Taivo Laevastu, U. S. Fleet Numerical Weather Facility, U. S. Naval Postgraduate School, Monterey, California.

SESSION V

9:00 AM, Thursday, February 25
Room 201, Education Building
Florida State University

RESEARCH IN AIR-SEA INTERACTION PROBLEMS

Chairman: Dr. George S. Benton, Chairman, Department of Mechanics, Johns Hopkins University.

"Laboratory Studies of Wind Action on Water Standing in a Channel." Dr. George M. Hidy, National Center for Atmospheric Research, Boulder, Colorado.

"On the Instability of Ekman Boundary Flow." Dr. Douglas K. Lilly, National Center for Atmospheric Research, Boulder, Colorado.

"Federal Research Programs in Air-Sea Interaction." Feodor Ostapoff, Acting Director, Sea-Air Interaction Laboratory, U. S. Department of Commerce, Washington, D. C.

APPENDICES

II. PARTICIPANTS

Thomas S. Austin, Bureau of Commercial Fisheries, Washington, D.C.
Tim P. Barnett, Navy Oceanographic Office, Washington, D. C.
George S. Benton, Johns Hopkins University, Baltimore, Md.
Sherman Betts, Interagency Committee on Atmospheric Science, Washington, D. C.
Walter A. Bohan, The Walter A. Bohan Company, Park Ridge, Ill.
Andrew F. Bunker, Woods Hole Oceanographic Institution, Woods Hole, Mass.
Kirk Bryan, U. S. Weather Bureau, Washington, D. C.
José A. Colón, U. S. Weather Bureau, San Juan, Puerto Rico
Mariano A. Estoque, University of Miami, Coral Gables, Fla. (on leave from the University of Hawaii)
George M. Hidy, National Center for Atmospheric Research, Boulder, Colo.
William E. Hubert, Comdr., USN, U. S. Navy Numerical Weather Facility, Monterey, Calif.
Woodrow C. Jacobs, National Oceanographic Data Center, Washington, D. C.
Arnold B. Joseph, Atomic Energy Commission, Washington, D. C.
A. D. Kirwan, Jr., New York University, New York, N. Y.
Taivo Laevastu, U. S. Navy Numerical Weather Facility, Monterey, Calif.
Dale F. Leipper, Department of Oceanography and Meteorology, Texas A and M University, College Station, Texas
Douglas K. Lilly, National Center for Atmospheric Research, Boulder, Colo.
Donald P. Martineau, Office of Naval Research, Washington, D. C.
Banner I. Miller, U. S. Weather Bureau, Miami, Fla.
Richard Morse, Comdr. U.S.C.G., U. S. Coast Guard Oceanographic Unit, Washington, D. C.
Thomas H. R. O'Neill, Comdr. U.S.N., Naval Weather Service, Washington, D. C.
A. H. Oshiver, U. S. Coast and Geodetic Survey, Washington, D. C.
Feodor Ostapoff, Sea Air Interaction Laboratory, U. S. Department of Commerce, Washington, D. C.
Irving Perlroth, National Oceanographic Data Center, Washington, D. C.
Robert O. Reid, Department of Oceanography and Meteorology, Texas A and M University, College Station, Texas
Joanne Simpson, U. S. Weather Bureau, Washington, D. C.
S. Fred Singer, University of Miami, Coral Gables, Fla.
R. Bruce Snyder, U. S. Navy Weather Research Facility, Norfolk, Va.
Jerome Spar, U. S. Weather Bureau, Washington, D. C.
Dee F. Taylor, U. S. Forest Service, Macon, Ga.
Fred D. White, National Science Foundation, Washington, D. C.
John Young, ESSO Research and Engineering, Linden, N. J.
Bernard D. Zetler, U. S. Coast and Geodetic Survey, Washington, D. C.

Florida State University Participants

Reed S. Armstrong, Graduate Assistant, Oceanographic Institute
Philip A. Calabrese, U. S. Weather Bureau Scholarship Student, Department of Meteorology
Albert W. Collier, Director, Oceanographic Institute
Gordon A. Dean, Research Associate, Department of Meteorology
George E. Fisher, U. S. Weather Bureau Scholarship Student, Department of Meteorology
Michael Garstang, Research Associate in the Oceanographic Institute and Assistant Professor of Meteorology
Joseph H. Golden, Graduate Assistant, Department of Meteorology
John C. Gille, Assistant Professor of Meteorology
Seymour L. Hess, Professor of Meteorology
Charles L. Jordan, Professor of Meteorology
Noel E. LaSeur, Professor of Meteorology
Hans U. Roll, N.S.F. Senior Foreign Scientist, Visiting Professor of Meteorology
Robert E. Stevenson, Research Associate in the Oceanographic Institute and Associate Professor of Meteorology
Detlef A. Warnke, Research Associate, Oceanographic Institute
Victor Wiggert, Graduate Assistant, Department of Meteorology
William L. Woodley, Graduate Assistant, Department of Meteorology
Edward J. Zipser, Research Associate, Department of Meteorology